UNIVERSITY OF NEUCHÂTEL

- FACULTY OF BIOLOGY -

Laboratory of Plant Physiology

Ph.D. Thesis

FUNCTIONAL CHARACTERIZATION OF THREE ABC1-LIKE KINASES FOUND IN THE PLASTOGLOBULE PROTEOME

PhD Candidate: Jacopo Martinis

Supervisor: Prof. Felix Kessler

Thesis committee: Prof. Michel Goldschmidt-Clermont
Prof. Jean-Marc Neuhaus
Prof. Samuel Zeeman

Academic Year 2012/2013

UNIVERSITÉ DE NEUCHÂTEL

Faculté des sciences
Secrétariat-décanat de Faculté
Rue Emile-Argand 11
2000 Neuchâtel - Suisse
Tél: + 41 (0)32 718 2100
E-mail: secretariat.sciences@unine.ch

IMPRIMATUR POUR THESE DE DOCTORAT

La Faculté des sciences de l'Université de Neuchâtel autorise l'impression de la présente thèse soutenue par

Monsieur Jacopo MARTINIS

Titre: Functional characterization of three ABC1-like kinases found in the plastoglobule proteome

sur le rapport des membres du jury:

- Prof. Felix Kessler, Université de Neuchâtel, directeur de thèse
- Prof. Jean-Marc Neuhaus, Université de Neuchâtel
- Prof. Michel Goldschmidt-Clermont, Université de Genève
- Dr Samuel C. Zeeman, ETH Zürich

Neuchâtel, le 22 janvier 2013

Le Doyen, Prof. P. Kropf

ABSTRACT

In bacteria and mitochondria, the members of the ABC1/ADCK/UbiB family regulate ubiquinone synthesis, and their mutations cause severe respiration defects, including progressive neurological disorders in humans. Little is known about plant ABC1-like kinases: in *Arabidopsis thaliana* five are predicted in mitochondria, but surprisingly six are located at lipid droplets (plastoglobules) in chloroplasts. These are a known site of carotenoid (β-carotene, lutein) and prenylquinone (including Vitamin E, K and plastoquinone) metabolism and contain a large proportion of the tocopherol cyclase (VTE1) required for Vitamin E synthesis and Redox recycling. Although the key enzymes involved in carotenoid and prenylquinone biosynthesis are mostly known, the regulation of these pathways is still poorly understood. Therefore, ABC1-like kinases may be suitable candidates for such regulators and be involved in the modulation of chloroplast lipid metabolism.

Using a non-targeted lipidomics approach we demonstrate that plants lacking either of the plastoglobule kinase ABC1I (At1g79600) or ABC1k3 (At4g31390) are defective both in the production of tocopherols and plastochromanol-8 (a plastoquinone-derived lipid antioxidant) as well as in the Redox recycling of α-tocopherol (Vitamin E). All of these pathways require tocopherol cyclase (VTE1) activity. However, in both mutants VTE1 levels are strongly reduced post-transcriptionally. Our results strongly indicate that both kinases are directly involved in the regulation of the activity of the tocopherol cyclase VTE1, likely by phosphorylation. This may stabilize VTE1 levels at plastoglobules or influence its activity.

At the same time, we demonstrate that the plastoglobule kinase ABC1k3 is allelic to the photosynthetic mutant *pgr6*, identified in a screening of *A. thaliana* plants with low NPQ, possibly because of a low carotenoid content. The *abc1k3/pgr6* mutant is also characterized by a defect in Fv/Fm and ETR after short high light treatment. Remarkably however, mutant plants are able to acclimate to high light, concurrently with a recovery in the cellular content of the xanthophylls lutein and β-carotene and a drastic alteration in the starch-to-sucrose ratio.

A knock-down mutant line for a third kinase, ABC1V (At5g05200), was also produced and subjected to preliminary characterization.

In conclusion, our results indicate that plastoglobule ABC1-like kinases may regulate prenylquinone, carotenoid and sugar metabolism and that VTE1 is a highly probable kinase substrate. However, the ABC1-like kinases may also have other targets and thereby act as major regulators in a wide chloroplast regulatory network.

KEYWORDS

ABC1-like kinases, Plastoglobules, Carotenoids, Tocopherols, Plastochromanol, Photosynthesis, VTE1.

ACKNOWLEDGMENTS

I would like to thank Prof. Dr. Felix Kessler for giving me the opportunity to perform my Ph.D. thesis in his group at the Laboratory of Plant Physiology, University of Neuchâtel.
I would also like to acknowledge Dr. Gaétan Glauser of the Chemical Analytical Service of the Swiss Plant Science Web, University of Neuchâtel, for his valuable help in the development of the method for the prenylquinone profiling by UHPLC-MS and for performing the lipidomics measurements. At the same time, my thanks go to Dr. Michaela Stettler and Prof. Dr. Samuel Zeeman of the Institute of Agricultural Sciences, ETH Zurich, for their precious contribution to the understanding of the possible role of the plastoglobule ABC1-like kinases in the regulation of sugar and starch metabolism.
I would also like to thank Prof. Dr. Toshiharu Shikanai of the Department of Botany, Graduate School of Science, Kyoto University (Japan), for sharing with us his previous experience on the *pgr6* mutant, which put us on the good path for better understanding the biological role of the kinase ABC1k3/PGR6 in the regulation of plant photoacclimation. I'm also grateful to Dr. Birgit Agne and Prof. Dr. Sasha Baginsky of the Institute of Biochemistry and Biotechnology, Halle University (Germany), for the effort they put in the preliminary analysis of the plastoglobule proteome, hoping that the collaboration between our groups can lead to significant advances in the understanding of the role of plastoglobules in chloroplasts.
Last but not least, I would like to thank Dr. Michel Havaux and Dr. Dominique Rumeau of the CEA Cadarache (France) for their initial involvement in the characterization of the plastoglobule ABC1-like kinases, and Michèle Vlimant of the University of Neuchâtel for introducing me to electron microscopy.

TABLE OF CONTENTS

CHAPTER 1

~ Introduction ~

1.1 - PLASTOGLOBULES

1.1.1 - Overview of plastid lipid droplets

1.1.1.1 - Plastoglobules are highly dynamic structures in plastids

Early observations of different plastid types in transmission electron microscopy revealed the presence of "osmiophilic globules"[1-3], small lipid-filled vesicles which carried similarities to the lipid bodies formed at the endoplasmic reticulum (ER) in both animal and plant cells[4].

The average diameter of these lipid bodies, later termed plastoglobules, ranges from 30 to 100 nm in chloroplasts of vegetative leaf cells, but their number and size can significantly change (up to several μm) depending to the developmental stage and in response to particular environmental conditions[5]. In particular, etioplasts with poorly developed thylakoids are characterized by a high number of plastoglobules which decreases during the light-induced conversion to chloroplasts[5-7], while an increased accumulation of plastoglobules was observed in mutants defective in thylakoid biogenesis[8,9]. On the contrary, in senescing chloroplasts plastoglobules enlarge and increase in number as thylakoid membranes are disassembled[5,10-12] It has been also demonstrated that plastoglobules play a role in the formation of the carotenoid-rich colored fibrils during the chloroplast to chromoplasts transition in flowers and fruits[10,13,14]. At the same time, both the size and the number of plastoglobules have been reported to increase in response to environmental conditions that aggravate oxidative stress on the photosynthetic apparatus. These include abiotic stress like the exposure to high light intensities[15], increased CO_2 concentrations[16], drought[17] and salinity[18], as well as in plants growing under nitrate starvation[19] and in soils containing high levels of heavy metals[20,21].

1.1.1.2 - Functional association with thylakoid membranes in chloroplasts

Plastoglobules consist of a neutral lipid core surrounded by a polar lipid monolayer that has been demonstrated to originate from the outer thylakoid membrane leaflet[22]. Electron tomography analysis showed that plastoglobules "blister" from the thylakoid surface and are physically attached to the thylakoid membrane, which is consistent with reports that

plastoglobules are part of the thylakoid network[23,24] and is in disagreement with previous hypotheses proposing a plastoglobule origin at the inner chloroplast membrane[25] or their presence as independent plastid entities which float freely in the stroma[26]. Moreover, the observation that plastoglobules are associated with highly curved regions of the thylakoids suggests that membrane curvature may be an important factor for their formation. It was also observed that in young chloroplasts most plastoglobules occur as single but they appear interconnected in small groups under stress conditions or during senescence, suggesting that new globules may also blister from previously-existing plastoglobules and form clusters not directly connected to thylakoids but linked to each other[22]. Similarly, it was observed that fibrils elongate from plastoglobule surface during chloroplast transition to chromoplast[13].

1.1.1.3 - The algal eyespot apparatus

A particular case related to plastoglobules is represented by the *Chlamydomonas reinhardtii* eyespot apparatus, a primordial visual system responsible for sensing light direction, quality and intensity in unicellular green algae, thus representing an important biological model in the study of the evolution of photoreceptors[27].

Interestingly, a key component of this chloroplast light-sensing complex is represented by an highly organized lens system formed by one to several layers of carotenoid-rich lipid globules separated by single stroma thylakoid lamellae and which functionally correspond to plastoglobules. Moreover, early electron microscopy observations by thin sectioning and freeze fracturing revealed the presence of protein particles exactly outlining the shape of green algal eyespot globules, strongly suggesting the existence of a specialized protein interface towards the stroma[28-30].

1.1.1.4 - Plastoglobules as lipoprotein particles

Similarly to the lipid globules of the algal eyespot apparatus, plastoglobules from higher plants are characterized by the presence of proteins in addition to the lipid component. In particular, the detection of nitrogen in early biochemical experiments performed on purified plastoglobules suggested the presence of proteins associated with the lipid

globules[1,10], while later experiments demonstrated that these proteins were not contaminants from thylakoid membranes but were specific of plastoglobules[13,25,31,32].

Among these, both the fibrillin/plastoglobulin FBN1a/PGL35 and the tocopherol cyclase VTE1 were initially localized to plastoglobules by immunogold labelling of high-pressure frozen and freeze-substituted chloroplasts, thus confirming that these proteins are plastoglobule specific and do not occur elsewhere in the chloroplasts[22]. Besides, these labelling experiments suggested that both proteins partially extends across the membrane monolayer that surround plastoglobules and into the neutral lipid core.

Owing to their structure and composition, plastoglobules are easily separated from thylakoid membranes by sonication or mechanical homogenization and can be conveniently isolated by flotation density centrifugation because of their low density that is due to the high lipid content. Highly pure plastoglobules allowed to investigate their lipid and protein composition while minimizing the possible contaminations from other chloroplast fractions, the thylakoids in particular.

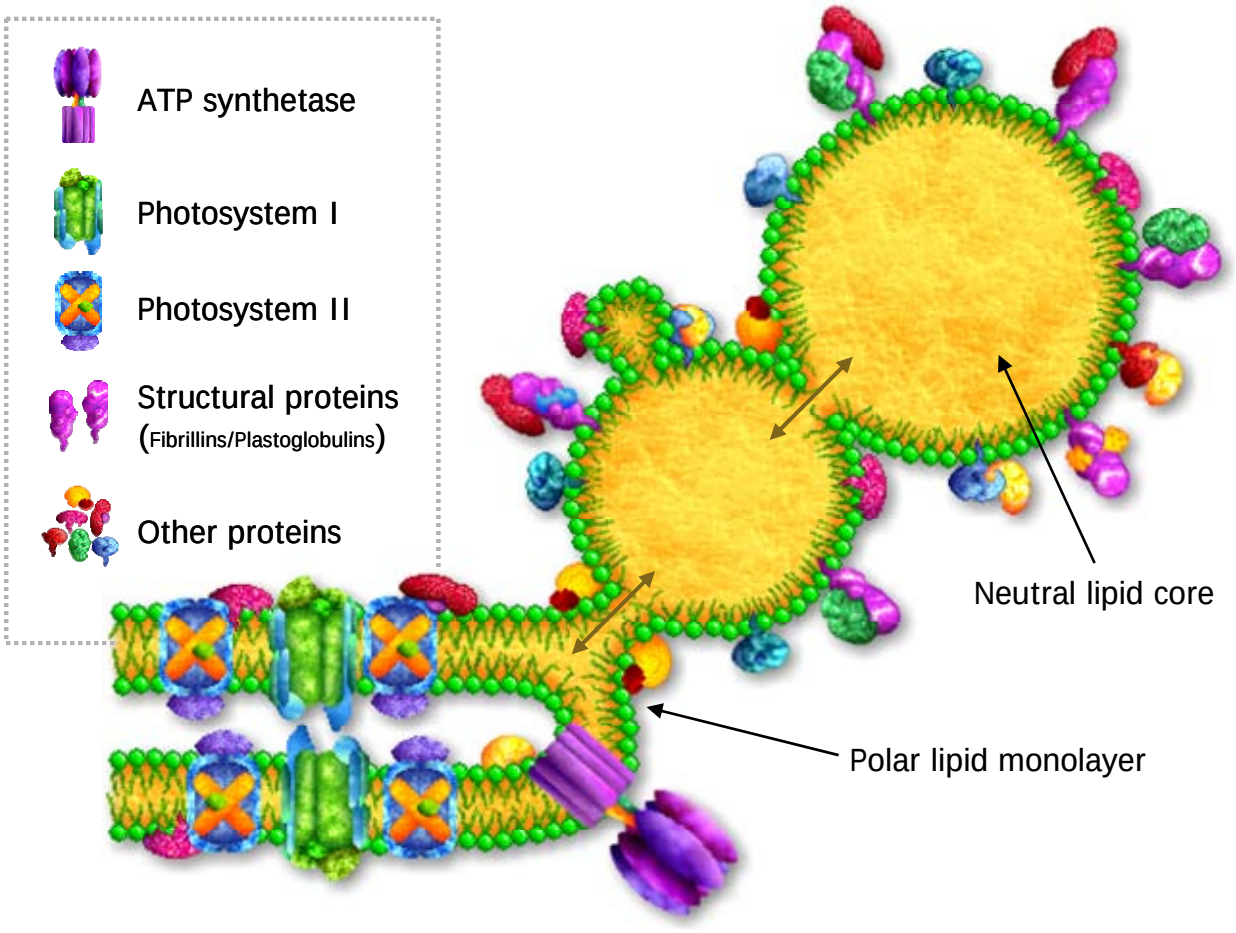

Figure 1.1: Model of coupling of plastoglobules to thylakoids.

1.1.2 - Lipid composition

The lipid composition of plastoglobules extracted from chloroplasts is markedly different from that of non-green plastids. It has been demonstrated that plastoglobules contain prenylquinones like plastoquinone (PQ-9)[5,10,33,34], its derivate plastochromanol (PC-8)[34,35], tocopherols (Vitamin E)[36] and phylloquinone (Vitamin K)[33,34]. In particular, experimental evidence suggested that plastoglobules have a role as a sink for the deposit of excess K that does not associate with PSI[33] and for a significant amount of the PQ-9 pool in chloroplast membranes[35].

Traces of carotenoids (β-carotene, lutein) and chlorophylls, as well as phospho- and galactolipids have also been detected in lipid globules purified from chloroplast fractions[2], although their presence in plastoglobule preparations at the time was attributed to contamination by thylakoids[10]. Conversely, a significant carotenoid accumulation is observed in correlation with the chloroplast to chromoplast transition, during which carotenoids localize primarily in plastoglobules[10]. Moreover, it was observed that carotenoids within plastoglobules exhibit much higher stability than those within chloroplast membranes, possibly because of the presence of other lipid-soluble antioxidants. In turn, their accumulation could also contribute to the protection from spontaneous photo-oxidation of triacylglycerols, unsaturated lipids and other light sensitive molecules[37].

Plastoglobules extracted from gerontoplasts ("old" chloroplasts) in senescing leaves accumulate free fatty acids, oxidised prenylquinones and carotenoid esters[10], the latter of which accumulate in the hydrophobic core of chromoplast plastoglobules and fibrils, contributing to color development in fruits and petals[13]. Moreover, under stress conditions like nitrogen starvation membrane-destabilizing compounds are released that include phytol from chlorophyll degradation and acyl groups from membrane lipids. However, their incorporation in fatty acid phytyl esters (FAPE) inside plastoglobules prevents plastid membrane damage[19].

Plastoglobules also have a major role as lipid deposits in elaioplasts, particular types of leucoplasts enriched in oil bodies and present notably in tapetum cells, in which lipids are deposited in maturing pollen[32].

Molecule		PG	↔	ENV	↔	THY	Reference
Fatty acid phytyl esters	(FAPE)	38 %	17 %	10 %	17 %	17 %	(19)
Plastoquinone-9	(PQ-9)	48 %	14 %	14 %	7 %	17 %	(33,34)
Plastochromanol-8	(PC-8)	56 %	23 %	3 %	2 %	16 %	(34)
Phylloquinone	(K)	14 %	17 %	10 %	20 %	39 %	(38)
α-Tocopherol	(α-T)	36 %	25 %	5 %	21 %	13 %	(36)

Table 1.1: Reported relative distribution of selected neutral lipids between chloroplast sub-fractions. PG. Plastoglobules. ENV. Envelope. THY. Thylakoids.

1.1.3 - Protein composition

In an effort to precisely determine the protein composition of plastoglobules, several independent proteome studies were performed on highly purified fractions by mass spectrometry analysis[36,39,40]. These resulted in the identification of about forty proteins that constitute the *Arabidopsis* plastoglobule proteome (Figure 1.2 on page 17).

More recently, in an attempt to identify the proteins highly enriched in plastoglobules and likely specific for these sub-organellar compartments, an *in silico* statistical filtering was applied to distinguish the "PG core" proteins from potential contaminants from outside plastids or localized primarily in other sub-organellar compartments[40]. As a consequence, some of the proteins previously included in the plastoglobule proteome were removed, leaving only about thirty proteins in the *bona fide* "PG core". However, this does not imply that the excluded proteins are absent from plastoglobules and simply correspond to contaminants but it strongly suggests that their primary localization is elsewhere inside chloroplasts, suggesting that their presence in plastoglobules might not be necessary to carry out their primary biological role.

Independently from the number of candidate proteins included in each study, plastoglobule proteins were further divided into three main groups: structural proteins, known metabolic enzymes and proteins of unknown function.

Gene ID	Protein name	Molecular weight (kDa)
At5g01730.1	WAVE3	128.62
At3g24190.1	ABC1K6	85.37
At3g07700.1	ABC1K7	78.28
At5g41120.1	Esterase 1	77.38
At1g54570.1	Diacylglycerol Acyltransferase 3 (**DGAT-3**)	75.13
At1g79600.1	ABC1I	74.46
At1g71810.1	ABC1K5	73.25
At3g26840.1	Diacylglycerol Acyltransferase 4 (**DGAT 4**)	71.82
At4g31390.1	ABC1k3	67.96
At4g19170.1	9-*cis* -epoxy-carotenoid dioxygenase (**NCED4**)	61.81
At5g42650.1	Allene oxide synthase (**AOS**)	54.57
At5g05200.1	ABC1V	53.84
At5g08740.1	NAD(P)H dehydrogenase C1 (**NDC1**)	51.38
At1g26090.1	Anion-transporting ATPase	46.14
At1g73750.1	Unknown SAG	44.52
At4g32770.1	Tocopherol cyclase (**VTE1**)	43.57
At1g09340.1	Rap38/CSP41B	42.62
At2g21330.1	Fructose bisphosphate aldolase 1 (**FBPA-1**)	41.91
At1g51110.1	FBN10	39.60
At2g01140.1	Fructose bisphosphate aldolase 3 (**FBPA-3**)	38.08
At4g38970.1	Fructose bisphosphate aldolase 2 (**FBPA-2**)	38.00
At1g06690.1	Aldo/keto reductase	37.89
At3g43540.1	Unknown 2 (DUF1350)	37.30
At2g35490.1	FBN2 [AtPGL40]	36.60
At3g63140.1	Rap41/CSP41A	36.30
At1g78140.1	UbiE methyltransferase-related 1	34.11
At2g41040.1	UbiE methyltransferase-related 2	33.42
At3g27110.1	M48 protease	32.95
At4g04020.1	FBN1a [AtPGL35]	28.80
At3g58010.1	FBN7a [AtPGL34]	28.40
At2g42130.4	FBN7b [AtPGL30]	27.70
At3g10130.1	**SOUL** domain protein	27.52
At4g22240.1	FBN1b [AtPGL33]	27.20
At2g46910.1	FBN8	27.10
At1g32220.1	Flavin-reductase-related 1	25.89
At2g34460.1	Flavin-reductase related 2	24.71
At3g23400.1	FBN4 [AtPGL30.4]	22.90
At4g39730.1	PLAT/LH2-1	17.67
At3g26060.1	Peroxiredoxin Q (Prx Q)	17.51
At1g52590.1	unknown (DUF39)	16.98
At4g13200.1	Unknown 1	13.94
At4g01150.1	unknown	11.17
At1g28150.1	unknown	10.79

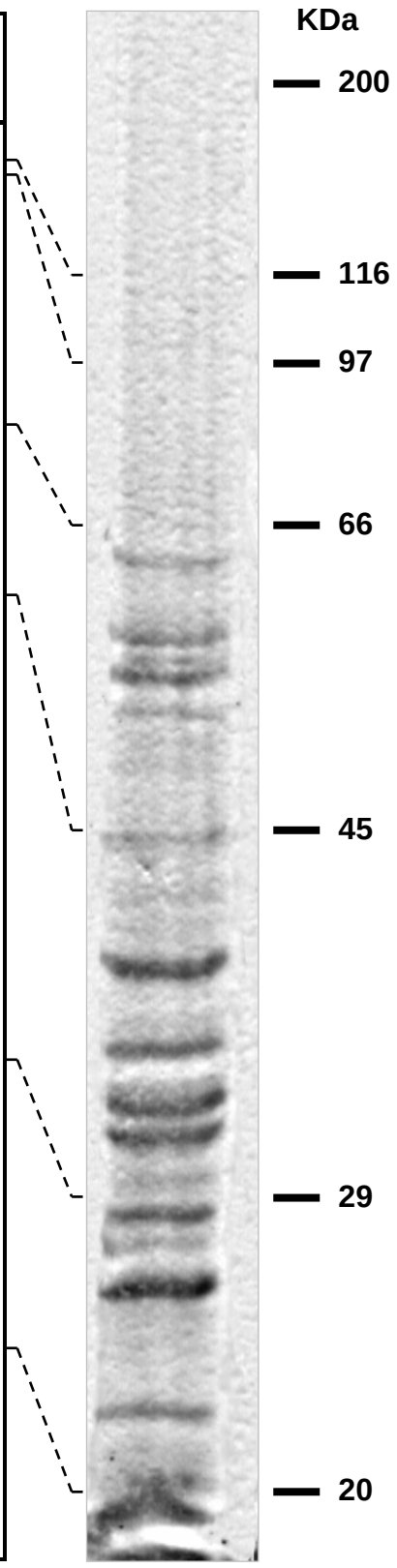

Figure 1.2: The plastoglobule proteome.

List of all the proteins currently identified in plastoglobule preparations. The predicted molecular weight and the relative position range after separation by SDS-PAGE are also indicated.

In particular, this last group includes members with sequence similarities with known proteins having annotated enzymatic or metabolic functions but for which no precise enzymatic or regulatory activity has been reported yet. Among these, this thesis gives particular attention to the description of the members of the ABC1/ADCK/UbiB kinase family (see Section 1.2).

1.1.3.1 - Plastoglobule structural proteins (PAP/fibrillins/plastoglobulins)

The PAP/fibrillin/plastoglobulin family in *Arabidopsis* consists of twelve fibrillin (FBN) proteins as well as an FBN-like homolog[41]. Interestingly, seven FBNs were identified principally in highly purified plastoglobules, while another member of this family (FBN10) is predicted to have a dual localization between plastoglobules and the stroma-exposed thylakoid surface[36,39,40] (see Figure 2.1 on page 54).

Fibrillins (FBN) are named after fibrils, the sub-organellar structures in chromoplasts in which the proteins were first identified. In chromoplasts, fibrils are tube- or thread-like structures of varying shape and thickness related to plastoglobules and correspond to the main site of pigment accumulation, in particular carotenoids as well as glyco- and phospho-lipids[42].Alternatively, considering their strong association with plastoglobules in other plastid types, other names have been proposed such as “Plastid lipid-Associated Proteins” (PAP) and “Plastoglobulins” (PGL)[43], although members of this family have been identified in thylakoids as well. For reference, the alternative names for the members of the PAP/fibrillin/plastoglobulin family are reported in Table 2.1 on page 53.

Fibrillins include proteins with different physical-chemical properties, having molecular weights that usually range from 20 to 40 kDa and isoelectric points (pI) comprised between 4 and 9[41] (see Table 2.1B on page 53), thus suggesting possible variations in the biological functions of each member of the fibrillin family. Furthermore, despite the plastid nature of all fibrillins, their selective distribution between different sub-organellar compartments suggests a specialization in their functions according to the plastid type and the precise localizations in specific plastid structures.

As previously discussed, fibrillins were first identified as protein components of chromoplast fibrils[13,42], and their presence is sufficient for the self-assembly of fibril-like structures in the presence of lipid droplets enriched in carotenoids[13]. Besides, eight of the *C. reinhardtii*

fibrillins are associated with the carotenoid-enriched globules of the eyespot apparatus, and their activity is necessary to stabilize the interactions between globule clusters during the formation of the highly ordered eyespot complex.[30,44]. Similarly, the degree of plastoglobule clustering in higher plants strongly correlates with the relative abundance of fibrillins, indicating that these proteins mediate plastoglobule clustering by preventing their coalescence and possibly mediating cross-links between lipoprotein particles[45,46].

In chloroplasts, several fibrillins are located on the surface of chloroplast plastoglobules and are required for their assembly as well as for the accumulation of lipids inside them[47,48]. On the other hand, fibrillins have also been identified in locations other than plastoglobules. In addition to the previously discussed FBN10, at least six fibrillins are also associated with thylakoid membranes, while only one FBN protein is located in the stroma.

Therefore, fibrillin sub-organellar localization is not fixed but appears to be highly dynamic. In particular, the two plastoglobule-predicted fibrillins FBN1a and FBN4 were found to be components of the Light-harvesting complex II (LHCII) in *Arabidopsis* plants exposed to light stress[49,50].

The differential regulation of the members of the fibrillin family by a variety of biological and environmental factors, as well as during different plant growth stages, strongly suggests the existence of a complex regulatory system for fibrillins both at the transcript and protein levels[51]. In particular, in various plant species the expression rate of the family member FBN1 is enhanced in correlation with the chloroplast to chromoplast transition, during fruit ripening[13,31], as well as in senescent leaves, while it is lowest in young leaves[52,53]. Similarly, treatment with abscissic acid (ABA) accelerates FBN1 accumulation in plants, while high auxin (IAA) levels significantly delays it[13].

At the same time, fibrillin gene expression is affected in response to stress, both biotic such as viruses, bacteria and pathogenic fungi, and to a larger extent abiotic[51]. In particular, complex and varied patterns in the regulation of both fibrillin transcript and protein levels are observed in response to heat, cold, drought, salinity, high light intensity and after exposure to herbicides or heavy metals such as Cd^{2+} and Zn^{2+}.[39, 51,53-56] (see Table 2.1B on page 53).

Despite the substantial amount of information relative to the expression and post-transcriptional regulation of fibrillins in plants, relatively little is known about their biological functions and mechanisms of action.

In view of the wide range of molecules with known antioxidant activity accumulating inside plastoglobules, it is not surprising that fibrillins have previously been implicated in plant resistance to oxidative stress, their mutation significantly affecting plastoglobule formation and lipid content[47,48]. However, functional studies have been carried out only for three out of the twelve fibrillins identified in *Arabidopsis* (FBN1a/b, FBN2 and FBN4).

Other functions have been proposed for these fibrillins though. In particular, indications of a possible involvement in chloroplast development come from the increase in FBN1a and FBN1b levels in *Arabidopsis* mutants defective for the ClpPRS protease complex required in chloroplast biogenesis and characterized by a delayed development, a pale green phenotype, and an increased numbers of plastoglobules[9,57]. At the same time, the increase in plastoglobule size and number during senescence has been associated with the disassembly of thylakoid membranes and the accumulation of the catabolites originating from membrane lipid degradation[58]. As previously discussed, plastoglobules have been reported to contain triacylglycerol (TAG) but few galactolipids[10,19]. The increase in TAG levels in plastoglobules during senescence has been proposed to correlate with galactolipid mobilization from thylakoids, concomitantly with the conversion of thylakoid fatty acids to phloem-mobile sucrose[59]. Indications come from the identification of a putative TAG lipase localized in plastoglobules and which can mobilize the TAG accumulating there. Knock-down mutant plants for this protein have been reported to be delayed in the initiation of a senescence program and are characterized by smaller but more numerous plastoglobules and fewer and deformed thylakoids, which would be consistent with a delay in the onset of senescence in rosette leaves[60].

Besides, the observed increase in plastoglobule size in older chloroplasts has been also proposed to represent a response to the accumulation of reactive oxygen species (ROS) concentration during plant aging[17].

On the other hand, the analysis of fibrillin structure highlighted the presence of a conserved domain which is highly similar to the “motif 1” of lipocalins[61], a large protein family present in prokaryotes, insects, vertebrates, and plants whose members are characterized by the ability to bind small hydrophobic ligands and often work as part of protein complexes[62]. This would be consistent with the predicted biological activity of fibrillins, in particular with the

plastoglobule-based trafficking of small hydrophobic molecules such as carotenoids, plastoquinone and tocopherols[10]. Furthermore, the accumulation of FBN1a in *Arabidopsis* plants treated with ABA has also been reported to stabilize Photosystem II (PSII) and enhance its protection from photoinhibition[63].

1.1.3.2 - Chloroplast metabolic proteins

For at least seven among the proteins of the chloroplast plastoglobule proteome by mass spectrometry analysis[36,39,40] an enzymatic activity was previously known or demonstrated after further characterization.

The **tocopherol cyclase (VTE1)** was previously thought to associate exclusively with the chloroplast inner envelope membrane. However, the specific association with plastoglobules of VTE1 was independently confirmed by electron tomography[22]. In chloroplasts, VTE1 is a key enzyme not only for tocopherol synthesis[64,65] and Redox recycling[66] but it is also responsible for the synthesis of plastochromanol-8 (PC-8), resulting from the cyclization of PQ-9[34,35,67]. Furthermore, the overexpression of VTE1 in transgenic plant lines resulted in the over-accumulation of PC-8, while tocopherol levels were only slightly affected[34,68], thus suggesting that VTE1 activity is a limiting factor for PC-8 rather than Vitamin E synthesis. At the same time, Northern Blot analysis revealed that *VTE1* expression is up-regulated in response to the exposure of plants to high light irradiance, further suggesting a connection of VTE1 activity with the response to oxidative stress in plants[34,69]. The activity and regulation of VTE1 will be discussed further with regard to its multiple roles in prenylquinone metabolism (see Section 1.3.1.2).

The precise sub-organellar localization of VTE1 in chloroplasts became the object of intense investigation. Interestingly, despite the fact that most of the enzymes involved in tocopherol metabolism have previously been localized to the inner envelope membrane[70], several independent screenings by mass spectrometry and immunolabeling strongly indicate that plastoglobules are the major site of VTE1 localization in chloroplasts[22,36,39,40]. Moreover, observations performed at different developmental stages demonstrated that VTE1 localizes to plastoglobules throughout the whole *Arabidopsis* life cycle[36]. At the same time, the

intersection of PC-8 and Vitamin E synthesis in chloroplasts appears to be consistent with a plastoglobule localization of VTE1 activity[34].

Another protein whose involvement in prenylquinone metabolism has been recently investigated is the **NAD(P)H dehydrogenase C1 (NDC1)**, the only member of the type II NAD(P)H quinone oxidoreductase (NDH) gene family that localizes not only to mitochondria but to chloroplasts as well, and more specifically to plastoglobules[71-73]. In chloroplasts, the NDH complex is known to be involved in the cyclic electron flow around Photosystem I (PSI) by oxidizing ferredoxin using the PQ-9 pool as electron acceptor[74], similarly to the PGR5 complex[75]. However, the sub-organellar localization of the family member NDC1 and its ability to oxidize NADH in the presence of purified plastoglobules suggests that the enzyme may rely on the plastoglobule PQ-9 pool rather than that in the thylakoids[76].

At the same time, the *ndc1* mutant is characterized by the lack of phylloquinone (Vitamin K) and plants accumulate its direct precursor 2-phytyl-1,4-naphthoquinone. Furthermore, a moderate reduction in PC-8 content was also detected in mutant plants. Interestingly, the enzyme required for the last methylation step in K biosynthesis (MenG, At1g23360) does not appear to be present. In addition, *MenG* expression levels did not significantly change between wild-type and *ndc1* plants. It has been proposed that MenG activity may be dependent on the Redox state of the PQ-9 plastoglobule pool[76,77]. Most strikingly however, both *ndc1* and *menG* mutant had no visible phenotype. It has been previously demonstrated that in the absence of K, PS I recruits PQ-9 into the A1 site, where it functions as an efficient cofactor in electron transfer from A0 to the iron-sulfur clusters[78,79], while it has been also suggested that the 2-phytyl-1,4-naphthoquinone precursor might functionally replace K in PSI[76].

At the same time, the reduction in PC-8 levels was attributed to the selectivity of VTE1 for the reduced form of PQ-9 (PQH_2) as substrate for PC-8 synthesis[77]. For instance, a significant accumulation of the oxidized form of PQ-9 (PQ) was reported in *ndc1* plants extracted with MeOH[76]. However, the use of a solvent with relatively high polarity such as MeOH was found to be unsuitable for the extraction of apolar prenylquinones such as PQ-9 and PC-8, as well as in maintaining the original PQ/PQH_2 ratio, as previously reported[80].

With regard to the involvement of plastoglobules in carotenoid metabolism, the identification of a **9-*cis*-epoxy-carotenoid dioxygenase (NCED4)** in chloroplast plastoglobules needs to be discussed.

In plants, NCEDs are a subgroup of the carotenoid cleavage dioxygenases (CCD) family, responsible for the first enzymatic step in the formation of apocarotenoids, a class of terpenoid compounds generated by the oxidative cleavage of a carotenoid molecule at one of its double bonds[81-86]. The CCD gene family consists of nine putative members in *A. thaliana*, five of which encode chloroplast-localized proteins that differ in their sub-organellar location[84] and are believed to be involved in the synthesis of apocarotenoids such as the phytohormone ABA. In particular, the significant accumulation of NCED4 in plastoglobules from leaves kept in darkness suggests an active role of the protein in the dark- and probably senescence-induced breakdown of carotenoids[39]. Moreover, NCED4 has been reported to interact with the zinc-finger protein VAR3 (At5g17790). In *A. thaliana*, the *variegated 3* (*var3*) mutant is characterized by somatic areas lacking or containing developmentally-retarded chloroplasts and by a significant reduction in carotenoid levels as well as a minor reduction in chlorophyll content[87].

Interestingly, a significant accumulation of other enzymes involved in carotenoid metabolism was detected during the chloroplast to chromoplast transition in red bell pepper fruits[39]. In particular, the increase in the levels of enzymes required for the synthesis of bicyclic carotenoids (α/β-carotene and xanthophylls) such as the ζ-carotene desaturase (ZDS), the lycopene-β-cyclase (β-Lyc) and two β-carotene-β-hydroxylases (LUT5 or CrtR-β) further suggests an active role of plastoglobules in carotenoid synthesis.

Although its localization in plastoglobules is not exclusive and it is also present in envelope and thylakoid membranes, the identification of the **allene oxide synthase (AOS)** in chloroplast lipid globules is indicative of their possible involvement in plant response to abiotic stress involving jasmonic acid (JA) and it is also consistent with their predicted role during thylakoid membrane disassembly.[40]. During senescence, the thylakoid membrane is dismantled, resulting in the release of mono- and di-galactosyl glycerols, as well as free fatty acids. These can become the substrate of AOS, which is one of the first enzymes acting in the lipoxygenase pathway which leads to the formation of JA and it is responsible for the conversion of 13-hydroperoxylinolenic acid into an unstable epoxide. Considering the presence of high concentrations of potential fatty acid-containing substrates, it is possible that

the localization of AOS activity at plastoglobules might contribute to the massive production of JA during senescence. It is also possible that the free fatty acids released during thylakoid disassembling might become substrate for other putative enzymes identified in the plastoglobule proteome, such as two **diacylglycerol acyltransferases (DGAT-3/4)** and one putative **esterase/lipase/thioesterase**, although these proteins have not been characterized yet.

Most surprisingly, three stromal **fructose-bisphosphate aldolase (FBPA-1 to 3)** were highly abundant in plastoglobule preparations. Considering their high stroma:plastoglobule abundance ratio, it is doubtful whether these proteins should be considered *bona fide* plastoglobule proteins[(40)]. On the other hand, the certified presence of the three aldolases in plastoglobules (even higher than many "PG core" proteins) together with the absence of other abundant chloroplast enzymes involved in glycolysis and in the Calvin cycle strongly suggest that the three FBPAs may have a specific function in association with plastoglobules[(39)].

1.1.4 - The plastoglobule gene coexpression network

A genome-wide gene coexpression network has been recently proposed based on the mRNA expression data available for all the proteins specifically localizing to plastoglobules[(40)]. In particular, most of the "PG core" proteins had strong associations with the expression of other plastoglobule proteins, as well as that of chloroplast proteins not located in plastoglobules. Based on these *in silico* predictions, the existence of four distinct functional modules was highlighted, each of them enriched in specific biological, biochemical and physiological functions. In particular, one module was characterized by genes involved in protein and chlorophyll degradation during senescence, while another one contained proteins affecting plastid biogenesis and several enzymes involved in the Calvin cycle. On the other hand, a third module included Redox regulators, plastid proteases and phosphatases as well as nonlinear electron flow components involved in plant photoacclimation. However, the largest module was predicted to have a central role in plastoglobule metabolism, being characterized by genes required for carotenoid and prenylquinone metabolism, as well as regulators of photosynthetic activity and state transition.
Moreover, each module contained at least one fibrillin and one ABC1-like kinase, suggesting a specific role of each of these proteins in different metabolic and regulatory pathways.

1.2 - ABC1-LIKE KINASES

Among the about thirty proteins identified in plastoglobules by mass spectrometry analysis[36,39,40], only a few belonged to the fibrillin family of structural proteins or were known enzymes with an established biochemical function such as the tocopherol cyclase (VTE1) or the allene oxide synthase (AOS). Conversely, the biological role of most of the proteins predicted to localize to plastoglobules was still largely unknown. However, based on sequence similarities with known proteins, many of these putative enzymes have annotated enzymatic or metabolic functions.

The case of interest for this thesis is represented by the members of the ABC1/ADCK/UbiB family of atypical kinases, which is completely unrelated to the ABC (ATP Binding Cassette) family of transport proteins[88]. The ABC1/ADCK/UbiB family consists of putative kinases identified by sequence alignment methods (Psi-Blast and HMMs) and which have a domain that is similar to the eukaryotic protein kinase (ePK) domain. This includes the most conserved metal binding residues and catalytic motifs. An attempt to further define the ABC1 kinase domain has recently been carried out by multiple sequence alignment of ABC1-like homologs from different plant species as well as by comparison with model kinases belonging to the ePK superfamily[89].
Members of the ABC1 family were found both in bacteria and eukaryotes. These findings suggest that the family evolved in bacteria and entered early eukaryotes by horizontal transfer[90]. Moreover, the phylogenetic analysis of ABC1-like homologs in diverse species of eukaryotes, bacteria and Archaea further highlighted a common evolutionary origin preceding that of the endosymbiotic events leading to the formation of mitochondria and chloroplasts[89].

The ABC1/ADCK/UbiB family includes **ABC1** (YGL119W) from yeast, Y**igR** from *E. coli* and **AarF** from *Providencia stuartii*. The prototypical family member, *S. cerevisiae* **ABC1/Coq8** (**A**ctivity of bc_1 complex/ **CO**enzyme **Q** biosynthesis), is defective in aerobic respiration because of a reduction in the activity of the mitochondrial bc_1 complex which can be overcome by exogenously supplied decylubiquinol[91,92]. Similarly, mutations of the human ABC1 homolog (CABC1 or ADCK3) cause ubiquinone deficiency and defects in the respiratory chain, resulting in a progressive neurological disorder with cerebellar atrophy, developmental delay, and hyperlactatemia[93]. To summarize, the inactivation of the *ABC1*

gene does not abolish the synthesis of cytochromes *b*, c_1, *c* and aa_3 but strongly decreases the *in situ* endogenous reduction of cytochromes c_l and *c*. The loss of NADH and succinate Cyt. *c* oxidoreductase activities seems to be due to the inability to reduce Cyt. *c*, suggesting a deficiency in the activity of the bc_1 segment.

Studies performed on bacteria showed that *YigR*, the *E. coli* homologue of *ABC1*, corresponds to *UbiB*, a gene required for the first monooxygenase step in ubiquinone biosynthesis[(94)]. Both the *P. stuartii aarF* and *E. coli ubiB* (*yigR*) disruption mutant strains lack ubiquinone and accumulate octaprenylphenol, an intermediate in ubiquinone biosynthesis pathway. Moreover, ABC1 has been shown to be able to complement the yeast mutant coq8-1, defective in ubiquinone synthesis[(95)].

However, the data do not suggest an enzymatic function for ABC1 but point to a regulatory role in ubiquinone biosynthesis. Prior experiments identified a pool of octaprenylphenol that remained bound to a protein complex until it was activated in the presence of oxygen to continue the ring modifications required in ubiquinone biosynthesis[(96)]. The rapid conversion of octaprenylphenol to UQ-8 upon transfer from anaerobic to aerobic growth conditions is consistent with a mechanism that may require kinase regulation. In support to this hypothesis, it has been demonstrated in *S. cerevisiae* that Coq3, Coq5, and Coq7 polypeptides are phosphorylated in a ABC1/Coq8-dependent manner and that the expression of the human homolog ADCK3/CABC1 rescued the growth of yeast *coq8* mutants as well as the phosphorylation state of several of the Coq polypeptides, suggesting the existence of multiple enzyme targets of the kinase in the ubiquinone biosynthesis pathway[(97)].

Until recently, ABC1-like kinases have been mainly studied in mitochondria and bacteria, while little evidence was obtained on the role of their chloroplast homologs.

One of these putative kinases, **AtOSA1** (*A. thaliana* Oxidative Stress-related ABC1-like protein) was identified in the inner envelope membrane of *A. thaliana* chloroplasts[(98)]. The analysis of gene expression showed that *AtOSA1* transcription is induced by Cd^{2+} treatment and oxidative stress conditions, and knock-out plants for this gene permanently suffer from oxidative stress. However, AtOSA1 was unable to complement yeast strains lacking the endogenous *ABC1* gene, and this suggests a different function for this chloroplast kinase when compared to mitochondrial ABC1. Similarly, the expression of the maize homolog of AtOSA1 was enhanced in response to Cd^{2+}, while its mRNA levels were lower when plants were grown in darkness and after treatment with ABA and H_2O_2[(99)].

Another kinase belonging to the ABC1 family, the *C. reinhardtii* serine/threonine protein kinase EYE3, has been recently demonstrated to localize to the pigment granule arrays in the eyespot apparatus and to be required for their assembly[100] (see Section 1.1.1.3). Furthermore, a strong correlation in the expression of the *A. thaliana* homolog of EYE3 (ABC1K6, At3g24190) with the zeaxanthin epoxidase (ZEP) has been predicted as well, suggesting a possible involvement in the regulation of the xanthophyll cycle[40].

Interestingly, six out of the eight ABC1-like kinases currently identified in *A. thaliana* chloroplasts were highly enriched in the plastoglobule proteome[36,39,40]. Considering the coincident presence of several enzymes involved in prenylquinone metabolism in plastoglobules, it appears possible that the ABC1-like kinases are involved in the regulation of prenylquinone biosynthesis comparable to ABC1 in bacteria and mitochondria. Moreover, indications of a possible regulatory role of ABC1-like kinases in carotenoid biosynthesis, photoacclimation, plastid biogenesis and senescence come from the previously-reported genome-wide coexpression analysis[40], suggesting the existence of a wide plastoglobule regulatory network affecting multiple metabolic pathways.

In particular, the research project carried out during this PhD thesis was aimed at the functional characterization of three out of the six ABC1-like kinases located in plastoglobules: **ABC1I** (At1g79600), **ABC1k3** (At4g31390) and **ABC1V** (At5g05200).
A change in the nomenclature of ABC1 homologs has been recently proposed[40] but it was not embraced in this report to avoid inconsistencies with the experimental material produced during the PhD project and presented in this thesis. For reference, the alternative names for the three kinases are reported in Table 2.1 on page 53.

Relatively to **ABC1k3**, it has been recently demonstrated that this kinase is required to maintain the number of chlorophyll-binding proteins in the photosynthetic complexes and that knock-down plants accumulate chlorophyll degradation products, have a lower anthocyanin content and are more sensitive to photooxidative stress under high light conditions[101]. Moreover, it is here demonstrated that ABC1k3 corresponds to the photosynthetic mutant *pgr6* (*proton gradient regulation 6*), previously identified in a screening of *Arabidopsis* mutants showing a reduced quenching of chlorophyll fluorescence[102] and which will be described in details in the following sections (see Section 1.3.2.1).

1.3 - ROLE OF ABC1 HOMOLOGS IN CHLOROPLAST METABOLISM

1.3.1 - Lipid metabolism

Although plastoglobules were initially considered passive lipid storage sites, increasing evidence demonstrated that they play a fundamental role not only in chloroplast development, being directly involved in thylakoid membrane formation as well as in its disassembly during senescence, but also in the transition to chromoplast and the accumulation of carotenoid pigments. Most strikingly however, the identification in the plastoglobule proteome of several enzymes belonging to prenylquinone and carotenoid biosynthetic pathways demonstrated that plastoglobules play an active role not only in the accumulation but also in the synthesis of these molecules. Considering their strategic position at the intersection of different pathways in plastid lipid metabolism, it is then conceivable that plastoglobule activity is highly regulated, suggesting the existence of a dynamic regulatory network. Although, on the one hand, the key enzymes involved in carotenoid and prenylquinone biosynthesis are known for the best part, the regulation of these pathways is still poorly understood. On the other hand, the identification of six ABC1-like kinases in chloroplast lipid globules makes them suitable candidates for such regulators.

In order to highlight possible key regulatory nodes shared between biochemical pathways apparently different but being part of a common metabolic network, an understanding of the biosynthesis of both carotenoids and prenylquinones is required. At the same time, a particular reference will be given in the following sections to the intersection of plastoquinone and tocopherol synthetic pathways in plastoglobules, which both represent a potential target of the activity of the chloroplast ABC1-like kinases, comparable to ubiquinone synthesis regulation by ABC1 in bacteria and mitochondria.

1.3.1.1 - Carotenoids

Carotenoids are an assorted class of pigments naturally found in bacteria, fungi, algae and plants, in which they play various roles in development, photosynthesis as well as the synthesis of phytohormones such as strigolactones and abscisic acid. On the contrary, animals are unable to synthesize carotenoids but they can absorb them through their diet. The beneficial effects of carotenoids on human and animal health have been extensively reviewed, with particular reference to their antioxidant activity, their valuable effect on the immune system and their role as precursors of retinol (Vitamin A).[103-105].

Carotenoid biosynthesis is a highly regulated process throughout the life cycle of the plant and it is characterized by dynamic changes to match plant developmental requirements during germination, photomorphogenesis, photosynthesis, fruit development as well as in response to external environmental stimuli. A general model of the carotenoid biosynthetic pathway is reported in Figure 1.3.

Like all isoprenoids, carotenoids are assembled from the condensation of monomers of the isopentenyl diphosphate (IPP) and of its double-bond isomer dimethylallyl diphosphate (DMAPP). Although two independent pathways exist in plant cells for the synthesis of these prenyl diphosphate precursors, one in cytoplasm via mevalonate and one in plastids, carotenoids are mainly derived from the 2-C-methyl-D-erythritol 4-phosphate/1-deoxy-D-xylulose 5-phosphate (MEP/DOXP) pathway of terpenoid biosynthesis. This pathway is entirely localized in plastids and leads to the formation of geranylgeranyl diphosphate (GGPP)[106-108]. Defects in isoprenoid biosynthesis or changes in other metabolic pathways using GGPP as substrate can significantly affect carotenoid synthesis as well. Furthermore, the availability of isoprenoid precursors can be significantly influenced by abiotic factors such as light and oscillations of the circardian rhythm as well as biotic factors such as the colonization of plant roots by arbuscular mycorrhizal fungi[109].

Figure 1.3: Model of carotenoids, xanthophylls and abscissic acid biosynthetic pathways and their regulation in *Arabidopsis*. The modifications introduced in each enzymatic step are indicated with grey triangles.

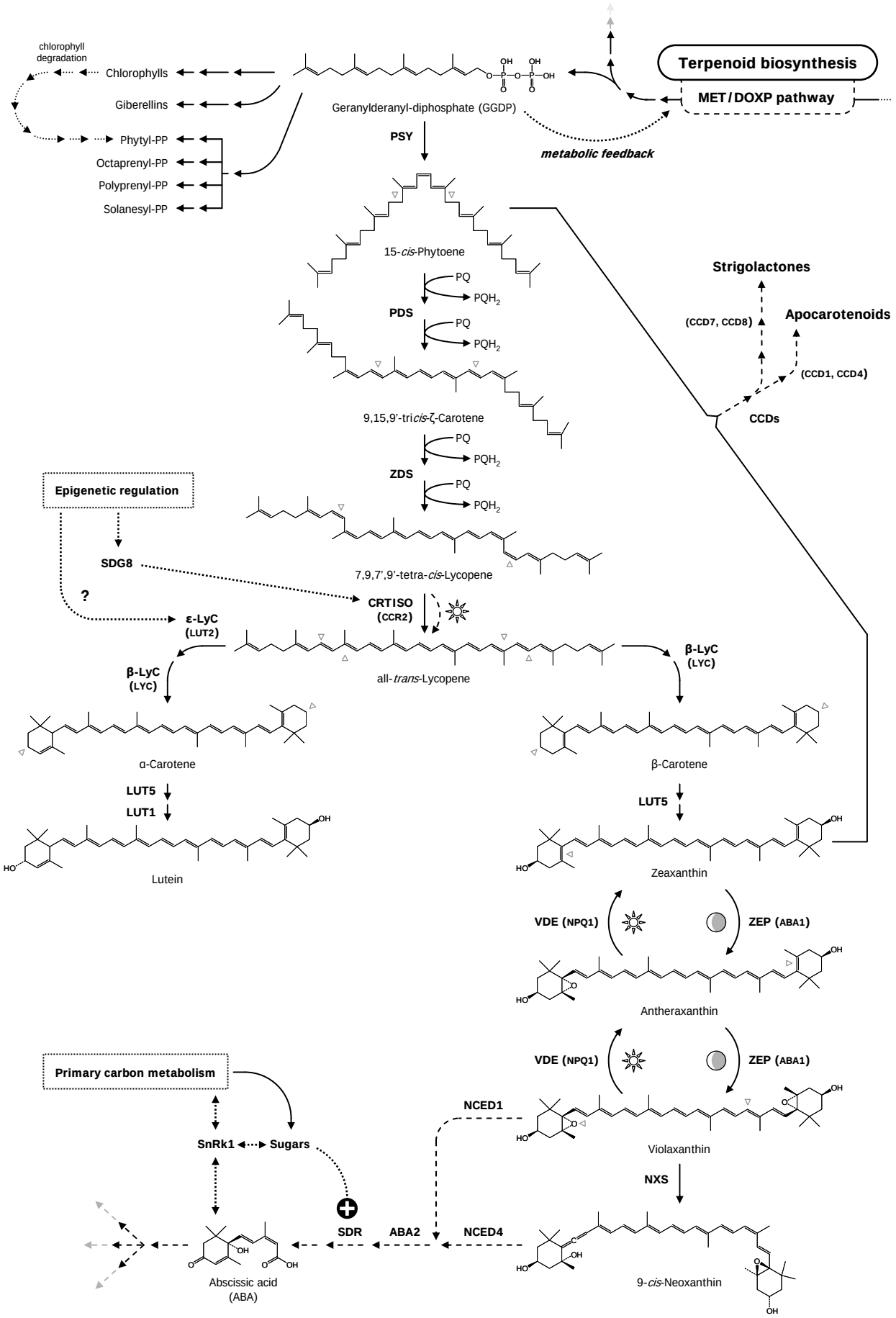
chlorophyll degradation
Chlorophylls
Giberellins
Phytyl-PP
Octaprenyl-PP
Polyprenyl-PP
Solanesyl-PP
Geranylderanyl-diphosphate (GGDP)
Terpenoid biosynthesis
MET / DOXP pathway
metabolic feedback
PSY
15-cis-Phytoene
PQ
PQH2
PDS
9,15,9'-tri-cis-ζ-Carotene
ZDS
7,9,7',9'-tetra-cis-Lycopene
Strigolactones
(CCD7, CCD8)
Apocarotenoids
(CCD1, CCD4)
CCDs
Epigenetic regulation
SDG8
?
CRTISO (CCR2)
ε-LyC (LUT2)
β-LyC (LYC)
all-trans-Lycopene
α-Carotene
β-Carotene
LUT5
LUT1
Lutein
Zeaxanthin
VDE (NPQ1)
ZEP (ABA1)
Antheraxanthin
Violaxanthin
NXS
9-cis-Neoxanthin
Primary carbon metabolism
SnRk1
Sugars
NCED1
SDR
ABA2
NCED4
Abscissic acid (ABA)

Figure 1.3

The condensation of two GGPP molecules by the phytoene synthase (PSY) results in the synthesis of **phytoene**, the precursor molecule for all the other carotenoids. PSY regulation is probably the most relevant rate-limiting step in carotenoid biosynthesis. In particular, *PSY* expression is enhanced by salinity, drought and high ABA levels[110,111]. Despite this, it has been demonstrated that stress-induced variations in *PSY* transcript abundance do not always result in changes in carotenoid flux[112], and that *PSY* mRNA levels are also upregulated during photomorphogenesis by both red and far-red light treatments via a phytochrome-mediated pathway[113]. Interestingly, the transcription of the maize homolog *ZmPSY2* can be induced by blue photoreceptors (phototrophins and cryptochromes) activity as well[110]. Moreover, a *cis*-acting motif (ATCTA) identified in the *PSY* promoter region is also present in other photosynthesis-related genes and it is believed to be important in mediating their transcriptional regulation[114].

The conversion of phytoene to **lycopene** consists of a two-step desaturation requiring the sequential activity of the phytoene desaturase (PDS) and the ζ-carotene desaturase (ZDS), followed by an isomerization mediated by the carotenoid isomerase (CRTISO), which catalyses cis-trans reactions conversion of the four cis-bonds introduced by the desaturases[115-118]. Moreover, the characterization of *CRTISO* mutants such as *ccr2* demonstrated that the biosynthetic pathway can proceed anyway via a spontaneous photoisomerization, although at lower efficiency, resulting in a delayed plant greening during plant de-etiolation as well as a significant reduction in lutein content[115].

Indications of a possible PDS regulation via a phytochrome-mediated pathway come from the transcriptional analysis of genes involved in carotenoid, chlorophyll and isoprenoid biosynthesis during photomorphogenesis[113,119].

At the same time, both of the desaturases require PQ-9 as electron acceptor[120-122], further suggesting a functional relationship between carotenoid synthesis and prenylquinone metabolism in chloroplasts[123]. A defect in the activity of the plastid terminal oxidase (PTOX), required for the oxidation of the PQ-9 pool, has been demonstrated to severely impair both PDS and ZDS activity[123] and to be responsible for the *immutans* (*im*) variegation mutant in *Arabidopsis*[124]. In particular, *im* leaves are characterized not only by the presence of white sectors in which carotenoid synthesis is impaired and that accumulate the non-colored phytoene, but also by severe defects in chloroplast development, suggesting that the Redox state of the PQ-9 pool may also affect other pathways than carotenoid biogenesis[125].

Regarding a possible epigenetic regulation of lycopene synthesis, the chromatin-modifying histone methyltransferase SDG8 (Set Domain Group 8) was demonstrated to be required for CRTISO expression, mutations leading to alterations in the methylation of the chromatin associated with the *CRTISO* gene and resulting in a reduction in its expression[126].

The branch point in carotenoid synthesis after lycopene, leading either to **α-** or **β-carotene**, represents a key step in the modulation of the ratio between α- and β-xanthophylls, the oxygenated derivatives of carotenes, and specifically between **lutein**, the most abundant xanthophyll, and the members of the xanthophyll cycle (**zeaxanthin**, **antheraxanthin** and **violaxanthin**).

Theoretically and considering that the β-lycopene cyclase (β-Lyc) is shared by both biosynthetic branches, the activity of the ε-lycopene cyclase (ε-Lyc) would appear to be critical for the synthesis of α-carotene and lutein. However, it was observed that the downregulation of ε-Lyc lead to an increase in total carotene levels, both β-carotene and its derivates and, most surprisingly, lutein[127]. Conversely, in plants lacking β-Lyc, β-carotene and its derivates are absent and mutants accumulate a number of unusual carotenes produced by ε-Lyc including δ-carotene, ε-carotene and lactucaxanthin (ε,ε-carotene-3,3'-diol)[128].

Lutein content appears to be affected in mutants defective for the previous isomerization step catalyzed by CRTISO[115], suggesting either a metabolite feedback regulation or a differential affinity of the two cyclases for the lycopene substrate[129,130]. At the same time, it has recently been demonstrated that *ε-LYC* transcript levels are affected in both the *crtiso* and *sdg8* mutants previously discussed, indicating a possible epigenetic regulation of ε-Lyc as well.

Lutein is the most abundant xanthophyll in the photosynthetic apparatus of higher plants and the only ligand for the L1 site of all Lhc proteins, where its presence is required to successfully quench chlorophyll triplets[131]. Similarly, β-carotene is bound to the Lhc complex of PSI[132], while the conversion between zeaxanthin, antheraxanthin and violaxanthin under different light conditions constitute the xanthophyll cycle.

Considering its critical role in the generation of non photochemical quenching (NPQ) and in plant photoprotective response to excess light, xanthophyll cycle will be treated in detail in the following sections (see Section 1.3.2.1). Regarding the effect of light intensity on the modulation of the two enzymes involved in this cycle, it has been demonstrated that under low or limiting light zeaxanthin epoxidase (ZEP) converts zeaxanthin to violaxanthin via the

intermediate antheraxanthin, while under excessive light and after the acidification of the thylakoid lumen reaches a critical threshold, violaxanthin deepoxidase (VDE) is activated and converts violaxanthin back to antheraxanthin and then zeaxanthin[133-137]. Moreover, it has also been demonstrated that the expression of *ZEP* and *VDE* is induced and repressed by high light, respectively[138], and that VDE activity is modulated by pH[139]

In addition to carotenoid role as antioxidants and in plant photoprotection, an essential biological function has also been demonstrated for their oxidative cleavage products, **apocarotenoids**. In animals, retinol is derived from the enzymatic cleavage of pro-vitamin A, while in plants a large spectrum of molecules is obtained from the carotenoid pool. Examples are plant hormones such as ABA[140], strigolactones[141] and mycorradicin, an apocarotenoid synthesized by plant roots during symbiosis with arbuscular mycorrhyza[142]. Moreover, other carotenoid derivates accumulating in fruits and flowers are involved in the formation of colour (α-crocin, the main pigment of the spice saffron)[83] and aroma (α/β-ionone, two major component of the aroma of roses and largely used in perfumery)[143].

While the oxidative cleavage of a carotenoid molecule at one of its double bonds can occur nonenzymatically in plants, the predominant mechanism requires the activity of the carotenoid cleavage dioxygenases (CCD) family[81-86]. The *A. thaliana* genome contains nine members of the CCD family, among which the four enzymes CCD1, -4, -7, and -8 as well as five members of the 9-*cis*-epoxy-carotenoid dioxygenase subfamily (NCED2, 3, 5, 6, and 9).

NCEDs are a group of enzymes that show a specificity for 9-cis-epoxycarotenoids as substrates. In particular, the family members NCED1 and NCED4 cleave the 11,12 and 11',12' double bonds of the 9-*cis* isomers of violaxanthin and neoxanthin, respectively, and both lead to the synthesis of xanthoxin, the precursor of ABA. Interestingly, the identification of NCED4 in plastoglobules and its accumulation during the dark-induced breakdown of carotenoids[36,39,40] strongly suggests an involvement of plastid lipid globules in carotenoid turnover and apocarotenoid synthesis, as previously discussed (see Section 1.1.3.2).

The remaining members of the CDD family have low sequence homologies to the NCEDs and are also characterized by a different substrate specificity and enzymatic activity. In particular, CCD7 and -8 are expressed predominantly in the root, where they act in concert leading to the synthesis of strigolactones[85,86], a group of compounds originally identified in root exudates for their ability to trigger the seed germination of parasitic weeds of the genera *Striga* and *Orobanche*[144]. Furthermore, strigolactones act as hyphal branching factors, which

stimulate root colonization by symbiotic arbuscular mycorrhizal fungi[145,146]. Among the other functions of CCDs, CCD4 activity has been reported to be responsible for the white color in flower petals because of its role in the degradation of colored carotenoid pigments[147], while CCD1 has previously been shown to have activity on multiple carotenoid substrates and possibly be involved in the production of β-ionones as well as substrates for the other members of the CCD family[82].

1.3.1.2 - Prenylquinones

Prenylquinones make up a class of lipophilic molecules, which includes essential electron carriers in bacterial respiration, mitochondria and chloroplasts (ubiquinone, plastoquinone, phylloquinone) and compounds with physiological antioxidant activity (tocopherols, tocotrienols, plastochromanol), some of which (tocopherol/Vitamin E and phylloquinone/Vitamin K) are required as Vitamins in human nutrition[148,149].

A general model of the prenylquinone biosynthetic pathway is reported in Figure 1.4. Prenylquinones derive in part from the Shikimate pathway via p-hydroxy-phenylpyruvate (plastoquinone, plastochromanol and tocopherols) or chorismate (phylloquinone, ubiquinone and menaquinones), and from isoprenoid metabolism via derivates of GGDP, which are shared with carotenoid biosynthesis and other metabolic pathways. At the same time, despite prenylquinones having quite diverse chemical structures, their synthesis is characterized by a common set of enzymatic reactions, which in some cases are performed by the same enzyme on different substrates. For these reasons, the reactions required for the synthesis of each prenylquinone will not be analyzed in detail in this section, which will focus instead on the biological role of these molecules and the modulation of their metabolism.

Figure 1.4: Biosynthetic pathways of tocopherol, plastoquinol, plastochromanol, ubiquinone, and phylloquinone in *Arabidopsis*. The modifications introduced in each enzymatic step are indicated with grey triangles.

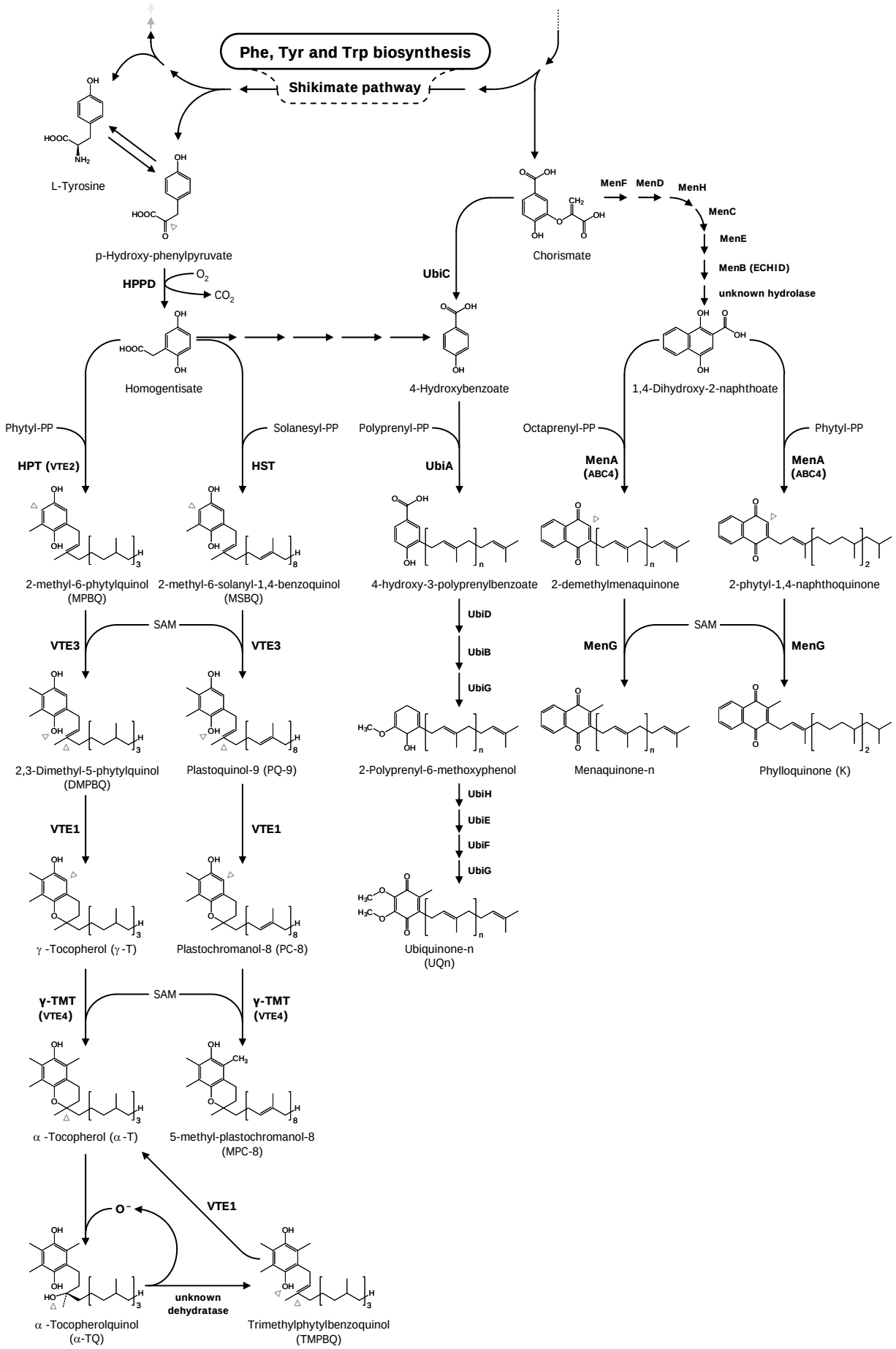
Phe, Tyr and Trp biosynthesis
Shikimate pathway
L-Tyrosine
p-Hydroxy-phenylpyruvate
HPPD
Homogentisate
Chorismate
MenF
MenD
MenH
MenC
MenE
MenB (ECH1D)
unknown hydrolase
UbiC
4-Hydroxybenzoate
1,4-Dihydroxy-2-naphthoate
Phytyl-PP
Solanesyl-PP
Polyprenyl-PP
Octaprenyl-PP
Phytyl-PP
HPT (VTE2)
HST
UbiA
MenA (ABC4)
MenA (ABC4)
2-methyl-6-phytylquinol (MPBQ)
2-methyl-6-solanyl-1,4-benzoquinol (MSBQ)
4-hydroxy-3-polyprenylbenzoate
2-demethylmenaquinone
2-phytyl-1,4-naphthoquinone
SAM
VTE3
VTE3
UbiD
UbiB
UbiG
MenG
SAM
MenG
2,3-Dimethyl-5-phytylquinol (DMPBQ)
Plastoquinol-9 (PQ-9)
2-Polyprenyl-6-methoxyphenol
Menaquinone-n
Phylloquinone (K)
VTE1
VTE1
UbiH
UbiE
UbiF
UbiG
γ -Tocopherol (γ-T)
Plastochromanol-8 (PC-8)
Ubiquinone-n (UQn)
SAM
γ-TMT (VTE4)
γ-TMT (VTE4)
α -Tocopherol (α-T)
5-methyl-plastochromanol-8 (MPC-8)
VTE1
O⁻
unknown dehydratase
α -Tocopherolquinol (α-TQ)
Trimethylphytylbenzoquinol (TMPBQ)

Figure 1.4

Tocochromanols (Vitamin E) are a group of amphipathic, lipid-soluble organic molecules further distinguished in tocopherols and tocotrienols according to their isoprenyl side chain (derived from phytyl-PP or GGDP, respectively). With regard to **tocopherol** biosynthesis, the 2-methyl-6-phytylbenzoquinol (MPBQ) derived from condensation between homogentisate and phytyl-PP can be methylated on the C-3 position on the aromatic ring by the methyl transferase VTE3 to give 2,3-dimethyl-6-phytyl-1,4-benzoquinone (DMPBQ). The cyclization of either MPBQ or DMPBQ by the tocopherol cyclase VTE1 leads to the formation of δ- and γ-tocopherol (δ- and γ-T), respectively. The further methylation at the C-5 position of these two molecules, mediated by the γ-tocopherol methyltransferase VTE4, finally generates β- and α-tocopherol (β- and α-T), respectively.

In *A. thaliana*, α-T is the predominant form of tocopherol in photosynthetic tissues, while seeds accumulate mainly γ-T, although relative tocopherol composition can significantly vary from plant species to species[(150)]. VTE4 overexpression in seeds of transgenic *A. thaliana* and soybean plants resulted in a dramatic increase in α-T levels, which rose up to about 95% of the total tocopherol content, demonstrating that the low VTE4 expression level in wild-type plants represents the rate-limiting step in α-T storage in seeds[(151,152)]. However, the tocopherol synthetic rate in both leaves and seeds appears to be determined by the availability of the precursor MPBQ. In particular, a significant α-T accumulation was observed in plants overexpressing of the homogentisate-phytyl transferase HPT/VTE2, which in turn strongly indicates that the following enzymatic steps are not the limiting factor in α-T biosynthesis[(153)]. On the other hand, changes in the expression of the methyl transferase VTE3 severely influence the relative content of γ/α- and δ/β-T in plant tissues[(152)], while the overexpression of the tocopherol cyclase VTE1 did not result in a significant accumulation of γ- and α-T but of another product of the enzyme (PC-8, see forward), suggesting that VTE1 is the rate-limiting step for the synthesis of this PQ-9 derivate rather than tocopherols[(34)].

Regarding their distribution inside chloroplasts, almost all the enzymes responsible for tocopherol biosynthesis were localized to the inner envelope membrane[(105,149)] with VTE1 being the lone exception localizing to plastoglobules[(22,36,39,40)], as previously discussed (see Section 1.1.3.2).

The biological role of tocopherols as powerful lipophilic antioxidants has been extensively investigated during the past years both in animals and plants, in which they protect polyunsaturated fatty acids from lipid peroxidation[(154-157)].

Tocopherols (and more generally tocochromanols) directly interact with reactive oxygen- and nitrogen species (ROS and RNS, respectively) as well as lipid radicals and peroxides, resulting in the formation of a lipid hydroperoxide and a tocochromanol radical, more stable thus less reactive because of the delocalization of the unpaired electron on the chromanol ring. This radical can be reduced back to the corresponding tocochromanol by the reaction with other water- or lipid-soluble antioxidants (ascorbate, PQ-9, PC-8, UQ-9, etc.), or it can be further oxidized, resulting in the opening of the chromanol ring and the formation of the corresponding tocochromanol-quinone[158]. In *A. thaliana*, a significant accumulation of α-tocopherol quinone (α-TQ) was observed in wild-type plants exposed to high light (HL) conditions, while the predominant molecule was γ-tocopherol quinone (γ-TQ) in *vte4* mutants[158,159,160]. The reduction in the levels of these molecules after plant acclimation to HL or under low light conditions suggests the presence of a recycling mechanism[66]. Briefly, the incubation of [^{14}C] α-TQ with chloroplasts purified from wild-type plants resulted in the accumulation of α-T, while the reaction stopped at the level of the intermediate trimethylphytylbenzoquinol (TMPBQ) in *vte1* mutants, indicating that the tocopherol cyclase VTE1 is required for the formation of the chromanol ring during α-TQ recycling. At the same time, experiments using [^{14}C] γ-TQ in the *vte4* mutant were characterized by a significantly slower conversion to γ-T (about 4-fold more time required), suggesting a selectivity for the substrate either of VTE1 or of the unknown dehydratase responsible of the conversion of α- and γ-TQ to TMPBQ and DMPBQ, respectively.

The effect of Vitamin E in plant photoprotection under excess light conditions has been widely investigated in relation to the role of tocopherols both in protecting membrane lipids from photooxidation and for their potential ability in scavenging the singlet oxygen radicals produced by the PSII[161,162]. In *vte2* plants, the lack of tocopherols lead to PSII photoinhibition accompanied by the accumulation of fatty acid oxidation products[163,164]. Moreover, *vte2* mutants showed several abnormalities during germination such as the inhibition of root growth, cotyledon bleaching and morphological defects as well as the significant accumulation of lipid peroxides and hydroperoxide[165]. On the other hand, *vte1* mutants lacking α/β/γ/δ-T but accumulating the precursor DMPBQ instead did not display a visible phenotype and showed little sensitivity to light stress, except when it was associated with low temperatures[163,164]. However, *VTE1* expression is up-regulated in response to HL, resulting in a significant α-T accumulation, as previously discussed[34,35,69,166,]. A possible explanation that has been proposed relies on the potential antioxidant activity of DMPBQ[149].

At the same time, it has been demonstrated that *vte1* plants compensate for the lack of tocopherols with an increase in carotenoid biosynthesis and that they accumulate the xanthophyll zeaxanthin[163].

Similarly, it has been demonstrated in *C. reinhardtii* that the overexpression of VTE2 in the *npq1 lor1* double mutant, lacking both lutein and zeaxanthin, was sufficient to compensate for carotenoid deficiency in chloroplast protection against photooxidative stress, indicating an overlapping functions of carotenoids and tocopherols in PSII photoprotection and further suggesting that carotenoid and prenylquinone metabolic pathways closely functionally interact[167].

Another important molecule derived from homogentisate is **plastoquinone-9 (PQ-9)**, characterized by the incorporation of solanesyl-PP instead of phytyl-PP as isoprenyl side chain. In addition to the role PQ-9 as an electron carrier between PSII and Cyt. *b6f* in the chloroplast electron transport chain, it has been demonstrated that the reduced form of PQ-9 (PQH_2) has an *in vitro* antioxidant activity similar to or even superior to that of tocopherols[168,169] and that it is also active *in vivo* both by protecting membrane lipids from peroxidation and because of its role as a superoxide and singlet oxygen scavenger in PSII[170-172]. Moreover, the PQ-9 pool is used as electron acceptor in several chloroplast metabolic pathways such as the cyclic electron flow from PSI via PGR5[75] and NDC1[74] as well as during phytoene desaturation by PDS and ZDS[123], as previously discussed. At the same time, the changes in the Redox state of the PQ-9 pool are largely responsible for the activation of the state transition under excess light conditions[173] and have also been associated with retrograde signaling to the nucleus and the regulation of genes involved in antioxidant biosynthesis[174,175].

Furthermore, plants lacking PQ-9 are severely affected in the light cycle of photosynthesis and in chloroplast development. Considering the importance of this prenylquinone for the correct assembly of PSII and the role of this complex in the stabilization of thylakoid grana, mutants lacking PQ-9 are defective in thylakoid assembly and show an albino or pale-green phenotype[176].

Considering the structural similarities between PQ-9 and DMPBQ, it has been recently demonstrated that the tocopherol cyclase VTE1 can recognize either of the two prenylquinones as a substrate, leading to the alternative synthesis of γ-T and of the

chromanol-derivate of PQ-9, **plastochromanol-8 (PC-8)**[35]. Furthermore, the overexpression of VTE1 in *A. thaliana* transgenic plants resulted in a 7-fold increase in PC-8 levels while tocopherol content was only slightly affected, indicating that VTE1 activity is the rate-limiting step for the synthesis of PC-8 rather than that of γ- and δ-T. Therefore, PC-8 should not simply be considered a side-product of VTE1 activity, as previously discussed[34].
The molecular structure of PC-8 is similar to γ-T but for the longer side chain, thus suggesting a possible antioxidant activity[149]. In fact, both the chromanol ring and the polyunsaturated side chain have been demonstrated to be active in preventing lipid peroxidation and as singlet oxygen scavengers, resulting in the formation of the oxidative-derivate hydroxy-plastochromanol (PC-OH)[177,178]. Moreover, the significant accumulation of both PC-8 and PC-OH in senescing leaves and independently from light intensity further suggests that both molecules are efficient antioxidants *in vivo*, similarly to PQ-9 and tocopherols[35,179].

1.3.2 - Photosynthesis and primary metabolism

Historically, the research on plastoglobules focused on the presence of pigments and lipophilic molecules active both as electron carriers in photosynthetic reactions and involved in the protection of chloroplast membranes from oxidative stress. The identification of structural proteins associated with chloroplast lipid droplets and the characterization of the corresponding mutants supported the hypothesis of a potential role of plastoglobules not only as storage for carotenoids and prenylquinones but in their active trafficking between envelope sources and thylakoid sinks during chloroplast morphogenesis, senescence and in response to changes in photosynthetic conditions. A further development was represented by the identification of enzymes required for the synthesis of those molecules, which demonstrated that plastoglobules have an active metabolic role at the intersection of different biosynthetic pathways.
For these reasons, the identification of six homologs of the mitochondrial kinase ABC1 strongly suggests the existence of a plastoglobule regulatory network which not only immediately affects carotenoid and prenylquinone biosynthesis but also the chloroplast metabolic and photosynthesis machineries on longer periods of time.

Considering the evidence emerging as result of the research described in this thesis, a connection between the regulation of chloroplast lipid metabolism and the modulation of photosynthesis has been established for at least one of the ABC1-like kinases under study. Therefore, in order to elucidate some of the aspects treated in the discussion, a short overview of some of the regulatory mechanisms of photosynthesis will be given in the following sections.

1.3.2.1 - Photosynthetic efficiency and the *pgr* phenotypes

The dissipation of excess light energy is a fundamental process to avoid photoxidative damage in algae and higher plants. Among the mechanisms these organisms evolved to protect themselves in environments in which light absorption exceeds the capacity for its utilization, Non Photochemical Quenching (NPQ) of chlorophyll fluorescence is the most relevant for the thermal dissipation of excess energy. NPQ can be further divided into three distinct components (qE, qT and qI), of which the ΔpH- or Energy-dependent component (qE) is the major and most rapid in most algae and plants[180,181]. Upon exposure to excess light conditions, the acidification of the thylakoid lumen induces qE via protonation of PSII and activation of the xanthophyll cycle[182,183], resulting in a conformational change of PSII antenna that puts PSII in a quenched state[184].

The screening of *Arabidopsis* mutants with low qE levels allowed to identify several mutants that were defective in photosynthetic electron transport and in the generation of the ΔpH across thylakoid membranes[102]. Although the molecular mechanisms affected in these mutants are different, they all lead to a reduced quenching of chlorophyll fluorescence and, for some of them, to a reduction in electron transport rate (ETR) as well.

Among these, the ***pgr1*** (*proton gradient regulation 1*) mutant is characterized by a specific mutation in the nuclear-encoded Rieske Fe-S subunit (*petC*) of the Cyt. b_6f complex[185,186]. Briefly, the point mutation does neither significantly affect the maximum quantum efficiency of PSII and PSI nor the electron flow between the two photosystems under low light conditions, but strongly reduces the simultaneous proton transfer from the stroma to the thylakoid lumen. As a consequence, *pgr1* plants are severely impaired in NPQ

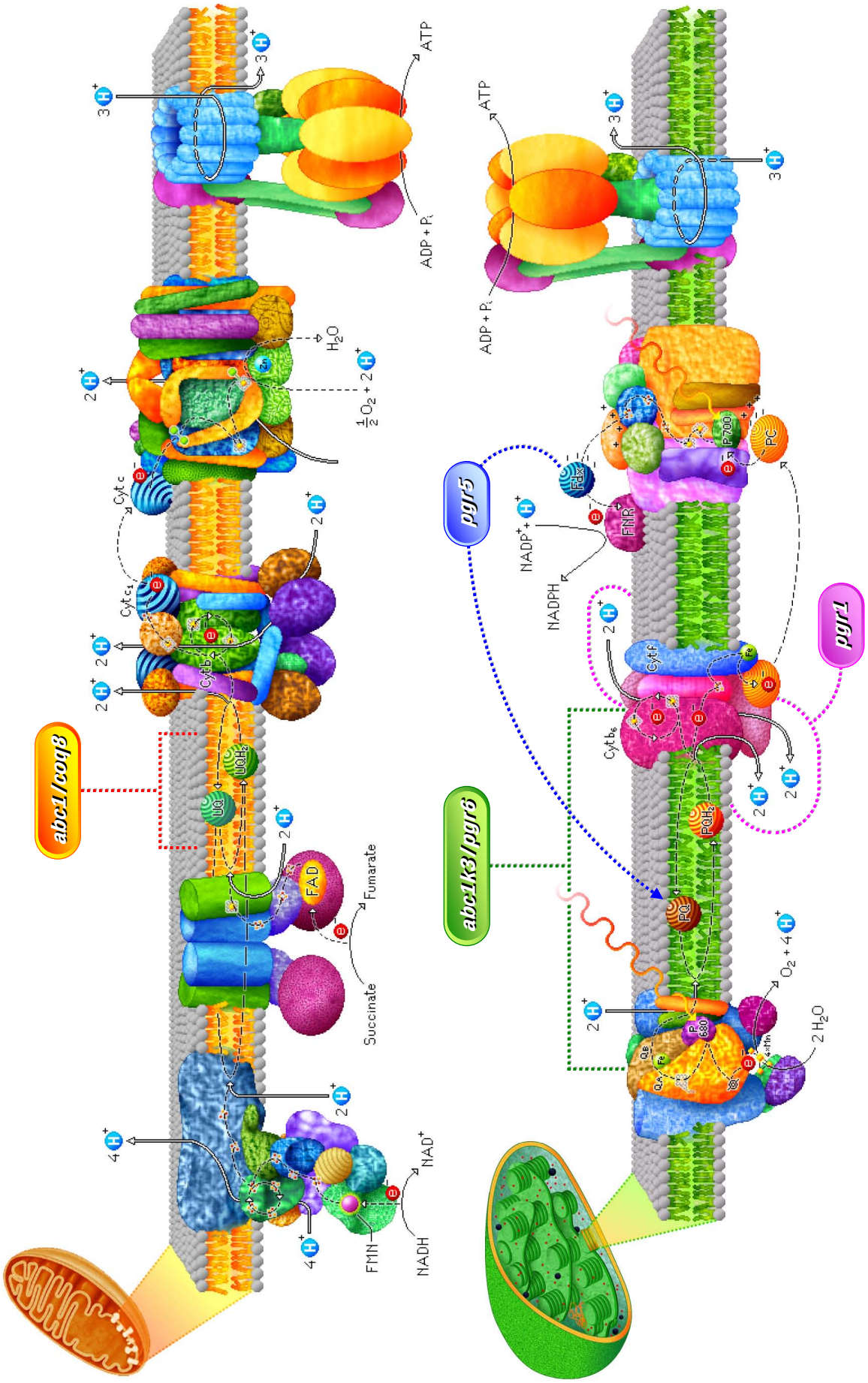

Figure 1.5: Comparison of the electron transport chains in mitochondria and chloroplasts.

formation because of the impossibility to activate the xanthophyll cycle via the acidification of the lumen. Conversely, the exposure of mutant plants to light intensities higher than 150 $\mu E \cdot m^{-2} \cdot s^{-1}$ also resulted in the saturation of the ETR levels and the photoinhibition of PSII.

On the contrary, ***pgr5*** mutant plants are defective for a thylakoid protein involved in the cyclic electron flow around PSI from reduced ferredoxin to PQ-9 with a mechanism that is independent from the chloroplast NAD(P)H dehydrogenase (NDH) complex[(75)]. This leads to the over-reduction of PSI and most surprisingly to its photoinhibition under HL conditions, while in wild-type plants this phenomenon takes place only under limited conditions such as low temperature and light intensity which lead to the sequestration of electrons by the acceptor side of PSI and the formation of hydroxyl radicals[(187)]. Moreover, PGR5 activity appears to be required for the activation of NPQ, possibly by affecting the formation of the ΔpH gradient across thylakoids.

The ***pgr6*** mutant represents yet another case. Despite showing a reduction in non-photochemical quenching (NPQ) similarly to *pgr1*, in *pgr6* plants NPQ induction is still observed but it depends on light intensity and its overall level is lower than in the wild-type. Besides, only a mild reduction in the electron transport rate (ETR) is observed in this mutant under normal light intensities[(188)].

Considering its effect on NPQ activation, PGR6 was initially hypothesized to encode for a novel Cyt. b_6f subunit or to be directly involved in its assembling and/or regulation, similarly to PGR1. However, the *pgr6* locus was initially cloned by chromosome mapping at about 800 kb near the molecular marker prha (pos. 14650528) on chromosome 4, in the region between loci T10C21 (pos. 14977814) and F11C18 (pos. 15375547). Interestingly, no proteins with such a predicted function were encoded by the genes located in this region. After further characterization, it was demonstrated that the *pgr6* (CE11-8-1) allele corresponds to a single point mutation in the gene region encoding for the plastoglobule ABC1-like kinase **ABC1k3** (At4g31390, pos. 15233126-15236764), as described in this thesis in the following chapters.

1.3.2.2 - Sugar and starch metabolism

Starch and sucrose are the two main products of photosynthesis in chloroplasts and cytosol, respectively. In many species, starch represents the major storage metabolite that accumulates during the day, while its degradation supplies plant metabolism at night. In contrast, sucrose is the main sugar produced in leaves and exported to sinks in the plant. At the same time, sucrose levels represent a major modulator of gene expression[(189-192)] and, sucrose synthesis being the principal sink of the triose phosphates produced by the Calvin cycle in chloroplasts, changes in sucrose metabolism also have a feedback effect on photosynthesis[(193)]. A general model of the regulation of photosynthetic carbon metabolism is reported in Figure 1.6.

Figure 1.6: Simplified model of the photosynthetic carbon metabolism in *A. thaliana*. [modified from Lunn *et al.* (2003)[(210)] and Nielsen *et al.* (2004)[(196)]].

Used abbreviations for sugars:

2-phosphoglycerate (2-PGA), 3-phosphoglycerate (3-PGA), 1,3-bisphosphoglycerate (1,3-bPGA), glyceraldehyde-3-phosphate (G-3-P), dihydroxyacetone phosphate (DHAP), erythrose-4-phosphate (E-4-P), sedoheptulose-7-phosphate (Sd-7-P), sedoheptulose-1,7-bisphosphate (Sd-1,7-bP), xylulose-5-phosphate (Xy-5-P), ribose-5-phosphate (R-5-P), ribulose-5-phosphate (Ru-5-P), ribulose-1,5-bisphosphate (Ru-1,5-bP), fructose-6-phosphate (Fru-6-P), fructose-1,6-bisphosphate (Fru-1,6-bP), fructose-2,6-bisphosphate (Fru-2,6-bP), glucose-1-phosphate (Glc-1-P), glucose-6-phosphate (Glc-6-P), sucrose-6-phosphate (Suc-6-P), phosphoenolpyruvate (PEP).

List of the enzymes involved in the reductive pentose phosphate (Calvin-Benson) cycle, in starch synthesis and in sucrose biosynthetic pathway:

1) Ribulose-1,5-bisphosphate carboxylase/oxygenase (RuBisCO). 2) 3-phosphoglycerate kinase. 3) Glyceraldehyde-3-phosphate dehydrogenase. 4) Triose-phosphate isomerase. 5) Fructose-bisphosphate aldolase (FBPA). 6) Fructose-bisphosphate phosphatase (FBPase). 7) Transketolase. 8) Sedoheptulose-bisphosphate aldolase. 9) Sedoheptulose-bisphosphate phosphatase. 10) Ribose-phosphate isomerase. 11) Ribulose-phosphate epimerase. 12) Phosphoribulokinase. Phosphoglucose isomerase (PGI). Phosphoglucomutase (PGM). ADP-glucose pyrophosphorylase (AGPase). Starch synthase (SS). Branching enzyme (BE). Debranching enzyme (DBE). Pyrophosphate-dependent phosphofructokinase (PFP). Fructose-2,6-bisphosphatase (F2KP). Sucrose phosphate synthase (SPS). UDP-glucose pyrophosphorylase (UGPase).

Other proteins:

CO_2 conducting aquaporins (Aqp). Triose-phosphate/phosphate translocator (TPT). SNF1-related protein kinase (SnRK1).

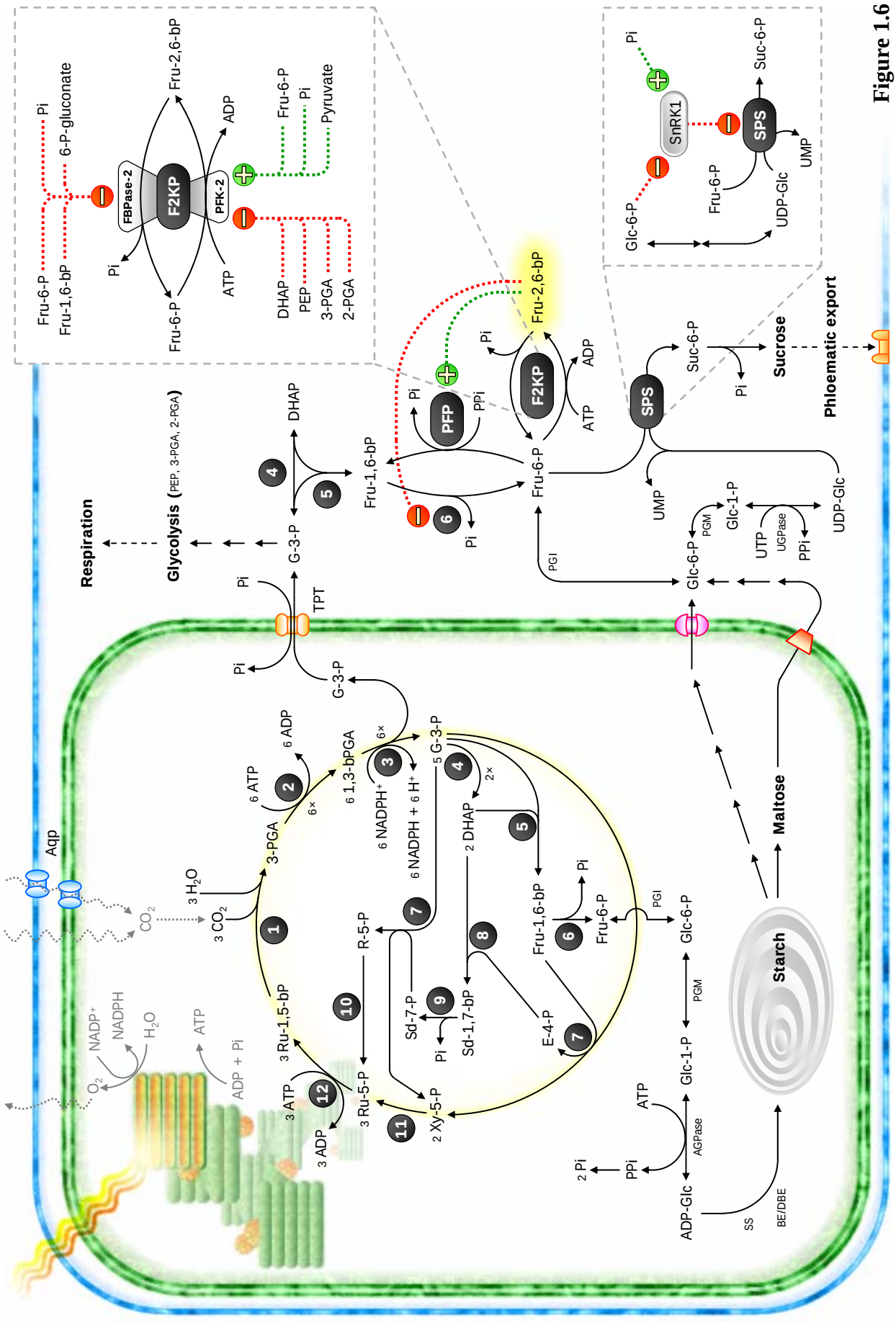
Fru-6-P
Fru-1,6-bP
Pi
6-P-gluconate
FBPase-2
F2KP
PFK-2
Fru-2,6-bP
ADP
Fru-6-P
Pi
Pyruvate
DHAP
PEP
3-PGA
2-PGA
ATP
Glc-6-P
SnRK1
SPS
Suc-6-P
Fru-6-P
UDP-Glc
UMP
PFP
PPi
Sucrose
Phloematic export
Respiration
Glycolysis (PEP, 3-PGA, 2-PGA)
DHAP
G-3-P
TPT
Fru-1,6-bP
Fru-6-P
PGI
Glc-6-P
PGM
Glc-1-P
UTP
UGPase
UDP-Glc
Aqp
CO_2
H_2O
3-PGA
6 ATP
6 ADP
6 1,3-bPGA
6 $NADPH^+$ + 6 H^+
6 NADPH + 6 H^+
5 G-3-P
2 DHAP
Fru-1,6-bP
Fru-6-P
R-5-P
Sd-7-P
Sd-1,7-bP
E-4-P
3 Ru-1,5-bP
3 Ru-5-P
2 Xy-5-P
3 ATP
3 ADP
O_2
NADP+
NADPH
H_2O
ATP
ADP + Pi
Maltose
Starch
ADP-Glc
AGPase
SS
BE/DBE
2 Pi
PPi

Figure 1.6

Among the mechanisms involved in the regulation of sucrose synthesis, two of the more studied are the enzymatic modulation of the **fructose-1,6-bisphosphatase (FBPase)** and of the **sucrose phosphate synthase (SPS)**.

In particular, the FBPase in the cytoplasm hydrolyzes the fructose-1,6-bisphosphate (Fru-1,6-bP) produced by the fructose-bisphosphate aldolase (FBPA) to fructose-6-phosphate (Fru-6-P), while the reverse reaction is catalyzed by the pyrophosphate-dependent phosphofructokinase (PFP). In plants, a feedback regulation of this enzymatic step is under the control of another derivate of (Fru-1,6-bP), fructose-2,6-bisphosphate (Fru-2,6-bP), which represses the activity of the FBPase and activates the PFP when present in high concentrations[194,195]. This favors the partitioning of carbon towards starch synthesis, while at low cytosolic Fru-2,6-bP levels sucrose biosynthesis is favored[196]. The interconversion between Fru-1,6-bP and Fru-2,6-bP is a critical step in the modulation of sucrose metabolism which relies mainly on the bifunctional role of the fructose-2,6-bisphosphatase F2KP, having both the fructose-6-phosphate,2-kinase (PFK-2) and fructose-2,6-bisphosphatase (FBPase-2) activity[197]. Both of them are subject to complex allosteric regulation by intermediates of the primary metabolism, among which are glyceraldehyde-3-phosphate (G-3-P), 3-phoshoglycerate (3-PGA), ortho- and pyrophosphate (Pi and PPi), Fru-6-P and several organic acids[195,198]. At the same time, it has been demonstrated that high levels of the FBPA product, Fru-6-P, induce the accumulation of Fru-2,6-bP by enhancing the PFK-2 activity and inhibiting the FBPase-2 component instead[195,199]. Moreover, this regulation mechanism is circumvented during night because the maltose obtained from starch degradation enters the sucrose biosynthetic pathway after the step regulated by Fru-2,6-bP.

The fructose-bisphosphate aldolase is present inside chloroplast as well, where it is required in the Calvin cycle for the reversible conversion of G-3-P and dihydroxyacetone phosphate (DHAP) to Fru-1,6-bP. At the same time, FBPA is one the enzymes of the Calvin cycle that are not regulated by effectors or post-translational modification, but only by transcriptional regulation or protein degradation[200].

Although the “nonregulated” enzymes catalyzing reversible reactions have usually been considered to have a minor influence on carbon fixation during photosynthesis[201], it has been shown that they have a potential role in the regulation of photosynthetic carbon flux *in vivo* through the Calvin cycle. In particular, the analysis of antisense tobacco and potato lines

demonstrated that even small decreases in the levels of the chloroplast FBPA lead to a reduction in RuBisCO content, resulting in a lower photosynthetic rate and decreased plant growth[202,203]. Conversely, FBPA overexpression in transgenic tobacco lines resulted in increased photosynthetic capacity, growth rate, and biomass yield as well as in a higher starch accumulation rate inside chloroplasts, but it did not affect the total starch content[204], as previously in tobacco plants overexpressing the bacterial FBPA[205].

In chloroplasts, the major rate-limiting step in carbon flux through the Calvin cycle is represented not only by the carboxylase activity of the RuBisCO because of its low affinity for CO_2 but also by the regeneration rate of ribulose 1,5-bisphosphate (Ru-1,5-bP), which is determined by the other enzymes in the Calvin cycle as well as by the capacity of the electron transport chain to supply enough ATP and NADPH[206]. For these reasons, it is conceivable that "nonregulated" enzymes such as the plastid aldolase may control the flux of photosynthesis by limiting the regeneration of Ru-1,5-bP.

Interestingly, three FBPA homologs (At2g21330, At4g38970 and At2g01140, respectively) have been previously reported to significantly contribute to the plastoglobule proteome[39], although they are not exclusive of plastoglobules and accumulate mostly in the stroma and thylakoid membranes[40]. It therefore appears possible that variations in their content or sub-organellar compartmentalization may have an effect on the photosynthetic carbon assimilation.

The enzymatic conversion of UDP-glucose + Fru-6-P to UDP + sucrose-6-phosphate, represents another fundamental step in the regulation of sucrose synthesis in the cytoplasm and it is mediated by the sucrose phosphate synthase (SPS)[207]. On the contrary, the ultimate reaction of the pathway, the hydrolysis of sucrose-6-P (Suc-6-P) to sucrose, does not appear to be involved in the modulation of sucrose biosynthesis[208]. In *A. thaliana* plants overexpressing SPS, a shift in the sucrose-to-starch ratio towards sucrose synthesis was observed in leaves[209]. Moreover, the isolation of three SPS gene families strongly indicates that SPS is essential for the regulation of the metabolic equilibrium between starch and sucrose[210,211].

The regulation of SPS activity takes place at the post-transcriptional level via phosphorylation by at least two types of kinases: an SNF1-related protein kinase (SnRK1) and a calmodulin-like domain protein kinase (CDPK)[212,213]. The sequence analysis of SPS showed that SnRK1 is mainly responsible for the regulation of the members of SPS family A in both mono- and

dicotyledons, while the SPSs belonging to family B can be regulated both by SnRK1 and CDPKs[210,213]. In particular, phosphorylation by SnRK1 inhibits SPS, resulting in decreased levels of sucrose synthesis. At the same time, SnRK1 activity is allosterically induced by Pi while it is repressed by high Glc-6-P, indicating the existence of a complex metabolic feedback regulation[199]. As a consequence, low cytosolic ATP levels favor starch degradation to support metabolism, while high sucrose concentrations are required in sink organs for its conversion to starch for storage, thus driving photosynthesis and carbon metabolism as more sucrose will be produced in leaves to compensate for the sugar flux in the phloem.

Interestingly, it has been demonstrated that members of the SnRK1 serine/threonine kinase family are involved not only in the regulation of sucrose metabolism but also play a key role in the mediation of ABA signaling during seed maturation, resulting in modifications of gene expression and in the activity of essential enzymes during germination[214,215].

1.4 - AIM OF THIS WORK

Plastoglobules were originally considered to have little function in plants besides a passive role as lipid storage particles and for the accumulation of carotenoid pigments during color deposition in flower petals and fruits.
After several years of investigation, we now know that plastoglobules have a major role in chloroplast metabolism instead. Their globular structure and their strategic position, at the interface between thylakoid grana and stroma, makes them a perfect exchange site between the two compartments, while their continuity with the external leaflet of thylakoid membranes allows for the rapid diffusion of lipophilic molecules whether required both during thylakoid (dis)assembly or in response to quick changes in the composition and Redox state of the antioxidant and electron transporter pools essential for the correct functioning of the photosynthetic apparatus. Moreover, it has been demonstrated that plastoglobules house proteins involved in the metabolism of carotenoids and prenylquinones, strongly indicating that chloroplast lipid droplets do not just represent a passage point for those molecules but also actively take part in their synthesis.

However, despite the intersection of several metabolic pathways at plastoglobules, little is known about their regulatory mechanisms. The identification of at least six ABC1-like kinases in the plastoglobule proteome suggests that they may have a role in controlling the synthesis of lipophilic molecules such as prenylquinones, similarly to the role of the prototypical family member ABC1 in the regulation of ubiquinone synthesis in mitochondria. Furthermore, a genome-wide analysis of the expression patterns of the genes encoding for these kinases has recently led to the hypothesis that plastoglobule ABC1 homologs are not redundant for the regulation of a single or few enzymes in prenylquinone synthesis but form a complex regulatory network affecting not only lipid metabolism but also photosynthetic activity, plant photoacclimation and plastid morphogenesis.

For these reasons, a systematic approach was taken in the characterization of these kinases and of their putative effect not only on plant lipid composition but also on its photosynthetic parameters and its efficiency in acclimating to different light conditions, as well as on the influence on primary carbon metabolism, plant growth rate and yield. At the same time, the possible effect of the ABC1-like kinases on plastoglobule architecture and

protein composition was investigated under different growth conditions. In order to do so, innovative experimental approaches were developed using state-of-the-art technology for the systematic lipidomics analysis of large numbers of samples.

The experimental work described in this thesis is focused on the functional characterization of two ABC1-like kinases identified inside plastoglobules. At the same time, effort was put in the creation of a suitable knock-down mutant for another kinase for which no knock-out mutant lines were previously available, and in the preliminary characterization of the resulting phenotype. On the other hand, the experimental evidence obtained for these three kinases and the novel techniques developed for their analysis will constitute the base for the investigation of the other homologs of ABC1 in chloroplasts, as well as for the systematic screening of different *A. thaliana* mutants and other plant species or cultivars.
Therefore, this PhD research project is part of a larger collaborative attempt aiming at the understanding of the physiological role of plastoglobules in chloroplast metabolism and in their dynamic adaptation to changing growth conditions.

CHAPTER 2

~ Results ~

2.1 - BIOINFORMATIC ANALYSES AND PREDICTIONS

Among the six ABC1-like kinases previously identified by tandem mass spectrometry in highly purified chloroplast fractions corresponding to plastoglobules[36,39,40], three of them were selected for further investigation: ABC1I (At1g79600.1), ABC1k3 (At4g31390.1) and ABC1V (At5g05200.1). In order to predict *a priori* some of the molecular and physiological features of the three ABC1-like kinases, as well as to obtain valuable information for the selection of the best conditions to use for their functional characterization, a series of bioinformatic analyses were performed on the publicly available data for these proteins. Expressed sequence tags (ESTs) for all the three genes were present in the TAIR database[216], ruling out the possibility that they are pseudogenes, and they were used as reference for all the analyses. The *ABC1k3* gene, however, can produce two splice variants without changes in the reading frame. In this case, only the full length transcript was used for predictions and for cloning.

2.1.1 - The ABC1-like kinase family in *Arabidopsis thaliana*

So far, thirteen putative ABC1-like kinases were identified in *A. thaliana* by sequence similarity (Table 2.1A on page 53). The sub-cellular localization of these proteins, either predicted *in silico* or experimentally confirmed, varies between mitochondria and chloroplasts, while no ABC1-like kinases have been identified or predicted outside these two organelles. Moreover, based on previous observations[36,39,40,98], chloroplast members can be further divided based on their sub-organellar distribution between plastoglobules, envelope, thylakoid membranes or as soluble stromal proteins.

Protein association with lipidic structures has been widely investigated both in prokaryotic and eukaryotic cells. In particular, for proteins lacking transmembrane domains, a correlation between the topology and physico-chemical properties of the protein and its mode of association with lipid surfaces has been proposed[217]. In order to provide a suitable model for the sub-cellular and sub-organellar localization of the ABC1-like kinases, two physical-chemical parameters were then taken into account that correlate well with protein polarity and affinity for membranes: the isoelectric point (pI) and the hydrophobicity, calculated as the grand average of hydropathy (GRAVY) index[218]. As a general rule, negative GRAVY values correspond to hydrophilic/soluble proteins while positive values indicate

hydrophobic/insoluble ones. These two parameters were calculated for the mature forms of all the ABC1-like kinases as well for the fifteen members of the *Arabidopsis* fibrillin (FBN) family (Table 2.1B), which were used as reference.

A

Gene ID	Protein name		Localization	MW (kDa)	pI	GRAVY	Regulation by (a)biotic stress	
	Used	Others					mRNA	Protein
At1g79600.1	**ABC1I**	ABC1K3	PG	74.46	5.46	-0.089	n/d	n/d
At4g31390.1	**ABC1k3**	ABC1K1	PG	67.96	5.01	-0.026	n/d	n/d
At5g05200.1	**ABC1V**	ABC1K9	PG	53.84	5.24	-0.047	n/d	n/d
At1g71810.1	**ABC1K5**		PG	73.25	5.70	-0.015	n/d	n/d
At3g24190.1	**ABC1K6**		PG	85.37	5.39	-0.007	n/d	n/d
At3g07700.1	**ABC1K7**		PG	78.28	9.13	-0.220	n/d	n/d
At5g64940.1	**AtOSA1**	ATH13, ABC1K8	ENV	83.04	9.18	-0.321	↑Cd	n/d
At4g24810.1			Chloroplast	54.64	9.22	-0.245	n/d	n/d
At1g11390.1			Mitochondria	65.25	9.61	-0.128	n/d	n/d
At1g61640.1			Mitochondria	45.90	9.59	0.132	n/d	n/d
At1g65950.1			Mitochondria	53.29	9.18	-0.078	n/d	n/d
At4g01660.1			Mitochondria	68.63	5.68	-0.254	n/d	n/d
At5g24970.1			Mitochondria	74.35	8.86	-0.038	n/d	n/d

B

Gene ID	Protein name		Localization	MW (kDa)	pI	GRAVY	Regulation by (a)biotic stress	
	Used	Others					mRNA	Protein
At4g04020.1	**FBN1a**	AtPGL35	PG	28.8	4.6 - 4.9	-0.239	↑C ↑D ↑HL	↑ABA ↑C ↑Cd ↑Zn ↑HL
At4g22240.1	**FBN1b**	AtPGL33	PG	27.2	4.7 - 4.9	-0.118	↑D	↑HL ↑HL+C ↓Da
At2g35490.1	**FBN2**	AtPGL40	PG	36.6	4.1 - 4.3	-0.320	↓C ↓D	↑↓HL
At3g26070.1	**FBN3a**		THY	21.8	(9.4)	-0.366	n/d	n/d
At3g26080.1	**FBN3b**		THY	24.8	(9.3)	-0.268	n/d	n/d
At3g23400.1	**FBN4**	AtPGL30.4	PG	22.9	4.9 - 5.4	-0.156	↑LPS	↓HL ↑S
At5g09820.1	**FBN5**		Stroma	23.9	(4.9)	-0.380	n/d	n/d
At5g19940.1	**FBN6**		THY	20.9	(7.9)	-0.148	n/d	n/d
At3g58010.1	**FBN7a**	AtPGL34	PG + Stroma	28.4	4.9	-0.173	n/d	↑HL
At2g42130.4	**FBN7b**	AtPGL30	PG	27.7	4.9	-0.070	n/d	↑Da
At2g46910.1	**FBN8**		PG	27.1	(5.2)	-0.050	n/d	n/d
At4g00030.1	**FBN9**		THY (?)	21.4	(7.3)	-0.283	n/d	n/d
At1g51110.1	**FBN10**		PG ↔ THY	39.6	(5.4)	-0.253	n/d	n/d
At1g18060.1	**FBN-like**		THY	n/d	(9.5)	-0.218	n/d	n/d
At5g53450.1	**FBN11**		n/d	75.8	(9.8)	-0.252	n/d	n/d

Table 2.1: Summary of the current information on the predicted localization, physical-chemical properties and known regulative factors of the indicated *A. thaliana* proteins.
A. ABC1-like kinases. B. Fibrillins/Plastoglobulins [modified from Singh *et al.* (2011)[51]]. Predicted pI values are indicated in brackets. Used abbreviations: ABA. Abscissic acid. C. Cold. Cd. Cadmium. D. Drought. DA. Dark. HL. High light intensity. LPS. Lipopolysaccharides. S. Salinity. Zn. Zinc.

Interestingly, the chosen model correlates well with the localization data predicted *in silico*[219] or experimentally determined for most of the ABC1-like kinases (Figure 2.1 on page 54)[22,36,39,40]. Plastoglobule ABC1-like kinases were characterized by a low pI and a higher hydrophobicity which is consistent with the association with chloroplast lipid globules, while

the majority of the mitochondrial kinases, despite having a similar affinity for membranes, showed a significantly more alkaline pI. At the same time, the ABC1-like kinase AtOSA1 clustered separately from the plastoglobule homologs, as expected from its localization on the inner envelope membrane[98]. Most surprisingly however, one kinase predicted to associate with plastoglobules (ABC1K7, At3g07700)[40] showed physical-chemical properties, which are more compatible with a thylakoid localization. Similarly, the mitochondrial kinase At4g01660 was characterized by a significantly more acidic pI and a higher solubility than the other mitochondrial ABC1-like kinases.

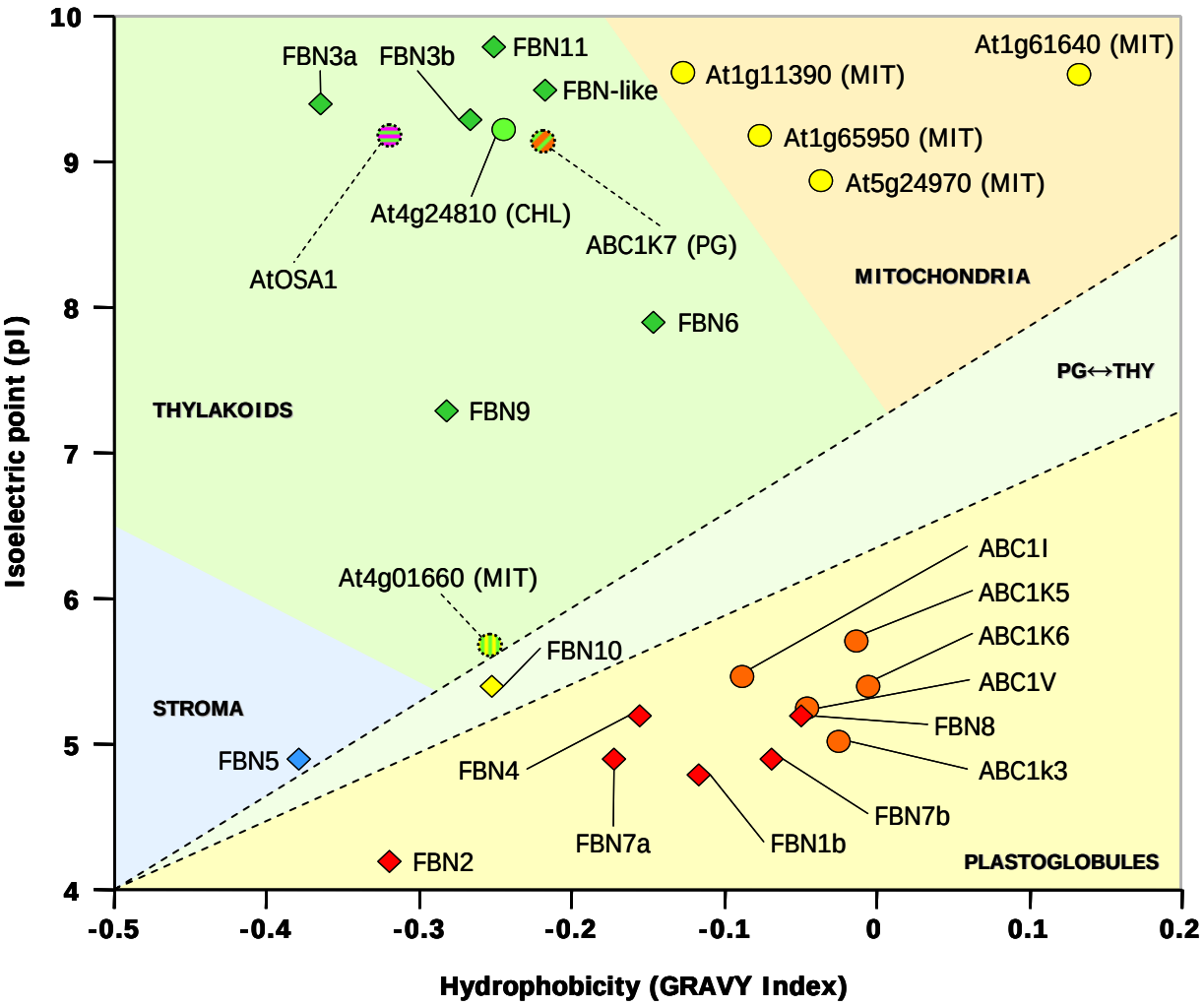

Figure 2.1: Predicted distribution of the ABC1-like kinases identified in *A. thaliana*.

The isoelectric point (pI) and hydrophobicity (GRAVY Index) of the twelve ABC1-like kinases currently identified in *A. thaliana* were calculated *in silico* after removal of the transit peptide using the ExPasy PredictProtein platform. These parameters were then used to plot the proteins and predict their sub-cellular and sub-organellar localization. The sequences of the fifteen members of the fibrillin/plastoglobulin family were used as reference.

Similarities in amino acid sequence and secondary structure between the members of the *A. thaliana* ABC1-like kinase family were also investigated by multiple sequence analysis (Figure 2.2A). The proteins showed a high degree of conservation of the ABC1/AarF/UbiB domain (yellow box) and of the most conserved eukaryotic protein kinase (ePK) catalytic motifs involved in ATP, substrate and Mg^{2+} binding. On the contrary, no significant conservation was observed in the position of the phosphorylated residues previously experimentally identified for the three chloroplast kinases ABC1k3, ABC1V and ABC1K7 and for the two mitochondrial homologs At1g65950 and At2g41040 (highlighted in red).

A phylogenetic analysis was also carried out on the obtained data, resulting in three separate branches (Figure 2.2B). The first group contained the majority of the kinases with predicted plastoglobule localization according to their physical-chemical properties (ABC1I, ABC1k3, ABC1K5 and ABC1K6; see Figure 2.1 on page 56) as well as the mitochondrial kinase At5g24970. The second branch included the three chloroplast kinases previously predicted to localize outside plastoglobules (AtOSA1, ABC1K7 and At4g24210; see Figure 2.1 on page 56) and the two mitochondrial kinases At1g65950 and At4g01660. Most surprisingly, the plastoglobule-localized ABC1V and the two mitochondrial kinases At1g11390 and At1g61640 clustered in the third group.

Figure 2.2: The ABC1-like kinase family in *A. thaliana*.

A. Multiple sequence alignment of the ABC1-like kinases identified in *A. thaliana* and identification of conserved regions with predicted secondary structure.
Red boxes represent α helices. Green arrow represent β strands. The yellow region corresponds to the conserved ABC1/AarF/UbiB domain. Similarities between residues are highlighted using a BLOSUM62 alignment score matrix. Experimentally identified phosphorylation sites are highlighted in red.

B. Dendrogram tree showing sequence similarities between the ABC1-like family members in *A. thaliana*. PG. Plastoglobule. ENV. Envelope. CHL. Chloroplast. MIT. Mitochondria.

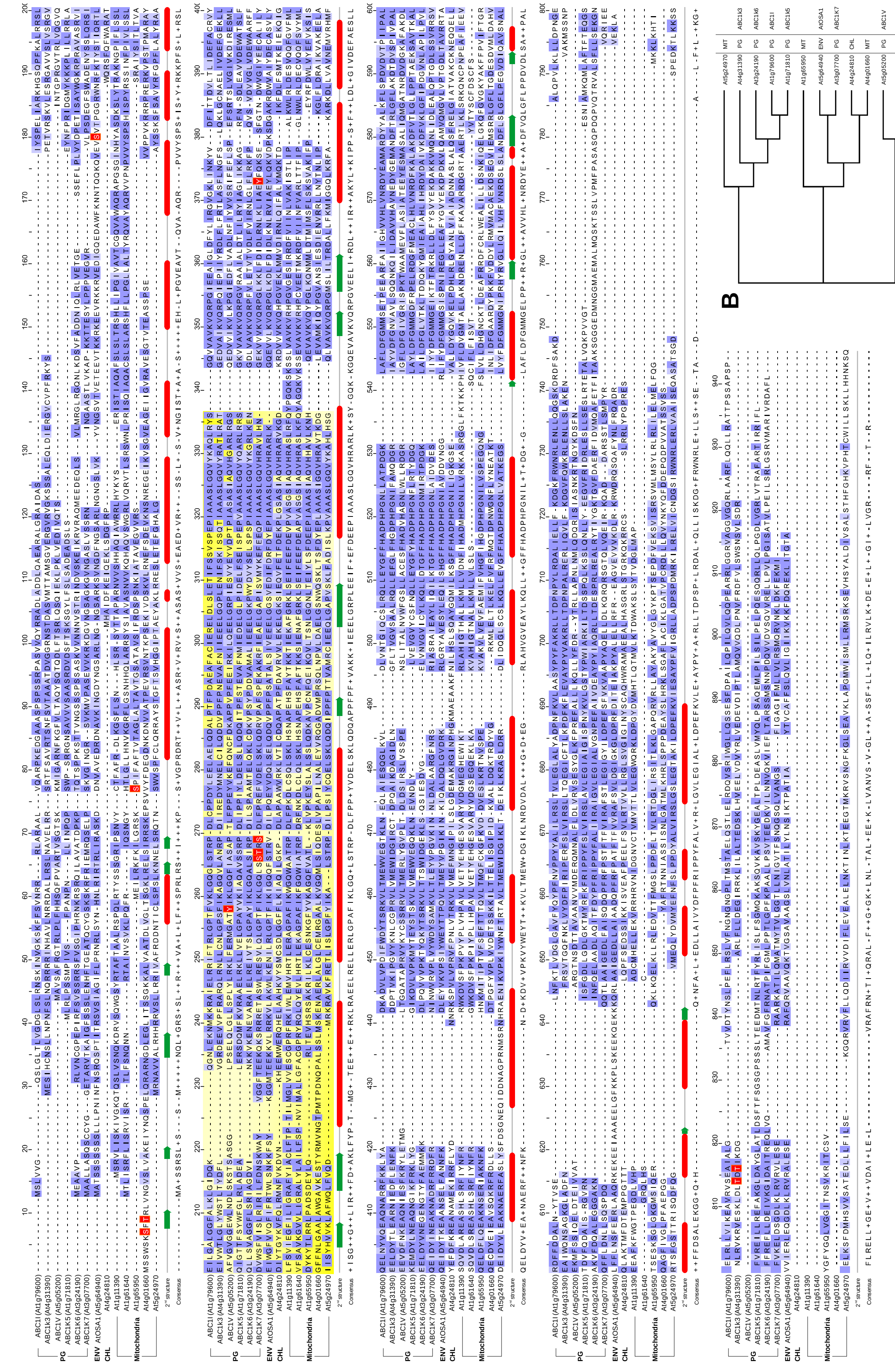

Figure 2.2: The ABC1-like kinase family in *A. thaliana*

Details on the length, solubility and conserved catalytic and regulatory domains for the three proteins ABC1I, ABC1k3 and ABC1V are reported in Figure 2.3 on page 58.

The three kinases are predicted to be globular, lack predicted transmembrane helixes and show a Kyte and Doolittle hydropathy plot compatible with soluble proteins.

Chloroplast transit peptides were predicted *in silico* using the TargetP 1.1 server and are indicated in light blue. Surprisingly however, ABC1V was predicted to localize inside mitochondria despite its identification in chloroplasts both in confocal laser scanning microscopy (Figure 2.7D on page 66) and by mass spectrometry analysis[36,39,40], probably because of a higher similarity of the ABC1V amino acid sequence with that of mitochondrial ABC1 homologs (Figure 2.2B on page 56). As a consequence, the indicated sequence may not correspond to the full-length chloroplast transit peptide.

Two overlapping conserved regions were also identified in all the proteins: the ABC1/UbiB/Aarf domain and the Protein Kinase C-like (PKc) superfamily catalytic domain. Moreover, the comparison of the three proteins (Figure 2.2A on page 56) suggests that ABC1V lacks the region at the C-terminus of the ABC1/UbiB/Aarf domain, putatively corresponding to the regulatory tail of the kinase.

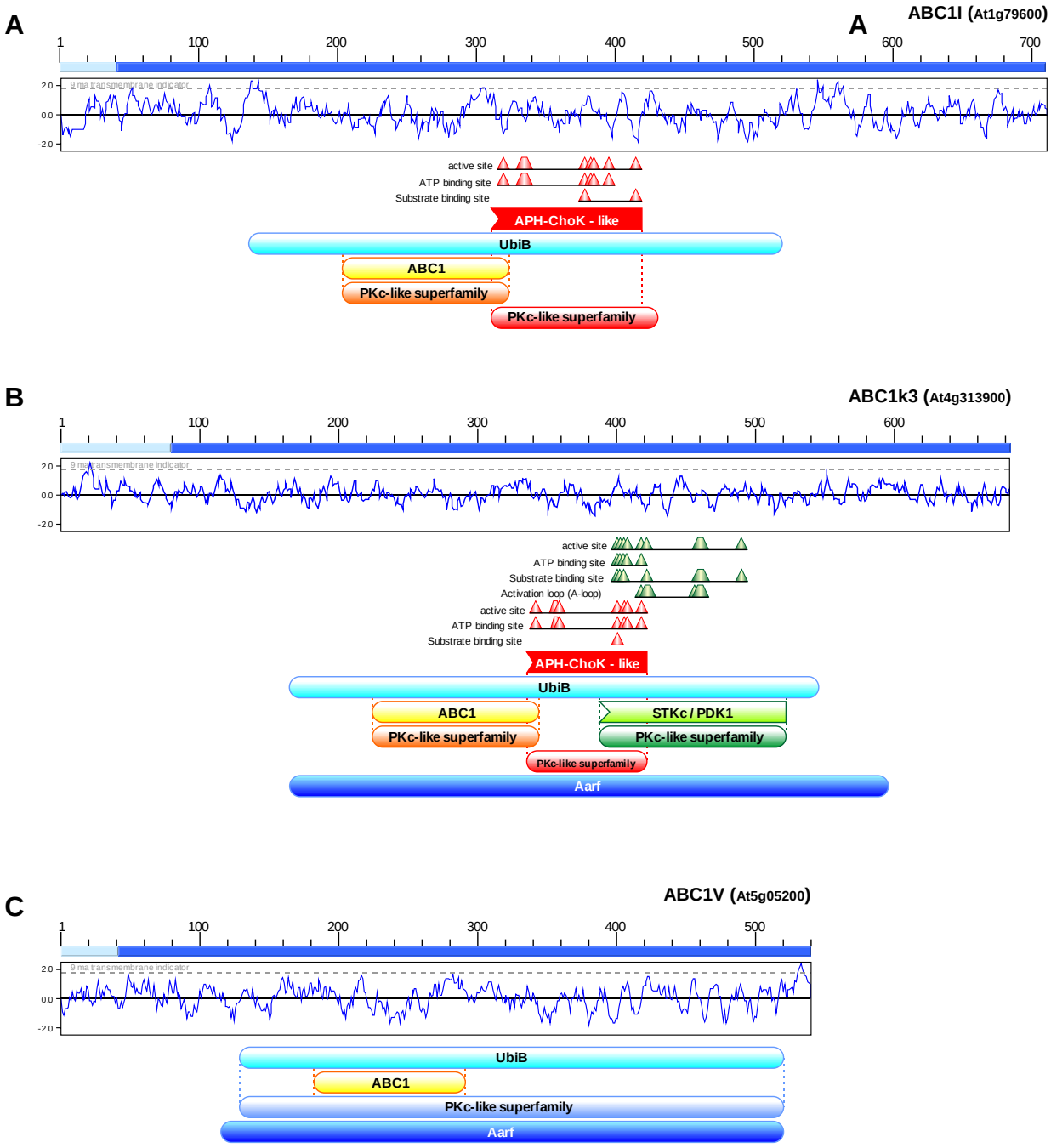

Figure 2.3: Protein solubility and conserved domains.

A-C. Comparison of the protein length, Kyte and Doolittle hydropathy plot and conserved catalytic and regulatory domains between ABC1I, ABC1k3 and ABC1V, respectively. The region corresponding to predicted transit peptide is indicated in light blue. The three ABC1-like kinases show and hydropathy profile which is compatible with soluble proteins. Abbreviations used for the conserved functional domains: APH-ChoK-like, Aminoglycoside 3'-phosphotransferase (APH) and Choline Kinase (ChoK) family. PKc-like superfamily, Protein kinase catalytic domain.

2.1.2 - Genetic regulation of the plastoglobule ABC1-like kinases

2.1.2.1 - Expression profiles and response to stimuli

In order to identify variations in the expression levels of the three ABC1-like kinases during plant development or after exposure to different growth conditions, publicly available microarray data were analyzed using the Genevestigator platform.

Under standard growth conditions, the expression rate of *ABC1I* was slightly higher than *ABC1k3* in all the analyzed organs and developmental stages, while *ABC1V* appeared to be expressed at significantly higher levels than the other two genes. However, a similar expression pattern was observed for the three kinases, which are more expressed in adult and senescent rosette leaves, in sepals and in mature siliques, while their expression decreases during bolting and in mature flowers after pollination (Figure 2.3A on page 58).

The variation of gene expression in response to selected stimuli and growth conditions was also analyzed (Figure 2.3B on page 58).
In particular, the transcription of the three kinases appears to be induced during senescence and by treatment with brassinolide, a brassinosteroid hormone that accelerates senescence in dying tissues[(220)], as well by exposure to high light intensities.
On the contrary, the gene expression is repressed in plants growing under extended night conditions and after treatment with norflurazon (4-chloro-5-methylamino-2-(3-trifluoromethylphenyl)pyridazin-3-one), a herbicide which inhibits the phytoene desaturase, resulting in reduced carotenoid biosynthesis[(221,222)]. As a consequence, considering the relevance of xanthopylls as the starting point for the synthesis of abscissic acid (ABA), plants treated with norflurazon are also characterized by a lower abscissic acid (ABA) production and a delayed senescence[(223)].

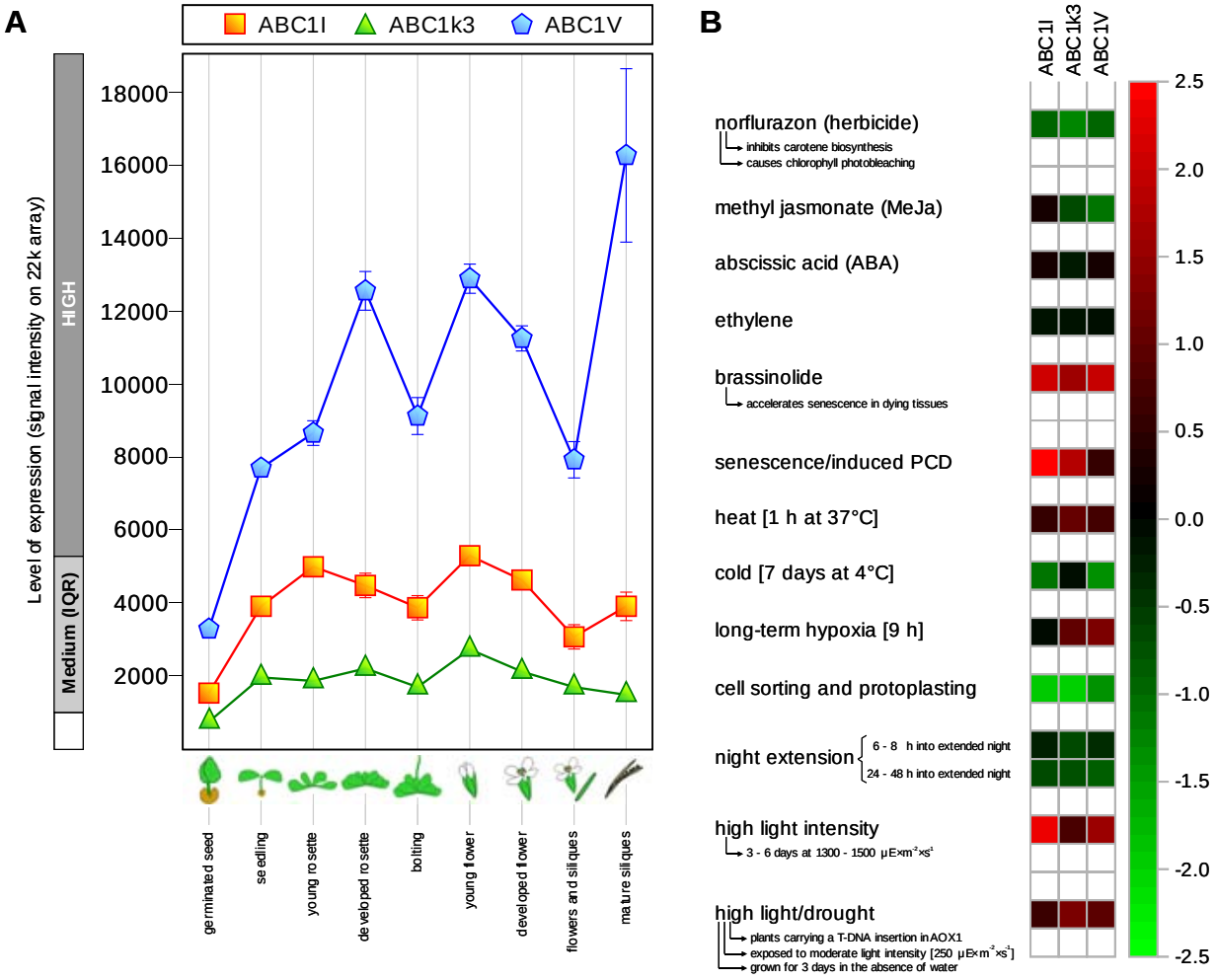

Figure 2.4: Variations in the gene expression of the three ABC1-like kinases based on microarray data obtained from the Genevestigator database.

A. Gene expression profile in different organs and developmental stages. B. Variations in transcript levels of the three genes registered in wild-type plants (Columbia-0) after exposure to specific growth conditions or treatments.

2.1.2.2 - The three kinases are part of a common gene coexpression network

The involvement of ABC1 in ubiquinone synthesis in bacteria and mitochondria has been extensively demonstrated, however the physiological functions of its chloroplast homologs are still unknown and potentially unrelated. In order to identify putative functions as well as possible phosphorylation targets for ABC1I, ABC1k3 and ABC1V, a genome-wide gene coexpression network was generated *in silico* using the ATTED-II database to highlight proteins having a similar expression pattern to the three ABC1-like kinases (Figure 2.4).

Interestingly, the three homologs under study coexpressed in the same cluster and associated with three other ABC1-like kinases localized in PGs (ABC1K5, ABC1K6 and ABC1K7, respectively), suggesting the existence of a common regulatory network for plastoglobule ABC1 homologs.

The functional relationship with single genes was then investigated for each kinase. In particular, *ABC1I* significantly associated with two other genes, the carotenoid cleavage dioxygenase 1 (*CCD1*) and the metalloprotease *FTSH8*. Moreover, a strong correlation under stress conditions was found between the expression of *ABC1I* and that of the tocopherol cyclase *VTE1*.

ABC1k3 also coexpressed with *VTE1*, although with a lower correlation score, while a strong association of *ABC1k3* with the expression of the sucrose-phosphate synthase (SPS4F) and the ζ-carotene desaturase (ZDS) was detected. *ABC1k3* also showed a slight association with the two fructose-biphosphate aldolases FBPA1 and FBPA2, which correlated more strongly with *ABC1V* expression instead.

On the other hand, ABC1V strongly coexpressed with several metallopeptidases among which the two genes *VAR1* and *VAR2*, required for chloroplast differentiation and responsible of the corresponding *VARIEGATED* phenotype in *Arabidopsis*. At the same time, a moderate association between *ABC1V* and the lycopene β-cyclase (LYC) was predicted in response to light signaling. On the contrary, no correlation between *ABC1V* and *VTE1* was determined from the available microarray data and the two genes appear to be independently expressed.

The detailed correlation analysis between each ABC1-like kinase and few selected genes from the previously illustrated gene coexpression network is reported in Figure 2.5A-E on page 63. In particular, the stability of the coexpression between *ABC1I*, *ABC1k3* and *ABC1V* was investigated (Figure 2.5B on page 63). Moreover, the association degree with the top coexpressors of the three kinases, corresponding to the proteins highlighted in Figure 2.4 on page 60 involved in prenylquinone and carotenoid synthesis, sugar metabolism, photosynthesis and plastid development, was also determined (Figure 2.5 C-E on page 63, respectively).

Figure 2.5: Predicted coexpression gene network for the three ABC1-like kinases.

Octagons represent plastoglobule proteins. Line thickness corresponds to the average correlation rank between two connected genes.

Figure 2.6: Correlation between the indicated ABC1-like kinases and few selected genes belonging to their predicted coexpression network**.**

A. Stability of the coexpression corresponding to the number of samples which support the focused gene-to-gene correlation. The symbols indicate the position of the focused gene pairs with the ABC1-like kinase in the background distribution calculated for the top 300 highly coexpressed gene pairs in the ATTED-II database.

B-E. Detail of the stability of gene coexpression with: B. The other two ABC1-like kinases. C. Enzymes involved in prenylquinone and carotenoid synthesis. D. Proteins implicated in sugar metabolism. E. Genes required for photosynthesis and plastid development. When the coexpression is supported by many factors, the PCA correlation will not change against subtractions of a few main factors, which indicates strong gene-to-gene functional relationship.

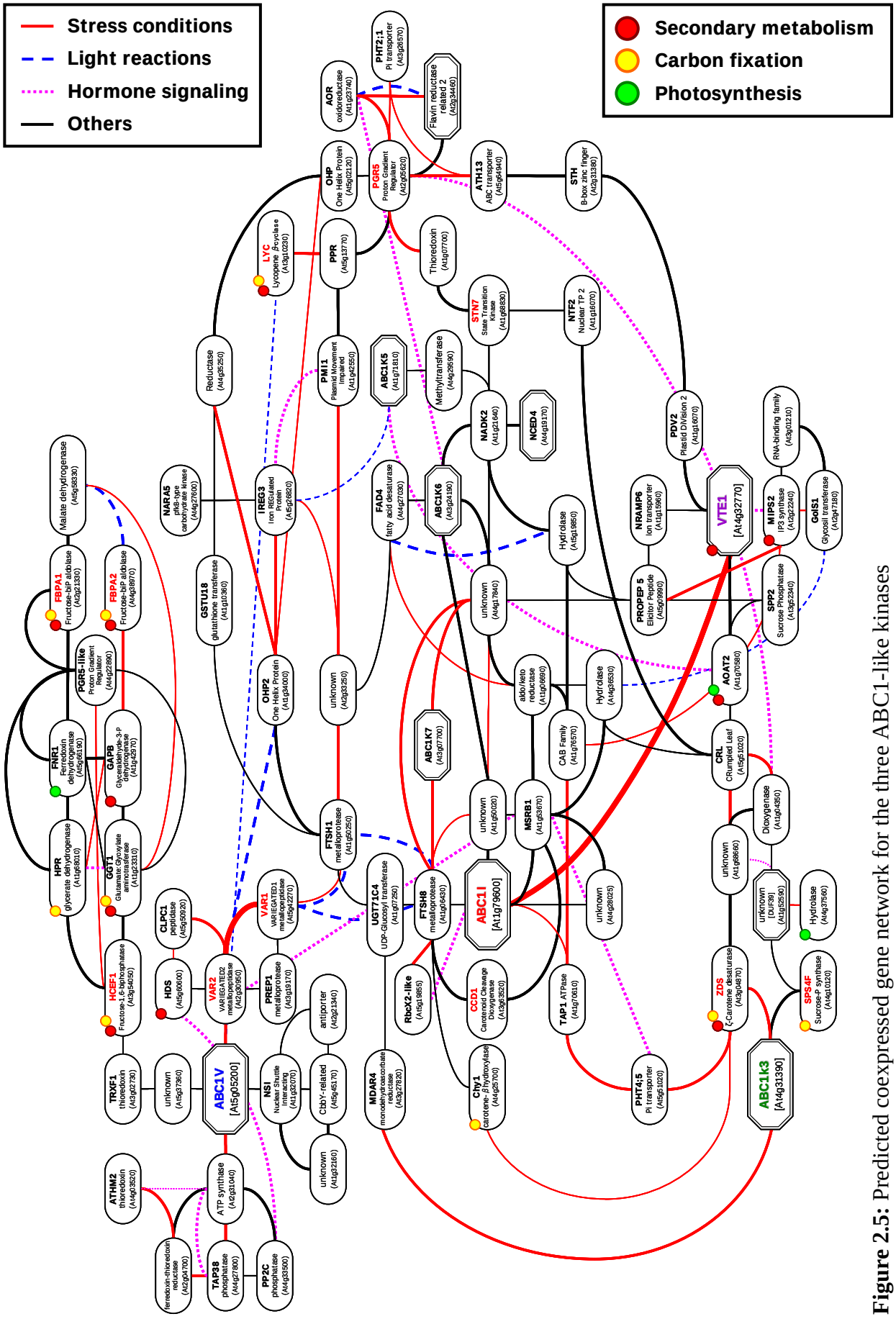

Figure 2.5: Predicted coexpressed gene network for the three ABC1-like kinases

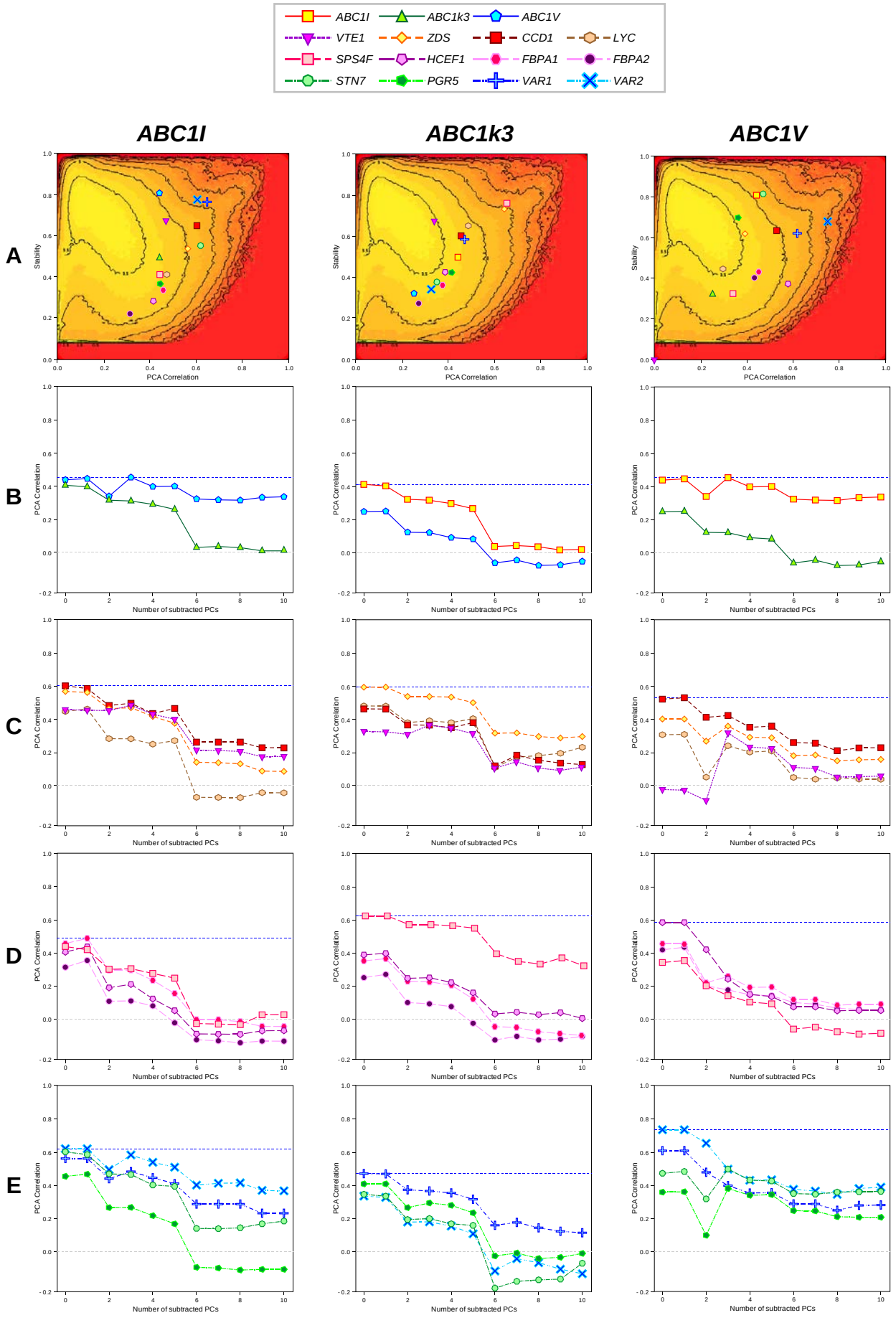
ABC1I
ABC1k3
ABC1V
VTE1
ZDS
CCD1
LYC
SPS4F
HCEF1
FBPA1
FBPA2
STN7
PGR5
VAR1
VAR2
A
B
C
D
E
Stability
PCA Correlation
Number of subtracted PCs

Figure 2.6

2.2 - EXPERIMENTAL SETUP

2.2.1 - The three ABC1-like kinases localize to plastoglobules *in vivo*

In order to confirm the plastoglobule localization of ABC1I, ABC1k3 and ABC1V, transgenic *Arabidopsis thaliana* plants were engineered to express a C-terminal YFP fusion protein under the 35S-promoter. The plastoglobule marker FBN1a fused to the Yellow Fluorescent Protein (YFP) was used as positive control (Figure 2.7A on page 66).
The observation in confocal laser scanning microscopy of *A. thaliana* leaves expressing the ABC1-like kinases fused to the YFP resulted in the detection of punctate fluorescence emission inside chloroplasts compatible with plastoglobule localization (Figure 2.7B-D on page 66). Moreover, in all the observed plant lines fluorescence was detectable neither at the thylakoids nor at the envelope. On the other hand, differences in the fluorescence emission pattern and chloroplast morphology were observed between plants expressing the three different recombinant fusion proteins.
In plants constitutively expressing ABC1I-YFP and ABC1V-YFP, fluorescence was associated with large and distinct globular structures similar to those observed in the FBN1a-YFP positive control and compatible with large plastoglobules.
However, in plants overexpressing the ABC1k3-YFP fusion protein the fluorescent emission associated with smaller globular structures inside chloroplasts, potentially compatible with smaller but more numerous plastoglobules (Figure 2.7C on page 66).

In order to confirm ABC1k3 sub-organellar localization, purified chloroplast fractions corresponding to plastoglobules (PG), envelope (ENV) and thylakoids (THY) were extracted from wild-type plants and a Western Blot analysis was performed using αABC1k3 antibodies (see Section 2.2.2), resulting in the detection of ABC1k3 only in the plastoglobule fractions (Figure 2.25 on page 97).

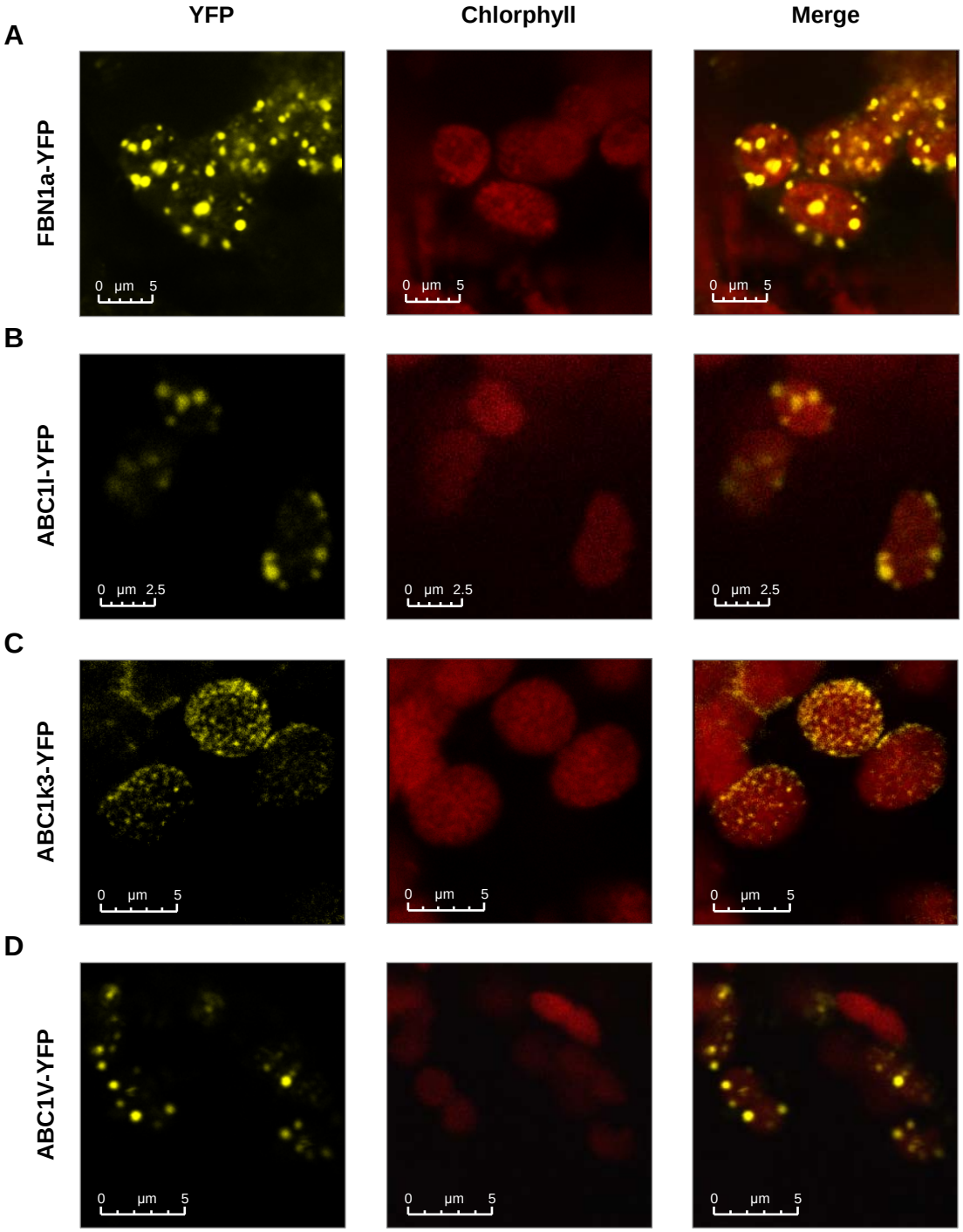

Figure 2.7: Sub-organellar localization of the ABC1-like kinases.

A. The plastoglobule marker FBN1a-YFP was used as positive control for plastoglobule localization. B-D. The complete coding sequences of the three ABC1-like kinases were fused at the C-terminal to the Yellow Fluorescent Protein (YFP) and stably expressed in *A. thaliana* plants. Leaves from ABC1I-YFP, ABC1k3-YFP and ABC1V-YFP plants, respectively, were then observed under confocal scanning microscopy. For all the three fusion proteins fluorescence co-localized with chloroplasts and a punctate YFP fluorescence emission consistent with plastoglobule localization was observed. Left panels, YFP emission. Central panels, chlorophyll autofluorescence. Right panels, merge of the two channels.

2.2.2 - Production of polyclonal antibodies

The production of a specific antibody represents an important step for both the biochemical localization of the protein and the analysis of the variation of its relative amount inside chloroplasts in response to a certain stimulus. For this reason, full-length ABC1I, ABC1k3 and ABC1V precursor proteins were fused at the C-terminus to a hexahistidinyl (His_6) tag and then expressed in *E. coli* (Figure 2.8A-B on page 68). For ABC1k3 and ABC1V a fragment of the appropriate molecular weight (77 and 60 kDa, respectively) was detected after induction with 0.5-1 mM IPTG for 3 h, while for ABC1I only a shorter polypeptide (around 45 kDa in weight) was recovered instead of the expected full-length protein (79 kDa).

ABC1k3 and ABC1V were purified under denaturing conditions by Ni-NTA affinity chromatography (Figure 2.8C-D on page 68) and used for the production of rabbit polyclonal antibodies. Sera obtained at different time points during the rabbit immunization program were tested by Western Blotting for their affinity for the two recombinant proteins as well for the presence of monomeric IgGs (data not shown). Antibodies were then purified by affinity chromatography and used for immunoblotting on plant samples. However, the lack of a knock-out mutant line for *ABC1V* (see Section 2.3.1) did not allow to confirm the specificity of αABC1V polyclonal antibodies. On the contrary, affinity purified antibodies against ABC1k3 recognized a single band at the expected molecular weight of the mature form of the kinase (68 kDa) which was absent in the *abc1k3* knock-out mutant line (Figure 2.25 on page 97).

Figure 2.8: Isolation of the recombinant ABC1-like kinases from bacterial extracts for the production of polyclonal antibodies.

A. Expression in *E. coli* BL21 (DE3) cells of the full-length coding sequences for the three kinases fused at the C-terminus to an hexahistidinyl (His6) tag. No significant increase in total protein amount was detected after induction with 0.5-1 mM IPTG over the indicated time.

B. Detection of the His6 tag by immunoblotting using commercial antibodies. The expected positions of the full-length recombinant proteins are indicated.

C-D. Purification of the recombinant ABC1k3-His6 and ABC1V-His6, respectively, by Ni-NTA affinity chromatography under denaturing conditions. Samples were collected at each step of the purification, separated by SDS-PAGE and transferred on nitrocellulose membrane. The presence of an His6 tag was then detected by Western Blotting.

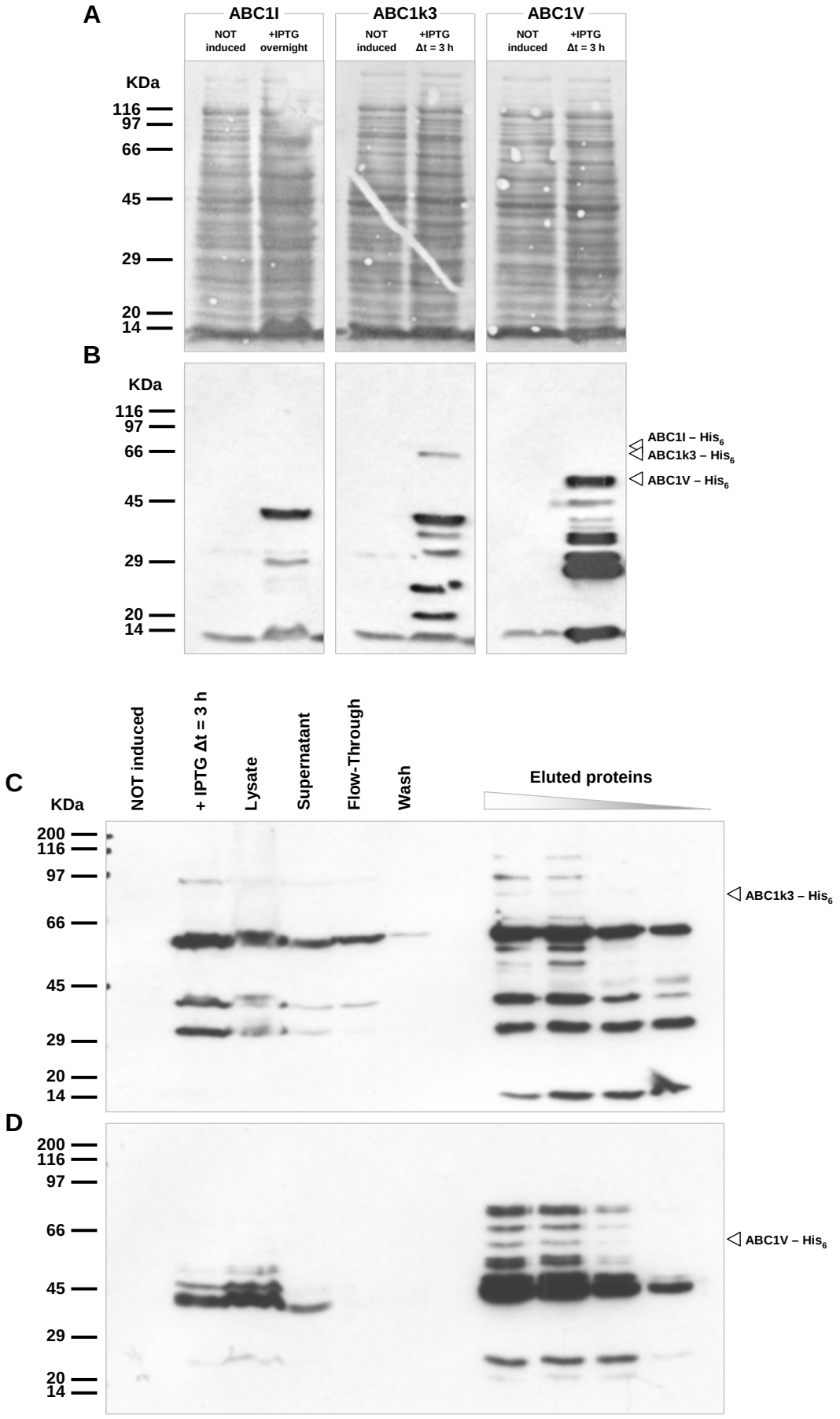
A
ABC1l
NOT induced
+IPTG overnight
ABC1k3
NOT induced
+IPTG Δt = 3 h
ABC1V
NOT induced
+IPTG Δt = 3 h
KDa
116
97
66
45
29
20
14
B
KDa
ABC1l – His6
ABC1k3 – His6
ABC1V – His6
C
NOT induced
+ IPTG Δt = 3 h
Lysate
Supernatant
Flow-Through
Wash
Eluted proteins
KDa
200
ABC1k3 – His6
D
ABC1V – His6

Figure 2.8

2.2.3 - Development of a novel method for prenylquinone and carotenoid profiling in plant tissues

In order to provide a rapid and reliable alternative to the conventional procedures used for the identification and quantification of prenylquinones and carotenoids in plants, a new method was developed that introduces for the first time the use of UHPLC-APCI-QTOFMS for lipid profiling in plant extracts. Compared to conventional analyses based on HPLC separation coupled to ultraviolet or fluorescence detection, this technique proves to be faster, very selective and sensitive for the analyzed molecules.

An optimized protocol was introduced for the rapid extraction of prenylquinones from plant tissues. In particular, different solvents were tested for their extraction yield, their ability to maintain the Redox state of molecules as well as their compatibility with reverse-phase UHPLC in terms of peak broadening and chemical resistance. For all prenylquinones, the highest extraction yield was obtained either with tetrahydrofuran (THF) and with a mixture of chloroform/methanol ($CHCl_3$/MeOH, 30:70, v/v). However, considering that the UHPLC system can accommodate all common solvents except chlorinated ones, $CHCl_3$ was excluded from further analyses.
Chromatography and mass spectrometry parameters were also optimized for speed, selectivity and sensitivity. Moreover, the influence of the extraction solvents on the chromatographic performance and the possible detrimental effects of the plant matrix on sample preparation recovery were evaluated as well.

The detailed approach to the development of this new analytical method for prenylquinone profiling is described in Martinis *et al.* (2011)**(80)** (see Appendix).
At the same time, sample extraction and chromatographic conditions were implemented in order to allow the simultaneous separation and detection of prenylquinones and carotenoids. A list of the identified prenylquinones and carotenoids is presented in Table 2.2 on page 70.

Compound	Abbreviation	Molecular Formula	RT (min)	m/z (–)
α-Tocopherol	α-T	$C_{29}H_{50}O_2$	2.28	429.3718
α-Tocopherol quinone	α-TQ	$C_{29}H_{50}O_3$	1.90	446.3746
γ-Tocopherol	γ-T	$C_{28}H_{48}O_2$	2.13	415.3562
δ-Tocopherol	δ-T	$C_{27}H_{46}O_2$	1.96	401.3404
2,3-dimethyl-5-phytyl-1,4-hydroquinone	DMPBQ	$C_{28}H_{48}O_2$	1.50	416.3650
Phylloquinone	K	$C_{31}H_{46}O_2$	2.67	450.3484
Plastoquinol	PQH_2	$C_{53}H_{82}O_2$	3.22	748.6152
Plastoquinone	PQ	$C_{53}H_{80}O_2$	3.99	748.6153
Hydroxy-plastoquinone	PQ-OH	$C_{53}H_{80}O_3$	3.22	764.6081
Plastochromanol-8	PC-8	$C_{53}H_{82}O_2$	3.66	749.6214
Hydroxy-plastochromanol	PC-OH	$C_{53}H_{81}O_3$	3.01	765.6161
Ubiquinol	UQH_2	$C_{54}H_{84}O_4$	3.40	794.6190
Ubiquinone	UQ	$C_{54}H_{82}O_4$	3.70	794.6188
β-carotene	β-Car	$C_{40}H_{56}$	3.48	536.4367
Lutein	Lut	$C_{40}H_{56}O_2$	1.50	568.4264
Stearate	C18:0	$C_{18}H_{36}O_2$	1.34	283.2629

Table 2.2: List of the molecules identified from UHPLC-APCI-QTOFMS data acquired in negative ionization mode. RT. Retention time.

2.3 - MUTANT CHARACTERIZATION

2.3.1 - Selection of mutant plant lines for the ABC1-like kinases

2.3.1.1 - Isolation of T-DNA insertion mutants

A preliminary search was performed on the SALK database[224] for *Arabidopsis* mutant lines carrying T-DNA insertions in the coding sequence of the genes corresponding to the three ABC1-like kinases under study. For *ABC1I*, only the two T-DNA insertion lines *abc1i*_A and *abc1i*_B (SALK_128696 and SAIL_918E10, respectively) were present in the database (Figure 2.9A), while three independent T-DNA insertion mutant lines were identified for *ABC1k3*: *abc1k3*_A (SALK_109079), *abc1k3*_B (SALK_068628) and *abc1k3*_C (SALK_057147). Moreover, another allele of *abc1k3* (*pgr6*) was independently mapped by forward genetics screening for a high chlorophyll fluorescence phenotype at high light intensity[102]. The *pgr6* (*proton gradient regulation 6*) mutant was originally isolated as CE11-8-1 and has a nonsense mutation in the second exon of *ABC1k3* which causes a premature translational termination (Figure 2.9D). On the other hand, no T-DNA insertion mutants are currently available for *ABC1V*. (Figure 2.9H).

Homozygous plants for each *abc1i* and *abc1k3/pgr6* mutant alleles were then selected by PCR genotyping (Figures 2.9B-C and 2.9E-G, respectively).

Figure 2.9: Isolation of mutant alleles for the three ABC1-like kinases.

A, D and H. Mapping of three T-DNA insertions and of a single point mutation inside *A. thaliana* genome in the region corresponding to *ABC1I* (At1g79600), *ABC1k3/pgr6* (At4g31390) and *ABC1V* (At5g05200), respectively. Squares represent exons and lines introns. Light grey regions correspond to the predicted UTRs. The position and the sequence of the SNP mutation in the *pgr6-1* mutant are indicated with a white triangle. No T-DNA insertion mutants were commercially available for *ABC1V*.

Genotyping of the mutant lines: B. SAIL_918E10. C. SALK_128696. E. SALK_109079. F. SALK_068628. G. SALK_057147. Genotyping was performed by PCR analysis using the indicated primers (see Table 4.1). Reactions were designed in order to detect the wild-type alleles or the T-DNA 5'/3' flanking sequence. DNA from wild-type plants (WT) was used as positive control (C+). Hm, Homozygous. Hz. Heterozygous. Nd. PCR product not detected.

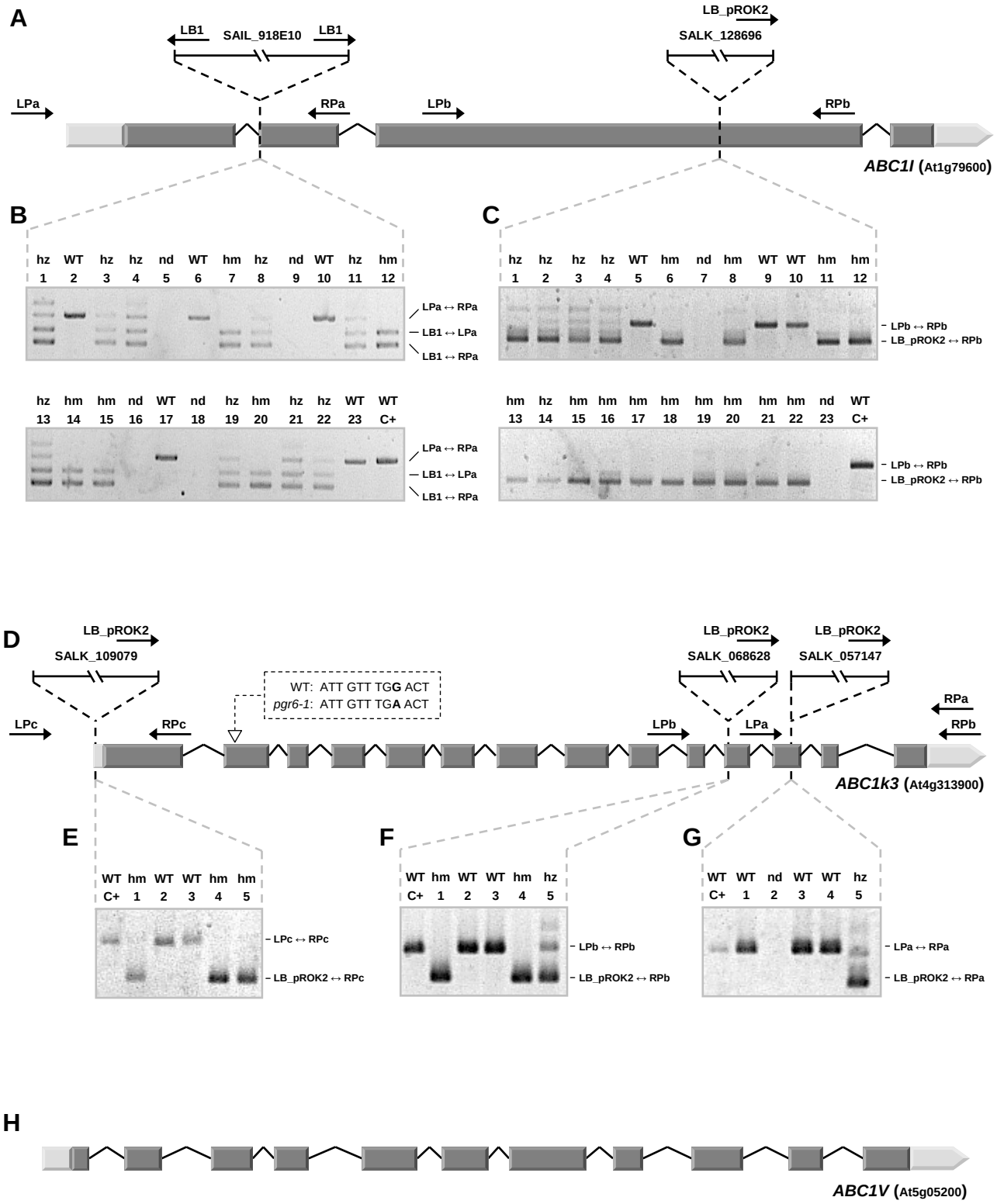

Figure 2.9: Isolation of mutant alleles for the three ABC1-like kinases.

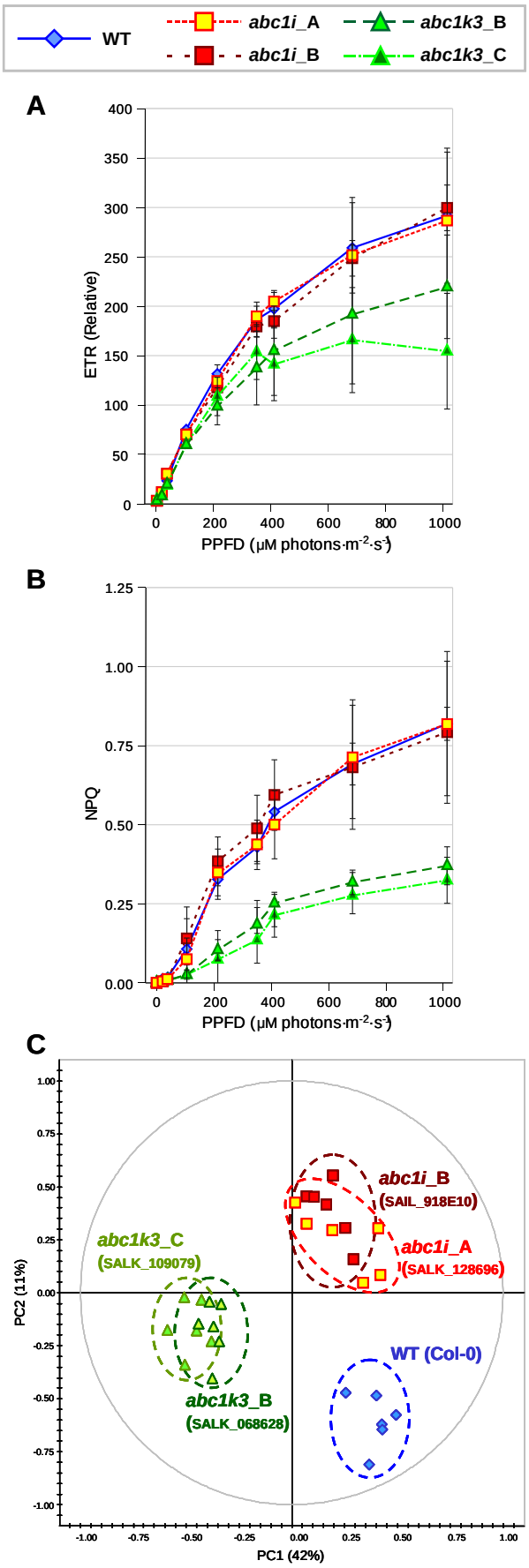

Figure 2.10: Comparison between wild-type plants and T-DNA insertion mutant alleles for the two kinases ABC1I and ABC1k3.

A. Light dependance of electron transport rate (ETR). B. Non-photochemical quenching (NPQ). Plants were grown under normal light conditions (150 µE × m^{-2} × s^{-1}) and leaves (n=5) were analyzed at intervals of 24 h.

C. Principal component analysis (PCA) performed on the lipid profiles of plants grown under normal light conditions. Prenylquinones and carotenoids were extracted and analyzed by UHPLC-APCI-QTOFMS. Colored squares correspond to the observations (n = 6 for each plant line). PC1 and PC2 are first and second principal components, respectively, with their percentage of explained variance.

In order to demonstrate that the mutation of the gene under investigation was responsible of the observed phenotype and to rule out the possibility that it was due to secondary mutations, a comparison was performed between the identified alleles for both *abc1i* and *abc1k3/pgr6* T-DNA insertion mutants. The visual phenotype of the alleles for the two mutants, their protein patterns and the photosynthetic parameters (ETR and NPQ) were identical (Figure 2.10A-B). Moreover, when the prenylquinone and carotenoid composition of wild-type and mutant plants was compared by principal component analysis (PCA), *abc1i* and *abc1k3/pgr6* clustered separately, while no significant differences were detected between the T-DNA insertion alleles for each mutant (Figure 2.10C).

A more detailed analysis of the two mutants *abc1i* and *abc1k3/pgr6* was also performed to establish whether they corresponded to null or knockdown mutant alleles. Considering the lack of a suitable antibody to determine ABC1I cellular content, a quantitative RT-PCR analysis was carried out on total RNA extracted from fresh wild-type and *abc1i* leaves. No *ABC1I* transcript was detected in *abc1i*, demonstrating that it corresponded to a null mutant (Figure 2.11).

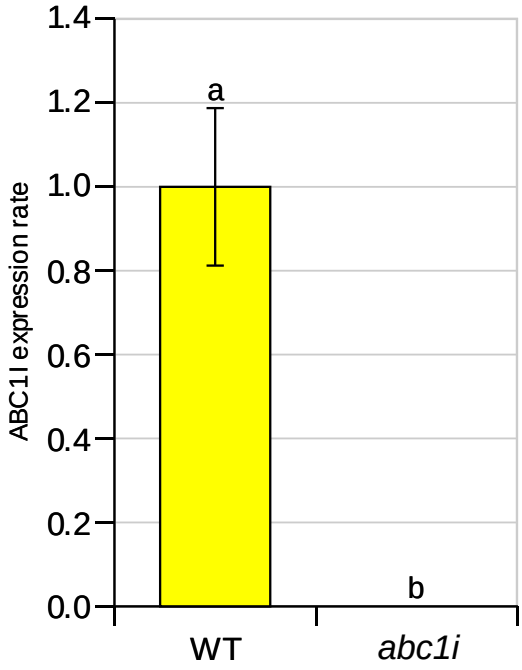

Figure 2.11: Determination of *ABC1I* gene expression rate by real-time RT-PCR.

Determination of the *ABC1I* (At1g79600) transcript levels in the T-DNA insertion mutant line SALK_128696.

Total RNA extracted from untreated wild-type and *abc1i* (SALK_128696) leaves was used for PCR assays.ACTIN2 expression levels were used for normalization. Significant differences between samples (n=3 for each plant line) were determined by a one-way ANOVA.

On the contrary, ABC1k3 levels in the mutant were investigated by Western Blotting using αABC1k3 antibodies. This resulted in the detection of the kinase only in plastoglobules extracted from wild-type plants, while ABC1k3 was undetectable in chloroplast fractions purified from *abc1k3/pgr6* plants, strongly suggesting that they correspond to null mutants (Figure 2.25 on page 97).

2.3.1.2 - *ABC1V* downregulation by RNA-mediated gene silencing

Considering that T-DNA insertion mutants were not available for *ABC1V*, a different approach was chosen to achieve *ABC1V* downregulation by gene silencing. The full length *ABC1V* coding sequence was cloned in the pHELLSGATE plasmid as inverted repeats separated by an intron from the pyruvate dehydrogenase kinase (PDK). The expression vector was then used for the stable transformation of wild-type *A. thaliana* plants, resulting in the formation of a *intron-containing* self-complementary "*hairpin*" RNA (*ihp* RNA) construct, which has been previously proven to efficiently trigger gene silencing[(225)].
Transformants were then selected on kanamycin-containing media and the integration of the transgene was further verified by PCR genotyping (Figure 2.12A-C on page 76). As a result, two T2 offsprings carrying the *ihp* RNA construct were selected and identified as ABC1V-pHSG 1 and ABC1V-pHSG 2, respectively. Interestingly, the visual phenotype of the two plants was significantly different and dissimilar from wild-type rosettes of the same age. In particular, the ABC1V-pHSG 2 seedling showed a significant growth defect and its central leaves were characterized by an albino phenotype (Figure 2.12A on page 76). Chlorophyll content in the adult rosette appeared to be normal instead, but the 6-week-old ABC1V-pHSG 2 was significantly smaller than wild-type plants at a similar developmental stage. On the contrary, ABC1V-pHSG 1 growth rate appeared to be significantly higher than the wild-type (Figure 2.12B on page 76).

In order to determine *ABC1V* transcript levels in the two RNAi mutant lines, a quantitative RT-PCR analysis was carried out on total RNA extracted from the two plants (Figure 2.13 on page 76). Only a weak, presumably background signal was detected in the ABC1V-pHSG 1 mutant. Most strikingly however, a 1.4-fold increase in the expression of *ABC1V* was detected in the ABC1V-pHSG 2 mutant line.

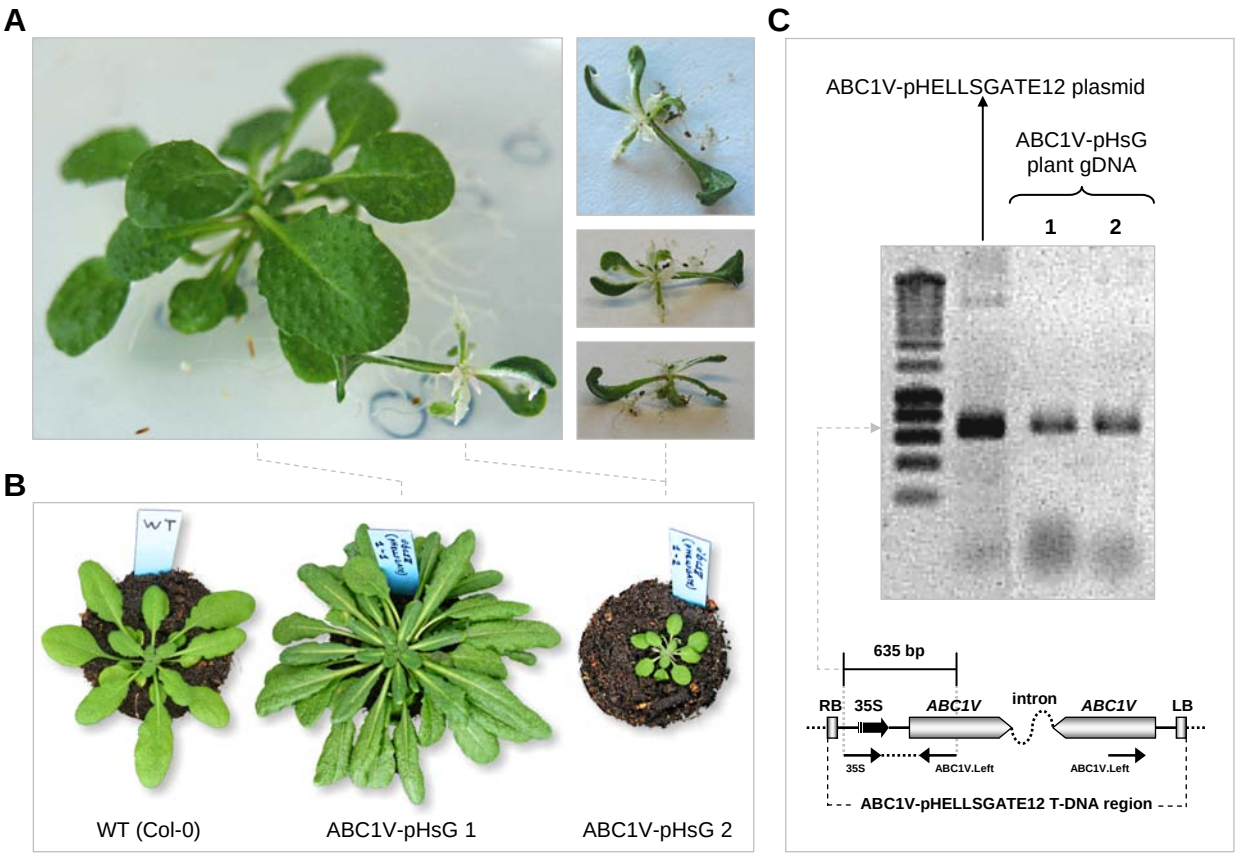

Figure 2.12: Isolation of *ABC1V* RNAi mutants.
A. Selection on ½ MS medium supplemented with 50 µg/mL kanamycin of 3-week-old seedlings obtained from the stable transformation of *A. thaliana* (Col-0) plants with the ABC1V-pHELLSGATE12 vector. Inserts on the right: detail view of the mutant seedling ABC1V-pHsG 2. B. Phenotypical comparison between a wild-type (Col-0) 6-week-old rosette and the two mutant plants previously isolated. C. Genotyping of the T-DNA insertion performed by PCR using the indicated primers. The undigested ABC1V-pHELLSGATE12 plasmid was used as positive control.

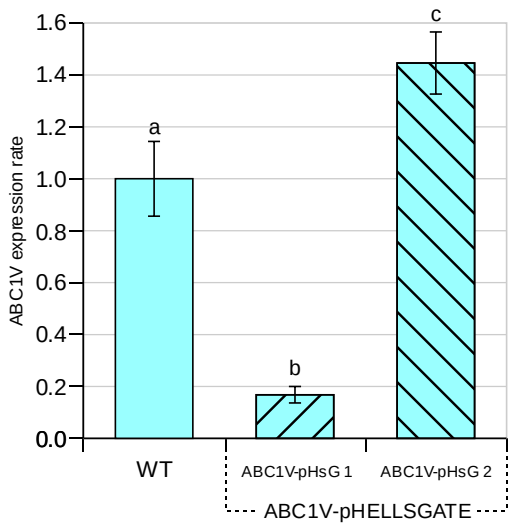

Figure 2.13: Determination of *ABC1V* gene expression rate by real-time RT-PCR.

Comparison of the *ABC1V* (At5g05200) expression levels between wild-type plants and the two RNAi lines ABC1V-pHsG 1 and ABC1V-pHsG 2. Both mutant lines were obtained by stable transformation with the full-lenght *ABC1V* sequence inside the pHELLSGATE12 vector under the control of the CaMV 35S promoter. Total RNA extracted from untreated wild-type and either of the mutant lines leaves was used for PCR assays. ACTIN2 expression levels were used for normalization. Significant differences between samples (n=3 for each plant line) were determined by a one-way ANOVA.

2.3.2 - *abc1k3/pgr6* affects growth rate and pigment content

In order to characterize the *abc1k3/pgr6* mutant, a phenotypical comparison was performed with wild-type plants both under normal light conditions and under continuous high light (HL) treatment. The growth rate of the *abc1k3/pgr6* mutant was affected in young rosettes (up to 3-week-old) growing under photoautotrophic culture conditions (Figure 2.14A), while *abc1k3/pgr6* adult rosettes (over 4-week-old) did not significantly differ from the wild-type neither in size nor in morphology (Figure 2.14B). However, after short exposure to HL intensities *abc1k3/pgr6* plants showed a pale phenotype with little or no anthocyanine synthesis, and were also characterized by a higher sensitivity to light stress, with diffused bleaching zones on the leaf surface (Figure 2.14B-C). Nevertheless, plants were able to grow under continuous HL treatment, and a partial recovery in anthocyanine accumulation was observed after prolonged HL exposure (Figure 2.14C).

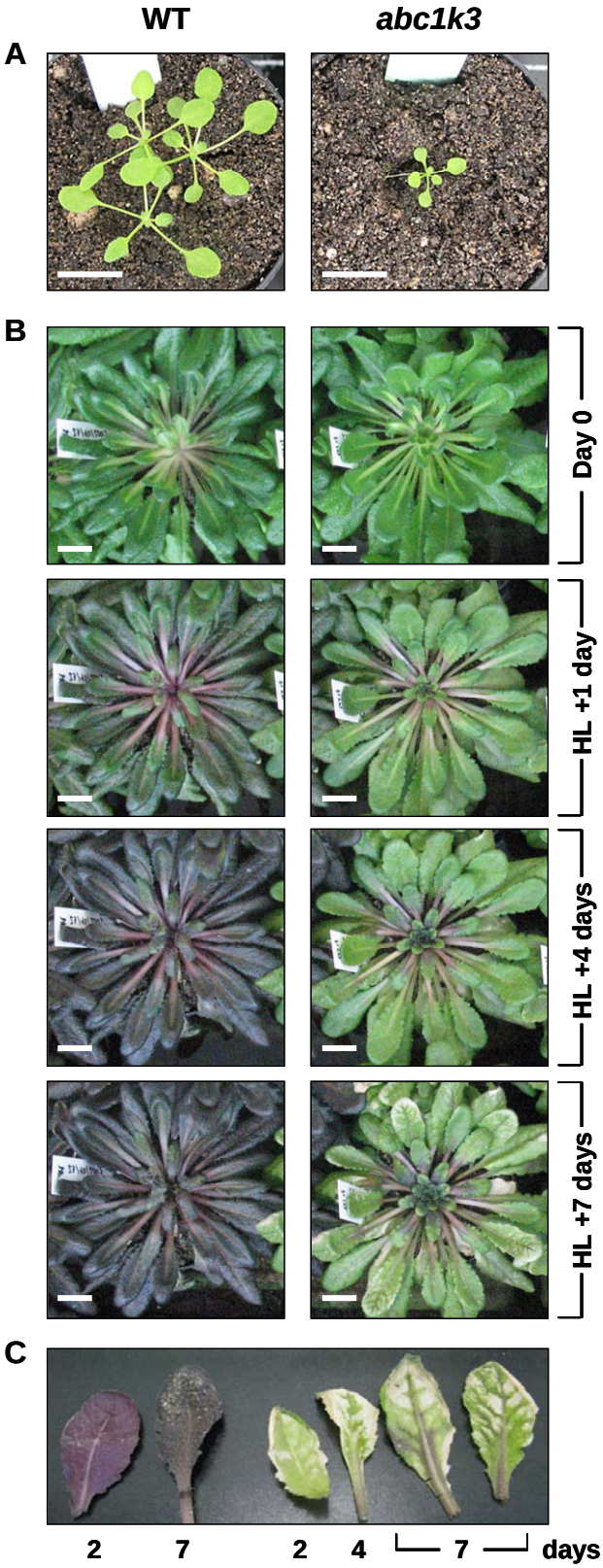

Figure 2.14: Phenotype of the *abc1k3* mutant and response to HL treatment.

A. Comparison of 3-week-old plants grown on soil under normal light conditions (150 µE × m-2 × s-1). B. Total rosettes exposed to continuous high light (500 µE × m-2 × s-1) for the indicated amount of days.
White bars correspond to a length of 1 cm.

C. Detail of leaves from plants exposed to continuous high light intensity.

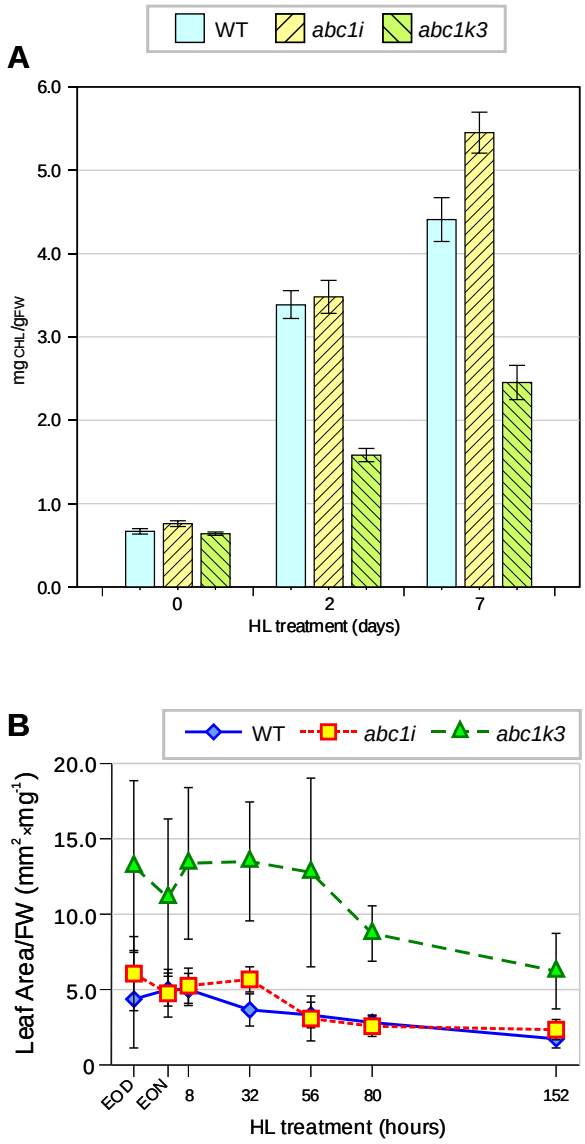

Figure 2.15: Pigment content variations and morphological changes in response to HL treatment.

A. Changes in chlorophyll content. Plants grown under normal light conditions (day 0, 150 µE × m^{-2} × s^{-1}) were exposed to continuous high light (500 µE × m-2 × s-1) for 2 and 7 days, respectively. Chlorophyll was then extracted from total leaves (n=3) in 80% acetone and measured spectrophotometrically.

B. Differences in leaf thickness. Leaf surface/Fresh Weight ratio determined in leaves (n=8) from wild-type, *abc1i* and *abc1k3/pgr6* mutant plants at different timesteps during HL treatment.

Interestingly, a significant difference in chlorophyll total content (about a 2-fold reduction compared to the wild-type) was observed in 2-month-old *abc1k3/pgr6* plants after exposure to HL intensity (Figure 2.15A). At the same time, under all light conditions *abc1k3/pgr6* plants were characterized by an higher leaf surface-to-fresh weight ratio, possibly indicating slightly thinner leaves than wild-type plants (Figure 2.15B).

On the other hand, no significant differences in plant morphology, growth rate and plant thickness were observed between the *abc1i* mutant and wild-type plants. The chlorophyll content in the two plant lines was also similar both under normal growth conditions and after a short HL treatment, while only a slight increase in chlorophyll levels was detected in *abc1i* plants when compared to the wild-type after prolonged exposure to continuous HL (Figure 2.15A-B).

2.3.3 - Chloroplast ultrastructure is severely affected in the two mutants

Semi-thin leaf sections from wild-type, *abc1i* and *abc1k3/pgr6* plants grown under different light intensities were observed in light microscopy, and differences were detected between the three plant lines (Figure 2.16A-B). In particular, a significant increase in the size and number of starch granules was observed in wild-type plants after exposure to HL intensity. On the contrary, despite chloroplast number and size in the *abc1i* mutant appeared to be similar to the wild-type under normal light conditions, no apparent increase in starch content was observed after HL treatment. Moreover, no starch granules were detectable in *abc1k3/pgr6* chloroplasts under any of the tested conditions.

Transmission electron microscopy was also used to analyze the chloroplast ultrastructure in both the *abc1i* and *abc1k3/pgr6* mutants and compare it to the wild-type.
Under normal light conditions, *abc1i* chloroplasts appeared to be morphologically similar to the wild-type but the thylakoid grana were more scattered and there were very few or no visible starch granules (Figure 2.16C). However, under HL treatment, *abc1i* chloroplasts significantly differed from the wild-type, presenting large scattered grana, extensive vacuolation as well as an increase in plastoglobule size and number of plastoglobule clusters. Moreover, as previously observed, no starch accumulation under HL was detected in *abc1i* chloroplasts (Figure 2.16D).
Under normal growth conditions, *abc1k3/pgr6* chloroplasts had small and very dense grana with loose stacking, while plastoglobules were small or absent (Figure 2.16C). Besides, under HL treatment grana were disassembled and scattered in the *abc1k3/pgr6* mutant, while plastoglobules appeared similar in size and number to the wild-type (Figure 2.16D). Interestingly, even at the higher resolution provided by transmission electron microscopy, no starch granules were detected in chloroplasts from *abc1k3/pgr6* plants grown both under normal and HL intensities (Figure 2.16C-D).

Figure 2.16: Changes in chloroplast ultrastructure observed under HL treatment.

Leaves were exposed to normal light intensity (A and C, 150 μE × m^{-2} × s^{-1}) or continuous high light (B and D, 500 μE × m-2 × s-1) for 4 days, respectively.
A-B. Semi-thin sections stained in toluidine blue and then observed with a compound light microscope.

C-D. Transmission electron micrographs of leaves exposed to normal and high light conditions, respectively. Black bars correspond to a length of 1 μm.

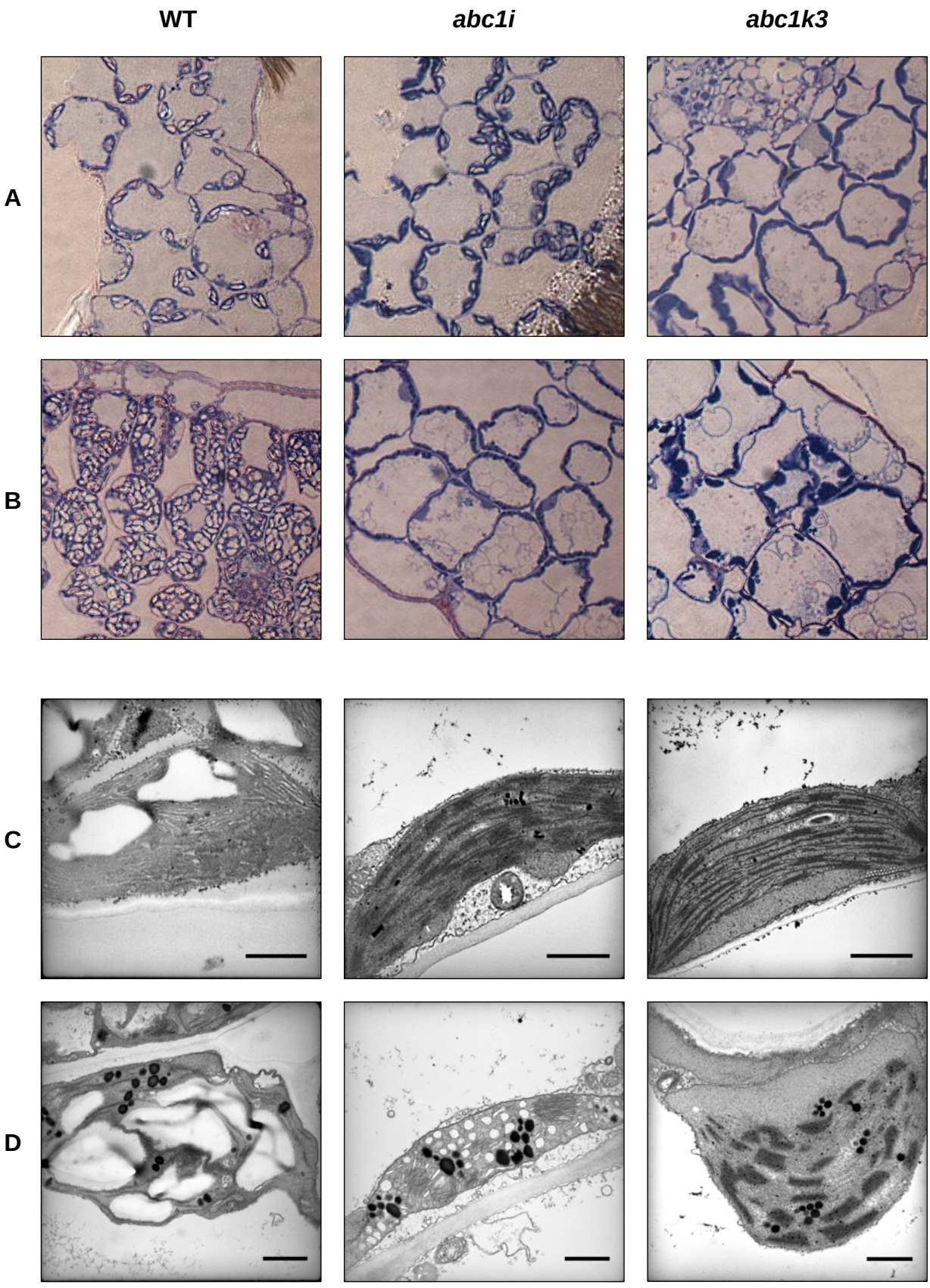

Figure 2.16: Changes in chloroplast ultrastructure observed under HL treatment.

2.3.4 - Photosynthetic activity and the *pgr6* phenotype

The measurement of chlorophyll fluorescence using a Mini-PAM device is a rapid and non-invasive technique giving an excellent indication of the plant photosynthetic functions. As a consequence, it was chosen for the fluorimetric determination of the photosynthetic parameters of *abc1i* and *abc1k3/pgr6* plants using wild-type plants (Col-0) as the control. At the same time, analyses were carried out on knock-out mutant plants for the tocopherol cyclase (*vte1*), which were used as a reference to investigate the effect of the lack of plastochromanol and tocopherols on the photosynthetic activity (see following sections). Measurements were performed at intervals of 24 h on leaves (n = 5) from rosettes grown either under normal light conditions (150 $\mu E \cdot m^{-2} \cdot s^{-1}$) or exposed to continuous high light intensity (HL, 500 $\mu E \cdot m^{-2} \cdot s^{-1}$) for a total duration of 7 days.

On the one hand, no significant differences in PSII quantum efficiency (Fv/Fm), CO_2 assimilation rate or total electron transport rate (ETR) were detected between wild-type, *abc1i* and *vte1* plant lines either under normal light intensity or after short HL treatment (Figure 2.17A-C on page 83). On the contrary, a significant reduction in PSII efficiency was observed in the *vte1* mutant starting from 4 days of continuous HL exposure (Figure 2.17A on page 83). Non-photochemical quenching (NPQ) in the *abc1i* mutant appeared to be slightly lower than in the wild-type, while in *vte1* plants NPQ levels were higher than in the wild-type after a short exposure (1-3 days) to continuous HL but they significantly decreased under prolonged HL treatment (Figure 2.17D on page 83).

On the other hand, photosynthetic activity was severely impaired in the *abc1k3/pgr6* mutant, as expected considering that the *pgr6* mutant was isolated on the basis of its high chlorophyll fluorescence phenotype[(102)]. In order to confirm the functional correspondence between *abc1k3* and *pgr6* mutations and evaluate the photosensitivity of *abc1k1/pgr6* mutant plants under light stress conditions, chlorophyll fluorescence measurements were carried out using a Mini-PAM device. At the same time, photosynthetic gas exchange was also measured in order to determine CO_2 assimilation rate in both wild-type (Col-0) and *abc1k3/pgr6* plants. A dramatic reduction in PSII quantum efficiency (Fv/Fm) was observed in the *abc1k3/pgr6* mutant after a short exposure (1-2 days) to HL conditions. Most strikingly however, maximum PSII activity recovered to almost normal levels after prolonged HL treatment

(Figure 2.17A). This result was confirmed by the analysis of photosynthetic gas exchanges in *abc1k3/pgr6* plants, showing an initial decrease in CO_2 assimilation but then recovering to normal levels after prolonged exposure to HL (Figure 2.17B). Consistently with the pgr6 phenotype, in the *abc1k3/pgr6* mutant ETR levels were also affected at normal light intensities and saturated at the half level of that in the wild-type (Figure 2.17C). NPQ was also severely impaired in the mutant, although *abc1k3/pgr6* plants still exhibited NPQ induction, which depended on light intensity (Figure 2.17D). On the other hand, after a short HL exposure a far more severe reduction in ETR and NPQ (Figures 2.17E and 2.17F, respectively) was observed. However, ETR recovered to normal levels after a prolonged HL treatment (Figure 2.17E), while only a partial increase in NPQ was detected (Figure 2.17F).

Figure 2.17: Plant photosynthetic parameters.

A. PSII activity (Fv/Fm) under continuous HL treatment.

C-D. Light dependance of electron transport rate (ETR) and non-photochemical quenching (NPQ) in plants grown under normal light conditions, respectively.

E-F. ETR and NPQ variations in response to continuous HL treatment, respectively. Leaves (n=5) from plants exposed to normal (150 $\mu E \times m^{-2} \times s^{-1}$) or high (500 $\mu E \times m^{-2} \times s^{-1}$) light intensity were analyzed at intervals of 24 h.

B. Photosynthetic gas exchange measurement. CO_2 assimilation was measured in three separate chambers for each plant line and photosynthetic rate was calculated based on the interpolated leaf area (per hour) to avoid fluctuations. Surfaces correspond to SE. EOD. End of day. EON. End of night.

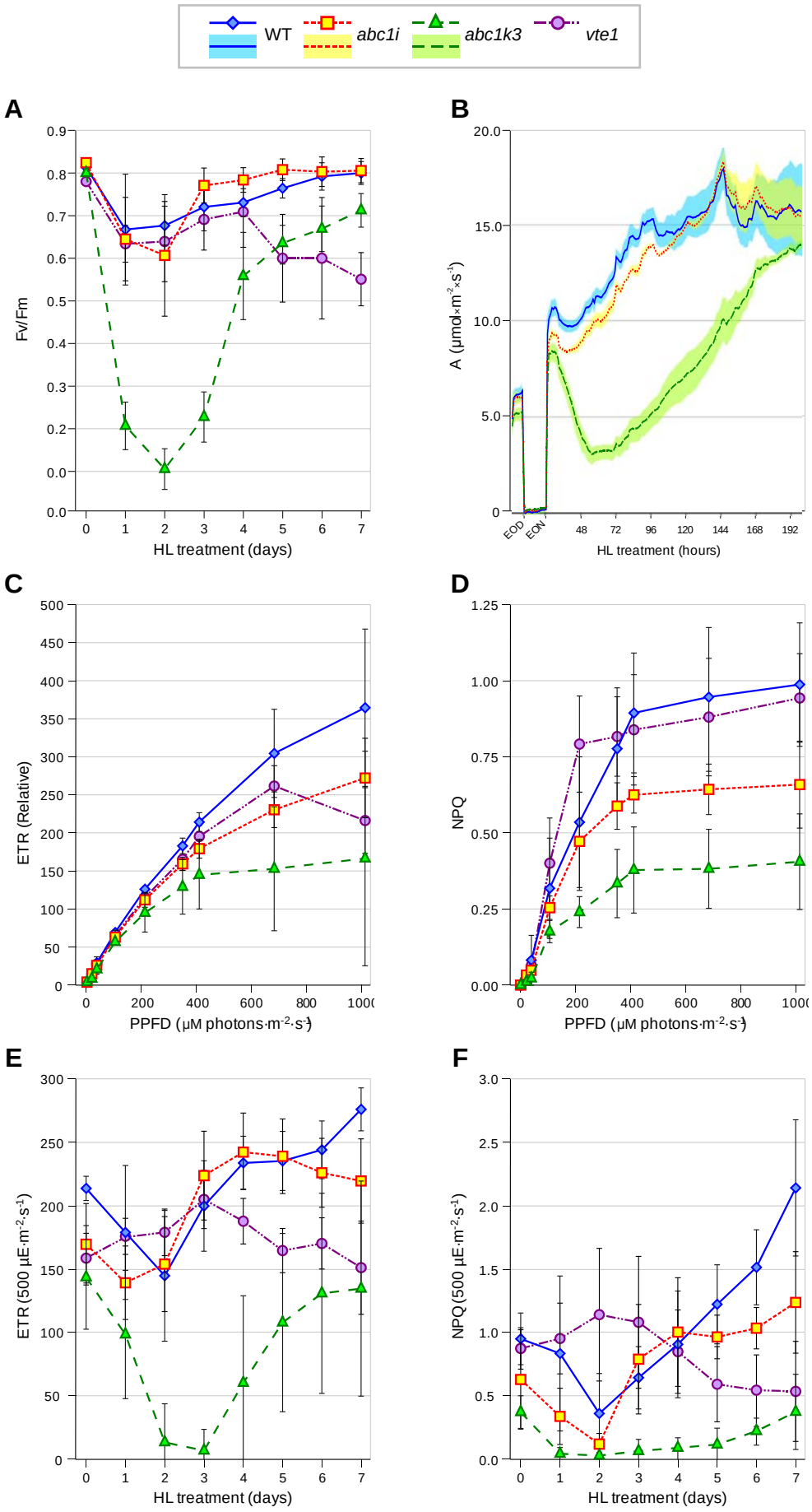
WT
abc1i
abc1k3
vte1
A
Fv/Fm
HL treatment (days)
B
A (µmol·m⁻²·s⁻¹)
EOD
EOW
HL treatment (hours)
C
ETR (Relative)
PPFD (µM photons·m⁻²·s⁻¹)
D
NPQ
PPFD (µM photons·m⁻²·s⁻¹)
E
ETR (500 µE·m⁻²·s⁻¹)
HL treatment (days)
F
NPQ (500 µE·m⁻²·s⁻¹)
HL treatment (days)

Figure 2.17

2.3.5 - Starch and sugar metabolism are affected in *abc1k3/pgr6*

In order to determine whether the absence of starch granules previously observed in *abc1i* and especially in *abc1k3/pgr6* chloroplasts (Figure 2.16 on page 80) depended exclusively on the reduction of the photosynthetic activity or on other mechanisms, starch content was determined in total rosettes exposed for increasing time to HL intensity.

In a preliminary experiment, a simple starch coloration with Lugol's iodine solution was used to visually determine its accumulation in leaves (Figure 2.18 on page 85). A significant increase in starch content was observed in wild-type leaves after 1-2 days of HL treatment, while the starch accumulation rate was slightly lower in the *abc1i* mutant. Conversely, no starch was detected by histochemical coloration in *abc1k3/pgr6* leaves both under normal light conditions and after exposure to HL intensity. Only after 6-7 days of continuous HL treatment a limited starch accumulation was observed in the *abc1k3/pgr6* mutant.

In order to achieve a precise measurement of starch content in total rosettes, samples were extracted in perchloric acid and starch concentration was enzymatically assayed after treatment with α-amylase and amyloglucosidase (Figure 2.19A on page 86).
Interestingly, no significant differences were detected between wild-type and *abc1i* starch levels, despite the previous phenotypic observations (Figures 2.16 and 2.18 on pages 80 and 85, respectively).
On the contrary, starch levels in the *abc1k3/pgr6* mutant were lower than in wild-type plants already under normal light conditions. Moreover, after short HL treatment starch accumulated in the wild-type, while a reduction in its content was observed in *abc1k3/pgr6* plants. However, after prolonged HL treatment, only a partial and delayed recovery in starch accumulation was detected in the *abc1k3/pgr6* mutant, in contrast with the significant recovery in PSII efficiency and CO_2 assimilation rate observed in the same plants (Figures 2.17A and 2.17B on page 83, respectively).

At the same time, in order to determine whether sugar metabolism or partitioning between starch and free sugars were also affected, the leaf content of glucose, fructose, maltose and sucrose was analyzed.

In the *abc1i* mutant, the detected levels for all the analyzed sugars were generally similar to the wild-type or slightly higher, especially after short exposure (2-3 days) to HL intensity (Figure 2.19B-E on page 86).

Conversely, glucose, fructose and maltose content in the *abc1k3/pgr6* mutant was significantly lower than in wild-type plants after short HL exposure but it recovered after prolonged HL treatment (Figure 2.19B-D on page 86). Moreover, sucrose content in the *abc1k3/pgr6* mutant was maximal at about half the level of the wild-type after 2 days of HL treatment, but it then accumulated to 1.5-fold the amount of the wild-type after 7 days of exposure to continuous HL (Figure 2.19E on page 86).

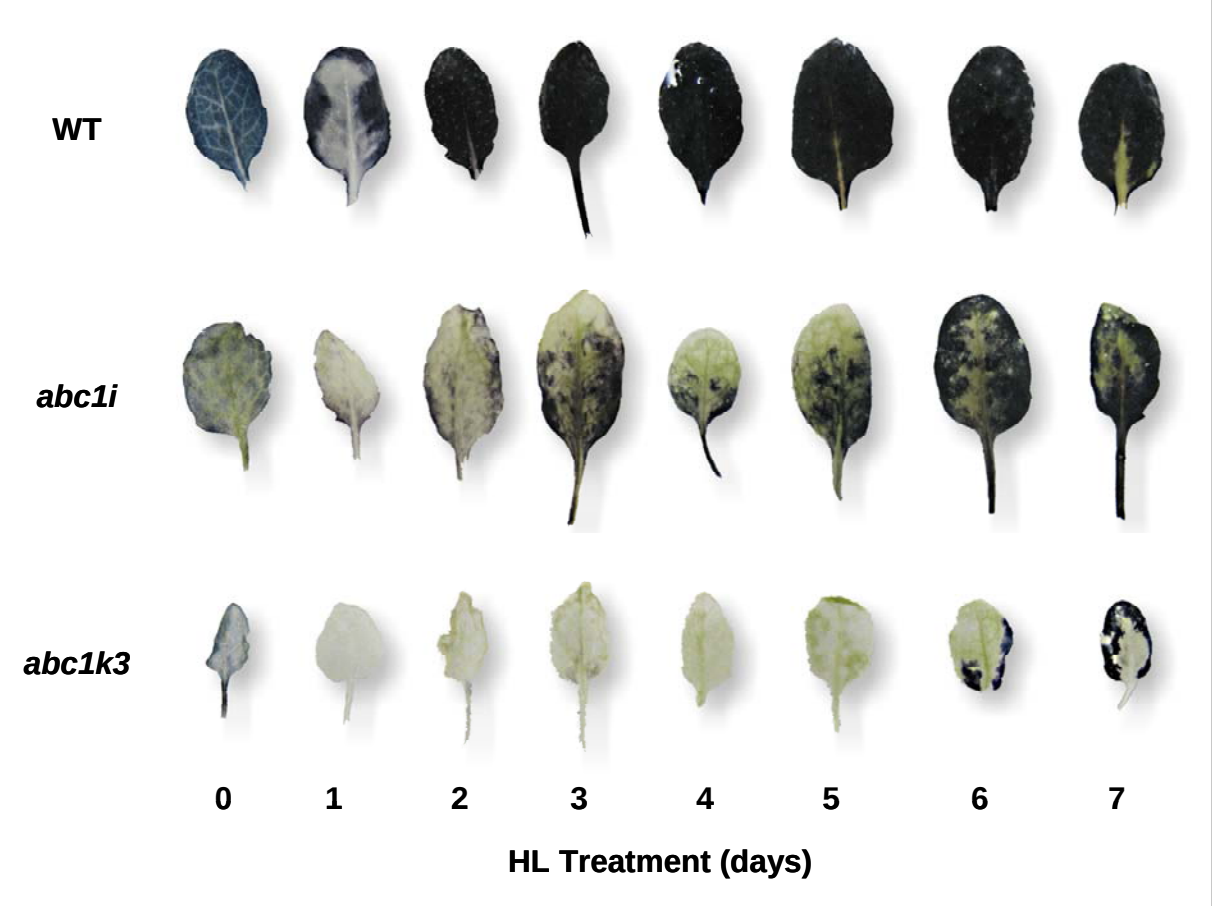

Figure 2.18: Visualization by Lugol's test of starch accumulation in *A. thaliana* leaves after exposure to HL.

Plants grown under normal light conditions (150 µE × m^{-2} × s^{-1}) or exposed to continuous high light (500 µE × m^{-2} × s^{-1}) for 7 days were boiled in water and washed in 80% EtOH to elute chlorophyll and other pigments, then starch was stained with Lugol's iodine solution.

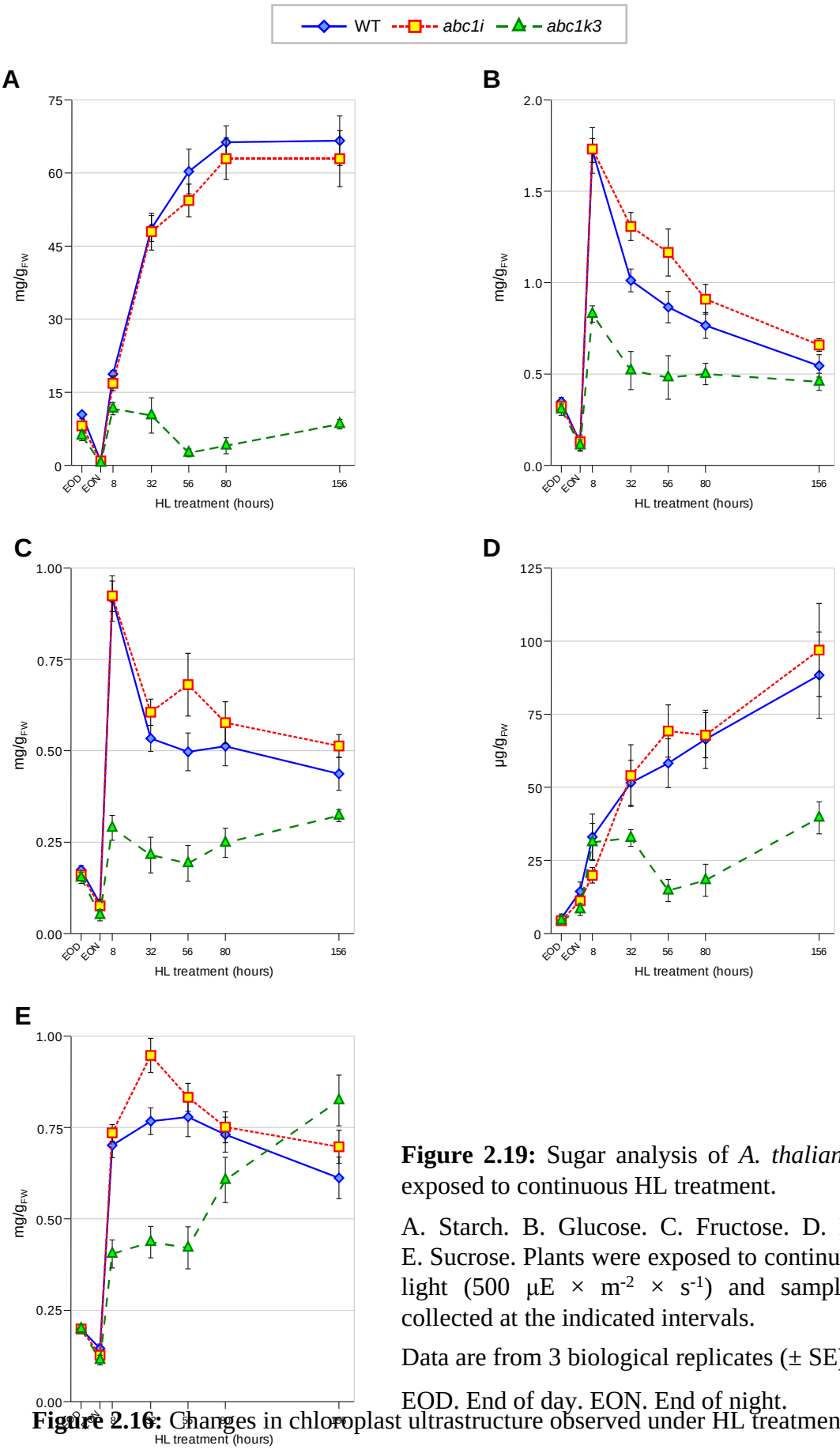

Figure 2.19: Sugar analysis of *A. thaliana* plants exposed to continuous HL treatment.

A. Starch. B. Glucose. C. Fructose. D. Maltose. E. Sucrose. Plants were exposed to continuous high light (500 µE × m^{-2} × s^{-1}) and samples were collected at the indicated intervals.

Data are from 3 biological replicates (± SE).

EOD. End of day. EON. End of night.

Figure 2.16: Changes in chloroplast ultrastructure observed under HL treatment.

2.3.6 - ABC1I and ABC1k3 have a major effect on prenylquinone and carotenoid composition of membranes

In order to investigate whether the *abc1i* and *abc1k3/pgr6* mutants are affected in prenylquinone and carotenoid composition, the lipid profiling of total rosette was carried out by ultra-high pressure liquid chromatography coupled to atmospheric pressure chemical ionization-quadrupole time of flight mass spectrometry (UHPLC-APCI-QTOFMS), a powerful analytical technique for rapid and reliable lipid profiling of plant samples. Analyses were carried out on the tocopherol cyclase knock-out mutant *vte1* as well, which is known to be defective in the synthesis of plastochromanol and tocopherols and instead accumulates the tocopherol precursor DMPBQ[(64)].

Total leaf extracts from 2-month-old *A. thaliana* rosettes grown under normal light conditions or exposed to continuous HL stress for an increasing period of time (1, 2 and 7 days, respectively) were subjected to analysis using the method previously described (see Section 2.2.3), resulting in the detection of more than 400 peaks in negative APCI mode. The identified prenylquinones and carotenoids are presented in Table 2.2 on page 70.

2.3.6.1 - Global effect on the lipid composition of mutant plants

Principal component analysis (PCA) represents a powerful statistical tool that allows to identify patterns in large datasets like those generated by lipid profiling, as well as the relative molecule distribution between samples. For this reason and to highlight differences between wild-type, *abc1i* and *vte1* plants and to investigate changes in the prenylquinone and carotenoid profile between wild-type and *abc1k3/pgr6* plants in response to HL treatment, untargeted PCA was applied on the obtained data.

Both under normal light conditions and after HL exposure, wild-type and *abc1i* samples clustered separately and were significantly different from *vte1*. Interestingly, the *abc1i* cluster co-localized with the α-T oxidative-derivate α-TQ but not with the other tocopherols, which were typical of wild-type samples. On the contrary, *vte1* samples co-localized with the xanthophyll lutein and the tocopherol precursor DMPBQ (Figure 2.20A-B on page 90).

At the same time, under normal light conditions wild-type and *abc1k3/pgr6* samples clustered separately, and a strong separation between them was observed starting after 1 day of HL exposure (Figure 2.21A-D on page 91). In particular, both under normal light conditions and after short HL exposure, wild-type samples co-localized with higher levels of tocopherols (α-, γ- and δ-T), plastoquinone (PQ-9), plastochromanol (PC-8) and of the xanthophyll lutein. On the contrary, *abc1k3/pgr6* co-localized with two oxidative-derivates of PQ-9 and PC-8 (PQ-OH and PC-OH, respectively). Besides, after 7 days of continuous HL treatment *abc1k3/pgr6* plants accumulated higher amounts of α-tocopherol quinone (α-TQ), an α-T oxidative-derivate generated in thylakoid membranes by spontaneous oxidation and recycled in a VTE1-dependent manner, but not of the other tocopherols, which were typical of wild-type samples (Figure 2.21D on page 91). Interestingly, the *abc1k3/pgr6* mutant also co-localized with higher levels of lutein after prolonged HL treatment (Figure 2.21D on page 91).

2.3.6.2 - *abc1i* and *abc1k3/pgr6* mutations affect carotenoid and prenylquinone content

A quantification of the identified prenylquinones and carotenoids was also performed to determine variations in their content between wild-type, *abc1i*, *abc1k3/pgr6* and *vte1* plants and in response to HL exposure (Figure 2.22A-I).

Relatively similar α-, γ- and δ-T levels were detected in wild-type, *abc1i* and *abc1k3/pgr6* plants under normal light conditions. However, their content did not increase in the *abc1k3/pgr6* mutant after HL exposure, in contrast with wild-type plants, while only a slightly slower accumulation rate was observed in *abc1i* mutants (Figure 2.22A-C on page 92). On the contrary, under HL treatment both *abc1i* and, to a lower extent, *abc1k3/pgr6* mutants accumulated significantly higher amounts of α-TQ, a tocopherol Redox cycle intermediate generated in thylakoid membranes by spontaneous oxidation and recycled to α-T in a VTE1-dependent manner (Figure 2.22D on page 92). In order to determine if the observed phenotype was simply a variant of the *vte1* phenotype, a comparison with the knock-out line for the tocopherol cyclase VTE1 was carried out. *Vte1* mutants completely lacked α-, γ- and δ-T and accumulated the precursor DMPBQ instead. However, DMPBQ was detected neither in *abc1i* nor in *abc1k3/pgr6* mutant plant lines (Figure 2.22E on page 92).

Most strikingly, in *abc1i* and *abc1k3/pgr6* plants the detected levels of another VTE1 product, plastochromanol-8 (PC-8), were 4-fold and 1-fold lower, respectively, than in the wild-type, and did not significantly change after HL exposure (Figure 2.22F on page 92). As expected, no PC-8 was detected in the *vte1* mutant.

The total content of the direct precursor of PC-8, plastoquinone-9 (PQ-9), was also significantly lower than in the wild-type in *abc1i*, *abc1k3/pgr6* and *vte1* mutant plants grown under normal light conditions, while PQ-9 levels in the four plant lines were similar after short exposure to HL (Figure 2.22G on page 92). Conversely, a significant reduction in total PQ-9 content (1-fold and 1.75-fold less than in the wild-type, respectively) was detected in both *abc1k3/pgr6* and *vte1* mutants after prolonged HL treatment, while in *abc1i* plants PQ-9 levels were similar to the wild-type. Moreover, the Redox state of the PQ-9 pool did not significantly change after HL exposure neither in the *abc1k3/pgr6* nor in the *vte1* mutant, in contrast with the significant accumulation of the reduced form (PQH_2) detected in the wild-type, as previously reported by[35,80].

Carotenoid content was affected as well in the mutants. In particular, β-Carotene levels in *abc1i*, *abc1k3/pgr6* and *vte1* plants were significantly lower than in the wild-type under both normal growth conditions and after short exposure to HL intensity but then recovered to wild-type levels after prolonged HL treatment (Figure 2.22H on page 92).

At the same time, under normal light intensity the leaf content of the xanthophyll lutein was lower than in the wild-type in both the *abc1i* and *abc1k3/pgr6* mutants, but it significantly accumulated in *abc1i* and *abc1k3/pgr6* plants after short or prolonged HL treatment, respectively (Figure 2.22I on page 92). In *vte1* mutant plants, lutein accumulation was observed both under normal growth conditions or after prolonged HL exposure, as previously reported[69].

As previously observed by PCA on total lipidomics data, other molecules appeared to be potentially affected either by the *abc1i* and the *abc1k3/pgr6* mutations, yet no precise identification could be achieved based on their *m/z* ratio.

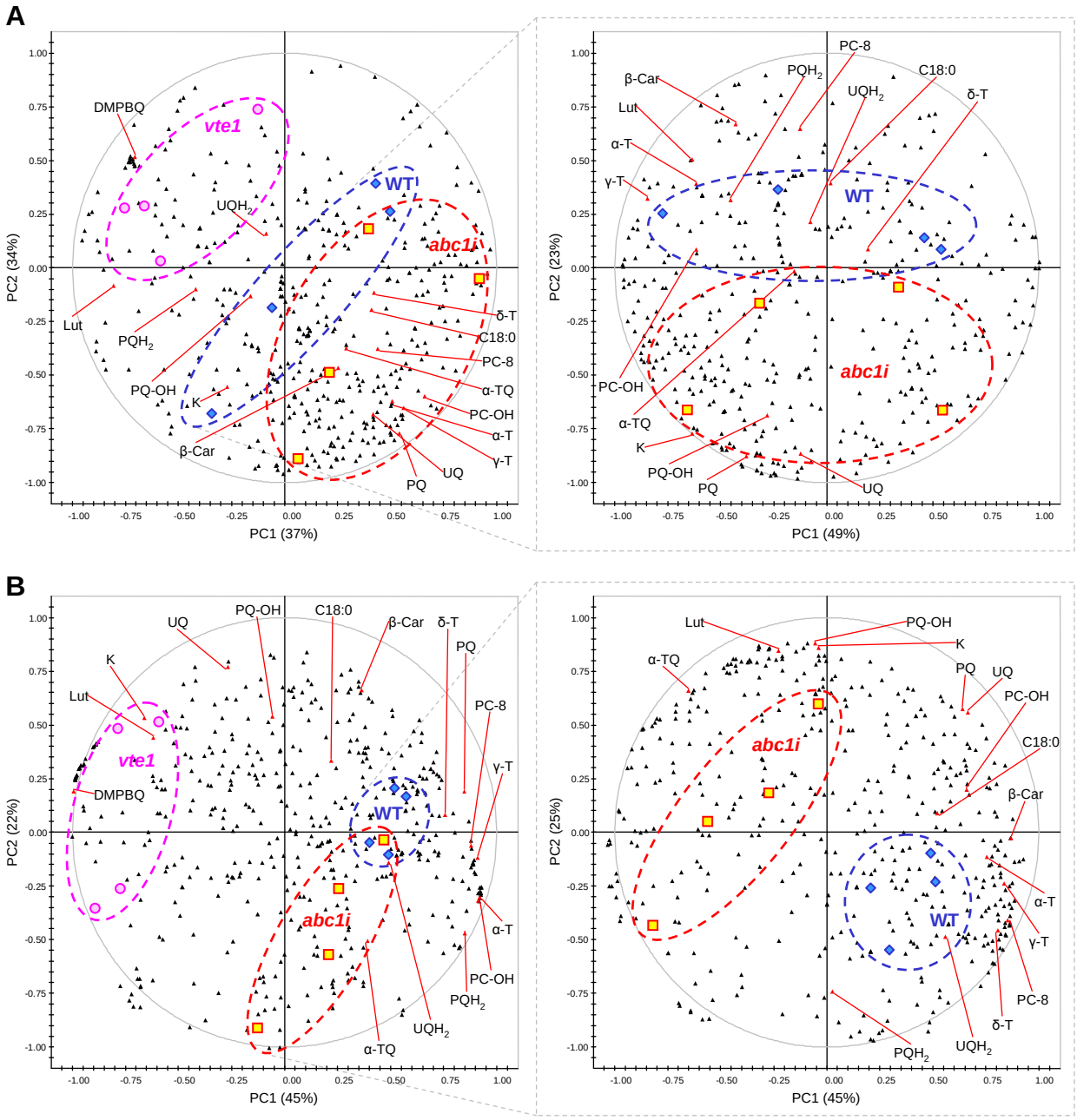

Figure 2.20: Bi-plots derived from an untargeted principal component analysis (PCA) showing differences between the lipid profiles of wild-type, *abc1i* and *vte1* plants.

A. Plants grown under normal light conditions (150 µE × m^{-2} × s^{-1}).

B. Plants exposed to continuous high light (500 µE × m^{-2} × s^{-1}) for 7 days. Inset on the right: Bi-plots from a PCA performed exclusively on wild-type (WT) and *abc1i* data. Colored squares correspond to the observations (n = 4 for each plant line) and black triangles represent the variables. PC1 and PC2 are first and second principal components, respectively, with their percentage of explained variance. The identified prenylquinones and carotenoids are indicated (confront with Table 2.2).

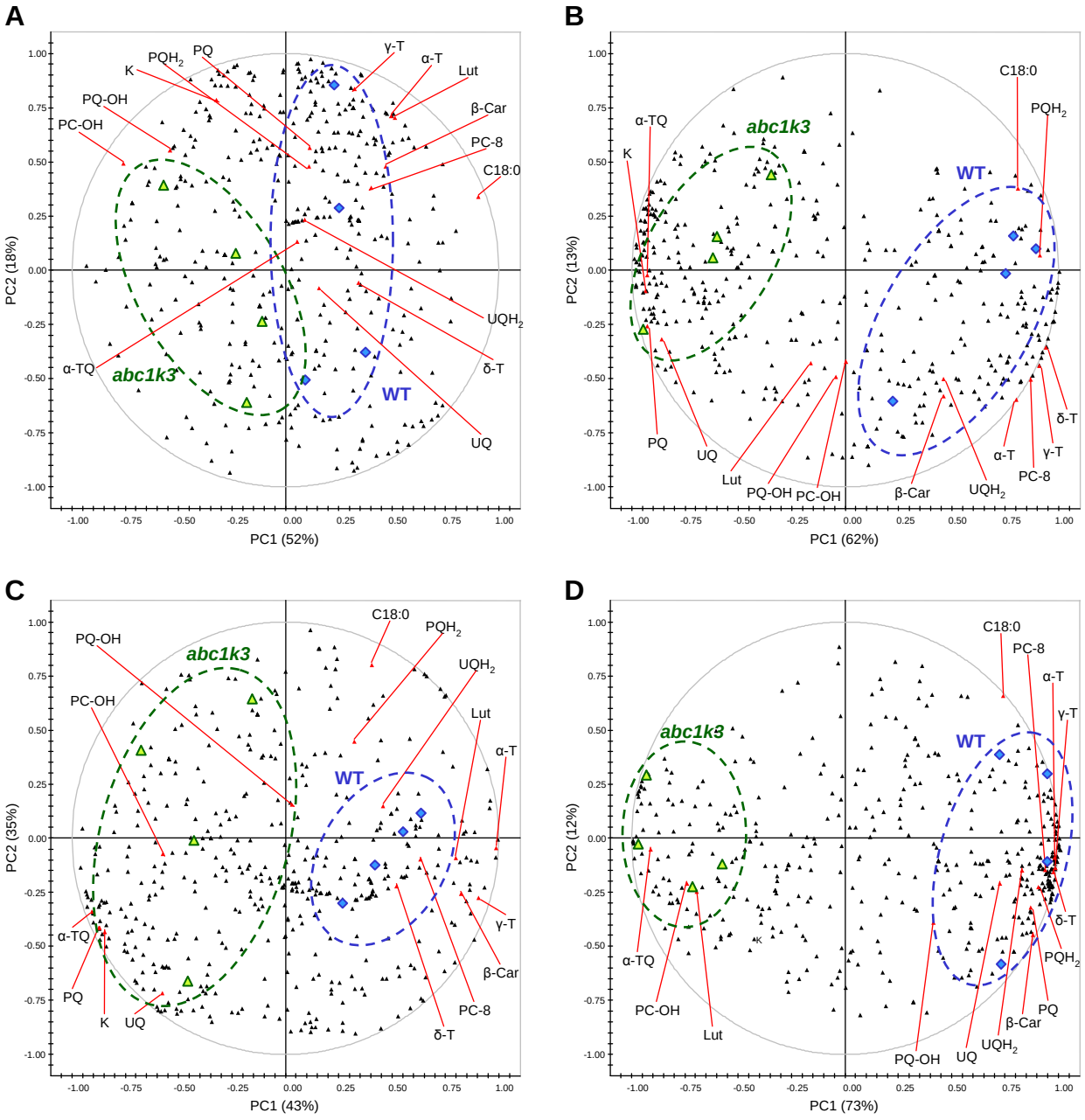

Figure 2.21: Bi-plots derived from an untargeted principal component analysis (PCA) showing differences between the lipid profiles of wild-type and *abc1k3* plants.

A. Plants grown under normal light conditions (150 µE × m^{-2} × s^{-1}).

B-D. Plants exposed to continuous high light (500 µE × m^{-2} × s^{-1}) for 1 day, 2 days and 7 days, respectively. Colored squares correspond to the observations (n = 4 for each plant line) and black triangles represent the variables. PC1 and PC2 are first and second principal components, respectively, with their percentage of explained variance. The identified prenylquinones and carotenoids are indicated (confront with Table 2.2).

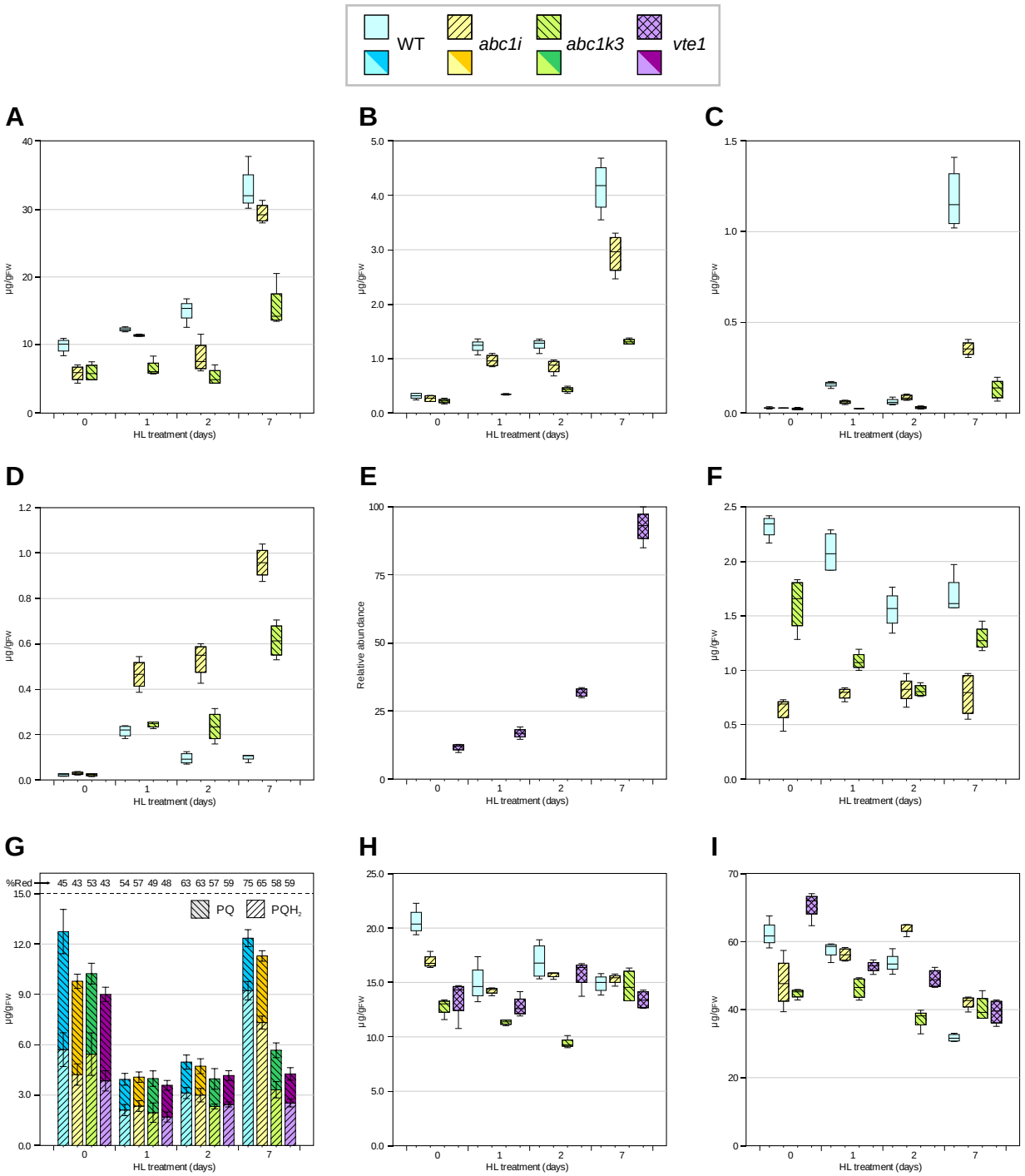

Figure 2.22: Comparison of the total leaf content of selected prenylquinones and carotenoids.

A. α-tocopherol. B. γ-tocopherol. C. δ-tocopherol. D. α-tocopherol quinone. E. 2,3-dimethyl-5-phytyl-1,4-hydroquinone (DMPBQ). F. Plastochromanol-8. G. Plastoquinone-9, oxidized (PQ) and reduced (PQH_2) forms. Reduction rate (PQH_2/total PQ-9) is indicated. H. β-carotene. I. Lutein. Plants grown under normal light conditions (day 0, 150 µE × m^{-2} × s^{-1}) were exposed to continuous high light (500 µE × m^{-2} × s^{-1}) for 1, 2 and 7 days, respectively. Data are from 4 biological replicates (± SD). Note that *vte1* lacks the compounds in panels A, B, C, D and F and accumulates E instead.

2.3.6.3 - Prenylquinone sub-organellar distribution

In an attempt to investigate changes in the prenylquinone distribution between plastoglobules and thylakoid membranes in response to HL treatment or caused by the knock-out mutation of the two ABC1-like or the tocopherol cyclase, the prenylquinone content of equal volumes of purified chloroplast fractions corresponding to plastoglobules and thylakoids was measured by UHPLC-APCI-QTOFMS.

Lipidomics analyses were performed on fractions extracted either from plants grown under normal light conditions (150 μE × m^{-2} × s^{-1}) or from wild-type and *abc1k3/pgr6* plants exposed to HL (500 μE × m^{-2} × s^{-1}) for 2 and 7 days, respectively.

The plastoglobule fraction was enriched in both α-T and PQ-9 (Figure 2.23A and C on page 94), as previously reported[5,33-36]. At the same time, the relative abundance of α-TQ and PC-8 was also determined (Figure 2.23B and D on page 94).

However, no significant differences were detected in the relative distribution of the indicated molecules between different plant lines or in response to HL stress.

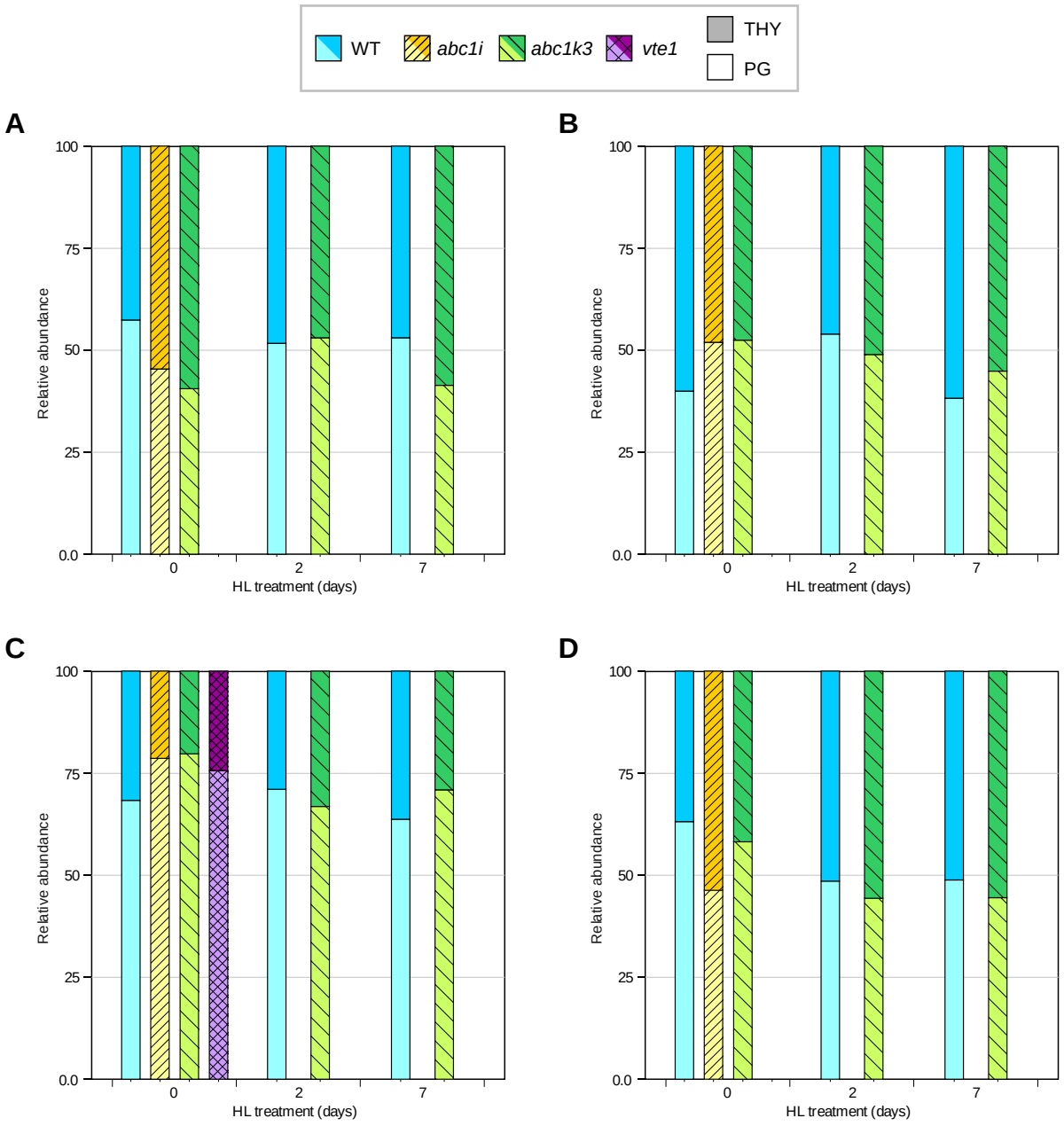

Figure 2.23: Relative distribution of selected prenylquinones between plastoglobules and thylakoid membranes.

A. α-tocopherol. B. α-tocopherol quinone C. Plastoquinone-9. D. Plastochromanol-8. Plants were grown under normal light conditions (day 0, 150 µE × m^{-2} × s^{-1}), then wild-type and *abc1k3/pgr6* were exposed to continuous high light (500 µE × m^{-2} × s^{-1}) for 2 and 7 days, respectively. Chloroplasts were then extracted and fractionated on linear sucrose gradients. Prenylquinones were extracted from equal volumes of purified fractions (n=4) corresponding to plastoglobules (PG) and thylakoid membranes (THY), then analyzed by UHPLC-APCI-QTOFMS.

Data refer to the relative abundance of the indicated prenylquinones between PG and THY. As a consequence, they are indipendent from the total molecule levels in samples as well from the variations in content registered between plant lines and in response to HL treatment (confront with Figure 2.22).

2.3.7 - The plastoglobule proteome is directly affected in both *abc1i* and *abc1k3/pgr6* mutant plants

2.3.7.1 - Plastoglobule analysis by immunoblotting

Considering the relevance of the enzymatic products of the tocopherol cyclase on the observed differences in prenylquinone composition of both *abc1i* and *abc1k3/pgr6* plants (Figures 2.20, 2.21 and 2.22 on pages 90-92, respectively), as well as the photoprotective activity of these molecules during HL acclimation, a possible variation in VTE1 content or sub-cellular localization was investigated by Western Blot analysis. For this reason, the knock-out mutant line *vte1* was used as reference.

Moreover, in order to investigate a potential effect of the two kinases on the protein composition of plastoglobules, envelope and thylakoid membranes, Western Blot analysis was carried out using antibodies raised against the two most abundant plastoglobule fibrillins FBN1a and FBN2[(40)], as well as the envelope and thylakoid markers Toc75 and LHCb2, respectively. Equal protein amounts of stromal and purified chloroplast membrane sub-fractions corresponding to plastoglobules, envelope and thylakoids were extracted from plants grown under normal light conditions, separated by SDS-PAGE, transferred to nitrocellulose and probed using αVTE1, αFBN1a/b, αFBN2, αToc75 and αLHCb2 antibodies (Figures 2.24 and 2.25 on pages 96 and 97, respectively).

Figure 2.24: Western blot analysis on wild-type, *abc1i* and *vte1* purified chloroplast sub-fractions.
Total proteins were extracted from: A. Total chloroplast membranes (MEM), plastoglobules (PG) and thylakoids (THY). B. Stroma. C. Chloroplast envelope. Proteins were separated by SDS-PAGE, transferred to nitrocellulose membrane and immunoblotted using the indicated antibodies raised against: the 75 kDa translocon at the outer envelope membrane (Toc75), the tocopherol cyclase (VTE1), the two most abundant plastoglobule fibrillins (FBN1a and FBN2, respectively) and the light-harvesting antenna type II chlorophyll a/b-binding protein (LHCb2). The positions of the detected proteins on the membrane are indicated by white triangles.

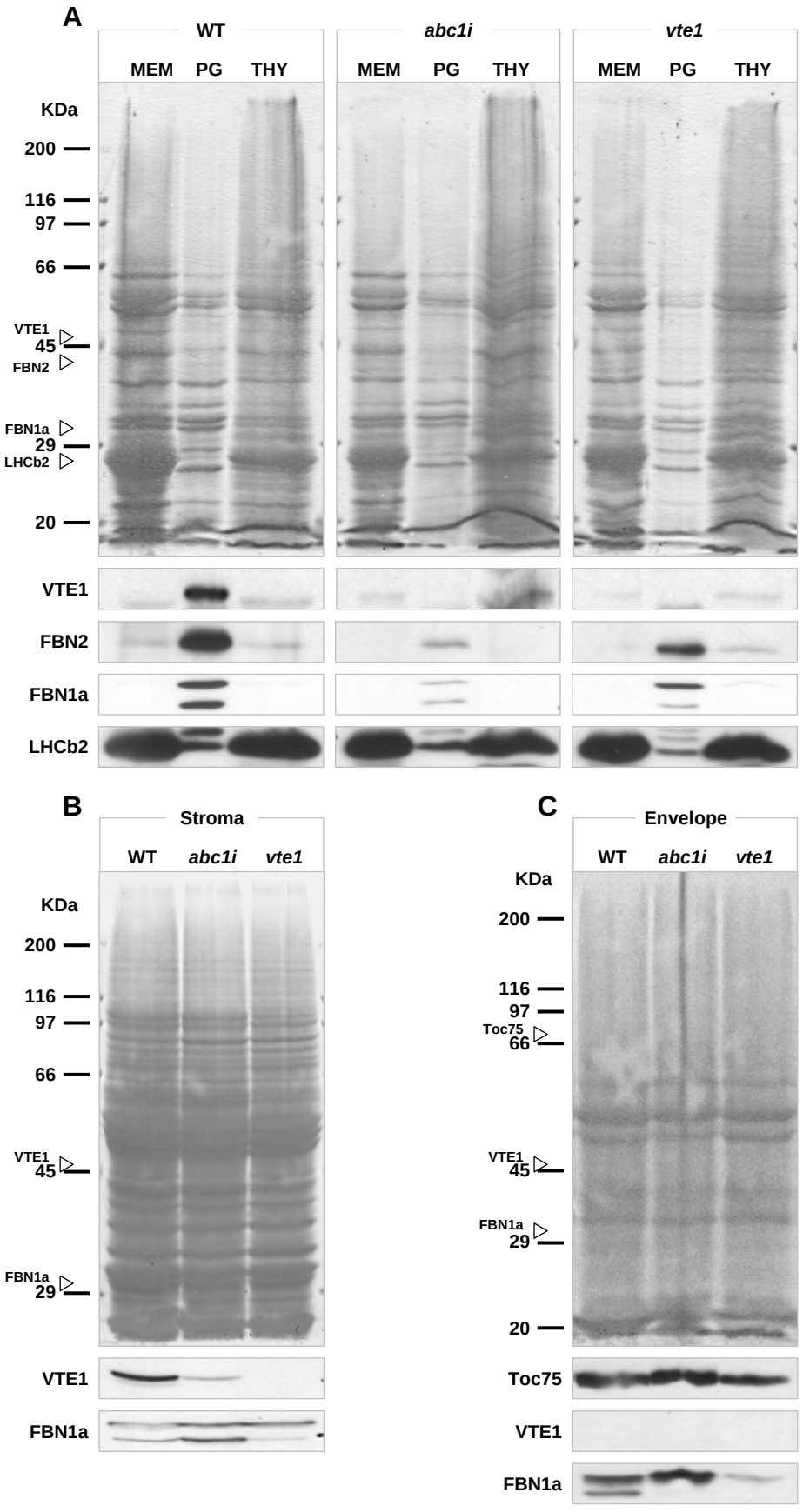
A
WT
abc1i
vte1
MEM PG THY
MEM PG THY
MEM PG THY
KDa
200
116
97
66
VTE1
45
FBN2
FBN1a
29
LHCb2
20
VTE1
FBN2
FBN1a
LHCb2
B
Stroma
WT abc1i vte1
KDa
200
116
97
66
VTE1
45
FBN1a
29
VTE1
FBN1a
C
Envelope
WT abc1i vte1
KDa
200
116
97
Toc75
66
VTE1
45
FBN1a
29
20
Toc75
VTE1
FBN1a

Figure 2.24

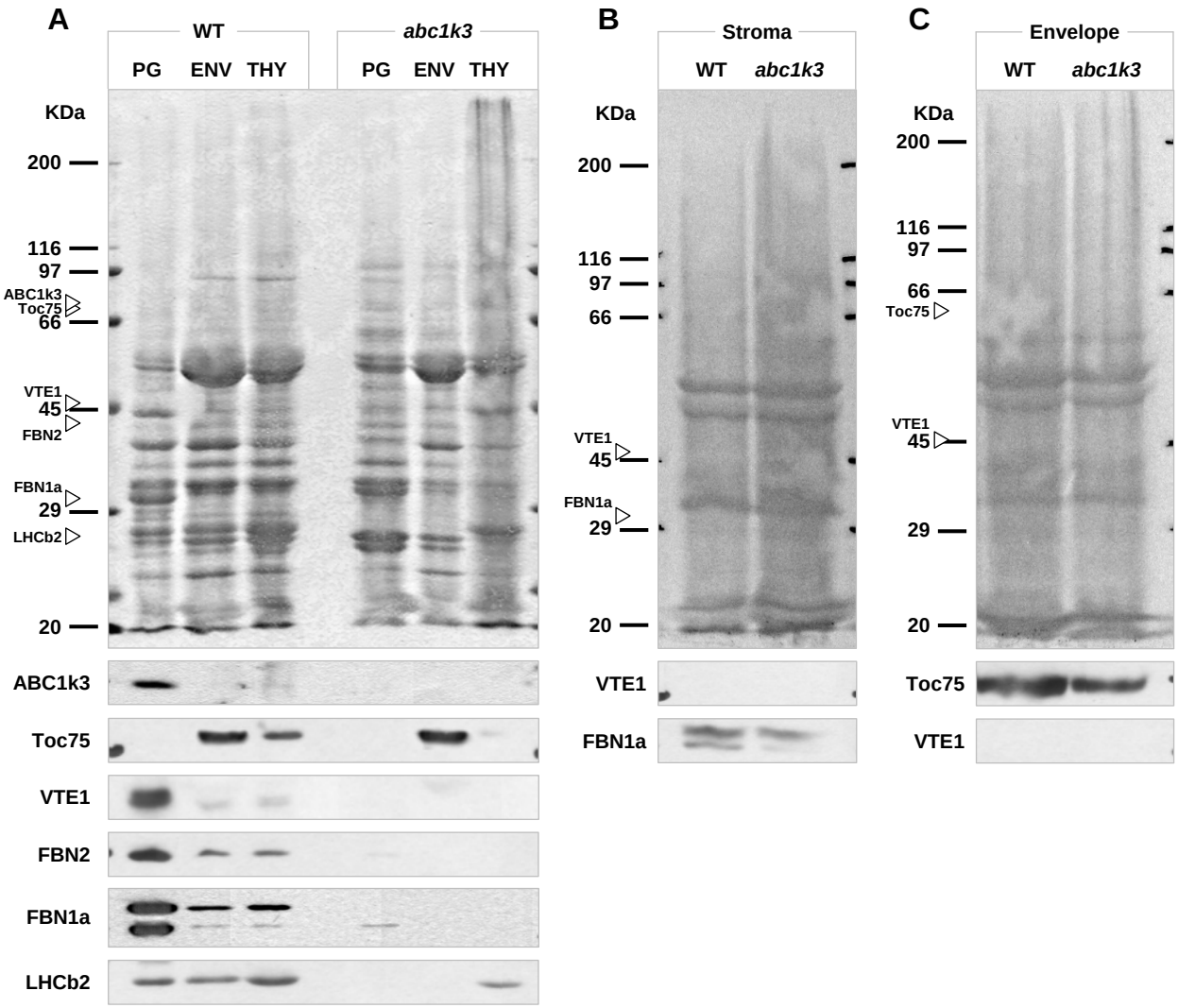

Figure 2.25: Western blot analysis on wild-type and *abc1k3* purified chloroplast sub-fractions. Total proteins were extracted from: A. Plastoglobules (PG), envelope (ENV) and thylakoids (THY). B. Stroma. C. Chloroplast envelope. Proteins were separated by SDS-PAGE, transferred to nitrocellulose membrane and immunoblotted using the indicated antibodies raised against: the ABC1-like kinase ABC1K1, the 75 kDa translocon at the outer envelope membrane (Toc75), the tocopherol cyclase (VTE1), the two most abundant plastoglobule fibrillins (FBN1a and FBN2, respectively) and the light-harvesting antenna type II chlorophyll a/b-binding protein (LHCb2). The positions of the detected proteins on the membrane are indicated by white triangles.

VTE1 was detected in wild-type plastoglobules but was below the detection limit in both *abc1i* and *abc1k3/pgr6* mutants (Figures 2.24A and 2.25A on pages 96 and 97, respectively). As expected, VTE1 was not present in the knock-out line *vte1* (Figure 2.24A). Moreover, no VTE1 accumulation in the stroma or in the envelope was detected neither in the *abc1i* nor in the *abc1k3/pgr6* mutant (Figures 2.24B-C and 2.25A-C on pages 96 and 97, respectively). In order to determine whether the expression of the *VTE1* gene was affected or whether the observed reduction occurred at a post-transcriptional level, quantitative RT-PCR experiments were carried out on total RNA extracted from fresh wild-type, *abc1i*, *abc1k3/pgr6* and *vte1* leaves. A significant increase in *VTE1* transcript levels was observed in the *abc1i* and the *abc1k3/pgr6* mutants compared to wild-type plants (2.75-fold and 2.5-fold, respectively), while only a weak, presumably background signal was detected in the *vte1* mutant (Figure 2.26).

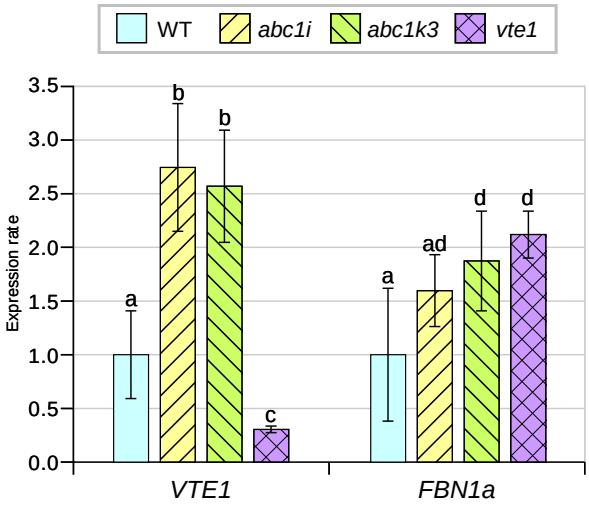

Figure 2.26: Changes in *VTE1* and *FBN1a* gene expression rate determined by real-time RT-PCR.

Total RNA extracted from untreated leaves was used for PCR assays. *ACTIN2* expression levels were used for normalization. Significant differences between samples (n=3 for each plant line) were determined by a one-way ANOVA.

Concerning the other proteins investigated by immunoblotting, the plastoglobule levels of the fibrillin FBN2 appeared to be significantly lower in both *abc1i* and *abc1k3/pgr6* plants, while its content in *vte1* samples was only moderately lower than in the wild-type (Figures 2.24A and 2.25A on pages 96 and 97, respectively).

The use of αFBN1a antibodies for immunoblotting resulted in the detection of two distinct proteins with a predicted molecular weight slightly higher than 30 kDa and corresponding to the two fibrillins FBN1a and FBN1b, as previously observed[(226)]. In *abc1i* plastoglobules, both proteins were less abundant than in wild-type, while *vte1* plants showed a similar content of the upper band (FBN1a), whereas the intensity of the lower one (FBN1b) was lower. Conversely, in *abc1k3/pgr6* plastoglobules the intensity of the upper band (FBN1a) was

below the detection limit and a significant reduction in the content of the lower one (FBN1b) was observed when compared to wild-type plants.
Similarly to what previously described for *VTE1*, in order to determine whether the *FBN1a* gene expression was reduced at a post-transcriptional level, a quantitative RT-PCR was also performed for the *FBN1a* transcript to determine a possible defect in its gene expression rate in the different plant lines (Figure 2.26 on page 98). A significant increase in the expression of *FBN1a* was detected in both *abc1i* and *abc1k3/pgr6* mutants (1.5 and 1.8-fold more, respectively) when compared to the wild-type. Most surprisingly however, a 2.2-fold increase in *FBN1a* expression rate was detected in *vte1* plants, indicating that the absence of the tocopherol cyclase induces the expression of *FBN1a*.

A reduction in the content of the chlorophyll binding protein LHCb2 was also observed in *abc1k3/pgr6* thylakoids (Figure 2.25A on page 97), while its content in *abc1i* and *vte1* mutant plants did not significantly differ from the wild-type (Figure 2.24A on page 96). Moreover, no significant differences between wild-type, *abc1i*, *abc1k3/pgr6* and *vte1* plants were observed with regard to the envelope marker Toc75 (Figures 2.24C and 2.25A and C on pages 96 and 97, respectively).

2.3.7.2 - Preliminary PG proteome profiling by mass spectrometry

In order to determine possible variations in the levels of plastoglobule proteins for which no antibodies were available, proteome profiling was attempted by mass spectrometry on purified chloroplast fractions extracted either from wild-type, *abc1i* and *vte1* plants grown under normal conditions and from wild-type and *abc1k3/pgr6* plants before and after prolonged HL treatment. Proteins were extracted from highly purified low-density fraction enriched in plastoglobules and briefly separated by 1-D SDS-PAGE. Total proteins were then excised from the gel, enzymatically digested with trypsin and they were then identified and quantified by UHPLC-Nanospray-QTOFMS analysis.
Unfortunately, several proteins predicted to constitute the plastoglobule proteome[36,39,40] were under the detection limit of the instrument. At the same time, contaminants from stroma and thylakoids were detected as well during this preliminary experiment (data not shown).
The relative content of the detected plastoglobule proteins in the four plant lines under different light conditions is reported in Figure 2.27.

A significant lower fibrillin (FBN4, FBN2, FBN1a, FBN1b and FBN7a) content was detected in the *abc1i* mutant when compared to the wild-type (Figure 2.27A on page 101), which is consistent with the previous observations performed for FBN2, FBN1a and FBN1b by immunoblotting (Figure 2.24A on page 96). Similarly, *vte1* plants were characterized by a fibrillin content similar or slightly lower than the wild-type, with the exception of FBN4 and FBN7a, which were significantly more abundant than in wild-type plants.
At the same time, significantly lower levels of the three fructose bisphosphate aldolases FBPA1, FBPA2 and FBPA3 were detected in the *abc1i* mutant, while their content in *vte1* plastoglobules was similar to the wild-type.
As a general rule, the *abc1i* mutant was characterized by low levels of the other plastoglobule proteins detected instead in both wild-type and *vte1* plants, with the exception of the allene oxide synthase (AOS), whose content was similar to the wild-type. Moreover, a significant accumulation of the lipase lipooxygenase PLAT/LH2-1 was observed in *abc1i* plastoglobules, while it was below the detection limit in both wild-type and *vte1* plants.
Interestingly, a significant accumulation of a protein with unknown function (At4g13200) was detected in the *vte1* mutant.

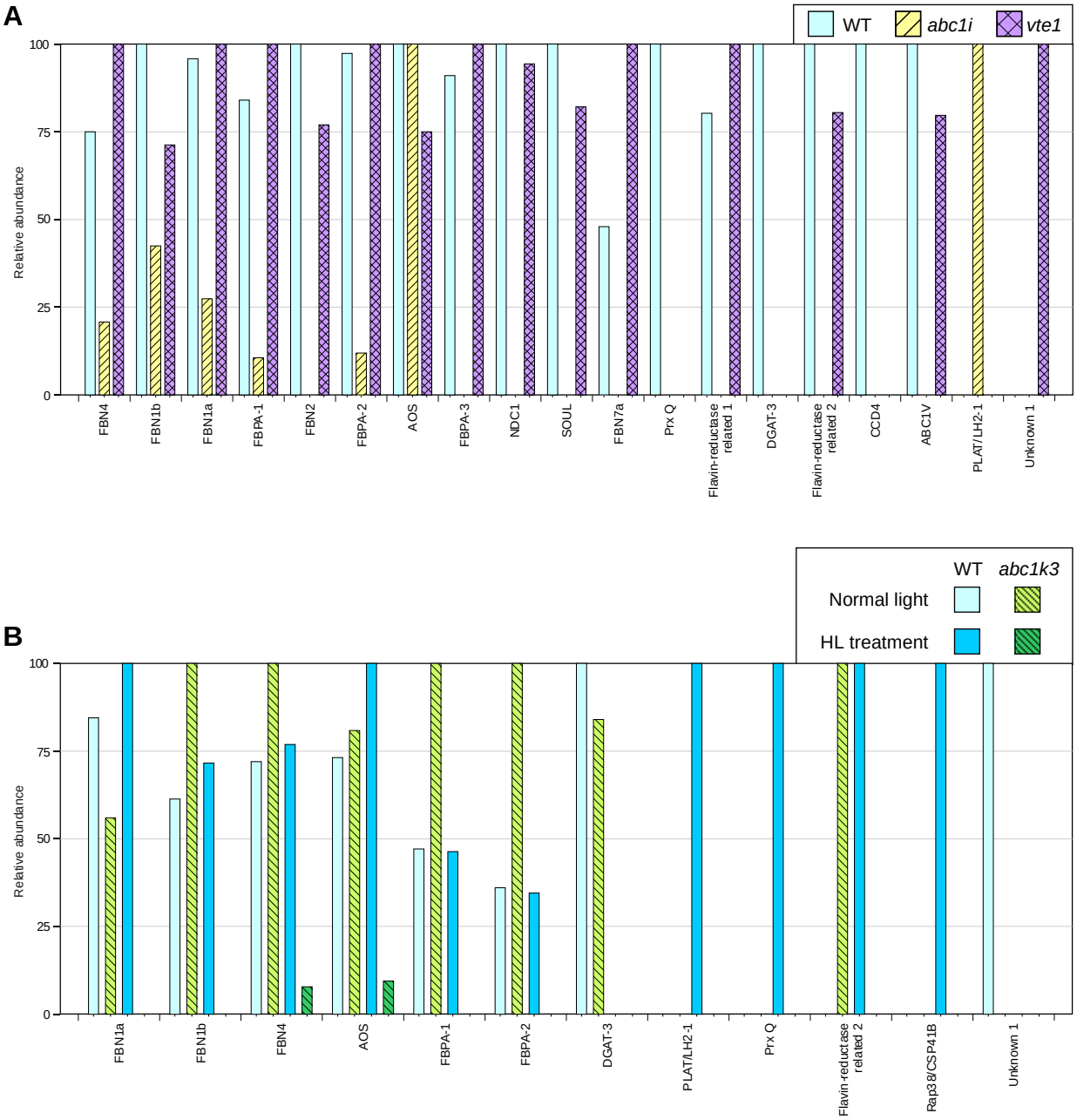

Figure 2.27: Variations in the protein composition of purified chloroplast fractions corresponding to plastoglobules.

A. Comparison between wild-type and *abc1i* plants grown under normal light conditions (day 0, 150 µE × m^{-2} × s^{-1}).

B. Detected changes in protein content between wild-type and abc1k3 plants exposed to normal light conditions (day 0, 150 µE × m^{-2} × s^{-1}) or to continuous high light (500 µE × m-2 × s-1) for 7 days.

Equal protein amounts were extracted from purified chloroplast fractions (n=3), digested with trypsin and analyzed by UHPLC-Nanospray-QTOFMS .

In a separate experiment, the effect of the *abc1k3/pgr6* mutation on plastoglobule protein composition was evaluated, together with the variations induced in the two plant lines by the exposure to HL intensity, (Figure 2.27B on page 101).

Under normal light conditions, a lower FBN1a content was detected in the *abc1k3/pgr6* mutant, as previously observed by immunoblotting (Figure 2.25A on page 97). Most surprisingly however, significantly higher FBN1b levels were detected in the mutant by UHPLC-Nanospray-QTOFMS analysis, in contrast with the lower FBN1b content observed by Western Blot analysis using antibodies raised against FBN1a (Figure 2.25A on page 97). Under HL conditions, a moderate increase in FBN1a and FBN1b content was observed in wild-type plants, as previously reported[39,226]. Conversely, a significant reduction in the levels of the two fibrillins was detected in the *abc1k3/pgr6* mutant after prolonged exposure to HL intensity.

Similarly, AOS content increased in wild-type plastoglobules after HL treatment, while in *abc1k3/pgr6* plants AOS levels were similar to the wild-type under normal light conditions but decreased after prolonged exposure to HL

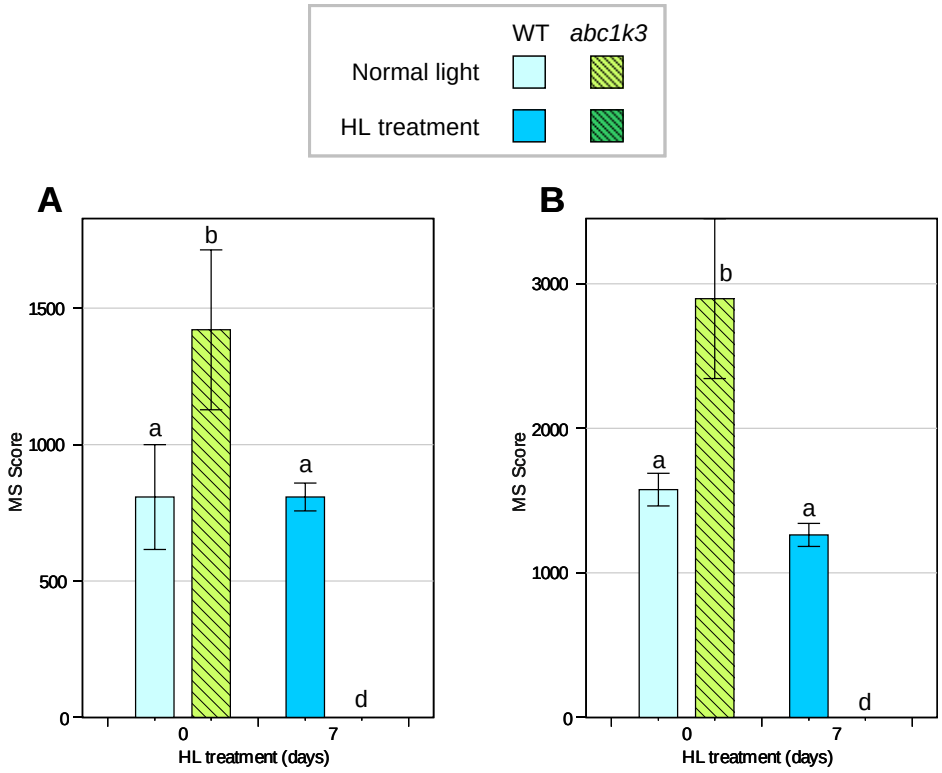

Figure 2.28: Detail of the variations in aldolase content in response to HL treatment.
A. FBPA1 B. FBPA2. Significant differences between samples (n=3 for each plant line and light intensity) were determined by a one-way ANOVA.

Interestingly, in the *abc1k3/pgr6* mutant a 1-fold accumulation of the two aldolases FBPA1 and FBPA2 was detected under normal light conditions. However, after prolonged HL treatment, their relative abundance was significantly lower in *abc1k3/pgr6*, while FBPA1 and FBPA2 content in wild-type plants did not significantly change, as previously reported[39]. In order to determine whether the observed difference was significant, a one-way analysis of variance (ANOVA) was conducted on the absolute MS scores obtained for FBPA1 and FBPA2 in the two plant lines and after HL treatment (Figure 2.28A-B on page 102).

2.3.8 - ABC1I and ABC1k3 phosphorylate VTE1

2.3.8.1 - Phosphorylation assays on purified chloroplast fractions

ABC1I and ABC1k3 are both predicted kinases located in plastoglobules. However, their targets are currently unknown. In order to identify such phosphorylation targets, a series of *in vitro* phosphorylation assays was carried out on purified plastoglobules extracted from wild-type, *abc1i* and *abc1k3/pgr6* plants. Moreover, to investigate the presence of potential kinase targets either at the plastoglobule surface or soluble in the stroma, experiments were performed in the absence or presence of a stromal extract from the same plant lines. Low-density chloroplast fractions corresponding to plastoglobules were pooled together and concentrated to enrich plastoglobule proteins, then phosphorylation reactions were assembled using radioactive-labelled [γ-^{33}P] ATP. Proteins were then separated by 1-D SDS-PAGE and phosphorylated ones were visualized by autoradiography.

Differences in the phosphorylation patterns were indeed detected between wild-type, *abc1i* and *abc1k3/pgr6* samples (Figure 2.29A-B on page 104, respectively).
Most strikingly, a phosphoprotein with an apparent molecular mass of about 45 kDa was absent in both the mutants in the presence of stromal extract. The same result was obtained in reactions using the purified plastoglobules alone, indicating the localization of this putative target of the two kinases in plastoglobules rather than in stroma. The detected phosphoprotein did not correspond to the mature form neither of ABC1I (75 kDa) nor ABC1k3 (68 kDa), thus excluding an autophosphorylation event. However, its predicted molecular weight was compatible with the mature form of VTE1 (43.5 kDa).

2.3.8.2 - The two kinases phosphorylates the recombinant VTE1 *in vitro*

In order to confirm VTE1 as one of the possible targets of ABC1I and ABC1k3, the mature forms of the two kinases and the full-length VTE1 coding sequence were *in vitro* translated in the presence or absence of [^{35}S] methionine. Radioactively-labeled proteins were then used as molecular mass references while the unlabeled IVT products were used to assemble *in vitro* phosphorylation reactions in the presence of [γ-^{33}P] ATP. The unlabeled rabbit reticulocyte lysate was used as a negative control (Figure 2.29C on page 104).

A phosphoprotein of about 97 kDa was detected in all the samples and possibly corresponds to the target of a kinase present endogenously in the *in vitro* translation mix. Most strikingly however, ^{33}P incorporation was detected in a protein with the same molecular mass as the [^{35}S]-labeled recombinant VTE1 exclusively after incubation with either ABC1I or ABC1k3, while it was absent in the negative control, in the VTE1 *in vitro* translation product and in the reactions containing either of the kinases alone. Moreover, the mass of this phosphoprotein did correspond neither to the recombinant ABC1I nor ABC1k3, thus excluding an autophosphorylation event.

At the same time, protein identification was performed by Western Blotting using specific antibodies raised against VTE1 or specific for the His_6 tag at the C-terminus of both of the recombinant kinases (Figure 2.29D). The antigen recognized by the purified serum raised against VTE1 co-localized with the radioactive band on the SDS-PAGE gel, thus supporting VTE1 as the phosphorylated target of the kinase. Moreover, the Western Blot analysis confirmed the relative distribution of the three proteins inside the phosphorylation reactions.

Figure 2.29: ABC1I and ABC1k3 *in vitro* phosphorylation assays.

A-B. SDS-PAGE separation of proteins extracted from purified plastoglobule sub-fractions (PG) incubated with [γ -33P] ATP alone or after addition of an equal amount of stromal extract. 33P incorporation was determined by autoradiography. The predicted position of the full-length kinases is indicated by an asterisk and their putative target is indicated by a white triangle.

C. Recombinant VTE1 *in vitro* phosphorylation by ABC1I and ABC1k3. Recombinant proteins were translated *in vitro* (IVT, left panel) in the absence or presence of [35S] methionine. Unlabeled IVT products were then used to assemble in vitro phosphorylation reactions with ABC1I and ABC1k3 (central and right panels, respectively). The IVT reaction mix was used as negative control. Corresponding [35S] methionine and 33P incorporation were determined by autoradiography. The position of the recombinant VTE1 is indicated by a white arrow.

D. Detail of the corresponding region on the SDS-PAGE gel stained with Comassie Blue. The presence of the two ABC1-like kinases and of VTE1 in the samples was determined by imunoblotting.

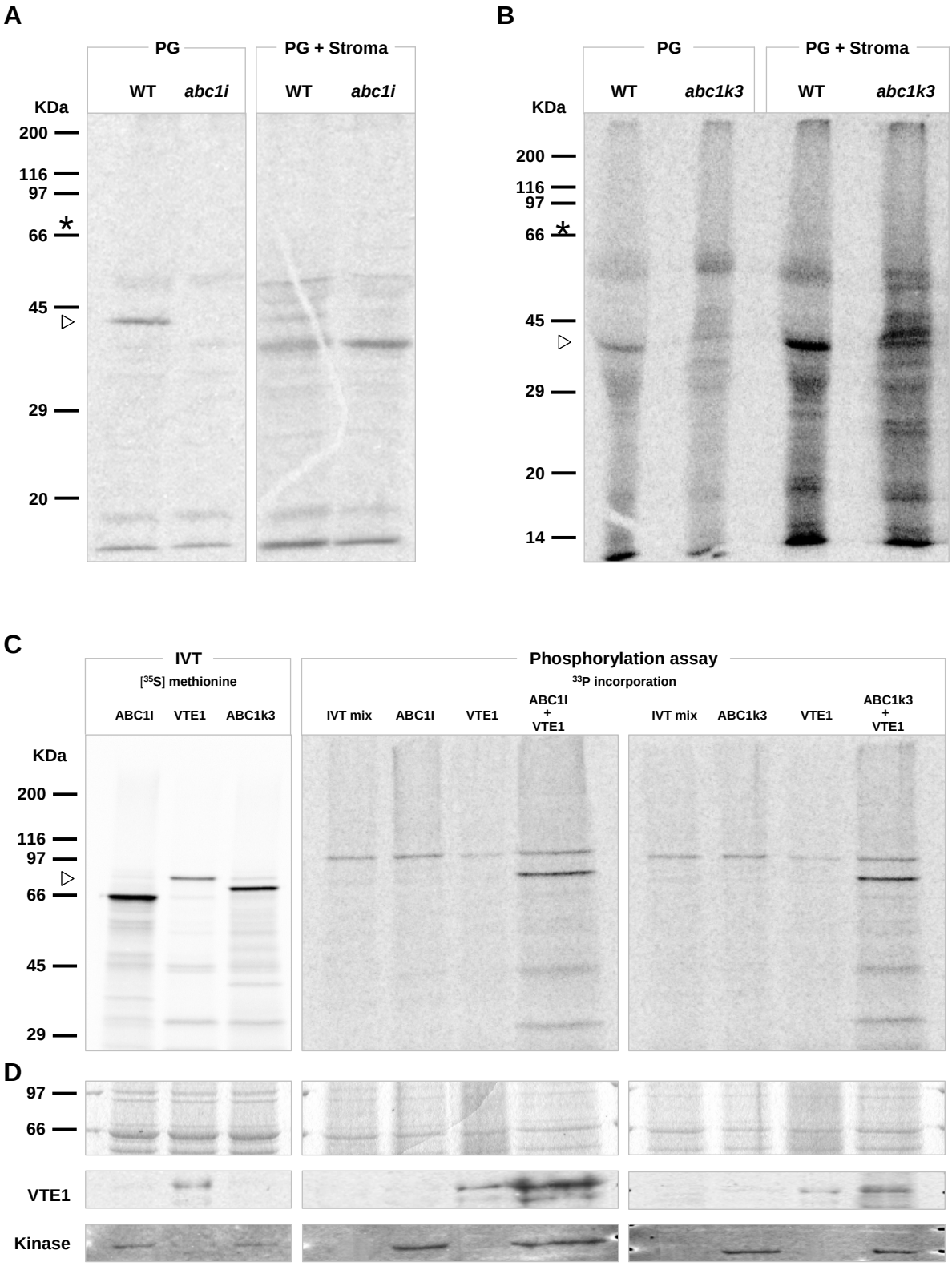

Figure 2.29: ABC1 and ABC1k3 *in vitro* phospohrylation assays.

CHAPTER 3

~ Discussion ~

3.1 - THE ABC1 PLASTOGLOBULE HOMOLOGS

3.1.1 - ABC1-like kinases are both in chloroplasts and mitochondria

The protein kinase-like (PKL) superfamily can be divided between the eukaryotic protein kinases (ePKs) and the atypical protein kinases (aPKs), that are prevalent in prokaryotes[(227)]. The members of the aPK family include proteins that are known to be involved in the phosphorylation-mediated regulation of a wide variety of cellular processes[(88)]. The determination of the crystal structure of these kinases demonstrated that many aPKs bear significant structural homology to ePKs despite the lack of sequence similarity. In particular, the members of the eukaryotic protein kinase-like (ELKs) group, which also include the ABC1-like kinases, only share a similarity to ePKs of about 5-15%, but this includes the most conserved catalytic and metal binding residues of the ePK kinase domain[(228,229)].

The evolutionary origin of the ABC1/ADCK/UbiB family of atypical kinases is ancient and precedes the endosymbiotic events which lead to the formation of mitochondria and chloroplasts. However, despite ABC1-like kinases having been identified in Archaea, bacteria, and eukaryotes, the phylogenetic analysis in diverse species of all three primary kingdoms demonstrated a significant expansion of the number of ABC1-like homologs in photosynthetic organisms[(90,40)].

3.1.2 - ABC1I, ABC1k3 and ABC1V localize to plastoglobules *in vivo*

Out of the eight ABC1-like kinases located in *A. thaliana* chloroplasts, six were identified in highly purified chloroplast lipid droplets (plastoglobules) in several independent screenings by mass spectrometry[(36,39,40)].

To independently give evidence for the plastoglobule localization of ABC1I, ABC1k3 and ABC1V, the three kinases were stably expressed as a YFP-fusion proteins in *Arabidopsis* plants. This resulted in a punctate fluorescence pattern which is consistent with plastoglobule localization, while in all plant lines fluorescence was detectable neither at the thylakoids nor at the envelope. Moreover, the identification of ABC1k3 by Western Blotting in purified chloroplast sub-fractions corresponding to plastoglobules further provides evidence for the plastoglobule localization of this protein.

On the other hand, previous experiments[89] showed that the three ABC1-like kinases ABC1I, ABC1k3 and ABC1V, despite being highly enriched in plastoglobules (11-, 16- and 440-fold more, respectively) are also present in thylakoid membranes but to a significantly lower extent. For this reason, it is not possible to completely exclude that the activity of these kinases is limited to plastoglobule substrates but it might contribute to the regulation of proteins located in the thylakoids as well.

3.1.3 - Chloroplast ABC1 homologs are involved in the regulation of diverse biological functions

The simultaneous presence of ABC1 homologs in mitochondria and chloroplasts rises questions relatively to their biological role in these two organelles.
The involvement of the prototypical family member in the synthesis of ubiquinone (UQ-9) both in non-photosynthetic bacteria and in yeast and human mitochondria has been widely investigated[91-97]. However, cyanobacteria do not synthesize UQ-9 and use instead plastoquinone (PQ-9) for both photosynthetic and respiratory electron transport[230]. At the same time, PQ-9 biosynthesis in plants differs from that in cyanobacteria[231]. For these reasons, it has been suggested that plants, through endosymbiosis with plastid and mitochondrial ancestors, have inherited multiple pathways for prenylquinone metabolism and possibly their regulatory mechanisms, among which the ABC1 homologs[89].

However, indications of an involvement of ABC1-like kinases in diverse pathways such as carotenoid metabolism come from the study of the formation of the eyespot apparatus in *C. reinhardtii*[100], which is related to chloroplast plastoglobules. At the same time, the recent genome-wide gene coexpression analysis performed on the six ABC1-like homologs identified in *A. thaliana* chloroplast lipid droplets strongly suggests that they are not redundant for the regulation of the same metabolic pathway but are potentially involved in the formation of a kinase network modulating different aspects of plastoglobule metabolism[40] (Figure 2.5 on page 63).

The findings presented in this thesis and discussed in the following sections are in agreement with such a hypothesis and strongly suggest that the two plastoglobule kinases ABC1I (At1g79600) and ABC1k3 (At4g31390) are not specifically involved in the synthesis of PQ-9 but, more in general, in the regulation of prenylquinone metabolism. Moreover, ABC1k3 appears to play a key role in plant photosynthetic response to excess light and in the modulation of carotenoid metabolism during the acclimation to these conditions.

At the same time, the *in silico* analysis of the genes coexpressing with the plastoglobule kinase ABC1V (At5g05200), as well as the preliminary characterization of its knock-down mutant, suggest a possible involvement of this kinase in chloroplast differentiation.

3.2 - INITIAL REMARKS

3.2.1 - Selection of the experimental conditions

In order to select the best experimental conditions to be used for the phenotypical characterization of the *abc1i* and *abc1k3/pgr6* mutants, publicly-available transcriptome profiles of *ABC1I* and *ABC1k3* were analyzed *in silico* to identify patterns in the expression of the two genes at different developmental stages of the plant as well as in response to selected growth conditions.

In particular, a significant increase in the transcript levels of both genes was observed after exposure to high light (HL) intensities. In order to keep experimental conditions as close as possible to those used for generating the microarray data annotated on the Genevestigator database, a strong light intensity (1300-1500 $\mu E \cdot m^{-2} \cdot s^{-1}$) was initially chosen to test the response of mutant plants to HL (data not shown).
However, the use of these light conditions led to a significant increase in leaf bleaching within 1-2 days of HL treatment, especially in the *abc1k3/pgr6* mutant. In order to reduce the risk of artefacts caused by extensive photooxidative damage at such light intensities and to match the light conditions previously reported in similar works[35,102,167,179], HL intensity was subsequently lowered to 500 $\mu E \cdot m^{-2} \cdot s^{-1}$. No significant phenotypical differences were observed in the response of both wild-type and mutant plants when compared with the earlier experiments.

At the same time, the expression rate of *ABC1I* and, to a lower extent, *ABC1k3* was predicted to be enhanced during senescence or after treatment with hormones that promotes it. A preliminary experiment was carried out to investigate a possible involvement of the two ABC1-like kinases in chloroplast response to dark-induced senescence. Briefly, leaves were detached from 8-week-old plants, put on a wet filter paper disk inside a Petri dish wrapped in aluminium and incubated up to 7 days in permanent darkness prior to observation.
However, the visual phenotype and protein patterns of the mutants were identical to the wild-type and no statistically significant differences were detected in chlorophyll content (data not shown). On the other hand, the determination of the photosynthetic parameters and the lipid profile of *abc1i* and *abc1k3/pgr6* mutant plants during leaf aging has not been performed yet.

3.2.2 - A new method was required for rapid lipid profiling

The majority of the methods used for the identification and quantification of prenylquinones and carotenoids in plants are based on their extraction by an organic solvent followed by the chromatographic analysis of selected molecules. However, conventional methods based on liquid chromatography (HPLC) coupled to ultraviolet or fluorescence analyzers[161,232,34] allow for the detection of a single or limited number of molecules at a time. Moreover, these techniques require long running times (several dozens of minutes) to obtain sufficient resolution and the identification of lipid constituents relies on the availability of pure standards. Mass spectrometry, despite its high potential for the detection and identification of various apolar lipids[233], has been scarcely employed in combination with liquid chromatography for the analysis of carotenoids and prenylquinones in plants. As a consequence, the conventional HPLC methods used for lipid profiling were not suitable to perform the simultaneous identification and quantification of multiple molecules in samples extracted from wild-type, *abc1i* and *abc1k3/pgr6* mutant plants under different light conditions.

For these reasons, a novel method was developed for the simultaneous profiling of prenylquinones and carotenoids using an optimized sample preparation procedure followed by ultra-high pressure liquid chromatography-atmospheric pressure chemical ionization-quadrupole time of flight mass spectrometry (UHPLC-APCI-QTOFMS).
The presented method proves to be fast, reliable, very selective and sensitive for the analyzed molecules, and consumes less solvent than conventional methods. In particular, by combining a simple and rapid sample preparation with the fast chromatographic separation provided by UHPLC columns, a single plant can be extracted and analyzed in less than 15 min and twelve samples can be processed in 90 min, thus allowing high-throughput analyses of mutant plant collections. Moreover, the use of a QTOFMS analyzer allows for the detection and tentative identification of molecules for which no pure standard is available.

Furthermore, the applicability of the developed method is not limited to the experimental work on the ABC1-like kinases described in this thesis but it can be used to profile prenylquinones and carotenoids in other *Arabidopsis* mutants as well as in other commercially relevant crop species.

3.3 - FUNCTIONAL CHARACTERIZATION OF ABC1I AND ABC1K3

3.3.1 - ABC1I and ABC1k3 modulate VTE1 activity

3.3.1.1 - ABC1I specifically affects PC-8 synthesis and α-TQ recycling

In order to analyze the role of ABC1I in prenylquinone metabolism, total leaf lipid extracts of wild-type and *abc1i* plants grown both under standard conditions and high light stress were analyzed by UHPLC-APCI-QTOFMS. At the same time, the knock-out mutant line *vte1* was used as reference, lacking both PC-8 and tocopherols and accumulating instead the metabolic intermediate DMPBQ.

Most strikingly, lower PC-8 and elevated α-TQ levels were observed in *abc1i* plants already under normal growth conditions, while α-, γ- and δ-T contents remained similar to the wild-type. Moreover, the *abc1i* mutant was characterized by a 10-fold increase of the cellular content of α-TQ after HL treatment (Figure 2.22 on page 92).
PC-8 is a chromanol-derivative of plastoquinone with a structure similar to γ-T that fulfills antioxidant function in thylakoid membranes[35,179], while α-TQ is an intermediate of the recently discovered tocopherol Redox cycle[66]. Both PC-8 synthesis and α-TQ recycling require the tocopherol cyclase (VTE1) activity and were absent from the *vte1* mutant. Interestingly though and in contrast to *vte1*, no significant variations in the levels of DMPBQ were observed in the *abc1i* mutant when compared to the wild-type.
These results demonstrate a very specific role of ABC1I in regulating a particular branch of VTE1 activity. At the same time, they are consistent with the finding that VTE1 activity can be a limiting factor for PC-8 but not for the synthesis of tocopherols[68,34]. Furthermore, a strong correlation between the expression of *ABC1I* and *VTE1* was predicted by genome-wide gene coexpression analysis in response to stress conditions (Figure 2.5 on page 63).

On the other hand, the comparison between the prenylquinone and carotenoid composition of wild-type, *abc1i* and *vte1* plant lines by principal component analysis showed that the *abc1i* mutant does not simply correspond to a variant form of the *vte1* phenotype but clusters separately from both wild-type and *vte1* plants, suggesting that prenylquinones other than PC-8 and α-TQ may be affected as well (Figure 2.20 on page 90).

3.3.1.2 - ABC1k3 activity is required both for the synthesis of tocopherols and PC-8 and for the recycling of α-TQ

Similarly to the *abc1i* mutant, *abc1k3/pgr6* plants were also characterized by a lower PC-8 content and by the an accumulation of α-TQ under HL treatment (Figure 2.22 on page 92). However, the levels of these two molecules were not as low as those detected in *abc1i* plants. Conversely, a severe reduction in the accumulation of tocopherols (α-, γ- and δ-T) was observed after exposure to HL intensity. This might be partially explained by a higher consumption rate of lipid-soluble antioxidants in the *abc1k3/pgr6* mutant under photooxidative stress conditions. On the other hand, the results obtained suggest that ABC1k3 may have a different role in the regulation of VTE1, generally affecting the activity of the tocopherol cyclase rather than its selectivity for the substrate.

3.3.1.3 - ABC1I and ABC1k3 phosphorylate the tocopherol cyclase, possibly regulating its activity and its sub-organellar localization

Chloroplast ABC1-like kinases have been suggested to function in prenylquinone metabolism due to their similarity to bacterial, yeast and human proteins that are implicated in ubiquinone metabolism. However, their targets are currently unknown.
Considering that the most relevant differences in prenylquinone composition detected between wild-type, *abc1i* and *abc1k3/pgr6* mutant plants depended on the enzymatic products of the tocopherol cyclase, VTE1 represented a potential target of the two kinases.
This hypothesis was confirmed both *in vitro*, by performing a phosphorylation assay using recombinant ABC1I, ABC1K3 and VTE1 *in vitro* translation products, and *in vivo*, by comparing the phosphorylation profiles of purified chloroplast sub-fractions corresponding to plastoglobules extracted from wild-type, *abc1i* and *abc1k3/pgr6* plant lines (Figure 2.29 on page 106).

Moreover, VTE1 levels were strongly reduced or totally depleted in plastoglobules derived from *abc1i* and *abc1k3/pgr6* plants, despite a significant increase in *VTE1* transcript levels (Figures 2.24, 2.25 and 2.26 on pages 96, 97 and 98, respectively). These findings strongly suggest that VTE1 is post-transcriptionally (down-) regulated in the two mutants. Moreover, the observed increase in *VTE1* gene expression is consistent with a feedback

signaling caused by the low protein content in the chloroplasts and rules out the hypothesis that the two ABC1-like kinases might be involved in the modulation of *VTE1* expression rate.

These lines of evidence suggest that the two kinases normally stabilize the tocopherol cyclase at plastoglobules by phosphorylation, while in *abc1i* and *abc1k3/pgr6* mutant plants VTE1 may be unable to correctly localize to plastoglobules and is possibly degraded by proteolysis. Furthermore, the significant differences observed between the lipid profiles of *abc1i* and *abc1k3/pgr6* mutants (Figures 2.10C and 2.22 on pages 73 and 92, respectively) strongly suggest a differential modulation of VTE1 activity by the two kinases and would not be explained by the absence of VTE1 from plastoglobules.

Another possible explanation is the simultaneous presence of VTE1 in plastoglobules and, to a lower extent, at the inner envelope membrane that has been recently proposed[76]. According to this hypothesis, the VTE1 pool in plastoglobules would be mainly responsible for α-TQ recycling and PQ-9 conversion to PC-8, while the lower VTE1 content in the envelope would still be sufficient for tocopherol synthesis. Conversely, a depletion of both the VTE1 pools would lead to a reduction in the levels of all the enzymatic products of the tocopherol cyclase.
Nevertheless, no significant VTE1 accumulation at the chloroplast envelope or as soluble protein in the stroma has been detected neither in the wild-type, which is consistent with previous observations[22,36,70], nor in the two mutants *abc1i* and *abc1k3/pgr6* (Figures 2.24 and 2.25 on pages 96 and 97, respectively).

The presented experimental evidence strongly suggests that both ABC1I and ABC1k3 are active kinases that both phosphorylate the recombinant VTE1 *in vitro*. However, when purified chloroplast fractions highly enriched in plastoglobules from either of the two mutants were used to perform phosphorylation assays, a phosphoprotein with a predicted molecular weight compatible with the mature form of VTE1 (approximately 45 kDa) was not detected (Figure 2.29 on page 106). As a consequence, it is conceivable that the simultaneous activity of two or more of the ABC1-like kinases located in plastoglobules could be required for VTE1 phosphorylation *in vivo*. This suggestion, together with the predicted involvement of ABC1-like kinases in the regulation of different metabolic pathways[40], strongly suggests the presence of a complex kinase network located at the plastoglobule level.

3.3.2 - Effects on primary photosynthetic metabolism

3.3.2.1 - ABC1k3 affects photosynthetic activity via the modulation of chloroplast lipid metabolism

The *abc1k3* T-DNA insertional mutants are allelic to the photosynthetic mutant *pgr6*, previously isolated on the basis of its high chlorophyll fluorescence phenotype[102] and affected at the level of the PSII - Cyt. b_6f segment of the chloroplast electron transport chain[188]. The *abc1k3/pgr6* mutant is characterized by low ETR and NPQ levels already under normal light conditions, and a further reduction in maximum PSII quantum efficiency (Fv/Fm), ETR and NPQ is observed after a short-term exposure to HL intensity (1-2 days). However, considering the plastoglobule localization of ABC1K3, it appears unlikely that the kinase is directly involved in the assembly of the Cyt. b_6f key complex or in affecting its activity and the formation of the proton gradient across thylakoid membranes, as has been demonstrated in the case of the *pgr1* mutant[185,186]. More probably, the effect of the *abc1k3/pgr6* mutation on the PSII - Cyt. b_6f segment of the chloroplast electron transport chain is likely to be indirect.

The *abc1k3/pgr6* mutation severely affects the cellular content of molecules belonging to carotenoid and prenylquinone classes that are known to participate either in photosynthesis or in the photoprotection of thylakoid membranes. In particular, the smaller pool of the electron transporter PQ-9 in the *abc1k3/pgr6* mutant potentially provides an explanation for the lower ETR observed under HL treatment. Moreover, a lower electron flow rate through the Cyt. b_6f complex leading to reduced acidification of the thylakoid lumen could partially explain the low NPQ levels detected after prolonged HL exposure, despite the recovery in maximal PSII efficiency.

At the same time, the NPQ defect after short-term HL treatment could also be explained by a defect in the regulation of xanthophyll metabolism, which has an essential role in protecting membranes from photooxidative damage and is largely responsible for the energy-dependent component of NPQ (qE)[180]. Under both normal light conditions of after a short exposure to HL intensity, *abc1k3/pgr6* plants were characterized by low β-carotene and lutein levels. Although zeaxanthin is the main player in the qE component of NPQ, lutein is responsible for the residual qE in *A. thaliana*[234]. In particular, it has been demonstrated that

in plants lacking zeaxanthin lutein accumulates instead and partially restores NPQ[181]. The observed increase in lutein and β-carotene levels in the *abc1k3/pgr6* mutant during acclimation to HL intensity is then consistent with the partial recovery of NPQ.
Besides, lutein binds to the L1 site of all light-harvesting complex (Lhc) proteins, whose occupancy is indispensable for protein folding and to successfully quench chlorophyll triplets[131]. As a consequence, a reduction in lutein content in *abc1k3/pgr6* plants would also explain the observed reduction in the numbers of chlorophyll-binding proteins of the photosynthetic complexes observed in this work and previously reported[101].

Furthermore, it has been predicted by genome-wide gene coexpression analysis that *ABC1k3* expression is tightly linked to that of the ζ-carotene desaturase (ZDS), an enzyme required for the synthesis of lycopene and affecting both α- and β-carotene biosynthetic pathways[40] (Figures 2.5 and 2.6 on pages 63 and 64, respectively). ZDS has been previously demonstrated to accumulate in plastoglobules during chloroplast conversion to chromoplast, together with other enzymes operating in carotenoid and xanthophyll synthesis[39]. Moreover, similarly to the other enzymes required for the conversion of phytoene to lycopene, ZDS requires PQ-9 as electron acceptor[120-122], further suggesting a functional relationship between carotenoid synthesis and the PQ-9 pool in chloroplasts[123]. Moreover, plants lacking ZDS and in which carotene synthesis is disrupted downstream ζ-carotene had a chlorophyll content that was half than in the wild-type and were also characterized by a downregulation in the expression of Lhc components, a lower maximum PSII efficiency and defects in chloroplast development[118].
These line of evidence suggest that ABC1k3 may regulate the activity of enzymes required for carotenoid synthesis. Nevertheless, it has previously been demonstrated that the *abc1k3/pgr6* mutation does not affect the expression of genes involved in chlorophyll and carotenoid metabolism[101]. Therefore, it may be possible that their down-regulation occurs at a post-transcriptional level, similarly to what demonstrated for VTE1.

To summarize, the *abc1k3/pgr6* mutant was very sensitive to the short-term HL treatment (during 2 days), suggesting that ABC1k3 activity is required for the rapid acclimation to HL conditions and for protecting PSII from photooxidative stress. Most strikingly however, both Fv/Fm and CO_2 fixation rate were able to recover to near normal levels in the longer period (after 2-5 days), in contrast with other *pgr* mutants. Notably,

chlorophyll and Lhc levels as well as leaf thickness were also reduced in *abc1k3/pgr6* plants acclimating to HL, suggesting an acclimation strategy based on absorbing less light energy[235-237]. Moreover, the drastic differences in the levels of prenylquinones and carotenoids observed between WT and *abc1k3/pgr6* plants after the acclimation to HL strongly suggest a possible involvement in carotenoid metabolism. It has previously been observed that *npq1 lut2* double mutants, lacking both zeaxanthin and lutein and characterized by low NPQ, were able to acclimate to moderately high light intensities[234]. Moreover, these plants had lower chlorophyll levels and presented visible photooxidative damage in the older leaves after prolonged HL treatment while younger ones were relatively unaffected, similarly to what was observed in the *abc1k3/pgr6* mutant. For these reasons, it is possible to hypothesize that the photosynthetic phenotype observed in the *abc1k3/pgr6* mutant is caused at least in part by a defect in the modulation of chloroplast carotenoid metabolism in response to light intensity.

3.3.2.2 - The lack of PC-8 and Vitamin E alone does not explain the photosynthetic phenotype of *abc1k3/pgr6* mutants

When photosynthetic parameters and the response to HL intensity were measured in the *vte1* mutant, higher NPQ levels than in the wild-type were detected after a short HL exposure due to the increase of xanthophyll content[163]. However, after prolonged HL treatment, a reduction in both ETR and NPQ levels was observed in *vte1* plants, possibly because of photooxidative damage caused by the lack of PC-8 and tocopherols. However, in *abc1i* and *abc1k3/pgr6* mutants PC-8 and tocopherols are present, although at lower concentrations than in the wild-type and may explain the improved ETR and NPQ when compared to the *vte1* mutant. Moreover, *vte1* plants accumulated DMPBQ, which has been suggested to partially compensate for the absence of tocopherols when *vte1* plants are exposed to HL intensity[163].

At the same time, *vte1* plants were also characterized by a low PQ-9 content after prolonged HL treatment, similarly to the *abc1k3/pgr6* mutant (Figure 2.22G on page 92). As previously proposed for this mutant, it is possible that the partial saturation of the small PQ-9 pool could lead to a reduction in the electron flow rate through the Cyt. b_6f, thus affecting both ETR and NPQ.

The defect in tocopherol accumulation under prolonged HL treatment, together with the reduction in α-TQ recycling, are likely to contribute to the rapid PSII photoinactivation after short HL stress, as well as the higher degree of photooxidative damage observed in *abc1k3/pgr6* plants exposed for several days to continuous HL.

However, despite being involved together with xanthophylls in preventing PSII photoinactivation and protecting thylakoid membrane lipids from peroxidation[34,163,164], PC-8 and tocopherols do not appear to be the limiting factor for the rapid response of plants to HL intensities. On the contrary, they significantly contribute in protecting thylakoids from photooxidative damage under prolonged HL stress.

Consistent with this hypothesis, the photosynthetic parameters of the *abc1i* mutant did not significantly differ from the wild-type despite the lower PC-8 levels, although *abc1i* plants showed slightly lower NPQ levels both under normal light conditions and after short HL treatment, possibly because of a slightly lower xanthophyll content.

3.3.2.3 - Starch and sugar metabolism are affected in the *abc1k3/pgr6* mutant

The initial defect in starch accumulation observed in *abc1k1/pgr6* plants exposed to HL conditions could be explained by their lower photosynthetic rate under HL intensity, as previously reported[238]. In fact, a slightly lower CO_2 assimilation rate was observed in the *abc1k1/pgr6* mutant even under normal light conditions when its photosynthetic efficiency was similar to the wild-type, which is consistent with the slightly lower starch content detected under the same light conditions. Under HL treatment, *abc1k1/pgr6* plants were characterized by a significantly low carbon assimilation, which might have not been sufficient for the maintenance of the carbon metabolism, thus resulting in the observed reduction in starch accumulation, the conversion of all the assimilated carbon to sugars and possibly the activation of starch breakdown to release more maltose, which could then be exported from the chloroplast and used for further metabolism. However, despite the recovery of the CO_2 assimilation rate observed in *abc1k1/pgr6* plants after prolonged HL treatment, starch levels did not significantly increase in the mutant. A possible explanation may lie in an increase of starch turnover to compensate for the previous carbon starvation, which is consistent with the moderate increase in the steady state levels of maltose detected in the *abc1k1/pgr6* mutant.

Remarkably, a significant sucrose accumulation was detected in *abc1k1/pgr6* plants after prolonged HL treatment, in contrast with the wild-type. This evidence suggests that ABC1K1 may have a role in modulating the sucrose:starch ratio that could explain the deficiency in starch accumulation despite the recovery of the photosynthetic efficiency. One of the main regulatory mechanisms of this balance in plants is mediated by the activity of the fructose 1,6-bisphosphatase (FBPase), which converts the fructose-1,6-bisphosphate produced by the fructose-bisphosphate aldolase (FBPA) to fructose-6-phosphate. High levels of fructose-6-phosphate have been shown to increase the concentration of another sugar, fructose-2,6-bisphosphate[(199)], the accumulation of which favors the partitioning of carbon towards starch synthesis, while at low levels sucrose biosynthesis is favored[(196)]. Furthermore, it has been demonstrated that changes in the levels of the chloroplast FBPAs affect the carbon flux through the Calvin cycle, thus influencing carbon fixation rate and plant growth[(202-204)] (see Section 1.3.2.2).

Interestingly, three FBPA homologs (At2g21330, At4g38970 and At2g01140, respectively) have previously been reported to significantly contribute to the plastoglobule proteome[(39)], although they are not "*bona fide*" plastoglobule proteins and accumulate in stroma and thylakoid membranes as well[(40)].

Furthermore, preliminary mass spectrometry data showed a significant accumulation of both FBPA1 and FBPA2 under normal light conditions in the *abc1k3/pgr6* mutant. However, after prolonged HL treatment, their levels were significantly lower in *abc1k3/pgr6*, while FBPA1 and FBPA2 content did not change in the wild-type, as has been reported previously[(39)]. FBPA is considered one of the six "nonregulated" enzymes of the Calvin cycle[(200)], therefore its regulation by direct phosphorylation appears to be unlikely. On the other hand, a possible sequestration of FBPA at the plastoglobule level in the *abc1k3/pgr6* mutant would contribute to explain the observed defect in carbon assimilation and growth rate both under normal light conditions and after short HL treatment, while its release would be consistent with the recovery observed during plant acclimation to HL intensity. However, considering the preliminary nature of the proteomic experiments performed on purified plastoglobules extracted from *abc1k3/pgr6* plants, further analyses would be required to confirm this hypothesis.

At the same time, genome-wide gene coexpression analysis showed that *ABC1k3* is tightly linked to the sucrose phosphate synthase SPS4F in gene coexpression networks[(40)]

(Figures 2.5 and 2.6 on pages 63 and 64, respectively). In plants, SPS represents another key enzyme in the modulation of sucrose synthesis, being responsible of the conversion of UDP-glucose + D-fructose 6-phosphate to UDP + sucrose-6-phosphate[(207)]. Moreover, it has previously been demonstrated that SPS overexpression in *A. thaliana* resulted in an shift in the metabolic equilibrium towards sucrose synthesis in leaves[(209)].

This finding further supports the hypothesis that ABC1k3 may be involved in the modulation of sugar metabolism in a way which is probably independent from the regulation of the light cycle of photosynthesis.

3.3.3 - Other effects of the activity of the two kinases

3.3.3.1 - Pigment content is affected in the *abc1k3/pgr6* mutant under HL stress

Besides the defect in chlorophyll accumulation, *abc1k3/pgr6* plants were characterized by a significant delay in anthocyanin synthesis under HL treatment and which partially recovered only after prolonged HL exposure. Anthocyanin synthesis modulation in response to changes in light quality and intensity is tightly controlled in higher plants. Apart from direct light-sensing through photoreceptors such as phytochrome and cryptochrome, plants use other mechanisms to integrate this information. Sugars are common regulators of several genes involved in photosynthesis and carbohydrate metabolism, and they also contribute to the regulation of anthocyanin biosynthesis[(239-241)]. In particular, it has been demonstrated in *A. thaliana* that high sucrose levels induce anthocyanin synthesis and that light sensing alone is not sufficient to trigger this adaptation if sucrose is absent[(242)]. The partial recovery of anthocyanin accumulation observed in *abc1k3/pgr6* plants after prolonged HL treatment could then be explained by the significant increase in leaf sucrose content detected after 3 days of HL treatment. Moreover, it has also been suggested that the Redox state of the PQ-9 pool could play a role in sensing variations of the photosynthetic apparatus, being involved in the modulation of anthocyanin synthesis together with sugar and light signaling[(241,242)].

3.3.3.2 - Effects on chloroplast ultrastructure

The comparison of transmission electron micrographs of leaf sections from wild-type, *abc1i* and *abc1k3/pgr6* plants highlighted significant differences in the chloroplast ultrastructure of the two mutants, which were more relevant when plants were exposed to HL treatment (Figure 2.16 on page 80). In particular, *abc1i* chloroplasts were characterized by large plastoglobule clusters, extensive vacuolation and the absence of starch granules. Conversely, thylakoid grana in *abc1k3/pgr6* chloroplasts appeared small and very dense under normal light conditions, while they enlarged and became disassembled after exposure to HL intensity. Moreover, plastoglobule number and size was severely reduced in *abc1k3/pgr6* chloroplasts under normal growth conditions, but appeared to be similar to the wild-type under HL treatment.

It has previously been reported that mutants defective in PQ-9 synthesis are severely affected in chloroplast development and show an albino or pale-green phenotype because of defects in thylakoid assembly[176]. However, despite being significantly less abundant than in the wild-type, PQ-9 was not absent neither in the *abc1i* nor in the *abc1k3/pgr6* mutant. On the other hand, the lower content of carotenoids and other lipophylic antioxidant such as Vitamin E and PC-8 could potentially explain the photochemical damage sustained by thylakoid membranes as well as the higher chlorophyll degradation rate under photooxidative stress conditions previously described in *abc1k3/pgr6* plants[101].

In addition, the genome-wide coexpression analysis suggested a functional correlation between the expression of *ABC1I* and of several other genes encoding for chloroplast metalloproteases (Figure 2.5 on page 63). These enzymes have previously been associated with defects in plastid biogenesis and differentiation resulting in "variegated" phenotypes characterized by extended chloroplast vacuolation and the lack of organized lamellar structures[243-246]. Moreover, a connection between carotenoid synthesis, PQ-9 Redox state and chloroplast differentiation has previously been proposed for the *immutans* phenotype, characterized by an heterogeneous plastid population including vacuolated proplastids defective in internal lamellar organization and accumulating the non-colored carotenoid phytoene[123,125].
In conclusion, the diverse evidence suggests that the two ABC1-like kinases may be involved in a far-ranging regulatory network affecting not only carotenoid and prenylquinone synthesis but also chloroplast morphology.

3.3.3.3 - The plastoglobule proteome is severely affected in the two mutants

The findings presented in this thesis suggest that the two kinases are necessary for the correct localization of VTE1 to plastoglobules and could have a role in the modulation of its activity. However, the effects of the deletion of either *ABC1I* or *ABC1k3* on the protein composition of plastoglobules were not limited to the tocopherol cyclase, but other proteins were affected as well.
Remarkably, a significant reduction in the levels of the two most abundant plastoglobule fibrillins FBN1a/b and FBN2 was detected by Western Blot analysis (Figures 2.24, 2.25 and

2.27 on pages 96, 97 and 101, respectively). Moreover, the simultaneous increase in *FBN1a* transcript levels suggests that its down-regulation occurred at a post-transcriptional level, similarly to VTE1 (Figure 2.26 on page 98).
With regard to the predicted role of fibrillins in stabilizing lipid globules, it might be possible that the two kinases have a direct effect on either the content or the phosphorylation state of one or more plastoglobule structural proteins. As a consequence, it is conceivable that alterations in the size or morphology of plastoglobules could affect their protein and lipid composition as well as, resulting in significant changes of the chloroplast metabolic network associated with plastoglobules. Both in *Arabidopsis* and in other plant species, a reduction in FBN1a/b, FBN2 and FBN4 levels has previously been associated with low ascorbate and anthocyanin accumulation, greater sensitivity to photoinhibition and oxidative stress[47,48], reduced NPQ levels and growth defects[45,49], as previously discussed (see Section 1.1.3.1).

Further indications of an effect of the *abc1i* and *abc1k3/pgr6* mutations on the plastoglobule proteome come from the comparison of the SDS-PAGE profiles of plastoglobule fractions extracted from different plant lines (Figures 2.24 and 2.25 on pages 96 and 97, respectively), as well from a preliminary proteomic screening by mass spectrometry performed on purified chloroplast fractions highly enriched in plastoglobules (Figure 2.27 on page 101). To summarize, a lower relative abundance of almost all the detected proteins was observed in the two mutants *abc1i* and *abc1k3/pgr6* when compared to that of plastoglobules isolated from wild-type plants, with some exceptions. Most strikingly however, minor differences were also detected between the protein composition of wild-type and *vte1* plants.

In conclusion, the two kinases ABC1I and ABCk3 may be involved in a far-ranging regulatory network not only affecting the synthesis of VTE1-derived prenylquinone products but also plastoglobule morphology.
At the same time, it appears that perturbations limited to one component of the plastoglobule proteome affect the total plastoglobule composition as well, thus indicating that plastoglobules are highly dynamic structures.

3.4 - PRELIMINARY RESULTS ON ABC1V

Considering that no T-DNA insertional mutant lines were publicly available for *ABC1V*, an alternative strategy was selected to achieve *ABC1V* downregulation by gene silencing. As a result, two plants were selected during the screening of the T2 mutant lines showing opposite phenotypes: one rosette (ABC1V-pHSG 1) was significantly larger than wild-type plants of the same age, while the other (ABC1V-pHSG 2) showed a significant growth defect and its central leaves were characterized by an albino phenotype in the early stages of development (Figure 2.12 on page 76).
At the same time, the analysis of *ABC1V* expression in the two plants highlighted a strong reduction in *ABC1V* transcript levels in ABC1V-pHSG 1, indicating an successful silencing event (Figure 2.13 on page 76). On the contrary, ABC1V-pHSG 2 was characterized by a significant increase in *ABC1V* expression rate, possibly because of a partial integration of the T-DNA insert resulting in the overexpression of an incomplete *ihp* RNA construct, which did not activate the RNA silencing machinery.

This preliminary evidence suggests that ABC1V may have a role in plant growth and chloroplast differentiation. Moreover, genome-wide coexpression analysis highlighted a strong correlation between the expression of *ABC1V* and of several metallopeptidases involved in plastid differentiation, among which the two genes *VAR1* and *VAR2*, responsible of the corresponding *VARIEGATED* phenotype in *Arabidopsis* (Figure 2.6 on page 64). Conversely and in contrast with the other two ABC1-like kinases, ABC1V did not coexpress with VTE1, indicating that the kinase may not be involved in the regulation of prenylquinone synthesis, as previously suggested[40] (Figure 2.6 on page 64).

3.5 - FUTURE PERSPECTIVES

3.5.1 - Future characterization of ABC1I and ABC1k3

3.5.1.1 - Identification of other targets of the kinases

Although VTE1 is a target of both ABC1I and ABC1k3, the two kinases may affect other targets and pathways that we did not address. In particular, evidence for an involvement in the modulation of carotenoid synthesis was obtained for the *abc1k3/pgr6* mutant, together with strong indications of its possible involvement the regulation of starch and sugar metabolism. Moreover, both kinases appear to have a severe influence on plastoglobule morphology and protein composition.

In order to identify other potential targets of the two ABC1-like kinases a comparative approach such as 2D-SDS-PAGE could be applied (see Section 3.5.4). Alternatively and to confirm a functional interaction between either ABC1I or ABC1k3 and other chloroplast proteins, an approach by Tandem Affinity Purification (TAP) could be selected. However, considering the often transient nature of the interactions usually existing between kinases and their targets, it would be possible that the interaction between the two proteins is not stable enough to allow their co-precipitation, thus requiring the further stabilization by crosslinking of the protein complexes generated *in situ* prior to their immunoprecipitation.

At the same time, considering the relatively limited number of structural proteins and annotated enzymes in plastoglobules, their functional interactions with either ABC1I or ABC1k3 could be directly investigated by an aimed *in vitro* phosphorylation screening, using either *in vitro* translation products or purified proteins.

3.5.1.2 - Effects of the overexpression of the two kinases

The experimental work described in this thesis demonstrated the involvement of ABC1I and ABC1k3 in the regulation of photosynthesis, sugar and chloroplast lipid metabolism. In order to better understand their biological role and their possible involvement in the modulation of different metabolic pathways chloroplast, it would also be interesting to investigate the effects of the overexpression of the two ABC1-like kinases in plants.

However, an increase in the levels of the kinases could potentially lead to a more severe phenotype than the one observed in the knock-out, the preliminary observation reported here for the ABC1V overexpressing line (see Sections 2.3.1.2 and 3.4).

3.5.2 - ABC1V functional characterization

The lack of suitable knock-out mutant line did not allow to proceed further with the characterization of ABC1V. For this reason, a knock-down mutant line for the plastoglobule ABC1-like kinase was generated during the course of this thesis.

It will now be possible to investigate the effect of *ABC1V* downregulation, with particular reference to role of the kinase during seed germination and in plastid differentiation during seedling photoacclimation.

At the same time, some preliminary evidence for the *ABC1V* overexpressing line has already been collected, but they will need to be verified and broadened by further investigation in the future.

3.5.3 - Lipid profiling

3.5.3.1 - Identification of carotenoids by UHPLC-APCI-QTOFMS

The developed method for lipid profiling in plant samples efficiently allowed the rapid and simultaneous identification of all the principal molecules belonging to the class of prenylquinones.

Nevertheless, only a limited number of carotenoids could be resolved because of the short chromatographic separation, as well as the use of a solvent which allowed their co-extraction with prenylquinones instead of one exclusively suitable for highly apolar molecules like carotenoids. In particular, the identification of carotenoids of high biological relevance like α-carotene, lycopene and zeaxanthin was not possible because of the co-elution of their corresponding peaks with those of more abundant molecules having the same *m/z* ratio, namely β-carotene and lutein.

In order to achieve the complete chromatographic resolution of these carotenoids by UHPLC-APCI-QTOFMS, the development of an alternative method would be advisable. In particular, longer elution times would provide a more suitable chromatographic separation for carotenoids, although significantly increasing the time required for the analysis of a single sample. As a consequence, this choice would correspond to the use of normal HPLC columns for carotenoid separation, thus losing many of the advantages provided by the choice of an UHPLC system.

Alternatively, a possible solution would be represented by the use of C30 stationary phases instead of the classical C18 reverse-phase columns. The increased length and hydrophobicity of commercially-available C30 stationary phases would provide an enhanced interaction with long chained molecules like carotenoids. On the other hand, longer separation times would be required as well for the complete chromatographic resolution of these molecules, in addition to the use of highly apolar solvents in the mobile phase to reduce the risk of a possible retention of hydrophobic solutes in the column.

3.5.3.2 - Determine the lipid composition of chloroplast sub-fractions

A preliminary attempt to compare the relative sub-organellar prenylquinone distribution between different plant lines and in response to HL treatment was performed on highly purified chloroplast fractions (Figure 2.23 on page 94). However, no significant differences were observed between samples, which were also characterized by an high internal variability. It is conceivable that the *abc1i*, *abc1k3/pgr6* and *vte1* mutations are not affecting the prenylquinone distribution between different chloroplast membranes. On the other hand, the method used for chloroplast fractionation increases the risk of cross contamination with membranes from different sub-organellar compartments, as well as the detected variability between samples. Moreover, the longer experimental procedure promotes the spontaneous oxidation of molecules inside samples.

Another fundamental limitation in the lipid profiling of chloroplast fractions is represented by the lack of a suitable internal reference, in contrast with total leaf samples for which either the fresh weight, leaf surface or the chlorophyll content are usually used. In

particular, the procedure used for chloroplast extraction and fractionation leads to significant losses in plant material, thus making it impossible to directly compare pooled plant samples according to their original weight. The number and size of chloroplasts can also change between plant lines or in response to particular growth conditions (like HL treatment), together with the relative abundance of plastoglobules and thylakoid membranes inside chloroplasts. Moreover, chlorophyll content can not be used as reference for mutants showing pale or albino phenotypes (like *abc1k3/pgr6*) and its concentration in thylakoids is not representative for envelope and plastoglobule samples, in which chlorophyll is present only as a contaminant.

For these reasons it would be necessary to identify one or more molecules whose content remains constant in chloroplasts during the whole experiment. However, considering the plasticity of chloroplast lipid metabolism, this does not constitute an easily feasible option. A possible alternative would be represented by the analysis of the fluxes of an isotopic-labeled precursor to estimate its metabolism and distribution inside simplified experimental systems. However, considering the economic relevance and the many limitations of this approach, it would be suitable to investigate the kinetics of the synthesis of one or few selected molecules in purified protoplasts rather than for high-throughput mutant screenings.

3.5.4 - (Phospho)proteomics

3.5.4.1 - Extended profiling of the plastoglobule proteome

The precise detection of changes in the protein composition of isolated plastoglobules represents a fundamental step for the characterization of mutants affecting plastoglobule proteome. However, considering the high amount of starting plant material and the long experimental setup necessary for each analysis, a suitable experimental approach is required in order to investigate differences between diverse plant lines on a routine basis rather than achieve the absolute quantification of all the proteins present in plastoglobules extracted from a single plant line and under the same growth conditions.

During the experimental work previously described in this thesis, an attempt was made to directly carry out the proteomic profiling of total proteins extracted from purified plastoglobules by UHPLC separation coupled to QTOFMS analysis. However, this

preliminary approach resulted in the identification of a limited number of plastoglobule proteins, both because of the relatively low amount of starting material and the complex composition of samples.

On the one hand, the low number of proteins included in the plastoglobule proteome (between 30 and 45 according to the different interpretations[36,39,40]) and their enrichment in samples obtained from highly purified plastoglobule fractions should allow to reduce the risk of cross contamination with proteins from different sub-organellar compartments.

On the other hand, the use of an UHPLC-Nanospray-QTOFMS system for plastoglobule proteome profiling, although providing a high sensitivity and allowing the detection of less represented peptides in the samples obtained from the tryptic digestion of total plastoglobule proteins, does not exploit the physical-chemical differences of the proteins they originated from to distinguish between them. Moreover, the use of standard HPLC conditions for the chromatographic separation of peptides did not take full advantage of the use of an UHPLC system, resulting in long running times (about 90 min/sample).

Conversely, the method developed during this thesis for the profiling of complex mixtures of prenylquinones and carotenoids makes use of the polarity of these molecules to separate them prior to the MS analysis, while the improvements provided by the use of UHPLC technology allow to perform faster chromatographic separations (about 5 min/sample) while keeping a suitable resolution of the peaks.

As a consequence, it would be advisable to use a different approach to optimize the plastoglobule proteome profiling while allowing the rapid and sensitive screening of several samples. A possible solution would be represented by a simple two-dimensional separation of the extracted proteins based on their isoelectric point (pI) and their molecular weight. Considering the extremely low risk of co-migration of two proteins, 2D-SDS-PAGE protein profiles could then be compared to identify changes in the relative abundance of virtually all plastoglobule proteins between samples.

At the same time, UHPLC-Nanospray-QTOFMS analysis would be useful for the precise identification of isolated proteins on gel and for their absolute quantification. Moreover, the prior two-dimensional separation would help reducing the number of potential contaminants in the analyzed samples, thus increasing the sensitivity.

3.5.4.2 - Screening for phosphoproteins in plastoglobules

The suggested 2D-SDS-PAGE approach would also be suitable for the identification of differentially phosphorylated proteins in samples and for the potential identification of targets of the plastoglobule ABC1-like kinases or of other chloroplast kinases.
As normally done in this kind of routine screenings, the presence of phosphopeptides and the protein from which they originated could be determined by MS analysis. Alternatively, protein phosphorylation could be visualized directly on gel using antibodies specific for phosphorylated amino acids serine, threonine and tyrosine or with particular chemiluminescent of fluorescent dyes (e.g. SYPRO® Ruby protein gel stain, Pro-Q Diamond phosphoprotein dye, etc.). In contrast, approaches based on the mobility shift detection of phosphorylated proteins on gel (e.g. Phos-Tag™) would be less advisable because of the complex migration profiles generated on 2D-SDS-PAGE gels.

3.5.2.3 - Implementation of the *in vitro* phosphorylation assays

In this thesis, it has been established by an *in vitro* phosphorylation test that the recombinant VTE1 is phosphorylated by both the ABC1I and ABC1k3 recombinant kinases. However, the use of *in vitro* translation products highly increases the risk of artefacts caused by the simultaneous presence in the rabbit reticulocyte lysate of several kinases and phosphatases that could potentially interact with the newly-synthesized proteins.

For these reasons, it would be advisable to proceed with the purification of the recombinant proteins prior to the phosphorylation assay. This would also enrich samples with the both the kinase and its potential target, thus increasing the probability of a functional interaction between the two as well as the intensity of the resulting phosphorylation signal. However, the use of hexahistidinyl (His_6) tags for purification is not suggested because of the high affinity of the Fe-coordinating His residues on rabbit hemoglobin for the Ni-NTA stationary phase. At the same time, in order to preserve the activity of the kinase, protein separation from hemoglobin under denaturing conditions is not a possible option. Moreover, the use of large protein tags (e.g. MBP, GST, etc.) for purification is not advisable as well, because they could potentially affect the tertiary structure of the kinase or of its target.

A possible solution would be represented either by the purification of hemoglobin from the *in vitro* translation mix prior to the assembling of the translation reactions or the use of protein-specific antibodies for the immunoprecipitation of each recombinant protein.

CHAPTER 4

~ Materials and Methods ~

4.1 - MATERIALS

4.1.1 - Plants

Wild-type (wt) *Arabidopsis* plant always refers to *Arabidopsis thaliana* (L.) Heynh. var. Columbia 0. T-DNA insertion lines from the SALK collection were obtained from the Nottingham Arabidopsis Stock Centre (NASC, http://arabidopsis.info). For *ABC1I* (At1g79600) and *ABC1k3* (At4g31390) at least two knock-out lines were screened (SALK_128696 and SAIL_918_E10 for *ABC1I*; SALK_109079, SALK_068628 and SALK_057147 for *ABC1k3*, respectively). A single point mutation line for *ABC1k3* (*pgr6-1*) was a gift from Dr. T. Shikanai (Graduate School of Science, Kyoto University, Japan) and was previously described as CE11-8-1[(102)]. No phenotypical differences were observed between the screened alleles of both *abc1i* and *abc1k3* mutant lines. For this reason, unless stated otherwise, *abc1I* always refers to SALK_128696 and *abc1k3* refers to SALK_068628. On the contrary, no T-DNA insertion knock-out lines are commercially available for *ABC1V* (At5g05200) to our knowledge. The mutant line for *VTE1* (At4g32770) was a gift from Dr. P. Dörmann (Max Planck Institute, Golm, Germany) and was obtained by ethyl methanesulfonate mutagenesis as described in Porfirova *et al.* (2002)[(64)].
Nicotiana benthamiana seeds were obtained from a commercial variety.

4.1.2 - Micro-organisms

Escherichia coli DH5α and DB3.1 (ccdB survival competent cells) strains were purchased from Invitrogen (Basel, Switzerland) and *E. coli* BL21(DE3) cells were from Novagen (Madison, WI, USA). *Agrobacterium tumefaciens* strain C58 was kindly provided by Dr. Roger Kuhn (Institute of Plant Sciences, ETH Zurich, Switzerland).

4.1.3 - Oligonucleotides

Oligonucleotides were synthesized at Microsynth (Balgach, Switzerland).

4.1.4 - cDNA clones

cDNA clones for *ABC1I* and *ABC1k3* (G21246 and G24066, respectively) were obtained from the Arabidopsis Biological Resource Centre (ABRC, http://abrc.osu.edu/). cDNAs for both genes were inserted in a Gateway®-compatible pENTR223.1 plasmid (Invitrogen), flanked by two SfiI restriction sites and the two attL1 and attL2 Gateway® recombination sites (at the 5' and 3', respectively). On the contrary, *ABC1V* cDNA clone (BX831944) was purchased from Genoscope (Centre National de Séquençage, Evry, France), inserted in a modified pENTR207 plasmid, carrying the resistance genes to both kanamycin and gentamicin. In addition, the *ABC1V* cDNA lacks the stop codon and is flanked by two unannotated sequences which separate the insert from the attL1/2 recombination sites.

4.1.5 - Plasmids

The pGEMT-Easy system was purchased from Promega (Madison, WI, USA). pET21d was obtained from Novagen. Its derivate pET21d-H6 was described in Vidi *et al.* (2006)[(36)] and it encodes for a hexahistidinyl (His_6) tag in frame with the NcoI site. pCL61 was kindly provided by Dr. A. Hiltbrunner (Institute for Biology, Albert-Ludwigs University Freiburg, Germany) and it encodes for a Yellow Fluorescent Protein (YFP) tag in frame with the NcoI site at the 3' of the recombination cassette. The expression vector VTE1-pCL61 was kindly provided by Dr. C. Bréhélin (University of Neuchâtel, Switzerland) and was described in Vidi *et al.* (2006)[(36)]. The Gateway®-compatible plasmid pDONR221 and its derivate pENTR221 were obtained from Invitrogen. pEARLEYGATE100, pEARLEYGATE101, pEARLEYGATE205, p0GWA and pHMGWA were obtained from the Arabidopsis Biological Resource Centre (ABRC, http://abrc.osu.edu/). pEARLEYGATE100 and its two derivatives pEARLEYGATE101 and pEARLEYGATE205 are described in Earley *et al.* (2006)[(247)]. They all encode for a Gateway® recombination cassette flanked by the CaMV 35S promoter and the octopine synthase (OCS) terminator. pEARLEYGATE101 contains the coding sequence for a YFP tag and for an HA epitope (YPYDVPDYA) at the 3' of the Gateway® recombination cassette. pEARLEYGATE205, on the contrary, encodes for a Tandem Affinity Purification (TAP) peptide at the C-terminal of the target protein, consisting of calmodulin binding peptide and a 2X Protein A peptide (which will bind to IgG resin)

separated by a TEV protease cleavage site[248]. p0GWA and pHMGWA are both derivate of pET22d (Merck, Darmstadt, Germany) described in Busso *et al.* (2005)[249]. p0GWA encodes for a C-terminal His_6 tag only, while pHMGWA encodes for an additional His_6 tag and a maltose binding protein (MBP) at the 5' of the recombination cassette. pHELLSGATE12 is a CSIRO hairpinRNAi vector described in Wesley *et al.* (2001)[250] and was obtained from CSIRO Plant Industry (Canberra, Australia).

Since the Gateway® Donor and Destination vectors contain the *ccdB* lethal gene, they were propagated in the *E. coli* DB3.1 strain (parent strain RR1) containing a gyrase mutation (gyrA462).

4.1.6 - Antibodies

Antibodies raised against the plastoglobulin FBN1a have been previously described[36]. Serum against FBN2 was kindly provided by Dr. C. Bréhélin (University of Neuchâtel, Switzerland). Antibodies specific to the chlorophyll a/b binding protein (CAB) were kindly provided by Dr. K. Apel (Institute of Plant Sciences, ETH Zurich, Switzerland). Antibodies specific to the 75 kDa translocon at the outer envelope membrane (AtToc75) have been described in Bauer *et al.* (2000) and (Hiltbrunner 2001)[251,252]. Serum against AtVTE1 was a gift from Dr. P. Dörmann (Max Planck Institute, Golm, Germany). Mouse αHis_6 monoclonal IgG were purchased from Invitrogen. Horseradish peroxidase-conjugated rabbit αmouse and goat αrabbit monoclonal IgG were purchased from Millipore (Billerica, MA, USA). Sera against ABC1I and ABC1k3 are described below.

4.1.7 - Purified standards for Lipidomic analysis

α- and γ-tocopherol (α-T and γ-T, respectively) and phylloquinone (K) standards of HPLC grade (≥ 99.5 %) were purchased from Sigma-Aldrich (Steinheim, Germany). δ-tocopherol (δ-T) standard was purchased from Supelco (Bellefonte, PA, USA). α-tocopherol quinone (α-TQ), plastoquinone-9 (PQ-9) and plastochromanol-8 (PC-8) standards were kindly provided by Jerzy Kruk (Jagiellonian University, Kraków, Poland).

The oxidized and reduced PQ-9 standards were obtained as described in Suhara *et al.* (2005)[253] with slight changes[80]. Briefly, an excess (1 μg) of sodium borohydride (Fluka, Buchs, Switzerland) was added to the oxidized PQ standard (100 ng) to completely reduce it to PQH_2 and the retention time of both forms was then determined by UHPLC-APCI-QTOFMS. Lutein (Lut) and β-Carotene (β-Car) standards were purchased from Extrasynthese (Lyon, France).

4.1.8 - Chemicals

The solvents used for plant lipid profiling were tetrahydrofuran (THF, analytical grade, Normapur) from VWR (Leuven, Belgium) and ethylacetate (EtAc, analytical grade) from Acros Organics (Geel, Belgium). UPLC/MS grade MeOH and water from Biosolve (Valkenswaard, The Netherlands) were used for the UHPLC-APCI-QTOFMS analyses. Unless stated otherwise, all the other chemicals were purchased from Sigma-Aldrich.

4.2 - METHODS

4.2.1 - Plant Growth

4.2.1.1 - Growing *A. thaliana* on Murashige and Skoog medium

An appropriate volume of dried seeds (~100 µL) was put into a 1.5 mL Eppendorf tube and incubated for 10 min with 1 mL of sterilization solution (2% bleach, 50% ethanol, 0,1% Tween20) under moderate shaking. The solution was then removed and seeds were rinsed several times with 100% ethanol. Seeds were then dried under laminar air flow inside the sterile hood and plated on sterile Petri dishes containing 0.5× Murashige and Skoog medium (MS; Duchefa Biochemie, Haarlem, The Netherlands) added with 0.8% (w/v) Phyto Agar (Duchefa). Whether necessary for the selection of phosphinothricin-resistant plants, solid medium containing 10 µg/mL glufosinate ammonium (BASTA; Dr. Ehrenstorfer GmbH, Germany) was used. Seed germination was synchronized by incubating the seeds 2 days at 4°C in the dark. Plates were then moved to short day conditions (8/16 h light/dark period).

4.2.1.2 - Growing *A. thaliana* and *N.benthamiana* on soil

Non-sterile *A.thaliana* and *N.benthamiana* plants were grown on sandy soil (Top Dressing, Ricoter) containing 45% sand, 10% perlite, 25% compost and 20% peat. Germination was synchronized as above. *A.thaliana* plants were grown on soil under standard growth conditions (150 $\mu E \cdot m^{-2} \cdot s^{-1}$, 21/18°C, 55% relative air humidity) and under either short- (8/16 h light/dark period) or long- (16/8 h light/dark period) day conditions according to the protocol described in Hiltbrunner *et al.* (2001)[252] with slight modifications. A slightly higher light intensity (300 $\mu E \cdot m^{-2} \cdot s^{-1}$) was used for *N.benthamiana* plants, instead.

4.2.1.3 - High Light (HL) treatment

HL treatment was performed on 1 or 2-month-old rosettes grown under short days by exposure to continuous HL conditions (500 $\mu E \cdot m^{-2} \cdot s^{-1}$, 21°C, 55% relative air humidity) in a PGC 6HID growth chamber (Percival Scientific, Boone, IA) equipped with 400 W metal halide lamps (Philips).

4.2.1.4 - Plastoglobule purification from *A. thaliana*

Chloroplast membranes were extracted and fractionated as described in Vidi *et al.* (2006)[(36)] with slight modifications. Briefly, leaves from *A.thaliana* plants grown on soil for 1 or 2-months were harvested, accurately washed with cold tap water and immersed for 30 min in dH_2O in the dark at 4°C. All subsequent steps were also carried out at 4°C. Leaf material was homogenized in HB buffer [450 mM sorbitol, 20 mM Tricine/KOH pH 8.4, 10 mM EDTA pH 8.5, 10 mM $NaHCO_3$, 1 mM $MnCl_2$] inside a benchtop blender (Waring Laboratory, USA) and filtered through superposed layers of cheese cloth and Miracloth (Merck). Chloroplasts were then sedimented by centrifugation (5 min at 3,800 × g), washed in TE buffer [50 mM Tricine/HCl pH 7.5, 2 mM EDTA pH 8.5, 2 mM DTT] and hypertonically lysed in TE buffer supplemented with 0.6 M sucrose. Chlorophyll concentration was spectroscopically quantified as described in Arnon *et al.* (1949)[(254)] and then adjusted to 2 mg/mL. In order to prevent proteolytic degradation and spontaneous dephosphorylation, 0.5% (v/v) protease inhibitor cocktail for plant cell extracts (P9599, Sigma) and 1% (v/v) phosphatase inhibitor cocktail 2 (P5726, Sigma) was added. Lysed chloroplasts were then diluted with 3 volumes of TE buffer and homogenised with a Potter homogenizer. Total membranes were sedimented by centrifugation (1 h at 100,000 × g and 4°C) and an aliquot of stroma was collected for further use. Membranes were then resuspended in TE buffer supplemented with 45% sucrose to a final chlorophyll concentration of 7 mg/mL, further homogenized in a Potter homogenizer and loaded on a linear (5% - 45%) sucrose gradient in TE buffer. Chloroplast membranes were then fractionated by centrifugation (15 h at 100,000 × g and 4°C) and 1 mL fractions were collected starting from the top of the gradient, frozen in liquid nitrogen and stored at -80°C.

4.2.2 - Molecular biology techniques

4.2.2.1 - Molecular cloning

Cloning by restriction/ligation was performed using standard protocols[(255)]. EST clones from pre-existing plasmid constructs were used as templates for PCR together with primers including appropriate restriction sites. Stop codons were removed and a variable number of nucleotides were added (whether necessary) to keep the cloned sequence in frame with any sequence tag located at its 3'. PCR products and plasmids were then digested with the corresponding restriction enzymes (New England Biolabs or Promega) and purified from agarose gels using the QIAquick kit (Quiagen). Vectors were dephosphorylated using shrimp alkaline phosphatase (Roche) according to the manufacturer's recommendations. T4 DNA ligase (New England Biolabs) was then used to ligate vectors and inserts.

Alternatively, when PCR products had to be cloned in Gateway®-compatible plasmids (Invitrogen), adaptors containing the two attB1 (5'-GGGG-ACA-AGT-TTG-TAC-AAA-AAA-GCA-GGC-TNN) and attB2 (5'-GGGG-AC-CAC-TTT-GTA-CAA-GAA-AGC-TGG-GTN) recombination sites were included in the forward and reverse primers, respectively. PCR products were purified from agarose gels using the QIAquick kit (Quiagen) and recombined with a suitable Donor vector (pDONR221) containing two attP1/attP2 regions. The BP recombination was performed using the Gateway® BP Clonase II Enzyme Mix (Invitrogen), according to the manufacturer's recommendations, and it produced two attL1/attL2 regions flanking the cloned sequence in the obtained Entry vector. DNA sequences were subsequentely cloned by LR recombination in suitable Destination vectors containing two attR1/attR2 regions using the Gateway® LR Clonase II Enzyme Mix (Invitrogen). As a consequence, two attB1/attB2 regions flanking the cloned sequence were obtained in the Expression vector.

Both ligation and recombination products were transformed by heat shock into competent *E. coli* DH5α cells prepared according to (Inoue et al., 1990). Selection was performed on LB medium [25 g/L LB Broth Miller (Becton Dickinson Diagnostic Systems)] supplemented with 1.2% (w/v) Agar (bacteriological grade, ICN Biomedicals) and the

appropriate antibiotics. Clones were then selected both by PCR and restriction digestion and DNA sequences were verified by sequencing at Microsynth (Balgach, Switzerland).

A list of the primers used for cloning, for transformant screening by PCR analysis and for sequencing are presented in Table 4.3. The starting cDNA clones, the used plasmids and the resulting vectors, together with information on their structure and their antibiotic resistance are presented in Table 4.4.

4.2.2.2 - Plasmid isolation and purification

For small-scale plasmid isolation, the GenElute Plasmid Miniprep Kit (Sigma) was used. For plasmid isolation from larger culture volumes (≥ 100 mL), the NucleoBond® Xtra Midiprep System (Macherey-Nagel) was used according to the suppliers' instructions.

4.2.2.3 - Genomic DNA extraction from *A. thaliana* leaves

Rapid genomic DNA (gDNA) extraction from *A. thaliana* leaves was performed as described in Edwards *et al.* (1991)[256]. When a higher degree of purity was required, samples were further purified by precipitation in an equal volume of buffer-saturated phenol/chloroform (1:1). After brief centrifugation (5 min at 10,000 × g), the aqueous phase (top layer) was recovered and additioned with 0.1 volumes of 3 M sodium acetate (pH 5.2) and 2 volumes of 100% ethanol. Samples were stored for 30 min at -80°C, then DNA was pelleted (15 min at 10,000 × g), washed with 1 mL of cold 70% ethanol, lyophilised and dissolved in a suitable volume of sterile ddH_2O.

4.2.2.4 - Isolation of knock-out mutant plants

In order to select homozygous lines for T-DNA insertions, a three-primer PCR analysis was employed. The primer sets included a Left and Right genomic Primer designed on the regions flanking the predicted T-DNA insertion site (LP and RP, at the 5' and 3' of the T-DNA, respectively) and the left T-DNA Border Primer (BP), designed on the inserted

sequence. For SALK lines LBa1 of pBIN-pROK2 for was used, while LB1 of pCSA110-pDAP101 was selected for SAIL lines. LB and RP were designed using the T-DNA Primer Design tool from the Salk Institute Genomic Analysis Laboratory[257]. The complete list of the used primers and their sequences are presented in Table 4.1. DNA extracted from wild-type *A. thaliana* (Columbia-0) plants was used as reference. PCR reactions were then analysed by agarose gel electrophoresis according to standard protocols[255].

The *pgr6-1* mutant was obtained by ethyl methanesulfonate mutagenesis as previously described[102] and is characterized by a single nucleotide substitution in the second exon of the gene (5'-ATTGTTTG***G***ACT-3' mutated to 5'-ATTGTTTG***A***ACT-3') which generates a stop codon.

Table 4.1: List of primers used for knock-out plant genotyping.

LP, Left genomic Primer. RP, Right genomic Primer. BP, left T-DNA Border Primer.

Gene	Knock-out line		Primer Name	Primer Sequence
ABC1I (At1g79600)	SALK_128696	LP	ABC1I_A_LP	5'-TGTTGCTGTCAAAGTTCAACG-3'
		RP	ABC1I_A_RP	5'-CAAGCGTACTTTGAAGTTCCG-3'
	SAIL_918_E10	LP	ABC1I_B_LP	5'-GGGAGGAGGTAGTGACAAAGG-3'
		RP	ABC1I_B_RP	5'-AAGGTAATCGGGTGGACAGAG-3'
ABC1k3 (At4g31390)	SALK_057147	LP	ABC1k3_A_LP	5'-CAACGTCCAAGAGACCAAGAC-3'
		RP	ABC1k3_A_RP	5'-TGGTGTTTTCCAATGGAAAAG-3'
	SALK_068628	LP	ABC1k3_B_LP	5'-AGCTGATTCATCATCTGTCGG-3'
		RP	ABC1k3_B_RP	5'-TCCCTTCCCACACTAAAAGTG-3'
	SALK_109079	LP	ABC1k3_C_LP	5'-TTAAGACGGAGCAGAACAACG-3'
		RP	ABC1k3_C_RP	5'-GTTGTCATTACCGATGCATCC-3'
ABC1V (At5g05200)	*none available*			
SALK lines		BP	LBa1 (pBIN-pROK2)	5'-TGGTTCACGTAGTGGGCCATCG-3'
SAIL lines		BP	LB1 (pCSA110-pDAP101)	5'-GCCTTTTCAGAAATGGATAAATA GCCTTGCTTCC-3'

4.2.2.5 - *ABC1V* knock-down by gene silencing.

Since no T-DNA insertion knock-out lines are commercially available for *ABC1V* (At5g05200), CSIRO hairpinRNAi vectors were used to achieve gene silencing. ABC1V complete coding sequence, excluding the stop codon, was sub-cloned by Gateway® LR recombination from pENTR221-ABC1V in the corresponding recombination sites of pHELLSGATE12, resulting in the formation of a *intron-containing* self-complementary "*hairpin*" RNA (*ihp* RNA) construct, under the control of the CaMV 35S promoter and the ocs terminator. *A. thaliana* plants were then transformed as described in section 4.2.3.3 on page 149 and transformants were selected on solid medium containing 50 µg/mL kanamycin. The presence of the T-DNA insertion in the selected transformants was further investigated by PCR using the primer couple pCL60-35S and ABC1V.Left according to standard protocols[(255)].

4.2.2.6 - RNA extraction from *A. thaliana* leaves and cDNA preparation.

Total RNAs were purified from *A. thaliana* leaves using the RNeasy Plant Mini Kit (Qiagen), according to the supplier's recommendations, and DNase treatment was performed *on column* using the RNase-free DNase set (Qiagen). cDNAs were then prepared using the GoScript™ Reverse Transcriptase kit (Promega) in the presence of RNasin RNase inhibitors (Promega), and stored at -20°C.

4.2.2.7 - Determination of gene expression rate by quantitative PCR.

For quantitative PCR, the housekeeping gene ACTIN2 (At3g18780) was used as reference and amplified using the primer couple act2-S and act2-AS. In order to analyze *ABC1I* expression rate in the *abc1i* T-DNA insertion mutant and *ABC1V* transcript levels in the ABC1V-pHELLSGATE12 knock-down lines, the two primer couples ABC1I_q_F/ABC1I_q_R ABC1V_q_F/ABC1V_q_R were used, respectively. For the analysis of a possible ABC1I and ABC1k3 effect on *VTE1* (At4g32770) and *FBN1a* (At4g04020) expression, the primer couples VTE1_q_F/VTE1_q_R and PG35_q_F/PG35_q_R were designed. The complete list of the used primers and their

sequences are presented in Table 4.2. Real-Time PCR reactions were assembled in a final volume of 20 µL using the ABsolute™ qPCR SYBR® Green mix (ABgene, Epsom, UK), 10 µM of both 5' and 3' primers, and adjusted amounts of cDNA diluted 40 times in ddH_2O. The PCR program was as follows: 15 min, 95°C (thermo-start); 45x (20 s, 95°C; 30 s, 55°C; 45 s, 72°C); 1 min, 55°C, and was followed by an 80-step dissociation (55 to 95°C). SYBR® Green emission was detected in real-time in an iQ5 Optical System (Bio-Rad Laboratories, Reinach, Switzerland) and data were treated using the included software. A one-way analysis of variance (ANOVA) was conducted on the obtained data. When a significant difference was detected, a Tukey HSD test was applied at a significance level of $P < 0.05$ to separate the means.

Table 4.2: List of primers used to determine gene expression levels by Real-Time qPCR.

Gene	Primer Name	Primer Sequence	Position on chromosome
ACTIN2 (At3g18780)	act2-S	5'-TGGAATCCACGAGACAACCTA-3'	Chr.3: 006476434
	act2-AS	5'-TTCTGTGAACGATTCCTGGAC-3'	Chr.3: 006476821
ABC1I (At1g79600)	ABC1I_q_F	5'-GCTTTGATCCTGCTATTTTG-3'	Chr.1: 029950352
	ABC1I_q_R	5'-GTGGCTCGAAGAAGTTGTTG-3'	Chr.1: 029950133
ABC1V (At5g05200)	ABC1V_q_F	5'-GGCTACAGCTCGTGGAACAA-3'	Chr.5: 001544620
	ABC1V_q_R	5'-CAGAAGTGCAAACTCTCTCG-3'	Chr.5: 001544335
VTE1 (At4g32770)	VTE1_q_F	5'-GTGCTCCTACCACAGAAGTT-3'	Chr.4: 015807400
	VTE1_q_R	5'-TATCTCCACTGCTGCCATTG-3'	Chr.4: 015807652
FBN1a (At4g04020)	PG35_q_F	5'-CAAACCATTGATTCCGATAG-3'	Chr.4: 001933025
	PG35_q_R	5'-AGTCCCTATAACACCTTGCT-3'	Chr.4: 001933240

Table 4.3: List of the primers used for cloning, for transformant screening by PCR analysis and sequencing.

Universal primers used for sequencing		
Primer Name	**Primer Sequence**	**Function**
M13	5'-TGTAAAACGACGGCCAGT-3'	External left primer on pENTR# Gateway® plasmids
M13.R	5'-CAGGAAACAGCTATGACC-3'	External right primer on pENTR# Gateway® plasmids
T7 (pGEMT)	5'-TAATACGACTCACTATAGGGCGAATTG GGCC-3'	External left primer on pGEMT-derived vectors (T7 promoter)
T7 (pET21d)	5'-GAAATTAATACGACTCACTATAGGGG-3'	External left primer on pET21d-derived vectors (T7 promoter)
T7term (pET21d)	5'-GCTAGTTATTGCTCAGCGG-3'	External right primer on pET21d-derived vectors (T7 terminator)
pCL60-35S	5'-TCTCCACTGACGTAAGGGAT-3'	External left primer on Gateway® expression vectors (35S promoter)
pCL61-YFP	5'-AGCTTGCCGTAGGTGGCATC-3'	External right primer designed on C-terminal YFP fusion tag

ABC1I **(At1g79600)**		
Primer Name	**Primer Sequence**	**Function**
GATE.ABC1I.attB1.F	5'-GGGG-ACAAGTTTGTACAAAAAAGCA GGCT-ATGAGTCTGGTGGTTGGTCAG-3'	Forward attB1 primer
GATE.ABC1I.attB2.R	5'-GGGG-ACCACTTTGTACAAGAAAGCTG GGT-G-TGGGGATGGTGCAGAAGATGG-3'	Reverse attB2 primer (+ 1 nt C-terminal framekeeper)
ABC1I_NAT.GATE.F	5'-GGGG-ACAAGTTTGTACAAAAAAGCAG GCT-CG-ATGGCTAGGCCTAAGGAAGACG G-3'	Forward attB1 primer for native protein [transit peptide removed] (+ 2 nt N-terminal framekeeper)
ABC1I.F.seq	5'-GAACTTGCAGAGCTTCAGGATGCTT-3'	Inner forward sequencing primer
ABC1I.R.seq	5'-CTTAGATACGGGTTTGGATCAGTGA-3'	Inner reverse sequencing primer
ABC1I.LEFT2	5'-TCACTGATCCAAACCCGTATCTAAG-3'	Outer forward sequencing primer
ABC1I.RIGHT2	5'-AGAGATCTCAGAAACTCAGGAAGGG-3'	Outer reverse sequencing primer

ABC1k3 **(At4g31390)**		
Primer Name	**Primer Sequence**	**Function**
GATE.ABC1k3.attB1.F	5'-GGGG-ACAAGTTTGTACAAAAAAGCAG GCT-ATGGAGTCAATCCACTGCAATAG-3'	Forward attB1 primer
GATE.ABC1k3.attB2.R	5'-GGGG-ACCACTTTGTACAAGAAAGCTG GGT-G-TCTGTCGGATAATACTGAGTTGC-3'	Reverse attB2 primer (+ 1 nt C-terminal framekeeper)
ABC1k3_NAT.GATE.F	5'-GGGG-ACAAGTTTGTACAAAAAAGCA GGCT-CG-TGGGGAAATCGAGCTCCGCGC T-3'	Forward attB1 primer for native protein [transit peptide removed] (+ 2 nt N-terminal framekeeper)
ABC1k3.in.F	5'-CTCTTGGGTTGTATTGGTCTACCTT-3'	Inner forward sequencing primer
ABC1k3.in.R	5'-GGCTTCAGTGTGAAACATATACCCT-3'	Inner reverse sequencing primer
ABC1k3.out.LEFT	5'-TGAAGGTCCCAAATTGCACAACAGG-3'	Outer forward sequencing primer
ABC1k3.out.RIGHT	5'-ACGACTTTCCCATCCGTATCCCAGA-3'	Outer reverse sequencing primer

ABC1V **(At5g05200)**		
Primer Name	**Primer Sequence**	**Function**
GATE.ABC1V.attB1.F	5'-GGGG-ACAAGTTTGTACAAAAAAGCA GGCT-ATGGCGGTCTCAGCTTTCCGT-3'	Forward attB1 primer
GATE.ABC1V.attB2.R	5'-GGGG-ACCACTTTGTACAAGAAAGCTG GGT-G-GTTGAAGCTGTCCTTGTATCC-3'	Reverse attB2 primer (+ 1 nt C-terminal framekeeper)
ABC1V_NAT.GATE.F	5'-GGGG-ACAAGTTTGTACAAAAAAGCAG GCT-CG-ATGGCTAGGCCTAAGGAAGACG G-3'	Forward attB1 primer for native protein [transit peptide removed] (+ 2 nt N-terminal framekeeper)
ABC1V_STOP.GATE.R	5'-GGGG-ACCACTTTGTACAAGAAAGCTG GGT-TTA-GTTGAAGCTGTCCTTGTATCC-3'	Reverse attB2 primer introducing a TTA stop codon
ABCIV.XbaI.ATG	5'-CCTAGTCTAGAATGGCGGTCTCAGCTT TC-3'	Forward primer for (sub)cloning by restriction/ligation
ABCIV.XhoI	5'-TGCTCGAGGTTGAAGCTGTCCTTGTAT-3'	Reverse primer for (sub)cloning by restriction/ligation
Seq.ABC1V.F	5'-CTGGTGGATTACCAAGTGAATTGCA-3'	Inner forward sequencing primer
Seq.ABC1V.R	5'-TAGTTCCTGGATAGATGAGAACATC-3'	Inner reverse sequencing primer
ABC1V.LEFT	5'-AGGAGCTTTGTCAAAGCAGTTCTGA-3'	Outer forward sequencing primer
ABC1V.RIGHT	5'-TGTACATGCAGGAAACTTATGGCTG-3'	Outer reverse sequencing primer

Table 4.4: List of the used plasmids, with information on their main features and their antibiotic resistance.

Plasmid feature abbreviations:

LB, Left T-DNA border; RB, Right T-DNA border; MCS, Multiple Cloning Site; attB1/2, attP1/2, attL1/2, attR1/2, Gateway® recombination sites; *ccdB*, lethal gene (DNA gyrase); *CmR*, Chloramphenicol resistance gene; 35S, CaMV 35S promoter; NOS, NOpaline Synthase promoter; T7, bacteriophage T7 RNA polymerase promoter; RBS, Ribosome Binding Site; *lac* Op, *lac* operator; ATG, start codon; *, stop codon; OCS, OCtopine Synthase terminator; NOSterm, NOpaline Synthase terminator; T7term, bacteriophage T7 RNA polymerase terminator; TP, Transit Peptide; (#), restriction site; [#], added nucleotides; HA, Human influenza hemAgglutinin epitope; His_6, hexahistidinyl tag; MBP, Maltose Binding Protein; TAP, Tandem Affinity Purification tag; YFP, Yellow Fluorescent Protein; *NPT II*, Neomycin PhosphoTransferase gene; *bar*, phosphinothricin resistance gene.

Abbreviations for antibiotics:

Amp, Ampicilline (100 µg/mL); Cam, Chloramphenicol (33 µg/mL); Gen, Gentamicin (100 µg/mL); Kan, Kanamycin (100 µg/mL); Spc, Spectinomycin (100 µg/mL).

Untransformed plasmids		
Vector name	**Main features**	**Antibiotic resistance**
pDONR221	–attP1-*ccdB*-*CmR*-attP2–	Kan, Cam
pEARLEYGATE100	–LB-*bar*-35S-attR1-*ccdB*-*CmR*-attR2-OCS-RBv	Kan, Cam
pEARLEYGATE101	–LB-*bar*-35S-attR1-*ccdB*-*CmR*-attR2-YFP-HA-OCS-RB–	Kan, Cam
pEARLEYGATE205	–LB-*bar*-35S-attR1-*ccdB*-*CmR*-attR2-TAP-OCS-RB–	Kan, Cam
p0GWA	–T7-*lac* OP-RBS-attR1-*ccdB*-*CmR*-attR2-His_6-*-T7term–	Amp, Cam
pHMGWA	–T7-*lac* OP-RBS-ATG-His_6-MBP-attR1-*ccdB*-*CmR*-attR2--His_6-*-T7term–	Amp, Cam
pGEMT-Easy	Plasmid linearized in the region corresponding to the MPS (5'A, 3'T protruding); β-galactosidase selection (+ X-Gal)	Amp
pET21d-H6	–T7-*lac* OP-MCS-His_6-*-T7term–	Amp
pHELLSGATE12	–RB-35S-attR1-*ccdB*- attR2-PDK intron-*CmR*-attR2-*ccdB*--attR1-OCS-NOS-*NPT II*-NOSterm-LB–	Spc, Cam

ABC1I **(At1g79600)**		
Vector name	**Main features**	**Antibiotic resistance**
pENTR223.1-ABC1I (cDNA clone G21246)	–attL1-(SfiI)-*ABC1I*-*-(SfiI)-attL2–	Spc
pENTR221-ABC1I	–attL1-*ABC1I*-[C]-attL2–	Kan
pENTR221-ABC1I (*native*)	–attL1-[CG]-ATG-*ABC1I* (TP removed)-[C]-attL2–	Kan
pEARLEYGATE100-ABC1I	–LB-*bar*-35S-attB1- *ABC1I*-[C]-attB2-OCS-RB–	Kan
pEARLEYGATE101-ABC1I	–LB-*bar*-35S-attB1- *ABC1I*-[C]-attB2-YFP-HA-OCS-RB–	Kan
pEARLEYGATE205-ABC1I	–LB-*bar*-35S-attB1- *ABC1I*-[C]-attB2-TAP-OCS-RB–	Kan
p0GWA-ABC1I	–T7-*lac* OP-RBS-attB1- *ABC1I*-[C]-attB2-His_6-*-T7term–	Amp
p0GWA-ABC1I (*native*)	–T7-*lac* OP-RBS-attB1- *ABC1I* (TP removed)-[C]-attB2--His_6-*-T7term–	Amp
pHMGWA-ABC1I (*native*)	–T7-*lac* OP-RBS-ATG-His_6-MBP-attB1-[CG]-ATG--*ABC1I* (TP removed)-[C]-attB2-His_6-*-T7term–	Amp

ABC1k3 **(At4g31390)**		
Vector name	**Main features**	**Antibiotic resistance**
pENTR223.1-ABC1k3 (cDNA clone G24066)	–attL1-(SfiI)-*ABC1k3*-*-(SfiI)-attL2–	Spc
pENTR221-ABC1k3	–attL1-*ABC1k3*-[C]-attL2–	Kan
pENTR221-ABC1k3 (*native*)	–attL1-[CG]-ATG-*ABC1k3* (TP removed)-[C]-attL2–	Kan
pEARLEYGATE100-ABC1k3	–LB-*bar*-35S-attB1- *ABC1k3*-[C]-attB2-OCS-RB–	Kan
pEARLEYGATE101-ABC1k3	–LB-*bar*-35S-attB1- *ABC1k3*-[C]-attB2-YFP-HA-OCS-RB–	Kan
pEARLEYGATE205-ABC1k3	–LB-*bar*-35S-attB1- *ABC1k3*-[C]-attB2-TAP-OCS-RB–	Kan
p0GWA-ABC1k3	–T7-*lac* OP-RBS-attB1- *ABC1k3*-[C]-attB2-His_6-*-T7term–	Amp
p0GWA-ABC1k3 (*native*)	–T7-*lac* OP-RBS-attB1- *ABC1k3* (TP removed)-[C]-attB2--His_6-*-T7term–	Amp
pHMGWA-ABC1k3 (*native*)	–T7-*lac* OP-RBS-ATG-His_6-MBP-attB1-[CG]-ATG--*ABC1k3* (TP removed)-[C]-attB2-His_6-*-T7term–	Amp

ABC1V **(At5g05200)**		
Vector name	**Main features**	**Antibiotic resistance**
pENTR207(modified)-ABC1V (cDNA clone BX831944)	–attL1- *spacer* -*ABC1V*- *spacer* -attL2–	Kan, Gen
pENTR221-ABC1V	–attL1-*ABC1V*-[C]-attL2–	Kan
pENTR221-ABC1V (STOP)	–attL1-*ABC1V*-*-attL2–	Kan
pENTR221-ABC1V (*native*)	–attL1-[CG]-ATG-*ABC1V* (TP removed)-[C]-attL2–	Kan
pGEMT-XbaI/XhoI-ABC1V	–MPS-[T]-(XbaI)-ABC1V-(XhoI)-[A]-MPS–	Amp
pEARLEYGATE100-ABC1V	–LB-*bar*-35S-attB1- *ABC1V*-[C]-attB2-OCS-RB–	Kan
pEARLEYGATE101-ABC1V	–LB-*bar*-35S-attB1- *ABC1V*-[C]-attB2-YFP-HA-OCS-RB–	Kan
pEARLEYGATE205-ABC1V	–LB-*bar*-35S-attB1- *ABC1V*-[C]-attB2-TAP-OCS-RB–	Kan
pET21d-H6	–T7-*lac* OP-(XbaI)- *ABC1V*-(XhoI)-His_6-*-T7term–	
p0GWA-ABC1V (*native*)	–T7-*lac* OP-RBS-attB1- *ABC1V* (TP removed)-[C]-attB2--His_6-*-T7term–	Amp
pHMGWA-ABC1V (*native*)	–T7-*lac* OP-RBS-ATG-His_6-MBP-attB1-[CG]-ATG--*ABC1V* (TP removed)-[C]-attB2-His_6-*-T7term–	Amp
pHELLSGATE12-ABC1V	–RB-35S-attB1-*ABC1V* (sense)- attB2-PDK intron-*CmR*--attB2-*ABC1V* (antisense)-attB1-OCS-NOS-*NPT II*--NOSterm-LB–	Spc, (Cam)

VTE1 **(At4g32770)**		
Vector name	**Main features**	**Antibiotic resistance**
pCL61-VTE1	–M13-T7-(EcoRV)-35S-(EcoRV)-*VTE1*-(NcoI)-YFP--NOSterm-M13R–	Amp
pCL61(NO 35S)-VTE1	–M13-T7-(EcoRV)-*VTE1*-(NcoI)-YFP-NOSterm-M13R–	Amp

4.2.2.8 - Protein extraction from *A. thaliana* total leaves.

Total protein isolation from *Arabidopsis* leaves was performed according to[258]. To prevent proteolytic degradation, 0.5% (v/v) protease inhibitor cocktail for plant cell extracts (P9599, Sigma) was added. Proteins were then concentrated by chloroform-methanol precipitation[259] and resuspended in an appropriate volume of sample buffer [50 mM Tris/HCl pH 6.8, 0.1 M DTT, 2% (w/v) SDS, 0.1% (w/v) bromophenol blue, 10% (v/v) glycerol].

4.2.2.9 - Protein separation and Western blot analysis

Proteins extracted either from bacteria or plants were separated by SDS-PAGE and transferred on Protran® nitrocellulose membrane (Whatman, Dassel, Germany) inside a Mini-PROTEAN electrophoresis cell (Bio-Rad Laboratories), according to the manufacturer's instructions. Membranes were then stained in Amido Black and unspecific staining was removed with a standard destain solution [1 volume glacial acetic acid, 4 volumes EtOH, 5 volumes dH_2O] according to standard protocols[255].

In order to block the unspecific binding of antibodies, membranes were first incubated in either TBS [25 mM Tris/HCl, 150 mM NaCl, pH 7.5] or PBS [140 mM NaCl, 2.7 mM KCl, 10 mM Na_2HPO_4, 1.8 mM KH_2PO_4; pH 7.4] supplemented with 3% (w/v) BSA or 5% skimmed milk powder. Membranes were then washed in either TBS-T or PBS-T [TBS or PBS, 0.1% (v/v) Tween20] and incubated for 60 min or longer with adequate antibody dilutions in blocking buffer. After extensive wash with TBS-T/TBS or PBS-T/PBS, primary antibodies were revealed by incubating the membranes for 30 min in blocking buffer supplemented with a 1/3,000 dilution (v/v) of horseradish peroxidase-conjugated rabbit αmouse or goat αrabbit IgG, depending on the organism in which the primary antibody was produced. After washing with TBS-T/TBS or PBS-T/PBS buffer, membranes were incubated 1 min in [0.1 M Tris/HCl pH 8.5, 1.25 mM 3-aminophthalhydrazide (luminol), 0.2 mM p-coumaric acid, 0.009% (v/v) H_2O_2]. Signals were detected by Enhanced ChemiLuminescence (ECL) by exposing the membranes to high performance chemiluminescence films (GE Healthcare, Buckinghamshire, UK). Alternatively, luminescence was monitored using a ChemiDock system and quantified using the provided QuantityOne software (both from Bio-

Rad Laboratories). For a complete list of the antibodies and the conditions used for Western blot analysis see Table 4.4.

Table 4.4: Antibody dilutions used for Western blot analysis. Incubation buffers and approximate incubation times for immunoblotting are indicated. See the text for buffer compositions.

Antibody	Organism	Dilution (v/v)	Buffer	Incubation time
αHis_6	mouse	1/2000	TBS, 5% (w/v) BSA	1 h
αFBN2	rabbit	1/4000	PBS, 5% (w/v) milk	1 h
αFBN1a	rabbit	1/2000	PBS, 5% (w/v) milk	1 h
αLHCb2	rabbit	1/2000	PBS, 5% (w/v) milk	1 – 3 h
αToc75	rabbit	1/500	PBS, 3% (w/v) milk	1 h
αVTE1	rabbit	1/500	PBS, 2% (w/v) milk	1 – 6 h
αABC1k3	rabbit	1/500	PBS, 3% (w/v) milk	1 – 4 h
αABC1V	rabbit	1/500	PBS, 3% (w/v) milk	1 – 4 h

4.2.3 - Microbiology techniques

4.2.3.1 - *Agrobacterium tumefaciens* transformation by electroporation

In order to make them competent for electroporation, *A. tumafaciens*, strain C58 cells were grown in liquid YEB medium [0.5% (w/v) Bacto-Trypton, 0.5% (w/v) Bacto-Pepton, 0.1% (w/v) yeast-extract (BD Biosciences, Le Pont de Claix, France), 2 mM $MgCl_2$] until an optical density (600 nm) of 0.8 was achieved. Cells were pelleted (10 min at 2,000 × g and 4°C) and washed several times with decreasing volumes of a 10% glycerol solution.
A suitable volume (50-100 µL) of competent cells was loaded in a cuvette for electroporation with 10-50 ng of plasmid DNA. Electroporation was performed in a MicroPulser device (Bio-Rad Laboratories), according to the manufacturer's instructions. Transformants were selected on LB medium supplemented with 1.2% (w/v) agar (bacteriological grade) and the appropriate antibiotic, in addition to 50 µg/mL Rifampicine and 100 µg/mL Ampicilline for the selection of the *A. tumafaciens* strain and the *vir* helper plasmid, respectively.

4.2.3.2.- Transient transformation of tobacco leaf cells.

Transformed *A. tumafaciens* cells were grown in liquid LB medium until an optical density (600 nm) of 1.7 - 2.0 was achieved. Cells were pelleted (15 min at 2,000 × g) and resuspended in water to a final optical density (600 nm) of 0.4. This suspension was then infiltrated in the lower face of *N.benthamiana* leaves previously nebulized with water to induce stomata opening. Leaf samples from plants agroinfiltrated with constructs encoding for YFP-fusion proteins were observed in confocal laser scanning microscopy 48 to 80 h after transformation (see section 4.2.4.1).

4.2.3.3 - *Arabidopsis* stable transformation.

A. thaliana plants were transformed using the floral dip method as described by[260,261]. Transformants were then selected on solid medium containing 10 µg/mL glufosinate ammonium (see section 4.2.1.1 on page 135). The presence of the transgene was further verified by PCR analysis on gDNA extracted from phosphinothricin-resistant plants, as previously described (see section 4.2.2.3 on page 135). The primers sets were: pCL60-35S (on the CamV 35S promoter region from the pCL60 vector) as forward primer and the outer reverse primer (either ABC1I.R.seq, ABC1k3.out.LEFT or seq.ABC1V.R for *ABC1I*, *ABC1k3* and *ABC1V*, respectively). The complete sequences of these primers are presented in Table 4.3.

4.2.4 - Analytical techniques

4.2.4.1 - Protein sub-cellular localization.

The complete coding sequences, excluding the stop codon, were amplified from *ABC1I*, *ABC1k3* and *ABC1V* cDNA clones by PCR using 5' and 3' primers including attB1 and attB2 adaptors, respectively (GATE.ABC1#.attB1.F and GATE.ABC1#.attB2.R; see Table 4.3). PCR products were cloned in a suitable Gateway® Donor vector (pDONR221) and then sub-cloned by LR recombination in pEarleyGate101, resulting in a C-terminal YFP fusion under the control of the CaMV 35S promoter and the ocs terminator. Vectors were

either transiently expressed in agroinfiltrated tobacco leaves or used for *A. thaliana* stable transformation.

YFP fluorescence emission was monitored in total rosettes using a Nikon SMZ 1000 binocular equipped with a GFP long pass (GFP-L) filter. For high resolution imaging, leaf samples were observed under confocal laser scanning microscopy. The FITC (514 nm) laser line from a LEICA SP2 AOBS microscope (LEICA Microsystems, Renens, Switzerland) was used to detect YFP emission with a 520-588 nm detection windows. Chlorophyll autofluorescence was monitored using either 594 nm or TRITC (568 nm) excitation wavelengths.

ABC1k3 sub-organellar localization was also determined by Western Blot analysis on purified chloroplast fractions using αABC1k3 as primary antibody (see section 4.2.2.7 on page 140).

4.2.4.2 - Cloning for protein overexpression in plants.

In order to evaluate the effect of the overexpression of the protein without the influence of any exogenous tag, the complete coding sequences, including the stop codon, were sub-cloned from *ABC1I* and *ABC1k3* cDNA clones by LR recombination in pEarleyGate100, under the control of the CaMV 35S promoter and the ocs terminator. For ABC1V, on the contrary, the complete coding sequence was amplified from the *ABC1V* cDNA clone by PCR using the previously described 5' attB1 primer (GATE.ABC1V.attB1.F) and a 3' attB2 primer introducing a TAA stop codon (ABC1V_STOP.GATE.R; see Table 4.3). PCR products were then cloned in a suitable Gateway® Donor vector (pDONR221) and subsequently sub-cloned by LR recombination in pEarleyGate100.

4.2.4.3 - Cloning for Tandem Affinity Purification.

In order to identify the possible targets or interaction partners of ABC1I, ABC1k3 and ABC1V, their coding sequences were sub-cloned by Gateway® LR recombination from pENTR221-ABC1# in pEarleyGate205, resulting in a C-terminal fusion with a Tandem Affinity Purification (TAP) peptide, under the control of the CaMV 35S promoter and the ocs terminator.

4.2.4.4 - Production of polyclonal antibodies.

The coding sequences of ABC1I and ABC1k3 were sub-cloned by Gateway® LR recombination from pENTR221-ABC1I and pENTR221-ABC1k3 in p0GWA. On the other hand, ABC1V complete coding sequence, excluding the stop codon, was amplified by PCR using 5' and 3' primers including XbaI and XhoI restriction sites (ABC1V.XbaI.ATG and ABC1V.XhoI, respectively; see Table 4.3). PCR products were cloned in pGEMT according to the manufacturer's instructions and then sub-cloned in pET21d-H6 in frame with the XhoI site. In both p0GWA and pET21d-H6 expression vectors the coding sequences were inserted under the control of the T7 promoter and the T7 terminator and in frame at the C-terminal with a hexahistidinyl (His_6) tag.

The full length His_6-tagged precursor proteins were expressed in *E. coli* BL21 (DE3) cells and purified under denaturing conditions by Ni-NTA affinity chromatography (Qiagen), according to the supplier's recommendations. Purified proteins were dialyzed against PBS and lyophilized in 100 µg aliquots. For ABC1k3-His_6 and ABC1V-His_6, eight aliquots were used to produce rabbit polyclonal antibodies (Eurogentec, Seraing, Belgium).

In order to purify αABC1k3 and αABC1V antibodies from serum, the recombinant proteins were coupled to Affi-Gel 15 (Bio-Rad Laboratories), according to the manufacturer's instructions. Sera extracted from the immunized rabbits were filtered several times through the Affi-Gel slurry at 4°C, then beads were extensively washed with PBS 1x. Bound antibodies were eluted with 200 mM Glycine (pH 2.2) inside tubes already containing Tris-HCl (pH 8) to immediately tamponate the solution at pH 7.5. Eluates were then dialyzed against PBS and 0.2% (w/v) sodium azide was added for long-term storage.

4.2.4.6 - Determination of the photosynthetic parameters.

Maximum quantum efficiency of photosystem II (Fv/Fm), electron transport rate (ETR) and non-photochemical quenching (NPQ) were fluorometrically determined using a MINI-PAM Photosynthesis Yield Analyzer (Walz, Effeltrich, Germany).

Photosynthetic gas exchange was measured using a custom-built multi-chamber system connected in parallel to an infra-red gas analyzer (Licor7000, Licor, Lincoln, USA).

Arabidopsis plants were grown under short day conditions until both genotypes reached the same developmental stage, then individual plants were introduced into a separate analytic chamber. After an adaptation period of 2 days, gas exchange was measured for 7 days. After the first 24 h, growth conditions were switched to continuous high light. During the measurement, air with a 380 ppm CO_2 content and a relative humidity of 65% was channeled through the system at a flow rate of 200 μmol/s. Each chamber was measured consecutively for 6 min and the average value was taken for the light and for the dark period. At the end of the light period, a picture was taken to calculate the projected leaf area for each plant. Based on the projected leaf area, photosynthetic and respiration rates were calculated with the ΔCO_2 and ΔH_2O values gained from the gas exchange system.

4.2.4.7 - Chlorophyll quantification in total leaf extracts

For the measurement of chlorophyll in fresh leaf tissues, leaves were exactly weighted and extracted in 80% acetone. Total chlorophyll levels were then photometrically determined as described in [(262)].

4.2.4.8 - *Arabidopsis* chloroplast ultrastructural analysis.

Leaves from 4- to 5-week-old *A. thaliana* rosettes were fixed overnight in 0.1 M phosphate buffer (pH 6.8) containing 4% (w/v) formaldehyde and 5% (w/v) glutaraldehyde, washed three times in 0.1 M phosphate buffer (pH 6.8) for 20 min and post-fixed for 2 h with 1% (w/v) osmium tetraoxide (OsO_4) at 20°C. Samples were dehydrated in ethanol and acetone series and infiltrated overnight with a low viscosity epoxy resin (Spurr; Polyscience, Eppelheim, Germany). Leaf fragments were then placed in an appropriate mold, included in Spurr and heated for 4 h at 60°C to allow the resin to solidify.
Semithin sections of 0.75 μm were prepared using an Ultracut-E microtome (Reichert-Jung) equipped with a glass blade, placed on a clean glass slide, dried at 60-80°C, then stained with 1% Toluidine Blue in 7% ethanol at 80°C, briefly rinsed with 50% ethanol and dried at 80°C. Semithin sections were then observed with a compound light microscope.

Ultrathin sections of 90 nm were prepared using an Ultracut-E microtome equipped with a diamond knife (Diatome, Biel, Switzerland), mounted on copper grids and contrasted with a saturated uranyl acetate solution in 50% ethanol and with Reynolds' lead citrate according to[263]. Ultrathin sections were observed with a Philips CM-100 electron microscope operating at 60 kV.

4.2.4.9 - Analysis of starch and sugar metabolism

Starch accumulation in *A. thaliana* total leaves was visually determined by a standard Lugol's iodine test. Briefly, leaves were placed in boiling water for 1 min to disrupt cell membranes, incubated in 80% (v/v) EtOH at 78°C for 3 min to elute chlorophyll and other pigments, gently washed in cold ddH_2O, then stained with Lugol's iodine aqueous solution [5% I_2, 10% KI] and rinsed in cold ddH_2O.

For the precise measurement of starch in total rosettes, the perchloric acid extraction method described by[264] was used, with slight modifications. Briefly, samples comprising entire individual rosettes were frozen in Eppendorf tubes and pulverized while still frozen using a Mixer Mill (Retsch, Haan, Germany). The frozen powder was extracted in 800 µl ice-cold 1 M perchloric acid for 5 min with intermittent mixing. All the subsequent steps were carried out between 0 and 4°C. After centrifugation (3000 × g for 10 min at 4°C), the insoluble material in the pellet was washed once with water and three times with 80% (v/v) ethanol. Starch content in the insoluble material was then measured by determining the glucose released by treatment with α-amylase and amyloglucosidase as described in Smith *et al.* (2006)[265]. Briefly, starch granules were extracted in EtOH to remove free glucose, solubilized by heating and digested to glucose with a preparation of α-amyloglucosidase and α-amylase. Glucose content was then enzymatically assayed using hexokinase and glucose 6-phosphate dehydrogenase to convert glucose to 6-phosphogluconate with concomitant reduction of NAD to NADH[266].

For the measurement of sugars, the same perchloric acid extraction method was used. After centrifugation, the supernatant (soluble fraction) was adjusted to pH 5 by adding 2 M KOH and 0.4 M MES. Precipitated potassium perchlorate was removed by centrifugation (2000 × g for 15 min at 4°C) and sugars (glucose, fructose, sucrose and maltose) in the

supernatant were measured using HPAEC-PAD as described in Fulton *et al.* (2008)[267], with minor modifications. Samples of the neutralized soluble fraction (100 mL) were applied to sequential 1.5-mL columns of Dowex 50 W and Dowex1 (Sigma-Aldrich). The neutral compounds were eluted with 4 mL of water, lyophilized, and redissolved in 100 mL of water. The sugars were separated on a Dionex PA-20 column according to the following conditions: eluent A, 100 mM NaOH; eluent B, 150 mM NaOH and 500 mM sodium acetate. The gradient was as follows: 0 to 7 min, 100% A; 7 to 26.5 min, a concave gradient to 20% A, 80% B (elution of sugars); 26.5 to 32 min, 20% A, 80% B (column wash step); 32 to 40 min, 100% A (column re-equilibration). Peaks were identified by co-elution with known sugar standards. Peak areas were determined using the Chromeleon software (Dionex).

4.2.4.10 - *Arabidopsis* membrane prenylquinone and carotenoid profiling.

In order to prevent lipid oxidation or degradation prior to analysis, a simple and rapid extraction method was developed, as described in Martinis *et al.* (2011)[80] (see Appendix). Briefly, *Arabidopsis* leaves from 1- or 2-month-old rosettes were ground in a mortar with liquid nitrogen. 100-150 mg of leaf material was then exactly weighed, transferred to a 1.5 mL microcentrifuge tube (Eppendorf, Hamburg, Germany) and swiftly re-suspended in five volumes of THF. Care was taken that no thawing occurred before the solvent was added. Glass beads of about 1 mm of diameter (Assistent, Sontheim, Germany) were added and samples were further homogenized for 3 min at 30 Hz in a tissue lyser (Retsch MM 300, Haan, Germany). Tubes were centrifuged on a benchtop centrifuge (14,000 × g for 3 min at 4°C) and 400 μL of supernatant was then transferred to an appropriate glass vial for immediate UHPLC-APCI-QTOFMS analysis.

Conversely, for the detection and identification of prenylquinones in fractionated chloroplast membranes (see section 4.2.1.4 on page 136), 200-400 μL of purified fractions were diluted with ddH_2O to a final volume of 1 mL and extracted for three times in an equal volume of EtAc. Apolar phases were pooled together, evaporated in a refrigerated CentriVap centrifugal vacuum concentrators (Labconco, Kansas City, MO, USA) and resuspended in 50-100 μL of THF before UHPLC-APCI-QTOFMS analysis.

Liquid chromatography-mass spectrometry analysis of leaf samples was performed using a LC-MS system consisting of a Waters Acquity UPLC™ (Milford, MA) coupled to a Waters Synapt G2 MS QTOF equipped with an atmospheric pressure chemical ionization (APCI) source. Samples were separated on an Acquity BEH C18 column (50x2.1 mm, 1.7 μm) and data were acquired with a scan time of 0.4 s over an m/z range of 225-1200 in the negative ion MS mode. Positive and negative ion MS/MS experiments were also carried out for the identification of prenylquinones and carotenoids, while their absolute quantities were determined using standard curves obtained from standard compounds. Analyses were performed as described in Martinis *et al.* (2011)[(80)] (see Appendix) with the following modifications to allow the simultaneous separation and detection of prenylquinones and carotenoids: the initial MeOH percentage used for the chromatographic gradient was set to 80%, increased to 100% in 3 min, and maintained at 100% for 2 min. α-T, α-TQ, γ-T, δ-T, K, PQ-9, PC-8, lutein and β-carotene were quantified based on calibration curves built from standard compounds.

Data were then processed using Masslynx v4.1 (Waters) and multivariate analysis was carried out using MarkerLynx XS™ (Waters). The following parameters were used: initial and final retention times 0.7-3.0 min, mass range m/z 225-1200 Da, mass tolerance 0.03 Da, retention time window 0.10 min, automatic peak width detection, intensity threshold 1000 counts. The deisotope filtering function was applied. Non-normalized peak areas were generated. Variables were Pareto-scaled before applying principal component analysis (PCA).

4.2.4.11 - Plastoglobule proteome profiling.

In order to investigate a possible effect of the *abc1i* and *abc1k3* mutations on the protein composition of plastoglobules, low-density chloroplast fractions corresponding to plastoglobules were pooled and proteins were extracted as described in section 4.2.2.8 on page 147. Proteins were separated on 1D SDS-PAGE gel, then the regions of interest were excised and *in gel* tryptic digestion was performed using Sequencing Grade Modified Trypsin (Promega) according to the manufacturer's recommendations.

Lyophilized peptides were then extracted in a aqueous solution containing 2% ACN and 0,1% formic acid (FA), and directly analyzed by LC-MS. Peptides were chromatographically separated using a Waters Acquity UPLC™ system equipped with an Acquity BEH130 C18

column (75 µm x 200 mm, 1.7 µm particles). The solvent system consisted of 0.1% formic acid in water (solvent A) and 0.1% formic acid in acetonitrile (solvent B). The following conditions were used: 3% B in 3 min, 50% B for 88 min, 85% B for 5 min, re-equilibration at 3% B for 9 min. The flow rate was 300 µL/min and the injection volume was 2 µL. The temperature of the column was set to 35°C.

MS and MS/MS analyses were performed using a Waters Synapt G2 MS QTOF equipped with a nanospray ionization source consisting of a pre-cut PicoTip emitter (20 µm tubing ID, 10 µm tubing tip, 360µm tubing OD, 2.5" length) and a lock-mass system. Data were acquired in positive ion MS mode with a scan time of 0.6 s over an m/z range of 50-1600 Da. The capillary voltage was set at 2.5 kV and the source temperature was maintained at 70°C. Accurate mass measurements were obtained by infusing a 500 fmol/mL solution of the Glu-Fib peptide (m/z = 785.8426 Da; z = 2) at a flow rate of 0.7 µL/min through the Lock Spray™ probe. Data were acquired using Masslynx v4.1 (Waters) while data processing and database search were performed using the ProteinLynx Global Server v2.5.1 (Waters).

4.2.4.12 - *In vitro* production of recombinant proteins.

In order to conduct *in vitro* phosphorylation assays with the three ABC1-like kinases and to identify the tocopherol cyclase VTE1 as a possible target, the coding sequences for the three proteins were cloned in order to remove the chloroplast transit peptide. An *in silico* prediction of the transit peptides was performed for ABC1I, ABC1k3 and ABC1V using the TargetP 1.1 server[(219)] and three polypeptides of 42 aa, 79 aa and 58 aa were identified, respectively. The coding sequences corresponding to the "native" protein, excluding the transit peptide and the stop codon, were thus amplified from *ABC1I*, *ABC1k3* and *ABC1V* cDNA clones by PCR using a 5' attB1 primer (ABC1#_NAT.GATE.F) at the 3' of the predicted transit peptide region and the previously described 3' attB2 primers (GATE.ABC1#.attB2.R; see Table 4.3). PCR products were cloned in a suitable Gateway® Donor vector (pDONR221) and then sub-cloned by LR recombination either in p0GWA or pHMGWA, under the control of the T7 promoter and the T7 terminator. The former constructs encoded for a C-terminal His_6 tag only, while the latter encoded for an additional N-terminal fusion with a His_6 tag and a maltose binding protein (MBP), which increases

protein solubility but could potentially interfere with kinase activity, As a consequence, this construct was not used for the following *in vitro* phosphorylation assays.
For the *in vitro* translation of VTE1, the pre-existing VTE1-pCL61 expression vector was modified by restriction digestion with EcoRV in order to remove the region corresponding to the 35S promoter at the 5' of the *VTE1* coding sequence, putting it under the control of the T7 promoter and avoiding the formation of unspecific polypeptides.

Recombinant proteins were then expressed *in vitro* using the TNT® Quick Coupled Transcription/Translation System (Promega) in the absence or presence of 20 μCi [^{35}S] methionine and according to the manufacturer's recommendations. To verify protein expression rate, radioactively-labeled proteins were separated by SDS-PAGE, then gels were stained in Comassie blue and dried on 1-2 layers of Whatman filter paper. [^{35}S] methionine incorporation was detected by β-decay emission by exposing the dried gels for 3 or more days to high performance autoradiography films (Storage Phosphor Screen, Kodak), which were then scanned in a Personal FX Phosphorimager and analyzed using the QuantityOne software (both from Bio-Rad Laboratories).

4.2.4.13 - Phosphorylation assays.

In order to investigate differences in the phosphorylation state of plastoglobule proteins between wild-type, *abc1i* and *abc1k3* mutant plants, low-density chloroplast fractions corresponding to plastoglobules were pooled together and dialyzed overnight against [50 mM HEPES/KOH pH 7.5, 0.1 M NaCl, 1 mM DTT] at 4°C inside dialysis membranes with 6000-8000 MWCO (Molecular Weight Cut Off) (Spectra/POR 1; Spectrum Laboratories, Rancho Dominguez, CA, USA). Samples were then concentrated in the same buffer supplemented with 33% PEG 20000 (Applichem, Darmstadt, Germany) up to a final protein concentration of 0.25-0.5 μg/μL. A total amount of 20-40 μg protein were used, either alone or after addition of an equal amount of stromal proteins, to assemble 100 μL *in vitro* phosphorylation reactions in a suitable phosphorylation buffer [50 mM HEPES/KOH pH 7.5, 5 mM $MgCl_2$, 0.5 mM $MnCl_2$, 50 mM NaCl, 0.1 mM DTT] supplemented with 50 μM ATP and 2 μCi [γ-^{33}P] ATP. Reactions were incubated for 30 min at 25 °C and under gentle shaking (300 rpm), then proteins were swiftly precipitated in chloroform-methanol**(259)** and

resuspended in an appropriate volume of sample buffer [50 mM Tris/HCl pH 6.8, 0.1 M DTT, 2% (w/v) SDS, 0.1% (w/v) bromophenol blue, 10% (v/v) glycerol]. Proteins were separated by SDS-PAGE, then gels were stained in Comassie blue and dried on 1-2 layers of Whatman filter paper. ^{33}P incorporation was detected by γ-decay emission as previously described by gel exposure to high performance autoradiography films (see section 4.2.4.12 on page 156).

In order to identify VTE1 as a possible target of ABC1I and ABC1k3, equal amounts of non-labeled *in vitro* translation products (see section 4.2.4.12 on page 156) were pooled together in different combinations and used to assemble the *in vitro* phosphorylation reactions, as previously described. Co-localization of VTE1 with radioactive bands on gel was then performed by Western Blot (see section 4.2.2.9 on page 147).

4.2.4.13 - Bioinformatics.

Expressed sequence tags (ESTs) were retrieved from the TAIR database[(216)] and used as reference for all the bioinformatical analyses. Protein multiple sequence alignment was performed using ClustalX 2.0[(268)] and secondary structure was predicted by PROF method through the PredictProtein Platform[(269,270)], by the Swiss Model Server[(271-274)] and by the JPred 3.0 platform[(275,276)]. Data were then assembled using the Jalview 2.4 software[(277)]. Protein "globularity" was predicted according to[(278)]. Conserved domains were identified via the NCBI Conserved Domains Database[(279)]. Kyte and Doolittle hydropathy plots[(218)] were predicted through the PredictProtein Platform[(280,281)] or by using the Protean software included in the Lasergene suite (DNASTAR, Madison, WI, USA), while subcellular localization and chloroplast transit peptide length were predicted *in silico* using the TargetP 1.1 server[(219)]. The presence of known phosphorylated sites or the prediction of phosphorylable residues was determined according to the Arabidopsis Protein Phosphorylation Site Database (PhosPhAt 3.0)[(282,283)]. In order to analyze gene expression profiles and response to stimuli, DNA microarray data were retrieved from public database and analysed using the Geenevestigaror toolbox[(284)]. Gene coexpression was determined *in silico* using the ATTED-II 6.0 database[(285)].

~ Bibliography ~

1) Bailey, J.L., Whyborn, A.G., Williams, J.P., Leech, R.M., and Greenwood, A.D. (1963). **Osmiophilic globules of chloroplasts**. Biochemical Journal **88,** 27.

2) Greenwood, A.D., Leech, R.M., and Williams, J.P. (1963). **Osmiophilic globules of chloroplasts .1. Osmiophilic globules as a normal component of chloroplasts and their isolation and composition in *Vicia faba* L.** Biochimica Et Biophysica Acta **78,** 148-162.

3) Thomson, W.W., and Platt, K. (1973). **Plastid ultrastructure in barrel cactus, *Echinocactus acanthodes***. New Phytologist **72,** 791-797.

4) Fernandez, D.E., and Staehelin, L.A. (1987). **Does gibberellic-acid induce the transfer of lipase from protein bodies to lipid bodies in barley aleurone cells**. Plant Physiology **85,** 487-496.

5) Lichtenthaler, H.K. (1968). **Plastoglobuli and fine structure of plastids**. Endeavour **27,** 144-148.

6) Lichtenthaler, H.K., and Tevini, M. (1970). **Distribution of pigments, plastidquinones and plastoglobuli in different particle fractions obtained from sonicated spinach chloroplasts**. Zeitschrift Fur Pflanzenphysiologie **62,** 33-39.

7) Tevini, M., Herm, K., and Leonhardt, H.D. (1977). **Lipids and function of etiochloroplasts after UV, blue and red light-illumination**. Biochemical Society Transactions **5,** 95-98.

8) Kroll, D., Meierhoff, K., Bechtold, N., Kinoshita, M., Westphal, S., Vothknecht, U.C., Soll, J., and Westhoff, P. (2001). **VIPP1, a nuclear gene of *Arabidopsis thaliana* essential for thylakoid membrane formation**. Proceedings of the National Academy of Sciences of the United States of America **98,** 4238-4242.

9) Rudella, A., Friso, G., Alonso, J.M., Ecker, J.R., and van Wijk, K.J. (2006). **Downregulation of ClpR2 leads to reduced accumulation of the ClpPRS protease complex and defects in chloroplast biogenesis in *Arabidopsis***. Plant Cell **18,** 1704-1721.

10) Tevini, M., and Steinmuller, D. (1985). **Composition and function of plastoglobuli. 2. Lipid-composition of leaves and plastoglobuli during beech leaf senescence**. Planta **163,** 91-96.

11) Guiamet, J.J., Pichersky, E., and Nooden, L.D. (1999). **Mass exodus from senescing soybean chloroplasts**. Plant and Cell Physiology **40,** 986-992.

12) Ghosh, S., Mahoney, S.R., Penterman, J.N., Peirson, D., and Dumbroff, E.B. (2001). **Ultrastructural and biochemical changes in chloroplasts during *Brassica napus* senescence**. Plant Physiology and Biochemistry **39,** 777-784.

13) Deruere, J., Romer, S., Dharlingue, A., Backhaus, R.A., Kuntz, M., and Camara, B. (1994). **Fibril assembly and carotenoid overaccumulation in chromoplasts - a model for supramolecular lipoprotein structures**. Plant Cell **6,** 119-133.

14) Vishnevetsky, M., Ovadis, M., and Vainstein, A. (1999). **Carotenoid sequestration in plants: the role of carotenoid-associated proteins**. Trends in Plant Science **4,** 232-235.

15) Hall, J.D., Alabbas, A.H., Barr, R., and Crane, F.L. (1972). **Ultrastructure of chloroplasts in mineral-deficient maize leaves**. Plant Physiology **50,** 404-409.

16) Sallas, L., Luomala, E.M., Utriainen, J., Kainulainen, P., and Holopainen, J.K. (2003). **Contrasting effects of elevated carbon dioxide concentration and temperature on Rubisco activity, chlorophyll fluorescence, needle ultrastructure and secondary metabolites in conifer seedlings**. Tree Physiology **23,** 97-108.

17) Munne-Bosch, S., and Alegre, L. (2004). **Die and let live: leaf senescence contributes to plant survival under drought stress**. Functional Plant Biology **31,** 203-216.

18) Sam, O., Ramirez, C., Coronado, M.J., Testillano, P.S., and Risueno, M.C. (2003). **Changes in tomato leaves induced by NaCl stress: leaf organization and cell ultrastructure**. Biologia Plantarum **47,** 361-366.

19) Gaude, N., Brehelin, C., Tischendorf, G., Kessler, F., and Doermann, P. (2007). **Nitrogen deficiency in *Arabidopsis* affects galactolipid composition and gene expression and results in accumulation of fatty acid phytyl esters**. Plant Journal **49,** 729-739.

20) Panou-Filotheou, H., Bosabalidis, A.M., and Karataglis, S. (2001). **Effects of copper toxicity on leaves of oregano (*Origanum vulgare* subsp *hirtum*)**. Annals of Botany **88,** 207-214.

21) Molas, J. (2002). **Changes of chloroplast ultrastructure and total chlorophyll concentration in cabbage leaves caused by excess of organic Ni(II) complexes**. Environmental and Experimental Botany **47,** 115-126.

22) Austin, J.R., II, Frost, E., Vidi, P.-A., Kessler, F., and Staehelin, L.A. (2006). **Plastoglobules are lipoprotein subcompartments of the chloroplast that are permanently coupled to thylakoid membranes and contain biosynthetic enzymes**. Plant Cell **18,** 1693-1703.

23) Yao, K., Paliyath, G., Humphrey, R.W., Hallett, F.R., and Thompson, J.E. (1991). **Identification and characterization of nonsedimentable lipid protein microvesicles**. Proceedings of the National Academy of Sciences of the United States of America **88,** 2269-2273.

24) Ghosh, S., Hudak, K.A., Dumbroff, E.B., and Thompson, J.E. (1994). **Release of photosynthetic protein catabolites by blebbing from thylakoids**. Plant Physiology **106,** 1547-1553.

25) Kessler, F., Schnell, D., and Blobel, G. (1999). **Identification of proteins associated with plastoglobules isolated from pea (*Pisum sativum* L.) chloroplasts**. Planta **208,** 107-113.

26) Hansmann, P., and Sitte, P. (1982). **Composition and molecular structure of chromoplast globules of *Viola tricolor***. Plant Cell Reports **1,** 111-114.

27) Kreimer, G. (2009). **The green algal eyespot apparatus: a primordial visual system and more?** Current Genetics **55,** 19-43.

28) Walne, P., and Arnott, H. (1967). **The comparative ultrastructure and possible function of eyespots: *Euglena granulata* and *Chlamydomonas eugametos***. Planta **77,** 325-353.

29) Melkonian, M., and Robenek, H. (1980). **Eyespot membranes of *Chlamydomonas reinhardii* - a freeze-fracture study**. Journal of Ultrastructure Research **72,** 90-102.

30) Renninger, S., Backendorf, E., and Kreimer, G. (2001). **Subfractionation of eyespot apparatuses from the green alga *Spermatozopsis similis*: isolation and characterization of eyespot globules**. Planta **213,** 51-63.

31) Pozueta-Romero, J., Rafia, F., Houlne, G., Cheniclet, C., Carde, J.P., Schantz, M.L., and Schantz, R. (1997). **A ubiquitous plant housekeeping gene, PAP, encodes a major protein component of bell pepper chromoplasts**. Plant Physiology **115,** 1185-1194.

32) Wu, S.S.H., Platt, K.A., Ratnayake, C., Wang, T.W., Ting, J.T.L., and Huang, A.H.C. (1997). **Isolation and characterization of neutral-lipid-containing organelles and globuli-filled plastids from *Brassica napus* tapetum**. Proceedings of the National Academy of Sciences of the United States of America **94,** 12711-12716.

33) Lichtenthaler, H.K., Prenzel, U., Douce, R., and Joyard, J. (1981). **Localization of prenylquinones in the envelope of spinach-chloroplasts**. Biochimica Et Biophysica Acta **641,** 99-105.

34) Zbierzak, A.M., Kanwischer, M., Wille, C., Vidi, P.A., Giavalisco, P., Lohmann, A., Briesen, I., Porfirova, S., Brehelin, C., Kessler, F., and Dormann, P. (2010). **Intersection of the tocopherol and plastoquinol metabolic pathways at the plastoglobule**. Biochemical Journal **425,** 389-399.

35) Szymanska, R., and Kruk, J. (2010). **Plastoquinol is the Main Prenyllipid Synthesized During Acclimation to High Light Conditions in *Arabidopsis* and is Converted to Plastochromanol by Tocopherol Cyclase**. Plant and Cell Physiology **51,** 537-545.

36) Vidi, P.A., Kanwischer, M., Baginsky, S., Austin, J.R., Csucs, G., Dormann, P., Kessler, F., and Brehelin, C. (2006). **Tocopherol cyclase (VTE1) localization and vitamin E accumulation in chloroplast plastoglobule lipoprotein particles**. Journal of Biological Chemistry **281,** 11225-11234.

37) Merzlyak, M.N., and Solovchenko, A.E. (2002). **Photostability of pigments in ripening apple fruit: a possible photoprotective role of carotenoids during plant senescence**. Plant Science **163,** 881-888.

38) Lohmann, A., Schoettler, M.A., Brehelin, C., Kessler, F., Bock, R., Cahoon, E.B., and Doermann, P. (2006). **Deficiency in phylloquinone (vitamin K-1) methylation affects prenyl quinone distribution, photosystem I abundance, and anthocyanin accumulation in the *Arabidopsis AtmenG* mutant**. Journal of Biological Chemistry **281,** 40461-40472.

39) Ytterberg, A.J., Peltier, J.B., and van Wijk, K.J. (2006). **Protein profiling of plastoglobules in chloroplasts and chromoplasts. A surprising site for differential accumulation of metabolic enzymes**. Plant Physiology **140,** 984-997.

40) Lundquist, P.K., Poliakov, A., Bhuiyan, N.H., Zybailov, B., Sun, Q., and van Wijk, K.J. (2012). **The Functional Network of the *Arabidopsis* Plastoglobule Proteome Based on Quantitative Proteomics and Genome-Wide Coexpression Analysis**. Plant Physiology **158,** 1172-1192.

41) Laizet, Y., Pontier, D., Mache, R., eacute, gis, and Kuntz, M. (2004). **Subfamily Organization and Phylogenetic Origin of Genes Encoding Plastid Lipid-Associated Proteins of the Fibrillin Type**. Journal of Genome Science and Technology **3,** 19-28.

42) Winkenbach, F., Falk, H., Liedvogel, B., and Sitte, P. (1976). **Chromoplasts of *Tropaeolum majus* L. - Isolation and characterization of lipoprotein elements**. Planta **128,** 23-28.

43) Brehelin, C., Kessler, F., and van Wijk, K.J. (2007). **Plastoglobules: versatile lipoprotein particles in plastids**. Trends in Plant Science **12,** 260-266.

44) Schmidt, M., Gessner, G., Matthias, L., Heiland, I., Wagner, V., Kaminski, M., Geimer, S., Eitzinger, N., Reissenweber, T., Voytsekh, O., Fiedler, M., Mittag, M., and Kreimer, G. (2006). **Proteomic analysis of the eyespot of *Chlamydomonas reinhardtii* provides novel insights into its components and tactic movements**. Plant Cell **18,** 1908-1930.

45) Rey, P., Gillet, B., Romer, S., Eymery, F., Massimino, J., Peltier, G., and Kuntz, M. (2000). **Over-expression of a pepper plastid lipid-associated protein in tobacco leads to changes in plastid ultrastructure and plant development upon stress**. Plant Journal **21,** 483-494.

46) Simkin, A.J., Gaffe, J., Alcaraz, J.-P., Carde, J.-P., Bramley, P.M., Fraser, P.D., and Kuntz, M. (2007). **Fibrillin influence on plastid ultrastructure and pigment content in tomato fruit**. Phytochemistry **68,** 1545-1556.

47) Singh, D.K., Maximova, S.N., Jensen, P.J., Lehman, B.L., Ngugi, H.K., and McNellis, T.W. (2010). **FIBRILLIN4 Is Required for Plastoglobule Development and Stress Resistance in Apple and *Arabidopsis***. Plant Physiology **154,** 1281-1293.

48) Youssef, A., Laizet, Y., Block, M.A., Marechal, E., Alcaraz, J.P., Larson, T.R., Pontier, D., Gaffe, J., and Kuntz, M. (2010). **Plant lipid-associated fibrillin proteins condition jasmonate production under photosynthetic stress**. Plant Journal **61,** 436-445.

49) Monte, E., Ludevid, C., and Prat, S. (1999). **Leaf C40.4: a carotenoid-associated protein involved in the modulation of photosynthetic efficiency?** Plant Journal **19,** 399-410.

50) Galetskiy, D., Susnea, L., Reiser, V., Adamska, I., and Przybylski, M. (2008). **Structure and dynamics of photosystem II light-harvesting complex revealed by high-resolution FTICR mass spectrometric proteome analysis**. Journal of the American Society for Mass Spectrometry **19,** 1004-1013.

51) Singh, D.K., and McNellis, T.W. (2011). **Fibrillin protein function: the tip of the iceberg?** Trends in Plant Science **16,** 432-441.

52) Kim, H.U., Wu, S.S.H., Ratnayake, C., and Huang, A.H.C. (2001). **Brassica rapa has three genes that encode proteins associated with different neutral lipids in plastids of specific tissues**. Plant Physiology **126,** 330-341.

53) Langenkämper, G., Manac'h, N., Broin, M., Cuiné, S., Becuwe, N., Kuntz, M., and Rey, P. (2001). **Accumulation of plastid lipid‐associated proteins (fibrillin/CDSP34) upon oxidative stress, ageing and biotic stress in Solanaceae and in response to drought in other species**. Journal of Experimental Botany **52,** 1545-1554.

54) Pruvot, G., Cuine, S., Peltier, G., and Rey, P. (1996). **Characterization of a novel drought-induced 34-kDa protein located in the thylakoids of Solanum tuberosum L plants**. Planta **198,** 471-479.

55) Leitner-Dagan, Y., Ovadis, M., Shklarman, E., Elad, Y., David, D.R., and Vainstein, A. (2006). **Expression and functional analyses of the plastid lipid-associated protein CHRC suggest its role in chromoplastogenesis and stress**. Plant Physiology **142,** 233-244.

56) Lee, D.-G., Ahsan, N., Lee, S.-H., Kang, K.Y., Lee, J.J., and Lee, B.-H. (2007). **An approach to identify cold-induced low-abundant proteins in rice leaf**. Comptes Rendus Biologies **330,** 215-225.

57) Zybailov, B., Friso, G., Kim, J., Rudella, A., Rodriguez, V.R., Asakura, Y., Sun, Q., and van Wijk, K.J. (2009). **Large Scale Comparative Proteomics of a Chloroplast Clp Protease Mutant Reveals Folding Stress, Altered Protein Homeostasis, and Feedback Regulation of Metabolism**. Molecular & Cellular Proteomics **8,** 1789-1810.

58) Brehelin, C., and Kessler, F. (2008). **The Plastoglobule: A Bag Full of Lipid Biochemistry Tricks**. Photochemistry and Photobiology **84,** 1388-1394.

59) Kaup, M.T., Froese, C.D., and Thompson, J.E. (2002). **A role for diacylglycerol acyltransferase during leaf senescence**. Plant Physiology **129,** 1616-1626.

60) Padham, A.K., Hopkins, M.T., Wang, T.-W., McNamara, L.M., Lo, M., Richardson, L.G.L., Smith, M.D., Taylor, C.A., and Thompson, J.E. (2007). **Characterization of a plastid triacylglycerol lipase from *Arabidopsis***. Plant Physiology **143,** 1372-1384.

61) de Castro, E., Sigrist, C.J.A., Gattiker, A., Bulliard, V., Langendijk-Genevaux, P.S., Gasteiger, E., Bairoch, A., and Hulo, N. (2006). **ScanProsite: detection of PROSITE signature matches and ProRule-associated functional and structural residues in proteins**. Nucleic Acids Research **34,** W362-W365.

62) Flower, D.R., North, A.C.T., and Sansom, C.E. (2000). **The lipocalin protein family: structural and sequence overview**. Biochimica Et Biophysica Acta-Protein Structure and Molecular Enzymology **1482,** 9-24.

63) Yang, Y., Sulpice, R., Himmelbach, A., Meinhard, M., Christmann, A., and Grill, E. (2006). **Fibrillin expression is regulated by abscisic acid response regulators and is involved in abscisic acid-mediated photoprotection**. Proceedings of the National Academy of Sciences of the United States of America **103,** 6061-6066.

64) Porfirova, S., Bergmuller, E., Tropf, S., Lemke, R., and Dormann, P. (2002). **Isolation of an *Arabidopsis* mutant lacking vitamin E and identification of a cyclase essential for all tocopherol biosynthesis**. Proceedings of the National Academy of Sciences of the United States of America **99,** 12495-12500.

65) Sattler, S.E., Cahoon, E.B., Coughlan, S.J., and DellaPenna, D. (2003). **Characterization of tocopherol cyclases from higher plants and cyanobacteria. Evolutionary implications for tocopherol synthesis and function**. Plant Physiology **132,** 2184-2195.

66) Kobayashi, N., and DellaPenna, D. (2008). **Tocopherol metabolism, oxidation and recycling under high light stress in *Arabidopsis***. Plant Journal **55,** 607-618.

67) Szymanska, R., and Kruk, J. (2007). **Plastochromanol, a 'new' lipophilic antioxidant in *Arabidopsis* leaves, is synthesized by tocopherol cyclase. The effect of high-light on the level of prenyllipid antioxidants**. Photosynthesis Research **91,** 313-314.

68) Raclaru, M., Gruber, J., Kumar, R., Sadre, R., Luhs, W., Zarhloul, M.K., Friedt, W., Frentzen, M., and Weier, D. (2006). **Increase of the tocochromanol content in transgenic *Brassica napus* seeds by overexpression of key enzymes involved in prenylquinone biosynthesis**. Molecular Breeding **18,** 93-107.

69) Kanwischer, M., Porfirova, S., Bergmuller, E., and Dormann, P. (2005). **Alterations in tocopherol cyclase activity in transgenic and mutant plants of *Arabidopsis* affect tocopherol content, tocopherol composition, and oxidative stress**. Plant Physiology **137,** 713-723.

70) Soll, J., Schultz, G., Joyard, J., Douce, R., and Block, M.A. (1985). **Localization and synthesis of prenylquinones in isolated outer and inner envelope membranes from spinach chloroplasts**. Archives of Biochemistry and Biophysics **238,** 290-299.

71) Michalecka, A.M., Svensson, A.S., Johansson, F.I., Agius, S.C., Johanson, U., Brennicke, A., Binder, S., and Rasmusson, A.G. (2003). ***Arabidopsis* genes encoding mitochondrial type IINAD(P)H dehydrogenases have different evolutionary orgin and show distinct responses to light**. Plant Physiology **133,** 642-652.

72) Elhafez, D., Murcha, M.W., Clifton, R., Soole, K.L., Day, D.A., and Whelan, J. (2006). **Characterization of mitochondrial alternative NAD(P)H dehydrogenases in *Arabidopsis*: Intraorganelle location and expression**. Plant and Cell Physiology **47,** 43-54.

73) Carrie, C., Murcha, M.W., Kuehn, K., Duncan, O., Barthet, M., Smith, P.M., Eubel, H., Meyer, E., Day, D.A., Millar, A.H., and Whelan, J. (2008). **Type II NAD(P)H dehydrogenases are targeted to mitochondria and chloroplasts or peroxisomes in *Arabidopsis thaliana***. FEBS Letters **582,** 3073-3079.

74) Yamamoto, H., Peng, L., Fukao, Y., and Shikanai, T. (2011). **An Src Homology 3 Domain-Like Fold Protein Forms a Ferredoxin Binding Site for the Chloroplast NADH Dehydrogenase-Like Complex in *Arabidopsis***. Plant Cell **23,** 1480-1493.

75) Munekage, Y., Hojo, M., Meurer, J., Endo, T., Tasaka, M., and Shikanai, T. (2002). **PGR5 is involved in cyclic electron flow around photosystem I and is essential for photoprotection in *Arabidopsis***. Cell **110,** 361-371.

76) Eugeni-Piller, L., Besagni, C., Ksas, B., Rumeau, D., Brehelin, C., Glauser, G., Kessler, F., and Havaux, M. (2011). **Chloroplast lipid droplet type II NAD(P)H quinone oxidoreductase is essential for prenylquinone metabolism and vitamin K1 accumulation**. Proc Natl Acad Sci U S A **108,** 14354-14359.

77) Grütter, C., Alonso, E., Chougnet, A., and Woggon, W.-D. (2006). **A Biomimetic Chromanol Cyclization Leading to α-Tocopherol**. Angewandte Chemie International Edition **45,** 1126-1130.

78) Johnson, T.W., Shen, G., Zybailov, B., Kolling, D., Reategui, R., Beauparlant, S., Vassiliev, I.R., Bryant, D.A., Jones, A.D., Golbeck, J.H., and Chitnis, P.R. (2000). **Recruitment of a Foreign Quinone into the A1 Site of Photosystem I: I. Genetic and physiological characterization of phylloquinone biosynthetic pathway mutants in *Synechocystis* sp. pcc 6803**. Journal of Biological Chemistry **275,** 8523-8530.

79) Shinkarev, V.P., Zybailov, B., Vassiliev, I.R., and Golbeck, J.H. (2002). **Modeling of the P700(+) charge recombination kinetics with phylloquinone and plastoquinone-9 in the A(1) site of photosystem I**. Biophysical Journal **83,** 2885-2897.

80) Martinis, J., Kessler, F., and Glauser, G. (2011). **A novel method for prenylquinone profiling in plant tissues by ultra-high pressure liquid chromatography-mass spectrometry**. Plant Methods **7**.

81) Iuchi, S., Kobayashi, M., Taji, T., Naramoto, M., Seki, M., Kato, T., Tabata, S., Kakubari, Y., Yamaguchi-Shinozaki, K., and Shinozaki, K. (2001). **Regulation of drought tolerance by gene manipulation of 9-cis-epoxycarotenoid dioxygenase, a key enzyme in abscisic acid biosynthesis in *Arabidopsis***. The Plant Journal **27,** 325-333.

82) Schwartz, S.H., Qin, X.Q., and Zeevaart, J.A.D. (2001). **Characterization of a novel carotenoid cleavage dioxygenase from plants**. Journal of Biological Chemistry **276,** 25208-25211.

83) Bouvier, F., Suire, C., Mutterer, J., and Camara, B. (2003). **Oxidative remodeling of chromoplast carotenoids: Identification of the carotenoid dioxygenase CsCCD and CsZCD genes involved in crocus secondary metabolite biogenesis**. Plant Cell **15,** 47-62.

84) Tan, B.C., Joseph, L.M., Deng, W.T., Liu, L.J., Li, Q.B., Cline, K., and McCarty, D.R. (2003). **Molecular characterization of the *Arabidopsis* 9-cis epoxycarotenoid dioxygenase gene family**. Plant Journal **35,** 44-56.

85) Booker, J., Auldridge, M., Wills, S., McCarty, D., Klee, H., and Leyser, O. (2004). **MAX3/CCD7 is a carotenoid cleavage dioxygenase required for the synthesis of a novel plant signaling molecule**. Current Biology **14,** 1232-1238.

86) Schwartz, S.H., Qin, X., and Loewen, M.C. (2004). **The Biochemical Characterization of Two Carotenoid Cleavage Enzymes from *Arabidopsis* Indicates That a Carotenoid-derived Compound Inhibits Lateral Branching**. Journal of Biological Chemistry **279,** 46940-46945.

87) Naested, H., Holm, A., Jenkins, T., Nielsen, H.B., Harris, C.A., Beale, M.H., Andersen, M., Mant, A., Scheller, H., Camara, B., Mattsson, O., and Mundy, J. (2004). ***Arabidopsis* VARIEGATED 3 encodes a chloroplasttargeted, zinc-finger protein required for chloroplast and palisade cell development**. Journal of Cell Science **117,** 4807-4818.

88) LaRonde-LeBlanc, N., and Wlodawer, A. (2005). **The RIO kinases: An atypical protein kinase family required for ribosome biogenesis and cell cycle progression**. Biochimica Et Biophysica Acta-Proteins and Proteomics **1754,** 14-24.

89) Lundquist, P.K., Davis, J.I., and van Wijk, K.J. (2012). **ABC1K atypical kinases in plants: filling the organellar kinase void**. Trends in Plant Science **17,** 546-555.

90) Leonard, C.J., Aravind, L., and Koonin, E.V. (1998). **Novel families of putative protein kinases in bacteria and archaea: Evolution of the "eukaryotic" protein kinase superfamily**. Genome Research **8,** 1038-1047.

91) Bousquet, I., Dujardin, G., and Slonimski, P.P. (1991). **ABC1, a novel yeast nuclear gene has a dual function in mitochondria - it suppresses a cytochrome-*b* messenger-RNA translation defect and is essential for the electron-transfer in the *bc1* complex**. Embo Journal **10,** 2023-2031.

92) Brasseur, G., Tron, P., Dujardin, G., Slonimski, P.P., and Brivet-Chevillotte, P. (1997). **The Nuclear ABC1 Gene is Essential for the Correct Conformation and Functioning of the Cytochrome *bc1* Complex and the Neighbouring Complexes II and IV in the Mitochondrial Respiratory Chain**. European Journal of Biochemistry **246,** 103-111.

93) Mollet, J., Delahodde, A., Serre, V., Chretien, D., Schlemmer, D., Lombes, A., Boddaert, N., Desguerre, I., de Lonlay, P., de Baulny, H.O., Munnich, A., and Rotig, A. (2008). **CABC1 gene mutations cause ubiquinone deficiency with cerebellar ataxia and seizures**. American Journal of Human Genetics **82,** 623-630.

94) Poon, W.W., Davis, D.E., Ha, H.T., Jonassen, T., Rather, P.N., and Clarke, C.F. (2000). **Identification of *Escherichia coli* ubiB, a gene required for the first monooxygenase step in ubiquinone biosynthesis**. Journal of Bacteriology **182,** 5139-5146.

95) Do, T.Q., Hsu, A.Y., Jonassen, T., Lee, P.T., and Clarke, C.F. (2001). **A defect in coenzyme Q biosynthesis is responsible for the respiratory deficiency in Saccharomyces cerevisiae abc1 mutants**. Journal of Biological Chemistry **276,** 18161-18168.

96) Knoell, H.E. (1981). **Stand-by position of the dioxygen-dependent ubiquinone-8 synthesis apparatus in anaerobically grown *Escherichia-coli*-k-12**. Fems Microbiology Letters **10,** 59-62.

97) Xie, L.T.X., Hsieh, E.J., Watanabe, S., Allan, C.M., Chen, J.Y., Tran, U.C., and Clarke, C.F. (2011). **Expression of the human atypical kinase ADCK3 rescues coenzyme Q biosynthesis and phosphorylation of Coq polypeptides in yeast coq8 mutants**. Biochimica Et Biophysica Acta-Molecular and Cell Biology of Lipids **1811,** 348-360.

98) Jasinski, M., Sudre, D., Schansker, G., Schellenberg, M., Constant, S., Martinoia, E., and Bovet, L. (2008). **AtOSA1, a member of the Abc1-like family, as a new factor in cadmium and oxidative stress response**. Plant Physiology **147,** 719-731.

99) Gao, Q.-S., Yang, Z.-F., Zhou, Y., Zhang, D., Yan, C.-H., Liang, G.-H., and Xu, C.-W. (2010). **Cloning of an ABC1-like Gene ZmABC1-10 and Its Responses to Cadmium and Other Abiotic Stresses in Maize (Zea mays L.)**. Acta Agronomica Sinica **36,** 2073-2083.

100) Boyd, J.S., Mittelmeier, T.M., Lamb, M.R., and Dieckmann, C.L. (2011). **Thioredoxin-family protein EYE2 and Ser/Thr kinase EYE3 play interdependent roles in eyespot assembly**. Molecular Biology of the Cell **22,** 1421-1429.

101) Yang, S., Zeng, X., Li, T., Liu, M., Zhang, S., Gao, S., Wang, Y., Peng, C., Li, L., and Yang, C. (2012). **AtACDO1, an ABC1-like kinase gene, is involved in chlorophyll degradation and the response to photooxidative stress in *Arabidopsis***. J Exp Bot **63,** 3959-3973.

102) Shikanai, T., Munekage, Y., Shimizu, K., Endo, T., and Hashimoto, T. (1999). **Identification and characterization of *Arabidopsis* mutants with reduced quenching of chlorophyll fluorescence**. Plant and Cell Physiology **40,** 1134-1142.

103) Fraser, P.D., and Bramley, P.M. (2004). **The biosynthesis and nutritional uses of carotenoids**. Progress in Lipid Research **43,** 228-265.

104) Krinsky, N.I., and Johnson, E.J. (2005). **Carotenoid actions and their relation to health and disease**. Molecular aspects of medicine **26,** 459-516.

105) DellaPenna, D., and Pogson, B.J. (2006). **Vitamin synthesis in plants: Tocopherols and carotenoids**. In Annual Review of Plant Biology, pp. 711-738.

106) Hunter, W.N. (2007). **The Non-mevalonate Pathway of Isoprenoid Precursor Biosynthesis**. Journal of Biological Chemistry **282,** 21573-21577.

107) Phillips, M.A., Leon, P., Boronat, A., and Rodriguez-Concepcion, M. (2008). **The plastidial MEP pathway: unified nomenclature and resources**. Trends in Plant Science **13,** 619-623.

108) Ganjewala, D., Kumar, S., and Luthra, R. (2009). **An account of cloned genes of Methyl-erythritol-4-phosphate pathway of isoprenoid biosynthesis in plants**. Curr Issues Mol Biol **11 Suppl 1,** i35-45.

109) Strack, D., and Fester, T. (2006). **Isoprenoid metabolism and plastid reorganization in arbuscular mycorrhizal roots**. New Phytologist **172,** 22-34.

110) Li, F., Vallabhaneni, R., and Wurtzel, E.T. (2008). **PSY3, a new member of the phytoene synthase gene family conserved in the Poaceae and regulator of abiotic stress-induced root carotenogenesis**. Plant Physiol **146,** 1333-1345.

111) Welsch, R., Wuest, F., Baer, C., Al-Babili, S., and Beyer, P. (2008). **A third phytoene synthase is devoted to abiotic stress-induced abscisic acid formation in rice and defines functional diversification of phytoene synthase genes**. Plant Physiology **147,** 367-380.

112) Li, F., Vallabhaneni, R., Yu, J., Rocheford, T., and Wurtzel, E.T. (2008). **The maize phytoene synthase gene family: Overlapping roles for carotenogenesis in endosperm, photomorphogenesis, and thermal stress tolerance**. Plant Physiology **147,** 1334-1346.

113) Welsch, R., Beyer, P., Hugueney, P., Kleinig, H., and von Lintig, J. (2000). **Regulation and activation of phytoene synthase, a key enzyme in carotenoid biosynthesis, during photomorphogenesis**. Planta **211,** 846-854.

114) Welsch, R., Medina, J., Giuliano, G., Beyer, P., and von Lintig, J. (2003). **Structural and functional characterization of the phytoene synthase promoter from *Arabidopsis thaliana***. Planta **216,** 523-534.

115) Park, H., Kreunen, S.S., Cuttriss, A.J., DellaPenna, D., and Pogson, B.J. (2002). **Identification of the carotenoid isomerase provides insight into carotenoid biosynthesis, prolamellar body formation, and photomorphogenesis**. Plant Cell **14,** 321-332.

116) Isaacson, T., Ohad, I., Beyer, P., and Hirschberg, J. (2004). **Analysis in vitro of the enzyme CRTISO establishes a poly-cis-carotenoid biosynthesis pathway in plants**. Plant Physiology **136,** 4246-4255.

117) Breitenbach, J., and Sandmann, G. (2005). **zeta-Carotene cis isomers as products and substrates in the plant poly-cis carotenoid biosynthetic pathway to lycopene**. Planta **220,** 785-793.

118) Dong, H.L., Deng, Y., Mu, J.Y., Lu, Q.T., Wang, Y.Q., Xu, Y.Y., Chu, C.C., Chong, K., Lu, C.M., and Zuo, J.R. (2007). **The *Arabidopsis* Spontaneous Cell Death1 gene, encoding a zeta-carotene desaturase essential for carotenoid biosynthesis, is involved in chloroplast development, photoprotection and retrograde signalling**. Cell Res. **17,** 458-470.

119) Meier, S., Tzfadia, O., Vallabhaneni, R., Gehring, C., and Wurtzel, E.T. (2011). **A transcriptional analysis of carotenoid, chlorophyll and plastidial isoprenoid biosynthesis genes during development and osmotic stress responses in *Arabidopsis thaliana* 5,** 77.

120) Mayer, M.P., Nievelstein, V., and Beyer, P. (1992). **Purification and characterization of a nadph dependent oxidoreductase from chromoplasts of *Narcissus pseudonarcissus* - a redox-mediator possibly involved in carotene desaturation**. Plant Physiology and Biochemistry **30,** 389-398.

121) Norris, S.R., Barrette, T.R., and DellaPenna, D. (1995). **Genetic dissection of carotenoid synthesis in *Arabidopsis* defines plastoquinone as an essential component of phytoene desaturation**. Plant Cell **7,** 2139-2149.

122) Carol, P., and Kuntz, M. (2001). **A plastid terminal oxidase comes to light: implications for carotenoid biosynthesis and chlororespiration**. Trends in Plant Science **6,** 31-36.

123) Berthold, D.A., Andersson, M.E., and Nordlund, P. (2000). **New insight into the structure and function of the alternative oxidase**. Biochim. Biophys. Acta-Bioenerg. **1460,** 241-254.

124) Yu, F., Fu, A., Aluru, M., Park, S., Xu, Y., Liu, H., Liu, X., Foudree, A., Nambogga, M., and Rodermel, S. (2007). **Variegation mutants and mechanisms of chloroplast biogenesis**. Plant Cell and Environment **30,** 350-365.

125) Aluru, M.R., Bae, H., Wu, D.Y., and Rodermel, S.R. (2001). **The *Arabidopsis immutans* mutation affects plastid differentiation and the morphogenesis of white and green sectors in variegated plants**. Plant Physiology **127,** 67-77.

126) Cazzonelli, C.I., Cuttriss, A.J., Cossetto, S.B., Pye, W., Crisp, P., Whelan, J., Finnegan, E.J., Turnbull, C., and Pogson, B.J. (2009). **Regulation of Carotenoid Composition**

and Shoot Branching in *Arabidopsis* by a Chromatin Modifying Histone Methyltransferase, SDG8. Plant Cell **21,** 39-53.

127) Yu, B., Lydiate, D.J., Young, L.W., Schaefer, U.A., and Hannoufa, A. (2008). **Enhancing the carotenoid content of *Brassica napus* seeds by downregulating lycopene epsilon cyclase**. Transgenic Research **17,** 573-585.

128) Bai, L., Kim, E.-H., DellaPenna, D., and Brutnell, T.P. (2009). **Novel lycopene epsilon cyclase activities in maize revealed through perturbation of carotenoid biosynthesis**. Plant Journal **59,** 588-599.

129) Pogson, B.J., and Rissler, H.M. (2000). **Genetic manipulation of carotenoid biosynthesis and photoprotection**. Philosophical Transactions of the Royal Society of London Series B-Biological Sciences **355,** 1395-1403.

130) Cuttriss, A.J., Chubb, A.C., Alawady, A., Grimm, B., and Pogson, B.J. (2007). **Regulation of lutein biosynthesis and prolamellar body formation in *Arabidopsis***. Functional Plant Biology **34,** 663-672.

131) Dall'Osto, L., Lico, C., Alric, J., Giuliano, G., Havaux, M., and Bassi, R. (2006). **Lutein is needed for efficient chlorophyll triplet quenching in the major LHCII antenna complex of higher plants and effective photoprotection in vivo under strong light**. BMC Plant Biol. **6**.

132) Lam, E., Ortiz, W., and Malkin, R. (1984). **Chlorophyll a-b proteins of Photosystem-I**. FEBS Letters **168,** 10-14.

133) Demmig-Adams, B. (1990). **Carotenoids and photoprotection in plants: A role for the xanthophyll zeaxanthin**. Biochimica et Biophysica Acta (BBA) - Bioenergetics **1020,** 1-24.

134) Pfündel, E., and Bilger, W. (1994). **Regulation and possible function of the violaxanthin cycle**. Photosynth. Res.**,** 89-109.

135) Adams, W.I., Demmig-Adams, B., Verhoeven, A., and Barker, D. (1995). **'Photoinhibition' During Winter Stress: Involvement of Sustained Xanthophyll Cycle-Dependent Energy Dissipation**. Functional Plant Biology **22,** 261-276.

136) Gilmore, A.M., Hazlett, T.L., and Govindjee. (1995). **Xanthophyll cycle-dependent quenching of photosystem II chlorophyll a fluorescence: formation of a quenching**

complex with a short fluorescence lifetime. Proceedings of the National Academy of Sciences **92,** 2273-2277.

137) Eskling, M., Arvidsson, P.-O., and Åkerlund, H.-E. (1997). **The xanthophyll cycle, its regulation and components**. Physiologia Plantarum **100,** 806-816.

138) Rossel, J.B., Wilson, I.W., and Pogson, B.J. (2002). **Global Changes in Gene Expression in Response to High Light in *Arabidopsis***. Plant Physiology **130,** 1109-1120.

139) Rockholm, D.C., and Yamamoto, H.Y. (1996). **Violaxanthin de-epoxidase**. Plant Physiol **110,** 697-703.

140) Zeevaart, J.A.D., and Creelman, R.A. (1988). **Metabolism and Physiology of Abscisic Acid**. Annual Review of Plant Physiology and Plant Molecular Biology **39,** 439-473.

141) Gomez-Roldan, V., Fermas, S., Brewer, P.B., Puech-Pages, V., Dun, E.A., Pillot, J.P., Letisse, F., Matusova, R., Danoun, S., Portais, J.C., Bouwmeester, H., Becard, G., Beveridge, C.A., Rameau, C., and Rochange, S.F. (2008). **Strigolactone inhibition of shoot branching**. Nature **455,** 189-194.

142) Fester, T., Schmidt, D., Lohse, S., Walter, M.H., Giuliano, G., Bramley, P.M., Fraser, P.D., Hause, B., and Strack, D. (2002). **Stimulation of carotenoid metabolism in arbuscular mycorrhizal roots**. Planta **216,** 148-154.

143) Dudareva, N., Negre, F., Nagegowda, D., and Orlova, I. (2006). **Plant Volatiles: Recent Advances and Future Perspectives**. Critical Reviews in Plant Sciences **25,** 417-440.

144) Lopez-Raez, J.A., Matusova, R., Cardoso, C., Jamil, M., Charnikhova, T., Kohlen, W., Ruyter-Spira, C., Verstappen, F., and Bouwmeester, H. (2009). **Strigolactones: ecological significance and use as a target for parasitic plant control**. Pest Manag Sci **65,** 471-477.

145) Akiyama, K., Matsuzaki, K., and Hayashi, H. (2005). **Plant sesquiterpenes induce hyphal branching in arbuscular mycorrhizal fungi**. Nature **435,** 824-827.

146) Bouwmeester, H.J., Roux, C., Lopez-Raez, J.A., and Bécard, G. (2007). **Rhizosphere communication of plants, parasitic plants and AM fungi**. Trends in Plant Science **12,** 224-230.

147) Ohmiya, A., Kishimoto, S., Aida, R., Yoshioka, S., and Sumitomo, K. (2006). **Carotenoid Cleavage Dioxygenase (CmCCD4a) Contributes to White Color Formation in Chrysanthemum Petals**. Plant Physiology **142,** 1193-1201.

148) Bouvier, F., Rahier, A., and Camara, B. (2005). **Biogenesis, molecular regulation and function of plant isoprenoids**. Progress in Lipid Research **44,** 357-429.

149) Mene-Saffrane, L., and DellaPenna, D. (2010). **Biosynthesis, regulation and functions of tocochromanols in plants**. Plant Physiology and Biochemistry **48,** 301-309.

150) Horvath, G., Wessjohann, L., Bigirimana, J., Jansen, M., Guisez, Y., Caubergs, R., and Horemans, N. (2006). **Differential distribution of tocopherols and tocotrienols in photosynthetic and non-photosynthetic tissues**. Phytochemistry **67,** 1185-1195.

151) Shintani, D., and DellaPenna, D. (1998). **Elevating the vitamin E content of plants through metabolic engineering**. Science **282,** 2098-2100.

152) Van Eenennaam, A.L., Lincoln, K., Durrett, T.P., Valentin, H.E., Shewmaker, C.K., Thorne, G.M., Jiang, J., Baszis, S.R., Levering, C.K., Aasen, E.D., Hao, M., Stein, J.C., Norris, S.R., and Last, R.L. (2003). **Engineering vitamin E content: From *Arabidopsis* mutant to soy oil**. Plant Cell **15,** 3007-3019.

153) Collakova, E., and DellaPenna, D. (2003). **Homogentisate phytyltransferase activity is limiting for tocopherol biosynthesis in *Arabidopsis***. Plant Physiology **131,** 632-642.

154) Kamal-Eldin, A., and Appelqvist, L.-Å. (1996). **The chemistry and antioxidant properties of tocopherols and tocotrienols**. Lipids **31,** 671-701.

155) Munne-Bosch, S., and Alegre, L. (2002). **The Function of Tocopherols and Tocotrienols in Plants**. Critical Reviews in Plant Sciences **21,** 31-57.

156) Schneider, C. (2005). **Chemistry and biology of vitamin E**. Mol Nutr Food Res **49,** 7-30.

157) Wolf, G. (2005). **The Discovery of the Antioxidant Function of Vitamin E: the contribution of Henry A. Mattill**. The Journal of Nutrition **135,** 363-366.

158) Wu, J.H., and Croft, K.D. (2007). **Vitamin E metabolism**. Mol Aspects Med **28,** 437-452.

159) Dilley, R.A., and Crane, F.L. (1963). **Light-induced changes of alpha-tocopherylquinone in spinach chloroplasts**. Biochimica Et Biophysica Acta **75,** 142-143.

160) Liebler, D.C., Burr, J.A., and Ham, A.J.L. (1999). **Gas chromatography mass spectrometry analysis of vitamin E and its oxidation products**. Oxidants and Antioxidants, Pt A **299,** 309-318.

161) Kruk, J., Hollander-Czytko, H., Oettmeier, W., and Trebst, A. (2005). **Tocopherol as singlet oxygen scavenger in photosystem II**. J Plant Physiol **162,** 749-757.

162) Krieger-Liszkay, A., and Trebst, A. (2006). **Tocopherol is the scavenger of singlet oxygen produced by the triplet states of chlorophyll in the PSII reaction centre**. Journal of Experimental Botany **57,** 1677-1684.

163) Havaux, M., Eymery, F., Porfirova, S., Rey, P., and Dormann, P. (2005). **Vitamin E protects against photoinhibition and photooxidative stress in *Arabidopsis thaliana***. Plant Cell **17,** 3451-3469.

164) Maeda, H., and DellaPenna, D. (2007). **Tocopherol functions in photosynthetic organisms**. Current Opinion in Plant Biology **10,** 260-265.

165) Sattler, S.E., Gilliland, L.U., Magallanes-Lundback, M., Pollard, M., and DellaPenna, D. (2004). **Vitamin E is essential for seed longevity, and for preventing lipid peroxidation during germination**. Plant Cell **16,** 1419-1432.

166) Lichtenthaler, H.K. (2007). **Biosynthesis, accumulation and emission of carotenoids, alpha-tocopherol, plastoquinone, and isoprene in leaves under high photosynthetic irradiance**. Photosynth Res **92,** 163-179.

167) Li, Z., Keasling, J.D., and Niyogi, K.K. (2012). **Overlapping Photoprotective Function of Vitamin E and Carotenoids in *Chlamydomonas***. Plant Physiology **158,** 313-323.

168) Kruk, J., Schmid, G.H., and Strzalka, K. (1994). **Antioxidant properties of plastoquinol and other biological prenylquinols in liposomes and solution**. Free Radical Research **21,** 409-416.

169) Kruk, J., Jemioła-Rzemińska, M., and Strzałka, K. (1997). **Plastoquinol and α-tocopherol quinol are more active than ubiquinol and α-tocopherol in inhibition of lipid peroxidation**. Chemistry and Physics of Lipids **87,** 73-80.

170) Hundal, T., ForsmarkAndree, P., Ernster, L., and Andersson, B. (1995). **Antioxidant activity of reduced plastoquinone in chloroplast thylakoid membranes**. Archives of Biochemistry and Biophysics **324,** 117-122.

171) Kruk, J., Jemiola-Rzeminska, M., Burda, K., Schmid, G.H., and Strzalka, K. (2003). **Scavenging of superoxide generated in photosystem I by plastoquinol and other prenyllipids in thylakoid membranes**. Biochemistry **42,** 8501-8505.

172) Kruk, J., and Trebst, A. (2008). **Plastoquinol as a singlet oxygen scavenger in photosystem II**. Biochim. Biophys. Acta-Bioenerg. **1777,** 154-162.

173) Rochaix, J.D. (2007). **Role of thylakoid protein kinases in photosynthetic acclimation**. FEBS Lett **581,** 2768-2775.

174) Karpinski, S., Escobar, C., Karpinska, B., Creissen, G., and Mullineaux, P.M. (1997). **Photosynthetic electron transport regulates the expression of cytosolic ascorbate peroxidase genes in *Arabidopsis* during excess light stress**. Plant Cell **9,** 627-640.

175) Fey, V., Wagner, R., Brautigam, K., and Pfannschmidt, T. (2005). **Photosynthetic redox control of nuclear gene expression**. Journal of Experimental Botany **56,** 1491-1498.

176) Motohashi, R., Ito, T., Kobayashi, M., Taji, T., Nagata, N., Asami, T., Yoshida, S., Yamaguchi-Shinozaki, K., and Shinozaki, K. (2003). **Functional analysis of the 37 kDa inner envelope membrane polypeptide in chloroplast biogenesis using a Ds-tagged *Arabidopsis* pale-green mutant**. Plant Journal **34,** 719-731.

177) Olejnik, D., Gogolewski, M., and NogalaKalucka, M. (1997). **Isolation and some properties of plastochromanol-8**. Nahrung-Food **41,** 101-104.

178) Gruszka, J., and Kruk, J. (2007). **RP-LC for determination of plastochromanol, tocotrienols and tocopherols in plant oils**. Chromatographia **66,** 909-913.

179) Szymanska, R., and Kruk, J. (2010). **Identification of hydroxy-plastochromanol in *Arabidopsis* leaves**. Acta Biochimica Polonica **57,** 105-108.

180) Muller, P., Li, X.P., and Niyogi, K.K. (2001). **Non-photochemical quenching. A response to excess light energy**. Plant Physiol **125,** 1558-1566.

181) Li, Z.R., Ahn, T.K., Avenson, T.J., Ballottari, M., Cruz, J.A., Kramer, D.M., Bassi, R., Fleming, G.R., Keasling, J.D., and Niyogi, K.K. (2009). **Lutein Accumulation in the**

Absence of Zeaxanthin Restores Nonphotochemical Quenching in the *Arabidopsis thaliana npq1* Mutant. Plant Cell **21,** 1798-1812.

182) Bouvier, F., dHarlingue, A., Hugueney, P., Marin, E., MarionPoll, A., and Camara, B. (1996). **Xanthophyll biosynthesis - Cloning, expression, functional reconstitution, and regulation of beta-cyclohexenyl carotenoid epoxidase from pepper (Capsicum annuum)**. Journal of Biological Chemistry **271,** 28861-28867.

183) Bugos, R.C., and Yamamoto, H.Y. (1996). **Molecular cloning of violaxanthin de-epoxidase from romaine lettuce and expression in Escherichia coli**. Proceedings of the National Academy of Sciences of the United States of America **93,** 6320-6325.

184) Gilmore, A.M. (1997). **Mechanistic aspects of xanthophyll cycle-dependent photoprotection in higher plant chloroplasts and leaves**. Physiologia Plantarum **99,** 197-209.

185) Munekage, Y., Takeda, S., Endo, T., Jahns, P., Hashimoto, T., and Shikanai, T. (2001). **Cytochrome *b(6)f* mutation specifically affects thermal dissipation of absorbed light energy in *Arabidopsis***. Plant Journal **28,** 351-359.

186) Jahns, P., Graf, M., Munekage, Y., and Shikanai, T. (2002). **Single point mutation in the Rieske iron-sulfur subunit of cytochrome b(6)/f leads to an altered pH dependence of plastoquinol oxidation in *Arabidopsis***. Febs Letters **519,** 99-102.

187) Sonoike, K. (1996). **Photoinhihition of photosystem I: Its physiological significance in the chilling sensitivity of plants**. Plant and Cell Physiology **37,** 239-247.

188) Kimura, K., Munekage, Y., Endo, T., and Shikanai, T. (2001). **Disturbed H+/e- ratio in *Arabidopsis* mutant *pgr6* defective in cytochrome bf complex activity**. Science Access **3,** -.

189) Sheen, J. (1994). **Feedback control of gene expression**. Photosynthesis Research **39,** 427-438.

190) Koch, K.E. (1996). **Carbohydrate-modulated gene expression in plants**. Annual Review of Plant Physiology and Plant Molecular Biology **47,** 509-540.

191) Koch, K. (2004). **Sucrose metabolism: regulatory mechanisms and pivotal roles in sugar sensing and plant development**. Current Opinion in Plant Biology **7,** 235-246.

192) Loreti, E., Poggi, A., Novi, G., Alpi, A., and Perata, P. (2005). **A genome-wide analysis of the effects of sucrose on gene expression in *Arabidopsis* seedlings under anoxia**. Plant Physiology **137,** 1130-1138.

193) Stitt, M. (1986). **Limitation of Photosynthesis by Carbon Metabolism : I. Evidence for Excess Electron Transport Capacity in Leaves Carrying Out Photosynthesis in Saturating Light and CO(2)**. Plant Physiol **81,** 1115-1122.

194) Huber, S.C. (1986). **Fructose 2,6-bisphosphate as a regulatory metabolite in plants**. Annual Review of Plant Physiology and Plant Molecular Biology **37,** 233-246.

195) Stitt, M. (1990). **Fructose-2,6-bisphosphate as a regulatory molecule in plants**. Annual Review of Plant Physiology and Plant Molecular Biology **41,** 153-185.

196) Nielsen, T.H., Rung, J.H., and Villadsen, D. (2004). **Fructose-2,6-bisphosphate: a traffic signal in plant metabolism**. Trends in Plant Science **9,** 556-563.

197) Draborg, H., Villadsen, D., and Nielsen, T.H. (1999). **Cloning, characterization and expression of a bifunctional fructose-6-phosphate, 2-kinase/fructose-2,6-bisphosphatase from potato**. Plant Molecular Biology **39,** 709-720.

198) Markham, J.E., and Kruger, N.J. (2002). **Kinetic properties of bifunctional 6-phosphofructo-2-kinase/fructose-2,6-bisphosphatase from spinach leaves**. European Journal of Biochemistry **269,** 1267-1277.

199) Taiz, L., and Zeiger, E. (2006). **Plant Physiology, 4th Edition**. (Sinauer Associates Inc).

200) Graciet, E., Lebreton, S., and Gontero, B. (2004). **Emergence of new regulatory mechanisms in the Benson-Calvin pathway via protein-protein interactions: a glyceraldehyde-3-phosphate dehydrogenase/CP12/phosphoribulokinase complex**. Journal of Experimental Botany **55,** 1245-1254.

201) Raines, C.A. (2006). **Transgenic approaches to manipulate the environmental responses of the C(3) carbon fixation cycle**. Plant Cell and Environment **29,** 331-339.

202) Haake, V., Zrenner, R., Sonnewald, U., and Stitt, M. (1998). **A moderate decrease of plastid aldolase activity inhibits photosynthesis, alters the levels of sugars and starch, and inhibits growth of potato plants**. Plant Journal **14,** 147-157.

203) Haake, V., Geiger, M., Walch-Liu, P., Engels, C., Zrenner, R., and Stitt, M. (1999). **Changes in aldolase activity in wild-type potato plants are important for acclimation to growth irradiance and carbon dioxide concentration, because plastid aldolase exerts control over the ambient rate of photosynthesis across a range of growth conditions**. Plant Journal **17,** 479-489.

204) Uematsu, K., Suzuki, N., Iwamae, T., Inui, M., and Yukawa, H. (2012). **Increased fructose 1,6-bisphosphate aldolase in plastids enhances growth and photosynthesis of tobacco plants**. Journal of Experimental Botany **63,** 3001-3009.

205) Barry, G., Cheikh, N., and Kishore, G. (1998). **Expression of fructose 1,6 bisphosphate aldolase in transgenic plants. Patent Application WO/1998/058069**.

206) Von Caemmerer, S., and Farquhar, G.D. (1981). **Some relationships between the biochemistry of photosynthesis and the gas-exchange of leaves**. Planta **153,** 376-387.

207) Strand, A., Zrenner, R., Trevanion, S., Stitt, M., Gustafsson, P., and Gardestrom, P. (2000). **Decreased expression of two key enzymes in the sucrose biosynthesis pathway, cytosolic fructose-1,6-bisphosphatase and sucrose phosphate synthase, has remarkably different consequences for photosynthetic carbon metabolism in transgenic *Arabidopsis thaliana***. Plant Journal **23,** 759-770.

208) Krause, K.P., and Stitt, M. (1992). **Sucrose-6-phosphate levels in spinach leaves and their effects on sucrose-phosphate synthase**. Phytochemistry **31,** 1143-1146.

209) Signora, L., Galtier, N., Skot, L., Lucas, H., and Foyer, C.H. (1998). **Over-expression of sucrose phosphate synthase in *Arabidopsis thaliana* results in increased foliar sucrose/starch ratios and favours decreased foliar carbohydrate accumulation in plants after prolonged growth with CO_2 enrichment**. Journal of Experimental Botany **49,** 669-680.

210) Lunn, J.E., and MacRae, E. (2003). **New complexities in the synthesis of sucrose**. Current Opinion in Plant Biology **6,** 208-214.

211) Castleden, C.K., Aoki, N., Gillespie, V.J., MacRae, E.A., Quick, W.P., Buchner, P., Foyer, C.H., Furbank, R.T., and Lunn, J.E. (2004). **Evolution and function of the sucrose-phosphate synthase gene families in wheat and other grasses**. Plant Physiology **135,** 1753-1764.

212) Winter, H., and Huber, S.C. (2000). **Regulation of sucrose metabolism in higher plants: Localization and regulation of activity of key enzymes**. Critical Reviews in Biochemistry and Molecular Biology **35,** 253-289.

213) Huang, J.Z., and Huber, S.C. (2001). **Phosphorylation of synthetic peptides by a CDPK and plant SNF1-related protein kinase. Influence of proline and basic amino acid residues at selected positions**. Plant and Cell Physiology **42,** 1079-1087.

214) Radchuk, R., Radchuk, V., Weschke, W., Borisjuk, L., and Weber, H. (2006). **Repressing the expression of the SUCROSE NONFERMENTING-1-RELATED PROTEIN KINASE gene in pea embryo causes pleiotropic defects of maturation similar to an abscisic acid-insensitive phenotype**. Plant Physiology **140,** 263-278.

215) Jossier, M., Bouly, J.-P., Meimoun, P., Arjmand, A., Lessard, P., Hawley, S., Grahame Hardie, D., and Thomas, M. (2009). **SnRK1 (SNF1-related kinase 1) has a central role in sugar and ABA signalling in *Arabidopsis thaliana***. Plant Journal **59,** 316-328.

216) The *Arabidopsis* Information Resource [http://www.arabidopsis.org/].

217) Murphy, D.J. (2001). **The biogenesis and functions of lipid bodies in animals, plants and microorganisms**. Progress in Lipid Research **40,** 325-438.

218) Kyte, J., and Doolittle, R.F. (1982). **A simple method for displaying the hydropathic character of a protein**. Journal of Molecular Biology **157,** 105-132.

219) Emanuelsson, O., Brunak, S., von Heijne, G., and Nielsen, H. (2007). **Locating proteins in the cell using TargetP, SignalP and related tools**. Nature Protocols **2,** 953-971.

220) Sasse, J.M. (2003). **Physiological actions of brassinosteroids: An update**. J. Plant Growth Regul. **22,** 276-288.

221) Bartels, P.G., and Watson, C.W. (1978). **Inhibition of carotenoid synthesis by fluridone and norflurazon**. Weed Science **26,** 198-203.

222) Sandmann, G., and Böger, P. (1997). **Phytoene desaturase as a target for bleaching herbicides IOS Press, Amsterdam,** 1–10.

223) Quatrano, R.S., Bartels, D., Ho, T.H.D., and Pages, M. (1997). **New insights into ABA-mediated processes**. Plant Cell **9,** 470-475.

224) Alonso, J.M., Stepanova, A.N., Leisse, T.J., Kim, C.J., Chen, H.M., Shinn, P., Stevenson, D.K., Zimmerman, J., Barajas, P., Cheuk, R., Gadrinab, C., Heller, C., Jeske, A., Koesema, E., Meyers, C.C., Parker, H., Prednis, L., Ansari, Y., Choy, N., Deen, H., Geralt, M., Hazari, N., Hom, E., Karnes, M., Mulholland, C., Ndubaku, R., Schmidt, I., Guzman, P., Aguilar-Henonin, L., Schmid, M., Weigel, D., Carter, D.E., Marchand, T., Risseeuw, E., Brogden, D., Zeko, A., Crosby, W.L., Berry, C.C., and Ecker, J.R. (2003). **Genome-wide Insertional mutagenesis of *Arabidopsis thaliana***. Science **301,** 653-657.

225) Smith, N.A., Singh, S.P., Wang, M.B., Stoutjesdijk, P.A., Green, A.G., and Waterhouse, P.M. (2000). **Gene expression - Total silencing by intron-spliced hairpin RNAs**. Nature **407,** 319-320.

226) Giacomelli, L., Rudella, A., and van Wijk, K.J. (2006). **High light response of the thylakoid proteome in *Arabidopsis* wild type and the ascorbate-deficient mutant vtc2-2. A comparative proteomics study**. Plant Physiology **141,** 685-701.

227) Kannan, N., Taylor, S.S., Zhai, Y.F., Venter, J.C., and Manning, G. (2007). **Structural and functional diversity of the microbial kinome**. Plos Biology **5,** 467-478.

228) Manning, G., Whyte, D.B., Martinez, R., Hunter, T., and Sudarsanam, S. (2002). **The protein kinase complement of the human genome**. Science **298,** 1912-1934.

229) Scheeff, E.D., and Bourne, P.E. (2005). **Structural evolution of the protein kinase-like superfamily**. Plos Computational Biology **1,** 359-381.

230) Collins, M.D., and Jones, D. (1981). **Distribution of isoprenoid quinone structural types in bacteria and their taxonomic implications**. Microbiological Reviews **45,** 316-354.

231) Sadre, R., Pfaff, C., and Buchkremer, S. (2012). **Plastoquinone-9 biosynthesis in cyanobacteria differs from that in plants and involves a novel 4-hydroxybenzoate solanesyltransferase**. Biochemical Journal **442,** 621-629.

232) Yoshida, K., Shibata, M., Terashima, I., and Noguchi, K. (2010). **Simultaneous Determination of In Vivo Plastoquinone and Ubiquinone Redox States by HPLC-Based Analysis**. Plant and Cell Physiology **51,** 836-841.

233) Byrdwell, W. (2001). **Atmospheric pressure chemical ionization mass spectrometry for analysis of lipids**. Lipids **36,** 327-346.

234) Niyogi, K.K., Shih, C., Chow, W.S., Pogson, B.J., DellaPenna, D., and Bjorkman, O. (2001). **Photoprotection in a zeaxanthin- and lutein-deficient double mutant of *Arabidopsis***. Photosynthesis Research **67,** 139-145.

235) Melis, A., Murakami, A., Nemson, J.A., Aizawa, K., Ohki, K., and Fujita, Y. (1996). **Chromatic regulation in *Chlamydomonas reinhardtii* alters photosystem stoichiometry and improves the quantum efficiency of photosynthesis**. Photosynthesis Research **47,** 253-265.

236) Neidhardt, J., Benemann, J.R., Zhang, L., and Melis, A. (1998). **Photosystem-II repair and chloroplast recovery from irradiance stress: relationship between chronic photoinhibition, light-harvesting chlorophyll antenna size and photosynthetic productivity in *Dunaliella salina* (green algae)**. Photosynthesis Research **56,** 175-184.

237) Melis, A. (2004). **Excitation Energy Transfer: Functional and Dynamic Aspects of Lhc (cab) Proteins Oxygenic Photosynthesis: The Light Reactions**, D.R. Ort, C.F. Yocum, and I.F. Heichel, eds (Springer Netherlands), pp. 523-538.

238) Sharkey, T.D., Berry, J.A., and Raschke, K. (1985). **Starch and sucrose synthesis in *Phaseolus vulgaris* as affected by light, CO_2, and abscisic acid**. Plant Physiology **77,** 617-620.

239) Rolland, F., Baena-Gonzalez, E., and Sheen, J. (2006). **Sugar sensing and signaling in plants: Conserved and novel mechanisms**. In Annual Review of Plant Biology (Palo Alto: Annual Reviews), pp. 675-709.

240) Solfanelli, C., Poggi, A., Loreti, E., Alpi, A., and Perata, P. (2006). **Sucrose-specific induction of the anthocyanin biosynthetic pathway in *Arabidopsis***. Plant Physiology **140,** 637-646.

241) Das, P.K., Geul, B., Choi, S.-B., Yoo, S.-D., and Park, Y.-I. (2011). **Photosynthesis-dependent anthocyanin pigmentation in *Arabidopsis***. Plant signaling & behavior **6,** 23-25.

242) Jeong, S.W., Das, P.K., Jeoung, S.C., Song, J.Y., Lee, H.K., Kim, Y.K., Kim, W.J., Il Park, Y., Yoo, S.D., Choi, S.B., Choi, G., and Park, Y.I. (2010). **Ethylene Suppression**

of Sugar-Induced Anthocyanin Pigmentation in *Arabidopsis*. Plant Physiology **154,** 1514-1531.

243) Chen, M., Jensen, M., and Rodermel, S. (1999). **The yellow variegated mutant of *Arabidopsis* is plastid autonomous and delayed in chloroplast biogenesis**. Journal of Heredity **90,** 207-214.

244) Chen, M., Choi, Y.D., Voytas, D.F., and Rodermel, S. (2000). **Mutations in the *Arabidopsis* VAR2 locus cause leaf variegation due to the loss of a chloroplast FtsH protease**. Plant Journal **22,** 303-313.

245) Takechi, K., Sodmergen, Murata, M., Motoyoshi, F., and Sakamoto, W. (2000). **The YELLOW VARIEGATED (VAR2) locus encodes a homologue of FtsH, an ATP-dependent protease in *Arabidopsis***. Plant and Cell Physiology **41,** 1334-1346.

246) Sakamoto, W., Uno, Y., Zhang, Q., Miura, E., Kato, Y., and Sodmergen. (2009). **Arrested Differentiation of Proplastids into Chloroplasts in Variegated Leaves Characterized by Plastid Ultrastructure and Nucleoid Morphology**. Plant and Cell Physiology **50,** 2069-2083.

247) Earley, K.W., Haag, J.R., Pontes, O., Opper, K., Juehne, T., Song, K.M., and Pikaard, C.S. (2006). **Gateway-compatible vectors for plant functional genomics and proteomics**. Plant Journal **45,** 616-629.

248) Rigaut, G., Shevchenko, A., Rutz, B., Wilm, M., Mann, M., and Seraphin, B. (1999). **A generic protein purification method for protein complex characterization and proteome exploration**. Nature Biotechnology **17,** 1030-1032.

249) Busso, D., Delagoutte-Busso, B., and Moras, D. (2005). **Construction of a set Gateway-based destination vectors for high-throughput cloning and expression screening in *Escherichia coli***. Anal. Biochem. **343,** 313-321.

250) Wesley, S.V., Helliwell, C.A., Smith, N.A., Wang, M.B., Rouse, D.T., Liu, Q., Gooding, P.S., Singh, S.P., Abbott, D., Stoutjesdijk, P.A., Robinson, S.P., Gleave, A.P., Green, A.G., and Waterhouse, P.M. (2001). **Construct design for efficient, effective and high-throughput gene silencing in plants**. Plant J **27,** 581-590.

251) Bauer, J., Hiltbrunner, A., and Kessler, F. (2001). **Molecular biology of chloroplast biogenesis: gene expression, protein import and intraorganellar sorting**. Cellular and Molecular Life Sciences **58,** 420-433.

252) Hiltbrunner, A., Bauer, J., Vidi, P.A., Infanger, S., Weibel, P., Hohwy, M., and Kessler, F. (2001). **Targeting of an abundant cytosolic form of the protein import receptor at Toc159 to the outer chloroplast membrane**. J. Cell Biol. **154,** 309-316.

253) Suhara, Y., Kamao, M., Tsugawa, N., and Okano, T. (2005). **Method for the determination of vitamin K homologues in human plasma using high-performance liquid chromatography-tandem mass spectrometry**. Analytical Chemistry **77,** 757-763.

254) Arnon, D.I. (1949). **Copper enzymes in isolated chloroplasts. Polyphenoloxidase in *Beta vulgaris***. Plant Physiol **24,** 1-15.

255) Sambrook, J., and Russell, D.W. (2001). **Molecular cloning: a laboratory manual**. (Cold Spring Harbor, New York: Cold Spring Harbor Laboratory Press).

256) Edwards, K., Johnstone, C., and Thompson, C. (1991). **A simple and rapid method for the preparation of plant genomic dna for pcr analysis**. Nucleic Acids Research **19,** 1349-1349.

257) La Jolla, CA, USA [http://signal.salk.edu/tdnaprimers.2.html].

258) Rensink, W.A., Pilon, M., and Weisbeek, P. (1998). **Domains of a transit sequence required for in vivo import in *Arabidopsis* chloroplasts**. Plant Physiology **118,** 691-699.

259) Wessel, D., and Flugge, U.I. (1984). **A method for the quantitative recovery of protein in dilute-solution in the presence of detergents and lipids**. Anal. Biochem. **138,** 141-143.

260) Bechtold, N., Ellis, J., and Pelletier, G. (1993). **In-planta Agrobacterium-mediated gene transfer by infiltration of adult *Arabidopsis thaliana* plants**. Comptes Rendus De L Academie Des Sciences Serie Iii-Sciences De La Vie-Life Sciences **316,** 1194-1199.

261) Clough, S.J., and Bent, A.F. (1998). **Floral dip: a simplified method for Agrobacterium-mediated transformation of *Arabidopsis thaliana***. Plant Journal **16,** 735-743.

262) Wintermans, J.F.G.M., and Demots, A. (1965). **Spectrophotometric characteristics of chlorophylls a and b and their pheophytins in ethanol**. Biochimica Et Biophysica Acta **109,** 448-453.

263) Reynolds, E.S. (1981). **The use of lead citrate at high pH as an electron-opaque stain in electron microscopy**. Current Contents/Life Sciences**,** 16-16.

264) Delatte, T., Trevisan, M., Parker, M.L., and Zeeman, S.C. (2006). ***Arabidopsis* mutants Atisa1 and Atisa2 have identical phenotypes and lack the same multimeric isoamylase, which influences the branch point distribution of amylopectin during starch synthesis. (vol 41, pg 815, 2005)**. Plant Journal **45,** 870-870.

265) Smith, A.M., and Zeeman, S.C. (2006). **Quantification of starch in plant tissues**. Nature Protocols **1,** 1342-1345.

266) Kunst, A., Draeger, B., and Ziegenhorn, J. (1988). in **Methods in Enzymatic Analysis** 3rd edn. Vol. 6 (ed. Bergmeyer, H.U.) 163–171 (Chemie, Weinheim, Germany).

267) Fulton, D.C., Stettler, M., Mettler, T., Vaughan, C.K., Li, J., Francisco, P., Gil, D., Reinhold, H., Eicke, S., Messerli, G., Dorken, G., Halliday, K., Smith, A.M., Smith, S.M., and Zeeman, S.C. (2008). **beta-AMYLASE4, a noncatalytic protein required for starch breakdown, acts upstream of three active beta-amylases in *Arabidopsis* chloroplasts**. Plant Cell **20,** 1040-1058.

268) Larkin, M.A., Blackshields, G., Brown, N.P., Chenna, R., McGettigan, P.A., McWilliam, H., Valentin, F., Wallace, I.M., Wilm, A., Lopez, R., Thompson, J.D., Gibson, T.J., and Higgins, D.G. (2007). **Clustal W and clustal X version 2.0**. Bioinformatics **23,** 2947-2948.

269) Rost, B., and Sander, C. (1993). **Prediction of protein secondary structure at better than 70% accuracy**. J Mol Biol **232,** 584-599.

270) Rost, B., Fariselli, P., and Casadio, R. (1996). **Topology prediction for helical transmembrane proteins at 86% accuracy**. Protein Sci **5,** 1704-1718.

271) Schwede, T., Kopp, J., Guex, N., and Peitsch, M.C. (2003). **SWISS-MODEL: an automated protein homology-modeling server**. Nucleic Acids Research **31,** 3381-3385.

272) Arnold, K., Bordoli, L., Kopp, J., and Schwede, T. (2006). **The SWISS-MODEL workspace: a web-based environment for protein structure homology modelling**. Bioinformatics **22,** 195-201.

273) Kopp, J., and Schwede, T. (2006). **The SWISS-MODEL repository: new features and functionalities**. Nucleic Acids Research **34,** D315-D318.

274) Kiefer, F., Arnold, K., Kuenzli, M., Bordoli, L., and Schwede, T. (2009). **The SWISS-MODEL Repository and associated resources**. Nucleic Acids Research **37,** D387-D392.

275) Cuff, J.A., and Barton, G.J. (2000). **Application of multiple sequence alignment profiles to improve protein secondary structure prediction**. Proteins **40,** 502-511.

276) Cole, C., Barber, J.D., and Barton, G.J. (2008). **The Jpred 3 secondary structure prediction server**. Nucleic Acids Research **36,** W197-W201.

277) Waterhouse, A.M., Procter, J.B., Martin, D.M.A., Clamp, M., and Barton, G.J. (2009). **Jalview Version 2-a multiple sequence alignment editor and analysis workbench**. Bioinformatics **25,** 1189-1191.

278) Rost, B. (1999). **Short yeast ORFs: expressed protein or not?** In CUBIC Preprint (New York: CUBIC, Dept. of Biochemistry & Molecular Biophysics, Columbia University, New York [http://www.rostlab.org/papers/pre1999_globe/].

279) Marchler-Bauer, A., Lu, S., Anderson, J.B., Chitsaz, F., Derbyshire, M.K., DeWeese-Scott, C., Fong, J.H., Geer, L.Y., Geer, R.C., Gonzales, N.R., Gwadz, M., Hurwitz, D.I., Jackson, J.D., Ke, Z., Lanczycki, C.J., Lu, F., Marchler, G.H., Mullokandov, M., Omelchenko, M.V., Robertson, C.L., Song, J.S., Thanki, N., Yamashita, R.A., Zhang, D., Zhang, N., Zheng, C., and Bryant, S.H. (2011). **CDD: a Conserved Domain Database for the functional annotation of proteins**. Nucleic Acids Research **39,** D225-D229.

280) Heazlewood, J.L., Tonti-Filippini, J., Verboom, R.E., and Millar, A.H. (2005). **Combining experimental and predicted datasets for determination of the subcellular location of proteins in *Arabidopsis***. Plant Physiology **139,** 598-609.

281) Heazlewood, J.L., Verboom, R.E., Tonti-Filippini, J., Small, I., and Millar, A.H. (2007). **SUBA: The *Arabidopsis* subcellular database**. Nucleic Acids Research **35,** D213-D218.

282) Heazlewood, J.L., Durek, P., Hummel, J., Selbig, J., Weckwerth, W., Walther, D., and Schulze, W.X. (2008). **PhosPhAt: a database of phosphorylation sites in *Arabidopsis thaliana* and a plant-specific phosphorylation site predictor**. Nucleic Acids Research **36,** D1015-D1021.

283) Durek, P., Schmidt, R., Heazlewood, J.L., Jones, A., MacLean, D., Nagel, A., Kersten, B., and Schulze, W.X. (2010). **PhosPhAt: the *Arabidopsis thaliana* phosphorylation site database. An update**. Nucleic Acids Research **38,** D828-D834.

284) Zimmermann, P., Hirsch-Hoffmann, M., Hennig, L., and Gruissem, W. (2004). **GENEVESTIGATOR. *Arabidopsis* microarray database and analysis toolbox**. Plant Physiology **136,** 2621-2632.

285) Obayashi, T., Nishida, K., Kasahara, K., and Kinoshita, K. (2011). **ATTED-II Updates: Condition-Specific Gene Coexpression to Extend Coexpression Analyses and Applications to a Broad Range of Flowering Plants**. Plant and Cell Physiology **52,** 213-219.

~ Appendix ~

Martinis et al. Plant Methods 2011, 7:23
http://www.plantmethods.com/content/7/1/23

PLANT METHODS

METHODOLOGY Open Access

A novel method for prenylquinone profiling in plant tissues by ultra-high pressure liquid chromatography-mass spectrometry

Jacopo Martinis[1], Felix Kessler[1] and Gaetan Glauser[2*]

Abstract

Background: Prenylquinones are key compounds of the thylakoid membranes in chloroplasts. To understand the mechanisms involved in the response of plants to changing conditions such as high light intensity, the comprehensive analysis of these apolar lipids is an essential but challenging step. Conventional methods are based on liquid chromatography coupled to ultraviolet and fluorescence detection of a single or limited number of prenylquinones at a time. Here we present an original and rapid approach using ultra-high pressure liquid chromatography-atmospheric pressure chemical ionization-quadrupole time-of-flight mass spectrometry (UHPLC-APCI-QTOFMS) for the simultaneous profiling of eleven prenylquinones in plant tissues, including α-tocopherol, phylloquinone, plastochromanol-8 and plastoquinone-9.

Results and discussion: Mass spectrometry and chromatography parameters were optimized using pure standards. Sample preparation time was kept to minimum and different extraction solvents were evaluated for yield, ability to maintain the redox state of prenylquinones, and compatibility with chromatography. In addition to precise absolute quantification of 5 prenyllipids for which standards were available, relative quantification of 6 other related compounds was possible thanks to the high identification power of QTOFMS. Prenylquinone levels were measured in leaves of *Arabidopsis* grown under normal and high light intensities. Quantitatively, the obtained results were consistent with those reported in various previous studies, demonstrating that this new method can profile the full range of prenylquinones in a very short time.

Conclusion: The new profiling method proves faster, more sensitive and can detect more prenylquinones than current methods based on measurements of selected compounds. It enables the extraction and analysis of twelve samples in only 1.5 h and may be applied to other plant species or cultivars.

Keywords: Prenylquinones, ultra-high pressure liquid chromatography, quadrupole-time-of-flight mass spectrometry, light stress, *Arabidopsis thaliana*

Background

The exposure to high light (HL) intensities is a normal event for plants growing under field conditions and represents a source of stress to the photosynthetic apparatus, both by direct photodamage and because of the formation of reactive oxygen species (ROS). Higher plants have evolved an array of mechanisms in order to dissipate the excess energy and protect themselves from potential damage. In addition to state transition and changes in chloroplast ultrastructure, leaves acclimate to variations in light conditions through the accumulation of various antioxidants and the turnover of key photosystem components and reduced electron carriers. Prenylquinones, in particular, play a fundamental role in this process and include molecules with a broad action spectrum [1]. Plastoquinone-9 and ubiquinone-9, for example, are the two main lipophilic electron carriers in chloroplasts and mitochondria, respectively. In chloroplasts, α-tocopherol (vitamin E) acts as the major antioxidant together with the reduced form of plastoquinone-9

* Correspondence: gaetan.glauser@unine.ch
[2]Chemical Analytical Service of the Swiss Plant Science Web, University of Neuchâtel, 2000 Neuchâtel, Switzerland
Full list of author information is available at the end of the article

and its derivative plastochromanol-8, protecting membranes from photoxidative stress [2-8]. Phylloquinone (Vitamin K_1), on the other hand, is also a strong antioxidant but its main biological role is as one-electron carrier in the A_1 site of photosystem I. Moreover, it has been demonstrated that in cyanobacteria phylloquinone can be replaced by plastoquinone-9 in the active site, but this does not occur in higher plants [9-11]. There is increasing evidence that prenylquinone metabolic pathways closely intersect [12] (Figure 1) and thus a suitable analytical technique enabling the detection of global and subtle changes in the profile of these thylakoid lipids is required. Most of the current methods for the analysis of prenylquinones are based on their extraction by an organic solvent followed by chromatographic analysis of selected molecules. However, the solvent choice may represent a major limiting factor for the extraction and chromatography efficiency. In addition to their variable extractive power related to the polarity of each molecule, some of the commonly used protic solvents may promote the spontaneous oxidation of the reduced forms of some lipids. The extraction protocol can also influence the stability and the redox state of the extracted molecules: in particular, reduced forms can be easily oxidized by atmospheric oxygen if samples are exposed to air or to high temperatures for a prolonged period of time. The separation and detection of the components of thylakoid membranes represents another key factor to obtain unambiguous lipid profiles. Recent methods are based on normal or reverse-phase high performance liquid chromatography (HPLC) coupled to ultraviolet and fluorescence detection [12-14]. These techniques require long running times (several dozens of minutes) to obtain sufficient resolution and the identification of lipid constituents relies on the availability of pure standards. Mass spectrometry, despite its high potential for the detection and identification of various apolar lipids [15], has been scarcely employed in combination with liquid chromatography for the analysis of prenyllipids in plants.

In this paper we propose a novel method for prenylquinone analysis using an optimized sample preparation procedure followed by ultra-high pressure liquid chromatography-atmospheric pressure chemical ionization-quadrupole time of flight mass spectrometry (UHPLC-APCI-QTOFMS). Compared to conventional HPLC, UHPLC uses sub-2 μm particle supports which allows for higher efficiency and optimal velocity [16,17]. Consequently, high throughput separations can be obtained by reducing column lengths and increased flow rates. The QTOF mass spectrometer is particularly well adapted to coupling with UHPLC thanks to its rapid scanning rate [18]. Moreover its high mass accuracy gives access to the determination of molecular formula, an essential feature for reliable compound identification. Different solvents were tested for their extraction yield, their ability to maintain the redox state of molecules as well as their compatibility with reverse-phase UHPLC as injection solvent. Chromatography and mass spectrometry parameters were optimized for speed, selectivity and sensitivity. The applicability of the developed method was illustrated with the simultaneous quantification of several prenylquinones in *Arabidopsis thaliana* grown under normal and high light conditions.

Results and Discussion

Optimization of MS conditions

While there have been several publications on the LC-MS analysis of tocopherols [19,20] and vitamin K homologues [21,22] as they are essential vitamins for human metabolism, we are not aware of any report for plastoquinone-9 (PQ-9) and plastochromanol-8 (PC-8). Thus different QTOFMS parameters were evaluated to obtain maximal sensitivity for these latter molecules together with α-tocopherol (α-T) and phylloquinone (K). Electrospray and APCI were compared in both positive and negative ionization modes using standard solutions at 1 μg/mL. For PQ-9, the oxidized form (PQ) was used as standard. APCI was found largely superior to electrospray for all four compounds. K, PQ and PC-8 gave similar responses in positive and negative APCI but α-T was much better ionized in negative mode (ca. 8-fold), which was thus selected for further experiments. We then tested the effect of the probe temperature on the ionization efficiency. While α-T and K gave a higher signal at lower temperatures (350-500°C), PC-8 and PQ were best ionized at higher temperatures (475-600°C). A temperature of 475°C was selected as the best compromise for the detection of the four compounds. The source cone voltage was varied from 15 to 50 V and the highest response was obtained at 40 V. Other source parameters such as corona current (18 μA), source temperature (120°C) and desolvation gas flow (800 L/hr) had a less important effect on the MS signal. The influence of the mobile phase composition on the ionization efficiency was evaluated. Methanol (MeOH), acetonitrile (ACN) and tetrahydrofuran (THF) were compared and MeOH gave the best signal for all compounds. For α-T and K, the intensity of MS responses in MeOH was 2-5 fold higher than in ACN or THF. For PQ and PC-8 it was 10-40 fold higher. MeOH was thus selected as the organic solvent of choice for further LC method development.

Optimization of LC conditions

Prenyllipids are traditionally separated by isocratic normal-phase chromatography using diol columns and very apolar solvents or by reverse-phase (RP) chromatography using octadecyl (C18) columns and mixtures of

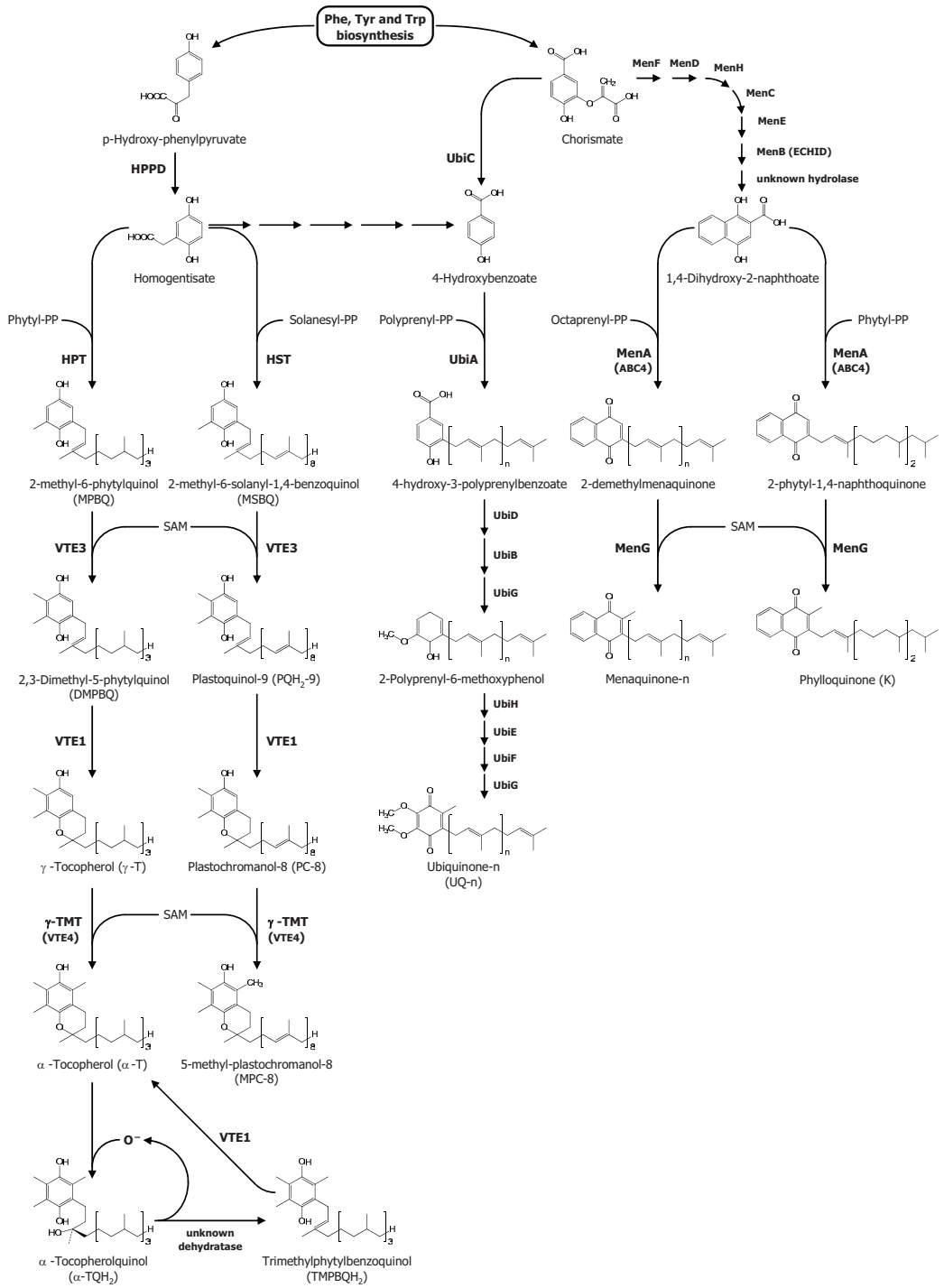

Figure 1 Biosynthetic pathways of tocopherol, plastoquinol, plastochromanol, ubiquinone, and phylloquinone in *Arabidopsis*.

MeOH/Ethanol or ACN/Ethanol as mobile phases. In RP mode, small amounts of hexane are sometimes used to accelerate the elution of PQ and PC-8 which are more hydrophobic than α-T and K. Run times are quite long (typically 20-40 min) because complete resolution of the peaks is needed for accurate quantification by ultraviolet and fluorescence detection. Using MS as a detector however, resolution becomes less important and chromatographic separations can often be shortened. In this study, UHPLC coupled to QTOFMS detection was evaluated for the high throughput analysis of prenyllipids. A 50 × 2.1 mm C18 column filled with

1.7 μm particles was selected for the separation. We first tested an isocratic 100% MeOH mobile phase at 25°C. Adequate retention factors (k) were obtained for α-T (k = 2.3) and K (k = 3.9), but PC-8 (k = 11.7) and PQ (k = 17) were too strongly retained leading to broad peaks and a decrease in sensitivity (Figure 2A). Since the use of MeOH as organic solvent was a required condition for MS sensitivity, we could not replace it by a solvent of higher eluting power. An alternative option to decrease the retention of PC-8 and PQ was to increase the temperature of the column. At 60°C, the retention factors for PC-8 and PQ were reduced to appropriate values, respectively 4.5 and 6.3. Meanwhile, the retention for α-T and K became slightly too weak with k values of 1.1 and 1.9 respectively (Figure 2B). To overcome this issue, a 1.5 min gradient from H_2O/MeOH (10:90, v/v) to 100% MeOH was implemented at the beginning of the run followed by a hold at 100% MeOH for 2.5 min. Using this optimized separation, all compounds of interest eluted between 0.9 and 2.5 min and gave symmetrical and sharp peak shapes (Figure 2C). We verified that no thermal degradation occurred at 60°C. Although prenyllipids are neutral molecules and their retention times are not likely to be affected by a possible change in pH, we also tested the impact of mobile phase additives such as formic acid in terms of retention and ionization efficiency. As expected, no change in retention times was observed. On the contrary, the ionization efficiency was reduced by one order of magnitude for K and PQ, and more than two orders of magnitude for α-T and PC-8. This is not surprising since strong gas phase acids suppress proton transfers in negative APCI. It was found that even the injection of an acidic solution of standards could slightly reduce the ionization efficiency of α-T even if mobiles phases without additive were used. For this reason it is recommended to remove any trace of formic acid in the system, including the injector wash lines (if partial loop mode is employed), before prenyllipids are analyzed. Acids are also frequently used for lipid extractions in order to inhibit enzymatic hydrolysis. In the case of prenyllipids, this should be avoided.

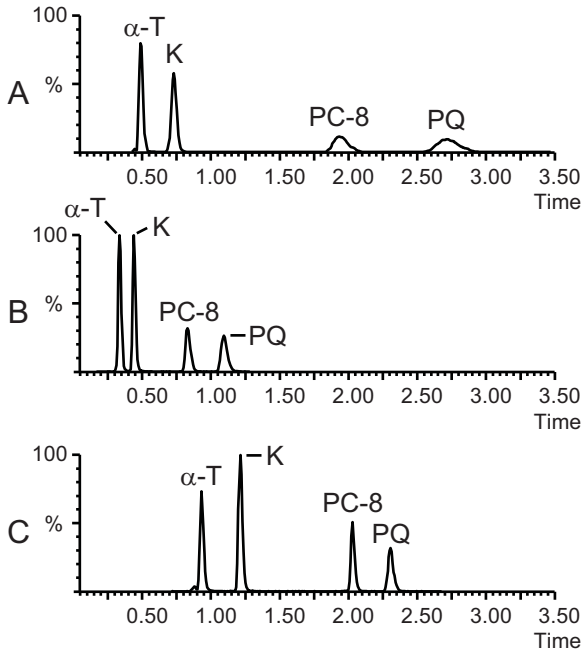

Figure 2 Optimization of the chromatographic separation using pure standards. A. Isocratic MeOH 100% as a mobile phase, T = 25°C. B. Isocratic MeOH 100% as a mobile phase, T = 60°C. C. Optimized gradient H_2O/MeOH (10:90, v/v) - MeOH 100% in 1.5 min, followed by MeOH 100% for 2.5 min, T = 60°C. Other conditions are given in Materials and Methods. α-T, α-tocopherol; K, phylloquinone; PC-8, plastochromanol-8; PQ: plastoquinone-9 (oxidized form).

Detection of prenylquinones in plant samples

To evaluate the performance of the developed UHPLC-APCI-QTOFMS method on biological samples, we extracted *Arabidopsis* plants grown under normal and high light conditions in a mixture of chloroform/methanol ($CHCl_3$/MeOH, 30:70, v/v). α-T, K, PC-8, and the oxidized (PQ) and reduced (PQH_2) forms of PQ-9 were easily detected. The presence of PQH_2 was confirmed by reducing the PQ standard with sodium borohydride and analyzing the resulting mixture. For these 5 molecules, positive identification was achieved based on the comparison of retention times and accurate masses with pure available standards. In addition, the QTOFMS allowed for the tentative identification of six other prenyllipids for which no standard was available, namely γ-tocopherol (γ-T), α-tocopherol quinone (α-TQ), hydroxyplastochromanol (PC-OH), hydroxyplastoquinone (PQ-OH) and the oxidized (UQ) and reduced (UQH_2) forms of ubiquinone-9 (UQ-9). UHPLC-APCI-QTOFMS data acquired in negative and positive APCI for the identified prenyllipids are presented in Table 1.

Optimization of sample preparation

The above used extraction solvent ($CHCl_3$/MeOH, 30:70 v/v) seemed to efficiently extract prenyllipids. However it had a serious drawback: $CHCl_3$ is chemically poorly compatible with the UHPLC system used which can accommodate all common solvents except chlorinated solvents. We therefore evaluated different extraction solvents based on the three following criteria: extraction yield for the prenylquinones, ability to maintain the redox state of PQ/PQH_2 and UQ/UQH_2, and compatibility with UHPLC in terms of peak broadening and chemical resistance. A preliminary condition was to avoid an evaporation-redissolution step which would

Table 1 Prenylquinones identified from UHPLC-APCI-QTOFMS data acquired in negative and positive ionization modes

No	RT (min)	APCI -	m/z (-)	APCI +	m/z (+)	formula	MS/MS (-)	Identification
1	0.76	$(M)^-$	446.3763	-[a]	-[a]	$C_{29}H_{50}O_3$	177.0919, 163.0764	α-tocopherol-quinone
2	0.92	$(M-H)^-$	415.3575	-[a]	-[a]	$C_{28}H_{48}O_2$	149.0605, 121.0655	γ-tocopherol
3	1.00	$(M-H)^-$	429.3734	$(M+H)^+$	431.3877	$C_{29}H_{50}O_2$	163.0760, 135.0812	α-tocopherol
4	1.28	$(M)^-$	450.3504	$(M+H)^+$	451.3572	$C_{31}H_{46}O_2$	210.0680, 185.0607	phylloquinone
5	1.52	$(M-H)^-$	765.6183	-[a]	-[a]	$C_{53}H_{81}O_3$	750.5956, 149.0608	hydroxyplastochromanol
6	1.71	$(M)^-$	764.6102	-[a]	-[a]	$C_{53}H_{80}O_3$	149.0604	hydroxyplastoquinone
7	1.72	$(M-2H)^-$	748.6158	$(M+H)^+$	751.6385	$C_{53}H_{82}O_2$	188.0836, 149.0605	plastoquinol
8	1.89	$(M-2H)^-$	794.6214	$(M+H)^+$	797.6448	$C_{54}H_{84}O_4$	779.5970, 219.0661	ubiquinol
9	2.12	$(M-H)^-$	749.6227	$(M+H)^+$	751.6395	$C_{53}H_{82}O_2$	734.6009, 149.0608	plastochromanol-8
10	2.16	$(M)^-$	794.6212	$(M+H)^+$	795.6300	$C_{54}H_{82}O_4$	779.5974, 219.0655	ubiquinone
11	2.43	$(M)^-$	748.6152	$(M+H)^+$	749.6232	$C_{53}H_{80}O_2$	188.0841, 149.0606	plastoquinone

[a], not detected. RT, retention time. Known chemical structures are available in Figure 1.

lengthen the sample preparation and possibly alter PQ/PQH_2 and UQ/UQH_2 redox ratios. Plants exposed to HL intensity (500 $\mu E \cdot m^{-2} \cdot s^{-1}$) were pooled and lipids were extracted using MeOH, isopropanol (IPA), ethylacetate (EtAC), THF and $CHCl_3$/MeOH (30:70, v/v) as control and further analyzed by UHPLC-APCI-QTOFMS (n = 4). A principal component analysis (PCA) was performed on the obtained data. Interestingly, the five solvents clustered separately (Figure 3) and showed a significant selectivity for different molecules. In general, polar lipids including α-TQ were extracted more efficiently using MeOH, while more apolar solvents showed a higher extractive power for apolar prenyllipids (e.g. PQ and UQ). For all prenylquinones, the highest extraction yield was obtained with $CHCl_3$/MeOH (30:70, v/v) and THF, while it was lower for EtAc and IPA (Figure 4A-F). MeOH represented a separate case because of its higher polarity, resulting in poor ability to extract PQ-9 and PC-8. Therefore MeOH is not a suitable solvent for PQ-9 and PC-8 analysis (Figure 4D and 4E).

Spontaneous variations in PQ/PQH_2 ratio under standard working conditions were determined in the five solvents using a purified PQ standard. No spontaneous reduction was detected (*data not shown*). Moreover, when spiking PQ in leaf extracts, no increase in PQH_2 was observed, suggesting that the reducing agents present in plant tissues are not concentrated enough to promote reduction. However, when ascorbic acid (30 mM) or butyl hydroxytoluene (BHT, 0.05%) were added to PQ solutions prepared in the different solvents, a slight reduction of PQ was observed (about 3% and 1% of the original amount of PQ using ascorbic acid or BHT, respectively). This phenomenon has previously been observed [13]. While anti-oxidant agents are often added to extraction experiments to prevent lipid peroxidation, this procedure does not appear useful for the determination of the redox state of PQ since reduction of the oxidized form may occur. When the PQ standard was chemically reduced with sodium borohydride and then exposed to air at room temperature, an increase of the oxidized form was detected for all solvents starting from 5-7 h after reduction. As a consequence, for the solvent to be effective in maintaining the original PQ/PQH_2 ratio, it needs to oxidize the PQH_2 present in plant tissues as little as possible. Using $CHCl_3$/MeOH (30:70, v/v), IPA and THF, a PQH_2/PQ_{TOT} ratio ≥ 0.5 was found in plants exposed to HL conditions, while EtAc led to a PQH_2/PQ_{TOT} ratio of only 0.3 (Figure 4D). This may be due to lower extraction yield for PQH_2 in EtAc rather than oxidation of PQH_2 into PQ. Interestingly, when plants grown under normal light intensity (150 $\mu E \cdot m^{-2} \cdot s^{-1}$) were extracted in IPA, a complete oxidation of PQH_2 was observed, while this did not happen in samples extracted by $CHCl_3$/MeOH (30:70, v/v) and THF (*data not shown*). This may be explained by the higher amount of antioxidants (tocopherols or other lipid-soluble molecules) naturally present in thylakoid membranes under HL conditions, which could have protected PQH_2 from spontaneous oxidation in IPA. A similar profile was observed for UQ-9 (Figure 4F).

The influence of the extraction solvents on the chromatographic performance was also evaluated. Indeed, it is well-known that injection solvents of higher elution strength than the initial mobile phase can lead to peak distortion and broadening, in particular for early eluting peaks. No significant peak broadening was observed for MeOH, $CHCl_3$/MeOH (30:70, v/v) and IPA (Figure 5A-C). Using THF, which is a stronger solvent, γ-T, α-T and K exhibited moderate peak broadening (Figure 5D). Not surprisingly, EtAc was the most problematic

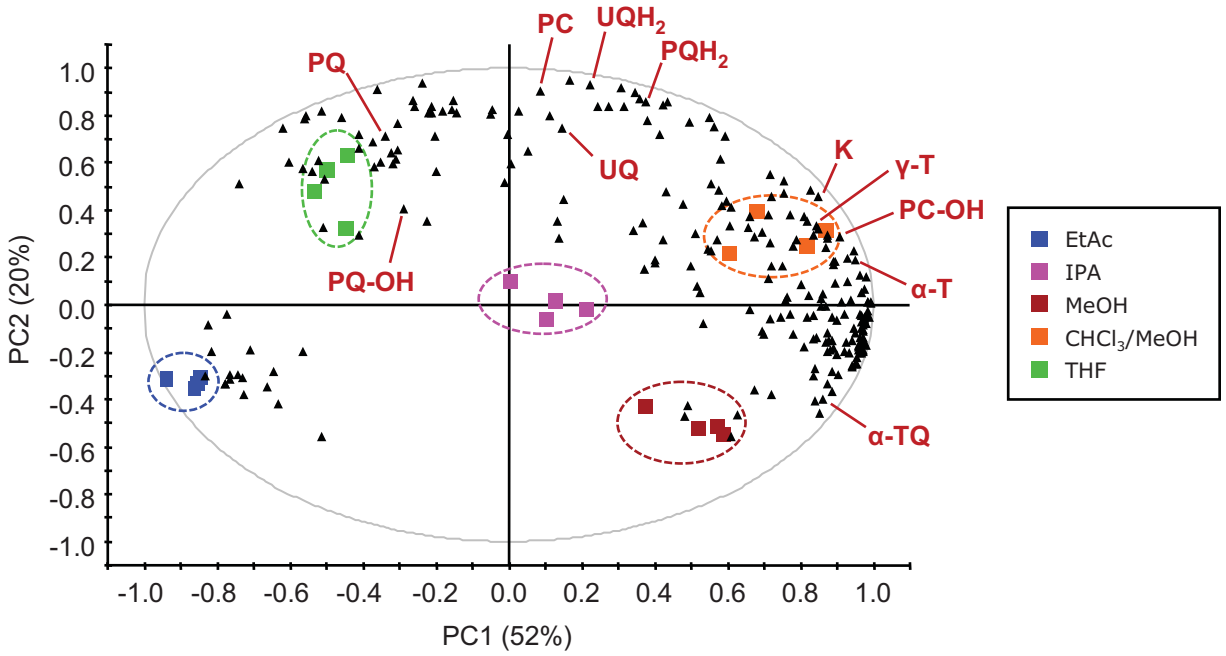

Figure 3 Bi-plot derived from a principal component analysis (PCA) showing the selectivity of the extraction solvent. Plants exposed to high light were pooled and extracted using the indicated solvents. Colored squares correspond to the observations (n = 4 for each solvent) and black triangles represent the variables. PC1 and PC2 are first and second principal components, respectively, with their percentage of explained variance. The identified prenyllipids are indicated (confront with Table 1). For abbreviations, see text.

solvent: strong peak distortion was observed for γ-T, α-T and K and even PQH_2 was affected (Figure 5E). We then diminished the injection volume from 5 to 2.5 μL, which substantially reduced peak broadening for THF but only slightly for EtAc (*data not shown*). In conclusion, 2.5 μL injections of solvents equally or more polar than THF could be used without negative effect on the chromatographic performance under the used conditions.

Overall, THF represented a good alternative to $CHCl_3$/MeOH (30:70, v/v) since it provided high and reproducible extraction yields, best maintained the redox state of PQ-9 and UQ-9, and was chromatographically compatible. It was thus selected as the solvent of choice for the extraction of biological samples. To determine whether the volume of extraction solvent (500 μL THF for 100 mg of fresh leaf material) was sufficient for extracting most of the prenylquinones, we extracted leaves exposed to HL in 1500 μL or 500 μL (for the latter, the extract was further diluted three times) and extraction yields were compared (n = 3). No significant difference was found, confirming that a volume of 500 μL is sufficient for the extraction of 100 mg of fresh leaves. We noticed that the oxidation of PQH_2 became significant about 2 and 5 hours after extraction for plants grown under normal and high light conditions respectively. For this reason, we took good care to always prepare and analyze samples within a maximum period of 1.5 hours. Given the speed of both extraction and analysis, 12 samples can be processed during that period of time. By performing sample preparation and analyses in parallel, a throughput of 100 samples in 8 h could be potentially achieved.

Extraction recovery, matrix effects and limits of quantification

To evaluate sample preparation recovery, two experiments were carried out: first pure standards of α-T, K, PC and PQ were submitted to the extraction procedure. Recovery greater than 95% was obtained for all molecules. To determine if the plant matrix had an impact on the recovery, decyl-plastoquinone was used as non-endogenous structural analogue and spiked before and after extraction of plant samples at identical concentration. Again a recovery greater than 95% was obtained.

APCI is usually less prone to matrix effects than electrospray because ionization occurs in the gas phase. We nevertheless checked if prenyllipids were subjected to suppression or enhancement effects from the *Arabidopsis* extract. Since these molecules are endogenous in *Arabidopsis*, a THF extract was prepared and an aliquot was spiked with standard solutions of each prenyllipid. The control extract (C), the standard solutions (SS) and the spiked extract (SE) were injected and the obtained

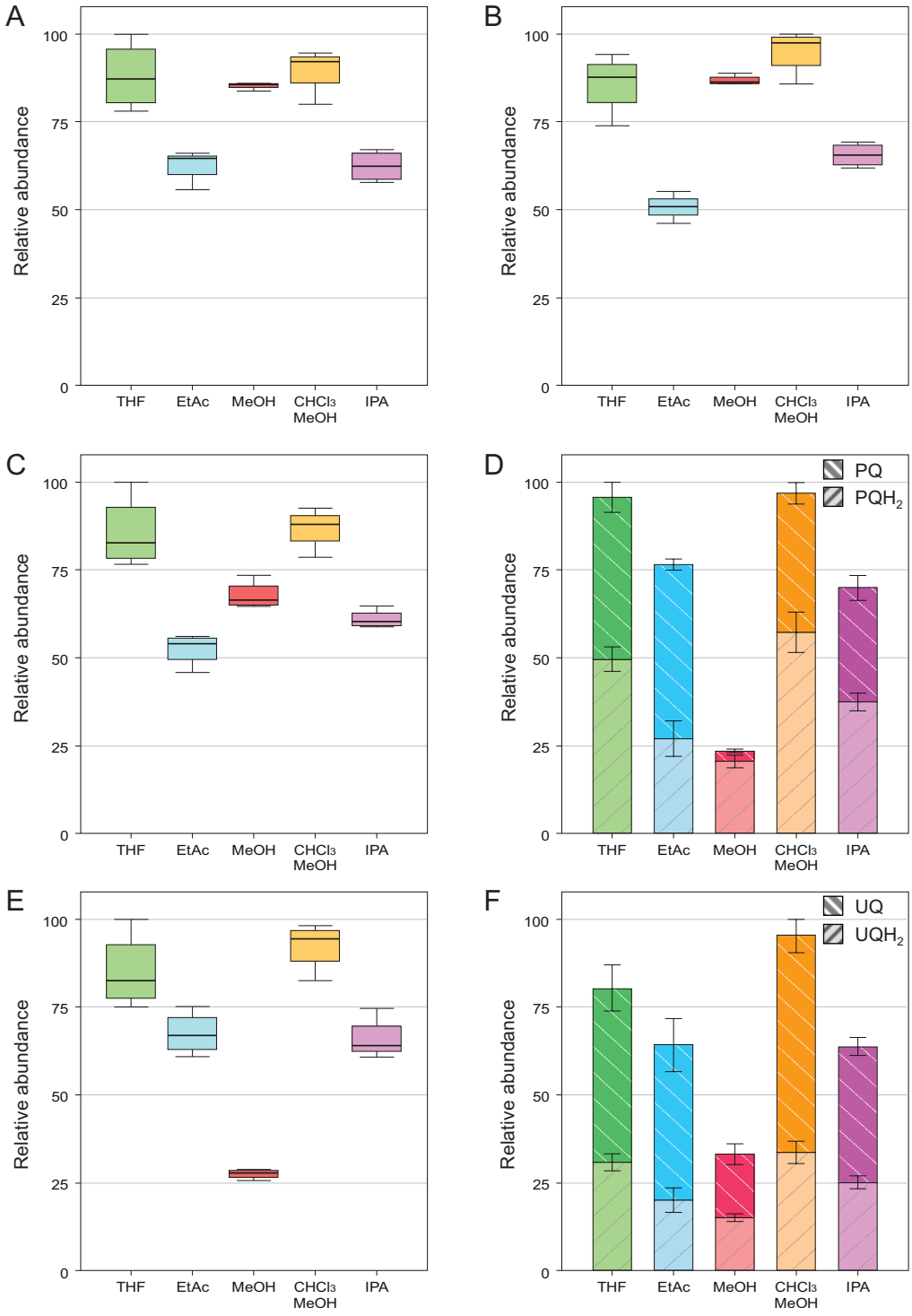

Figure 4 Comparison of the extraction yields for prenylquinones with the five selected solvents. A. γ-tocopherol. B. α-tocopherol. C. Phylloquinone. D. Plastoquinone-9, oxidized (PQ) and reduced (PQH_2) forms. E. Plastochromanol-8. F. Ubiquinone-9, oxidized (UQ) and reduced (UQH_2) forms. Plants exposed to high light were pooled and lipids were extracted using the indicated solvents. Data are from 4 replicates (± SD). For PQ-9 (D) and UQ-9 (F) the ability to maintain the redox state was also evaluated.

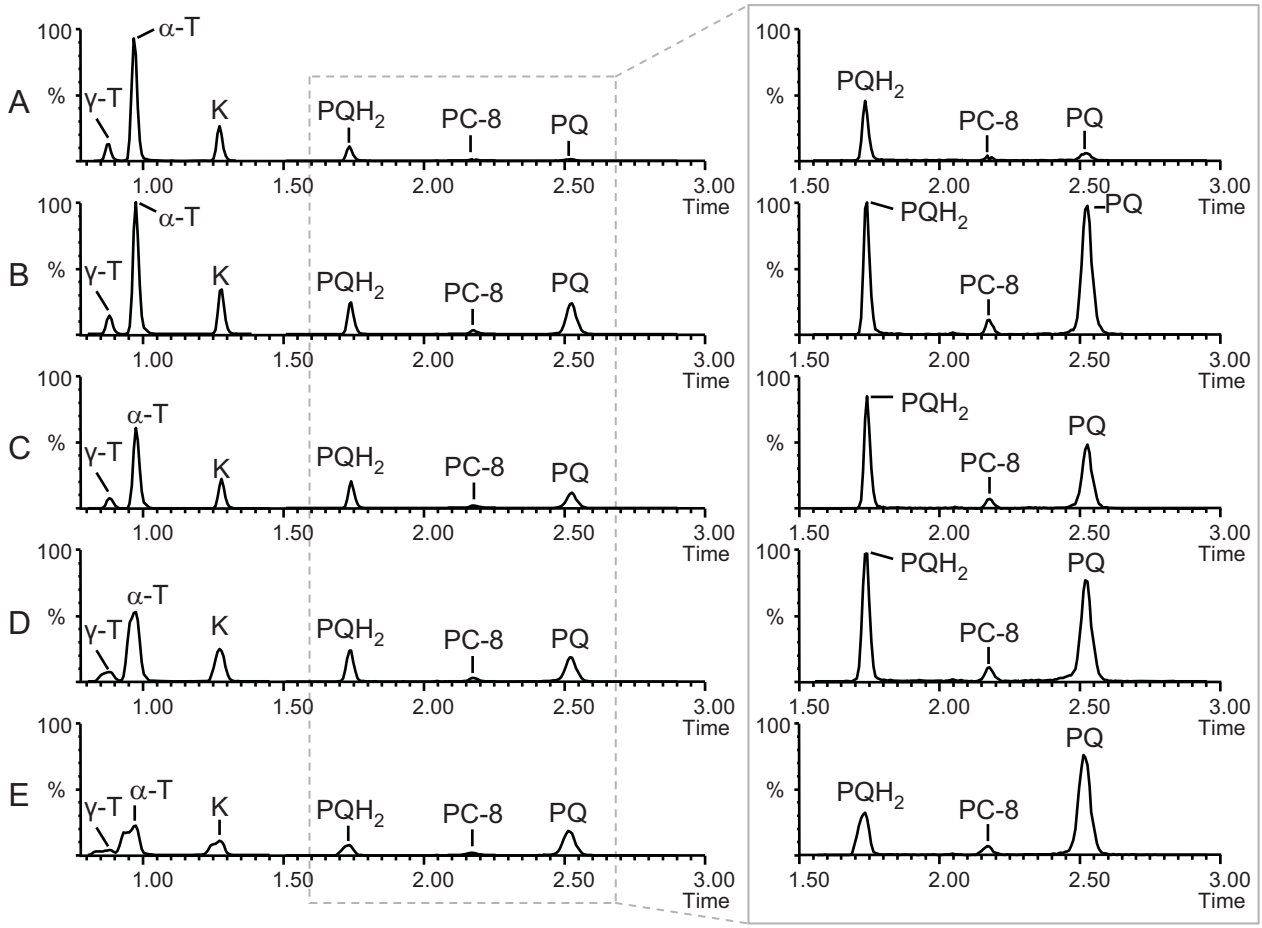

Figure 5 Extracted ion chromatograms illustrating the influence of the five extraction solvents on the chromatographic performance. A. MeOH 100%. B. $CHCl_3$/MeOH (30:70, v/v). C. IPA. D. THF. E. EtAc. Plants exposed to high light were pooled and extracted using the indicated solvents. 5 μL was injected. Inset on the right: zoom on the peaks corresponding to PQ/PQH_2 and PC-8. γ-T, γ-tocopherol; α-T, α-tocopherol; K, phylloquinone; PC-8, plastochromanol-8; PQ: plastoquinone-9 (oxidized); PQH_2: plastoquinone-9 (reduced).

area compared. For all the ions, the area of C+SS were equivalent to those of SE with a variation inferior to 5%. In other words, no significant matrix effect was observed for the analyzed compounds.

The quantification of prenyllipids was based on internal standard calibration. Decyl-plastoquinone was found suitable as an internal standard: it was structurally close to the studied prenylquinones, was readily detected in negative APCI with high selectivity (M^- ion at *m/z* 276.2087), eluted within the chromatographic gradient (retention time 0.44 min), and no matrix effect was observed. For α-T, PQ and PC-8, five calibrations points were used (0.05, 0.2, 1.0, 2.0, and 10.0 μg/mL for α-T; 0.05, 0.2, 1.0, 2.0, and 5.0 μg/mL for PQ-9 and PC-8). When PQ was completely reduced using sodium borohydride, the peak corresponding to PQH_2 had an identical area to that of PQ. As a result, PQH_2 could be quantified based on PQ calibration curve. For K, whose concentration does not significantly change after HL treatment, only four calibration points were used (0.1, 0.25, 1.0, and 2.5 μg/mL). For all compounds the response was linear over the range of the chosen concentrations with coefficients of determination > 0.99. A signal-to-noise ratio (s/n) of 10 was defined as limit of quantification (LOQ). For α-T, K and PC-8, the LOQ was 20 ng/mL. For PQ-9, an LOQ of 10 ng/mL was attained. The other identified prenyllipids (see Table 1) for which no pure standard was available were relatively quantified.

Effect of high light on prenylquinone profile

HL exposure induces biochemical and physiological changes in plants. In order to provoke a strong effect on prenyllipid content, 4 to 5-week-old *Arabidopsis thaliana* (Columbia-0) plants were exposed to continuous HL intensity for a prolonged period of time (7 days) and their prenyllipid profiles were compared to those obtained from plants grown under normal light. Under

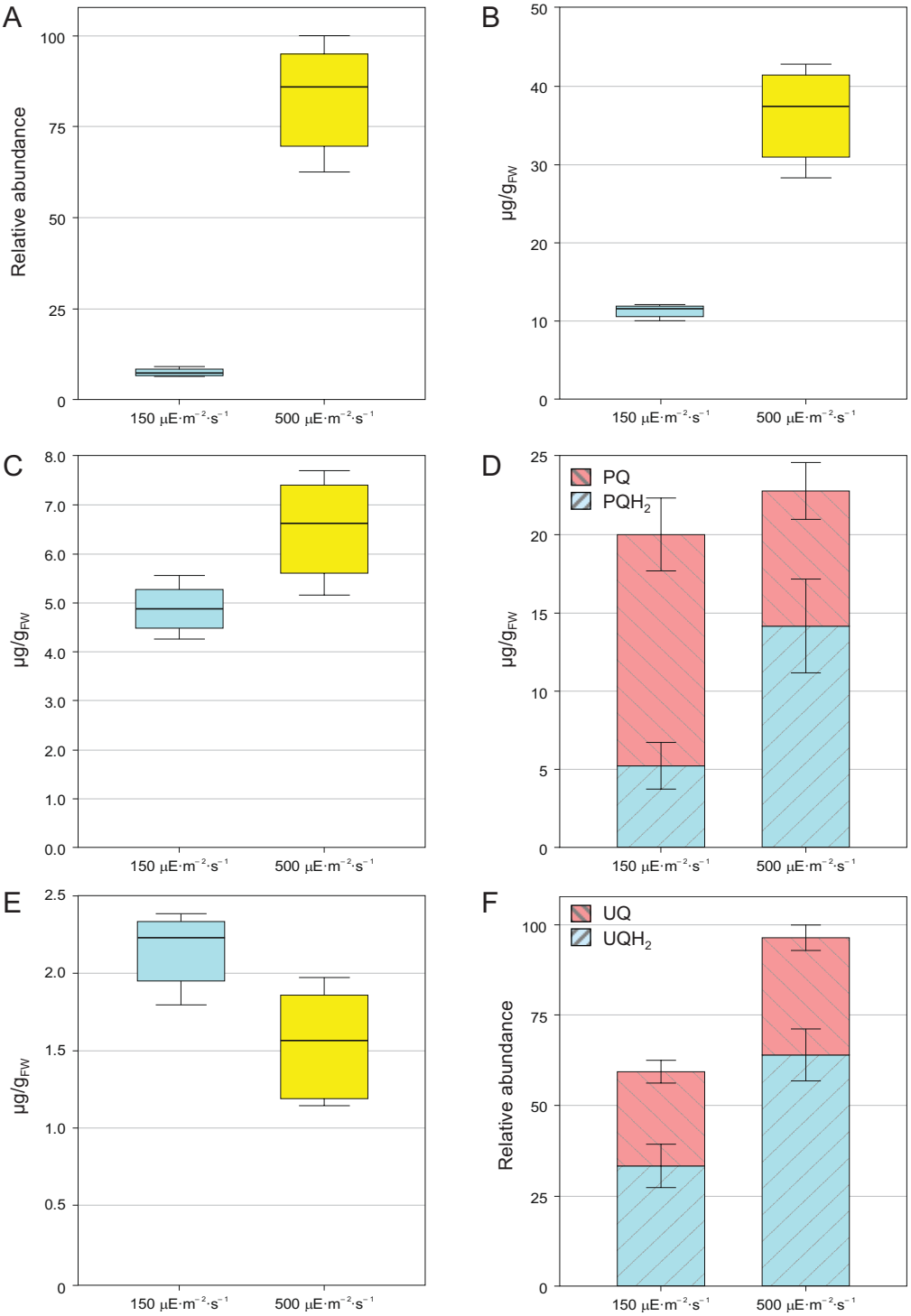

Figure 6 Effect of HL exposure on the total leaf content of prenylquinones. A. γ-tocopherol. B. α-tocopherol. C. Phylloquinone. D. Plastoquinone-9, oxidized (PQ) and reduced (PQH_2) forms. E. Plastochromanol-8. F. Ubiquinone-9, oxidized (UQ) and reduced (UQH_2) forms. Plants exposed to normal (150 µE × m^{-2} × s^{-1}) or high (500 µE × m^{-2} × s^{-1}) light intensities were extracted using THF. Data are from 4 biological replicates (± SD). For PQ-9 (D) and UQ-9 (F) the redox state of the total leaf pool was taken into account.

HL conditions γ- and α-tocopherol levels increased 8-fold and 3.5-fold respectively (Figure 6A and 6B). The synthesis of tocopherols and their accumulation in thylakoid membranes and plastoglobules is a well-known phenomenon which has been demonstrated to occur in response to oxidative stress [4,5]. After exposure to HL conditions plants produce more α-tocopherol, which mitigates photosystem II photoinactivation and protects thylakoids from photooxidative damage under chilling conditions [6,23]. No significant variation in phylloquinone levels was observed under HL (Figure 6C). As a matter of fact, even though its absence in plants lacking key enzymes in vitamin K biosynthetic pathway affects photosystem I activity [9], no direct evidence of its accumulation under HL has been reported [4]. In the future, we will apply this new method to profile simultaneously several tocochromanols/prenylquinones and assess the roles of each of them under various conditions.

Concerning plastoquinone-9, 4-week-old *A. thaliana* plants grown under normal light conditions showed a PQH_2/PQ_{TOT} ratio of about 0.25, in agreement with a previous study by Szymanska *et al.* [24] that used plants of similar age and a different method for prenyllipids extraction. After continuous HL exposure, plastoquinone-9 total content (oxidized + reduced) did not seem to be significantly altered. Yet, the redox state of the electron acceptor pool changed, with a significant accumulation of the reduced form (PQH_2), leading to a PQH_2/PQ_{TOT} ratio of 0.6 (Figure 6D). This result suggests that the accumulation of PQH_2 under HL may not be due to the *de novo* synthesis of the latter but on the reduction of the already available PQ pool. While these findings are distinct from the increase in PQH_2 synthesis reported by Szymanska *et al.* [24], this discrepancy may well be attributed to the different growth and light conditions or to the different reference units employed (μg/g fresh weight versus μg/mg chlorophyll).

Among the other prenyllipids identified, plastochromanol-8 levels did not significantly change when plants were exposed to HL (Figure 6E), while total ubiquinone-9 content increased about 1.5-fold. Moreover, the $UQH2/UQ_{TOT}$ ratio increased in response to the change in light conditions (Figure 6F), as previously observed by Yoshida *et al.* [14].

Conclusion

The presented method introduces for the first time the use of UHPLC-APCI-QTOFMS for simultaneously profiling several prenylquinones in plants. It proves to be fast, reliable, very selective and sensitive for the analyzed molecules, and consume less solvent than conventional methods. By combining it with simple and rapid sample preparation, a single plant can be extracted and analyzed in less than 15 min and twelve samples can be processed in 90 min. Moreover it allows for the detection and tentative identification of molecules for which no pure standard is available. The developed method will be used to profile prenylquinones in various *Arabidopsis* mutants as well as in other commercially relevant crop species.

Methods

Chemicals

The solvents used for extraction were methanol (MeOH, HPLC grade, Chromanorm), chloroform ($CHCl_3$, analytical grade, Normapur) and tetrahydrofuran (THF, analytical grade, Normapur) from VWR (Leuven, Belgium), isopropanol (IPA, HPLC grade) and ethylacetate (EtAc, analytical grade) from Acros Organics (Geel, Belgium). ULC/MS grade MeOH and water from Biosolve (Valkenswaard, The Netherlands) were used for the UHPLC-APCI-QTOFMS analyses.

α-T and K standards of HPLC grade (≥ 99.5%) were purchased from Sigma-Aldrich (Steinheim, Germany). Decyl-plastoquinone (~75%) was obtained from Sigma-Aldrich. PQ-9 and PC-8 standards were provided by Jerzy Kruk (Jagiellonian University, Kraków, Poland). The oxidized and reduced PQ-9 standards were obtained as described in [25] with slight changes. Briefly, an excess (1 μg) of sodium borohydride (Fluka, Buchs, Switzerland) was added to the oxidized PQ standard (100 ng) to completely reduce it to PQH_2. The retention time of both forms was then determined by UHPLC-APCI-QTOFMS. Ascorbic acid was purchased from Carl Roth (Karlsruhe, Germany) and butyl hydroxytoluene (BHT) from Sigma-Aldrich.

Plant material and treatments

Arabidopsis thaliana (Columbia-0) plants were grown on soil under standard growth conditions (150 $\mu E \cdot m^{-2} \cdot s^{-1}$, 8/16 h light/dark period, 21/18°C, 55% relative air humidity) according to the protocol described in [26] with slight modifications. HL treatment was performed on 4- to 5-week-old rosettes by exposure to continuous HL conditions (500 $\mu E \cdot m^{-2} \cdot s^{-1}$, 21°C, 55% relative air humidity) for 1 week in a PGC 6HID growth chamber (Percival Scientific, Boone, IA) equipped with 400 W metal halide lamps (Philips).

Prenyllipid extraction

Arabidopsis leaves from 4- to 5-week-old rosettes were ground in a mortar with liquid nitrogen. Approximately 100 mg of leaf material was then exactly weighed, transferred to a 1.5 mL microcentrifuge tube (Eppendorf, Hamburg, Germany) and swiftly re-suspended in five volumes of the selected solvent (e.g. 500 μL for 100 mg) containing decylplastoquinone at 2 μg/mL as internal standard. Care was taken that no thawing occurred

before the solvent was added. Glass beads of about 1 mm of diameter (Assistent, Sontheim, Germany) were added and samples were further homogenized for 3 min at 30 Hz in a tissue lyser (Retsch MM 300, Haan, Germany). Tubes were centrifuged on a benchtop centrifuge (14,000 × g for 3 min at 4°C) and 400 μL of supernatant was then transferred to an appropriate glass vial for immediate UHPLC-QTOFMS analysis.

Liquid chromatography-mass spectrometry analysis

The LC-MS system consisted of a Waters Acquity UPLC™ (Milford, MA) coupled to a Waters Synapt G2 MS QTOF equipped with an atmospheric pressure chemical ionization (APCI) source. Prenyllipids were separated on an Acquity BEH C18 column (50 × 2.1 mm, 1.7 μm) under the following conditions: Solvent A = water; Solvent B = MeOH; 90-100% B in 1.5 min, 100% B for 2.5 min, re-equilibration at 90% B for 0.5 min. The flow rate was 800 μL/min and the injection volume was 2.5 μL. The temperature of the column was set to 60°C and the autosampler chamber was kept at 15°C. Data were acquired with a scan time of 0.4 s over an *m/z* range of 225-1200 in the negative ion MS mode. The corona current was set to 18 μA and the cone voltage to 40 V. The source temperature was maintained at 120°C and the APCI probe temperature at 475°C. The desolvation gas flow was set to 800 L/hr. The mobile phase was diverted to waste for 0.3 min at the beginning of the gradient. Accurate mass measurements were obtained by infusing a 400 ng/mL solution of the small peptide leucin-enkephalin at a flow rate of 10 μL/min through the Lock Spray™ probe. For the identification of prenyllipids, positive and negative ion MS/MS experiments were carried out using a fixed collision energy of 40 eV and argon as collision gas at a flow of 2.1 mL/min. The quadrupole LM resolution was 4.7, and the HM resolution was 15. MS/MS product ion spectra were acquired over the *m/z* range 50-1200. Absolute quantities of prenyllipids were determined using standard curves obtained from standard compounds. The concentrations of the calibration points for α-T were 0.05, 0.2, 1.0, 2.0, and 10.0 μg/mL, for PQ-9 and PC-8 0.05, 0.2, 1.0, 2.0, and 5.0 μg/mL. For K, the concentrations were 0.1, 0.25, 1.0, and 2.5 μg/mL. All standard solutions contained decylplastoquinone (internal standard) at a concentration of 2 μg/mL.

Data treatment

Data were processed using Masslynx v4.1 (Waters). Multivariate analysis was carried out using MarkerLynx XS™ (Waters). The following parameters were used: initial and final retention times 0.7-3.0 min, mass range *m/z* 225-1200 Da, mass tolerance 0.03 Da, retention time window 0.10 min, automatic peak width detection, intensity threshold 1000 counts. The deisotope filtering function was applied. Non-normalized peak areas were generated. Variables were UV-scaled before applying PCA.

Acknowledgements

We thank Jerzy Kruk for kindly providing purified plastoquinone-9 and plastochromanol-8 standards. GG acknowledges support from the Swiss Plant Science Web. FK was supported by UniNE, SystemsX PGCE, NCCR Plant Survival and SNF 31003A_127380.

Author details

[1]Laboratory of Plant Physiology, University of Neuchâtel, 2000 Neuchâtel, Switzerland. [2]Chemical Analytical Service of the Swiss Plant Science Web, University of Neuchâtel, 2000 Neuchâtel, Switzerland.

Authors' contributions

JM grew, collected, and extracted plants. GG developed the UHPLC-APCI-QTOFMS method and conducted measurements. JM and GG carried out the optimization of the sample preparation, performed data analysis and treatment. GG and JM wrote the manuscript. FK contributed to the writing of the manuscript. All authors conceived the study. All authors read, commented and approved the final manuscript.

Competing interests

The authors declare that they have no competing interests.

Received: 19 May 2011 Accepted: 21 July 2011 Published: 21 July 2011

References

1. Nowicka B, Kruk J: **Occurrence, biosynthesis and function of isoprenoid quinones.** *BBA-Bioenergetics* 2010, **1797**:1587-1605.
2. Mene-Saffrane L, Jones AD, DellaPenna D: **Plastochromanol-8 and tocopherols are essential lipid-soluble antioxidants during seed desiccation and quiescence in Arabidopsis.** *P Natl Acad Sci USA* 2010, **107**:17815-17820.
3. Kobayashi N, DellaPenna D: **Tocopherol metabolism, oxidation and recycling under high light stress in Arabidopsis.** *Plant J* 2008, **55**:607-618.
4. Lichtenthaler HK: **Biosynthesis, accumulation and emission of carotenoids, alpha-tocopherol, plastoquinone, and isoprene in leaves under high photosynthetic irradiance.** *Photosynth Res* 2007, **92**:163-179.
5. Krieger-Liszkay A, Trebst A: **Tocopherol is the scavenger of singlet oxygen produced by the triplet states of chlorophyll in the PSII reaction centre.** *J Exp Bot* 2006, **57**:1677-1684.
6. Havaux M, Eymery F, Porfirova S, Rey P, Dormann P: **Vitamin E protects against photoinhibition and photooxidative stress in *Arabidopsis thaliana*.** *Plant Cell* 2005, **17**:3451-3469.
7. Kruk J, Trebst A: **Plastoquinol as a singlet oxygen scavenger in photosystem II.** *BBA-Bioenergetics* 2008, **1777**:154-162.
8. Szymanska R, Kruk J: **Identification of hydroxy-plastochromanol in Arabidopsis leaves.** *Acta Biochim Pol* 2010, **57**:105-108.
9. Lohmann A, Schottler MA, Brehelin C, Kessler F, Bock R, Cahoon EB, Dormann P: **Deficiency in phylloquinone (vitamin K-1) methylation affects prenyl quinone distribution, photosystem I abundance, and anthocyanin accumulation in the Arabidopsis *AtmenG* mutant.** *J Biol Chem* 2006, **281**:40461-40472.
10. Shimada H, Ohno R, Shibata M, Ikegami I, Onai K, Ohto M, Takamiya K: **Inactivation and deficiency of core proteins of photosystems I and II caused by genetical phylloquinone and plastoquinone deficiency but retained lamellar structure in a T-DNA mutant of Arabidopsis.** *Plant J* 2005, **41**:627-637.
11. Johnson TW, Shen GZ, Zybailov B, Kolling D, Reategui R, Beauparlant S, Vassiliev IR, Bryant DA, Jones AD, Golbeck JH, Chitnis PR: **Recruitment of a foreign quinone into the A(1) site of photosystem I - I. Genetic and physiological characterization of phylloquinone biosynthetic pathway mutants in *Synechocystis sp* PCC 6803.** *J Biol Chem* 2000, **275**:8523-8530.
12. Zbierzak AM, Kanwischer M, Wille C, Vidi PA, Giavalisco P, Lohmann A, Briesen I, Porfirova S, Brehelin C, Kessler F, Dormann P: **Intersection of the**

tocopherol and plastoquinol metabolic pathways at the plastoglobule. *Biochem J* 2010, **425**:389-399.
13. Kruk J, Karpinski S: **An HPLC-based method of estimation of the total redox state of plastoquinone in chloroplasts, the size of the photochemically active plastoquinone-pool and its redox state in thylakoids of Arabidopsis.** *BBA-Bioenergetics* 2006, **1757**:1669-1675.
14. Yoshida K, Shibata M, Terashima I, Noguchi K: **Simultaneous determination of *in vivo* plastoquinone and ubiquinone redox states by HPLC-based analysis.** *Plant Cell Physiol* 2010, **51**:836-841.
15. Byrdwell WC: **Atmospheric pressure chemical ionization mass spectrometry for analysis of lipids.** *Lipids* 2001, **36**:327-346.
16. Swartz ME: **UPLC (TM): An introduction and review.** *J Liq Chromatogr Relat Technol* 2005, **28**:1253-1263.
17. Nguyen DTT, Guillarme D, Rudaz S, Veuthey JL: **Fast analysis in liquid chromatography using small particle size and high pressure.** *J Sep Sci* 2006, **29**:1836-1848.
18. Plumb R, Castro-Perez J, Granger J, Beattie I, Joncour K, Wright A: **Ultra-performance liquid chromatography coupled to quadrupole-orthogonal time-of-flight mass spectrometry.** *Rapid Commun Mass Sp* 2004, **18**:2331-2337.
19. Lauridsen C, Leonard SW, Griffin DA, Liebler DC, McClure TD, Traber MG: **Quantitative analysis by liquid chromatography tandem mass spectrometry of deuterium-labeled and unlabeled vitamin E in biological samples.** *Anal Biochem* 2001, **289**:89-95.
20. Lanina SA, Toledo P, Sampels S, Kamal-Eldin A, Jastrebova JA: **Comparison of reversed-phase liquid chromatography-mass spectrometry with electrospray and atmospheric pressure chemical ionization for analysis of dietary tocopherols.** *J Chromatogr A* 2007, **1157**:159-170.
21. Kurilich AC, Britz SJ, Clevidence BA, Novotny JA: **Isotopic labeling and LC-APCI-MS quantification for investigating absorption of carotenoids and phylloquinone from kale (*Brassica oleracea*).** *J Agric Food Chem* 2003, **51**:4877-4883.
22. Suhara Y, Kamao M, Tsugawa N, Okano T: **Method for the determination of vitamin K homologues in human plasma using high-performance liquid chromatography-tandem mass spectrometry.** *Anal Chem* 2005, **77**:757-763.
23. Maeda H, Song W, Sage TL, DellaPenna D: **Tocopherols play a crucial role in low-temperature adaptation and phloem loading in Arabidopsis.** *Plant Cell* 2006, **18**:2710-2732.
24. Szymanska R, Kruk J: **Plastoquinol is the main prenyllipid synthesized during acclimation to high light conditions in Arabidopsis and is converted to plastochromanol by tocopherol cyclase.** *Plant Cell Physiol* 2010, **51**:537-545.
25. Kruk J: **Charge-transfer complexes of plastoquinone and alpha-tocopherol quinone *in vitro*.** *Biophys Chem* 1988, **30**:143-149.
26. Hiltbrunner A, Bauer J, Alvarez-Huerta M, Kessler F: **Protein translocon at the Arabidopsis outer chloroplast membrane.** *Biochem Cell Biol* 2001, **79**:629-635.

doi:10.1186/1746-4811-7-23
Cite this article as: Martinis *et al.*: A novel method for prenylquinone profiling in plant tissues by ultra-high pressure liquid chromatography-mass spectrometry. *Plant Methods* 2011 **7**:23.